Università degli Studi di Ferrara

DOTTORATO DI RICERCA IN
"Medicina molecolare e farmacologia"

CICLO XXXI

COORDINATORE Prof. Francesco Di Virgilio

Herpetic vectors for safe, long-term gene transfer in the central nervous system

Settore Scientifico Disciplinare BIO/14

Dottoranda
Dott.ssa Selene Ingusci

Tutore
Prof. Michele Simonato

Anni 2015/2018

Table of contents

Abstract

Herpetic vectors for safe, long-term gene transfer in the central nervous system

After a dramatic stop following the initial clinical trials in 1990s, gene therapy has had an encouraging new start in recent years. Significant improvements in vector engineering, delivery, and safety have placed viral vector-based therapy at the forefront of modern medicine for the treatment of many metabolic, cardiovascular, muscular and oncologic diseases, with nearly 3000 clinical trials completed by 2017. However, one of the major challenges of gene therapy remain the development of therapeutic strategies for central nervous system (CNS) disorders. No cure is available for the vast majority of CNS diseases, and gene therapy offers a promising new approach to compensate for lacking genes, to substitute abnormal genes or to produce therapeutic proteins. Unfortunately, many different hurdles are not yet overcome, including stability and regulation of transgene expression, and safety of both the vector and the expressed transgene(s). In addition, the brain adds several challenges that do not pertain to peripheral gene therapy paradigms, such as post-mitotic target cells (neurons), heterogeneity of cell types and circuits, and limited access to the tissue due to the presence of the blood-brain barrier (BBB). Among a variety of possible gene delivery systems, the Herpes Simplex virus type 1 (HSV-1) appears to be a promising viral vector for CNS gene therapy. Advantageous properties include natural neurotropism, high transduction efficiency, large payload capacity, and the ability of enter a latent state in neurons.

The primary aim of this PhD project was to develop new gene transfer tools based on herpetic vectors for application in CNS diseases.

The challenge has been to genetically engineer the HSV genome to prevent expression of toxic viral genes while retaining the ability to infect multiple cell types and express multiple therapeutic transgenes under independent transcriptional control. Specifically, this thesis focuses on the *in vitro* and *in vivo* characterization of a new family of replication-defective viral vectors (JΔNI) and the *in vivo* characterization of amplicon vectors based on HSV. Attention has been mainly given to safety and expression kinetics. in addition, we evaluated mechanisms to regulate the strength of transgene expression. The principal finding was that this new generation of HSV-1 based vectors exhibit a robust and long-lasting expression of reporter genes, essentially limited to neurons, together with the absence of signs of toxicity or infiltration of inflammatory cells. Therefore, these vectors represent a highly promising tool for gene deliver in many CNS pathologies.

Vettori erpetici per un trasferimento sicuro e a lungo termine nel sistema nervoso centrale

Dopo una battuta d'arresto seguita ai primi, problematici trial clinici negli anni ‘90, la terapia genica ha recentemente trovato un incoraggiante nuovo inizio. Significativi miglioramenti nell'ingegnerizzazione, nel *delivery* e nella sicurezza hanno posto la terapia genica in una posizione di avanguardia nella medicina moderna per il trattamento di varie malattie metaboliche, cardiovascolari, muscolari e oncologiche, con quasi 3000 studi clinici completati al 2017. Tuttavia, una delle principali sfide della terapia genica rimane lo sviluppo di strategie terapeutiche per i disturbi del sistema nervoso centrale (SNC). Per la stragrande maggioranza delle malattie del SNC non esistono ancora terapie curative, e la terapia genica offre un approccio nuovo che promette di compensare la mancanza di geni, di sostituire geni mutati o di produrre proteine terapeutiche. Rimangono molti ostacoli da superare, come la stabilità e la regolazione dell'espressione del transgene e la sicurezza del vettore e del transgene. Inoltre, l’approccio al cervello pone numerosi problemi che non si presentano nella terapia genica periferica, come la presenza di cellule-bersaglio post-mitotiche (i neuroni), l'eterogeneità dei tipi e dei circuiti cellulari e l'accesso limitato dovuto alla presenza della barriera emato-encefalica. Tra i tanti possibili sistemi di *delivery* di geni, il virus dell'Herpes Simplex di tipo 1 (HSV-1) sembra particolarmente promettente per la terapia genica del SNC. Le proprietà vantaggiose comprendono il neurotropismo naturale, l'elevata efficienza di trasduzione, la capacità di ospitare geni di elevate dimensioni e la capacità di entrare in uno stato di latenza nei neuroni.

Lo scopo principale di questo progetto di dottorato è stato sviluppare nuovi strumenti di trasferimento genico basati su vettori erpetici per applicazioni terapeutiche nel SNC.

La sfida è stata quella di ingegnerizzare il genoma di HSV in modo da prevenire l'espressione di geni virali tossici conservando la capacità di infettare più tipi cellulari e di esprimere più transgeni terapeutici in modo indipendente e controllato. Nello specifico, la tesi tratta la caratterizzazione in vitro e in vivo di una nuova famiglia di vettori virali difettivi per la replicazione (JΔNI), e la caratterizzazione in vivo di vettori ampliconi basati su HSV. L'attenzione è stata posta prima di tutto sulla sicurezza e sulla cinetica di espressione. In aggiunta, sono stati studiati meccanismi atti a regolare l’intensità di espressione del transgene. La scoperta principale è stata che questa nuova generazione di vettori HSV-1 esibisce una robusta e duratura espressione dei geni *reporter*, essenzialmente limitata ai neuroni, in assenza di segni di tossicità o di infiltrazione da parte di cellule infiammatorie. Questi nuovi vettori rappresentano quindi uno strumento promettente per la terapia genica in molte patologie del SNC.

This thesis is divided in seven parts: (1) the **introduction**, addressing the current state of the art and the scientific relevance of the project, consisting of two Reviews and enriched by an additional chapter providing general information on herpes viruses; (2) the **aims** of the project; (3) the **results**, reported in two papers and one abstract, showing the main advancements obtained in the development of HSV-1 based viral vectors as gene transfer tools for CNS application; (4) a summary of the results and the **discussion**; (5) a description of the **future perspectives**; (6) **reference**; (7) a short report on **other works** to which I contributed besides the thesis project.

1.1 Gene therapy tools for brain diseases

Gene therapy tools for brain diseases

Selene Ingusci[1], Gianluca Verlengia[1,2], Marie Soukupova[1], Silvia Zucchini[1,3], Michele Simonato[1,2]

[1] Department of Medical Sciences and National Institute of Neuroscience, University of Ferrara, Ferrara, Italy

[2] University Vita-Salute San Raffaele, Milan, Italy

[3] Technopole of Ferrara, LTTA Laboratory for Advanced Therapies, Ferrara, Italy

Corresponding author:

Selene Ingusci

Department of Medical Sciences, Section of Pharmacology

University of Ferrara

Via Fossato di Mortara, 17-19

44121 Ferrara, Italy

Email: selene.ingusci@unife.it

Keywords: gene therapy, central nervous system, viral vector, gene regulation, brain disease

Abstract

Neurological disorders affecting the central nervous system (CNS) are still incompletely understood. Many of these disorders lack a cure and are seeking more specific and effective treatments. In fact, in spite of advancements in knowledge of the CNS function, the treatment of neurological disorders with modern medical and surgical approaches remains difficult for many reasons, such as the complexity of the CNS, the limited regenerative capacity of the tissue and the difficulty in conveying conventional drugs to the organ due to the blood-brain barrier. Gene therapy, allowing the delivery of genetic materials that encodes potential therapeutic molecules, represents an attractive option. Gene therapy can result in a stable or inducible expression of transgene(s), and can allow a nearly specific expression in target cells. In this review, we will discuss the most commonly used tools for the delivery of genetic material in the CNS, including viral and non-viral vectors; their main applications; their advantages and disadvantages. We will discuss mechanisms of genetic regulation through cell-specific and inducible promoters, which allow to express gene products only in specific cells and to control their transcriptional activation. In addition, we will describe the applications to CNS diseases of post-transcriptional regulation systems (RNA interference); of systems allowing spatial or temporal control of expression (optogenetics and DREADDS); of gene editing technologies (Crispr/Cas9, Zinc finger proteins). Particular attention will be reserved to viral vectors derived from herpes simplex type 1, a potential tool for the delivery and expression of multiple transgene cassettes simultaneously.

1. Introduction

Neurodegenerative diseases are a heterogeneous group of diseases characterized by slow and progressive loss of neurons and nerve cells within specific neuronal networks, which consequently leads to inevitable and irreversible damage of brain functions. Neurons, the principal cells of the nervous tissue, are not only morphologically and physiologically heterogeneous, but also strictly organized to form complex circuits that regulate different functions. Depending on the number, position and type of damaged cells, alterations can cause cognitive deficits, dementia, motor impairments, severe behavioral and psychological disorders, with consequent serious disabling effects. Leaving aside inherited disorders with early life onset and brain tumors, neurodegenerative disorders like Alzheimer's disease (AD), Parkinson's disease (PD) and Huntington disease (HD) are undoubtedly among the most complex and widespread in the world population (Bertram and Tanzi, 2005; Brown et al., 2005; Van Deerlin, 2012; Hebert et al., 2013; Budd Haeberlein and Harris, 2015). These highly disabling diseases present a progressive course that is phenotypically evident only when the anatomical brain damage is already in an advanced phase. The continuous growth in the average age and life expectancy of the population leads to an increase in the incidence of these disorders, which until now, with the partial exception of levodopa for PD, have been treated with poor results through the administration of purely symptomatic drugs (Mueller et al., 2006).

Just considering AD, epidemiological data on a global scale estimate that the prevalence of dementia (that is mostly due to AD) was 35.6 million in 2010 and, according to statistical projections, these numbers are expected to duplicate every 20 years, up to 65.7 million in 2030 and 115.4 million in 2050. This will entail a huge cost for the community (Prince et al., 2013).

Scientific research has made great progress over the last decade in identifying pathogenic mechanisms and treatment strategies for neurodegenerative diseases. A primary focus of research is on the development of disease-modifying therapies, i.e. therapeutic strategies capable to act on the pathogenetic mechanisms of the disease (Cummings et al., 2017). In this context, gene therapy is making its way as a doable therapeutic approach. Although much remains to be done before it becomes "routine practice", the potential of gene therapy for the treatment of neurodegenerative disease is amply demonstrated by numerous preclinical and clinical studies (Simonato et al., 2013).

For example, monoclonal antibodies anti-amyloid β (Aβ), delivered by viral vectors, have been found to reduce Aβ deposition in the brain of AD mouse models (Fukuchi et al., 2006; Ryan et al., 2010; Shimada et al., 2013). Others explored the properties of growth and neurotrophic factors (Mandel, 2010; Rafii et al., 2014). Recent evidence supports a key role of insulin-like growth factor 2 (IGF2) in the consolidation of memory, and its delivery in AD mouse models reduced Aβ deposits and the rescued behavioral deficits (Pascual-Lucas et al., 2014). Similarly, neurotrophic factors like glial derived neurotrophic factor (GDNF) and its analog neurturin (NTN) have been evaluated in PD (Wang et al., 2002; Eslamboli et al., 2005; Kordower et al., 2006; Gasmi et al., 2007). No clinical benefits was observed by viral vector-mediated GDNF delivery in a phase I clinical trial (Lang et al., 2006), but delivering NTN into the putamen of PD patients led to a 36% improvement in the average Unified Parkinson's Disease Rating Scale (UPDRS) motor score at 12 months in a phase I clinical study (Marks et al., 2008; Marks et al., 2010; Bartus et al., 2013; Marks et al., 2016).

2. Gene therapy

The idea behind gene therapy derives from an assumption of great simplicity: by introducing into the cells the "correct" copy of a defective gene whose malfunction causes a disease, its product, generically a functional protein, will be able to revert the pathological phenotype. This assumption may be correct for monogenic diseases caused by alteration in the coding sequence or in regulatory regions of a single gene, and if these alterations lead to loss of function without production of a pathogenic protein. However, many diseases have a pattern of altered genes. Moreover, the regulation of gene expression is often complex and difficult to reconstruct artificially.

According to a new, broader definition, all drugs that contain an active substance that includes or consists of a recombinant nucleic acid (DNA or RNA), administered to a human being for the purpose to adjust, repair, replace, add or remove a gene sequence, can be defined as gene therapy.

The introduction of a functional gene, called transgene, within the cell nucleus is a complex operation that starts with the choice of a delivery vehicle in relation to the target tissue and route of administration. A good gene therapy vehicle should be capable of responding to the following requirements:

- Minimal invasiveness: the vector should not cause uncontrolled or undesired alterations of the host genome. The integration of a vector into the cellular genome can induce insertionalmutagenesis.
- Selectivity of the cellular target: the transgene should be expressed exclusively in the cells affected by the pathology.
- Absence of immunogenicity: the vector should not contain genes that induce immune responses or other factors that may be harmful to the body.
- High cloning capacity: the vector should be able to allow the introduction of one or more genes and regulatory sequences that guarantee the desired spatial and temporal restriction of transgene expression.
- Stability over time: the vector should be transmitted unaltered in the cell progeny and/or must allow a correct and prolonged expression of the transgene(s).
- Manipulation: the vector should be easily manipulated for recombination and propagation in suitable hosts.

Currently available gene therapy delivery tools belong to two broad categories: viral vectors and non-viral vectors.

2.1 Viral vectors

Regardless of their origin, order and family, viruses have evolved very fine strategies to reach and penetrate specific cellular targets. Their use in gene therapy lies in their innate ability to deliver and express genetic information into host cell (Bouard et al., 2009). Viral vectors therefore derive from wild-type viruses in which the "wild" genes, essential for replication and virulence, have been replaced with other heterologous, therapeutic genes. The key genes required for virus packaging, replication and host genome integration are deleted from the viral DNA and replaced as trans-acting factors through the development of specific cell lines or helper viruses capable to complementing these essential sequences. Among all viruses, the most characterized and used vectors have been derived from retroviruses, adenoviruses, adeno-associated viruses and herpes simplex viruses (Teschemacher et al., 2005; Bourdenx et al., 2014; Artusi et al., 2018). These viral

vectors mainly differ in payload capacity, cell tropism and in ability to integrate into the host genome, which may affect the duration of transgene expression. Advantages and disadvantages, potential CNS application and side effects for each of the above-mentioned vectors will be briefly discussed below.

2.1.1 Retroviral/lentiviral vectors

The Retroviridae family includes the gamma-retroviruses and lentiviruses, that are those more commonly tested for gene therapy (Cooray et al., 2012). Members of the Retroviridae family have a similar genomic structure with three major genes flanked by long terminal repeats: *gag*, encoding a structural protein; *pol*, encoding an enzyme required for reverse transcription and integration; and *env*, encoding the viral envelope glycoprotein. All retroviruses are single-stranded RNA viruses that can integrate into the host cell genome by retrotranscribing their RNA into a cDNA copy, that will be inherited during DNA replication (Escors and Breckpot, 2010). While lentiviruses are able to transduce non-dividing as well as dividing cells, gammaretrovirus can transduce only actively dividing cells, making their use less attractive for gene therapy of the CNS (Case et al., 1999; Sutton et al., 1999; Sakuma et al., 2012). We will therefore focus on lentiviruses.

The first developed lentiviral vectors derived from human immunodeficiency virus type 1 (HIV-1) and contained a significant portion of the HIV genome (Page et al., 1990). To create a safe, replication-defective retroviral vector, the essential viral components (*gag*, *pol*, *env*) must be split in separate plasmids (Kim et al., 1998). In order to reduce the risk of generating infectious particles due to recombination events, a three-vector system is used to provide in trans the essential genes required for replication. A suitable cell line (generally the 293T cell line) is co-transfected with three separate plasmids: the vector plasmid, containing the gene of interest, the two long terminal repeats (LTRs) necessary for integration into the genome of the host cell and the packaging signal; a plasmid which provides in trans the structural viral genes *gag* and *pol*; and a plasmid encoding for envelope proteins. None of the starting plasmids is capable of generating a viral particle by itself (Maetzig et al., 2011). The removal of most of the viral genome increases the cloning capacity to 9kb (Zhao and Lever, 2007). Engineering improvements have been achieved by pseudotyping the envelope glycoproteins (gp) to redirect viral particles to specific targets. Replacing the surface gp with the gpG of the vesicular somatitis virus (VSV-G) allowed to expand the host spectrum as well as to significantly increase stability (Yee et al., 1994; Sinclair et al., 1997). Other alternatives are the fusion of gp with protein fractions or antibodies that act as specific ligand for cellular receptors (Maurice et al., 2002; Verhoeyen et al., 2003). Integration into the host genome ensures stable and persistent expression of the transgene, but entails the risk of insertional mutagenesis. However, the gene editing technology allows to develop lentiviral vectors with specific integration sites. The insertion of transgenes into a predetermined genomic site creates a safe platform that avoids the risk of insertional mutagenesis (Lombardo et al., 2007).

Lentiviral vectors have been tested for the treatment of AD and PD. Lentiviral vectors expressing PPARγ-coactivator-1α (PGC-1α) reduce Aβ deposition and improve spatial and recognition memory in an AD mouse model (Katsouri et al., 2016). A tricistronic lentiviral vector (ProSavin) based on the equine infectious anemia virus (EIAV), engineered to encode three enzymes necessary for dopamine biosynthesis, was successfully tested in preclinical studies on OHDA-lesioned rats and MPTP-treated macaque monkeys, re-establishing dopamine production and improving motor function (Azzouz et al., 2002; Jarraya et al., 2009). Such positive results allowed to start a clinical study in patients with advanced PD resistant to treatment with L-DOPA. The vector was found to be safe and well tolerated. In addition, a significant improvement in motor behavior was observed in all patients (Palfi et al., 2014). Patients were then followed up 5 to 8 years for long term assessment of safety and efficacy, again with encouraging results (Palfi et al., 2018).

2.1.2 Adenoviral vectors

Adenoviruses (Ad) are linear double-stranded DNA viruses with a genome size of 35-40kb encoding approximately 30-40 genes. There are 100 serotypes of adenovirus, 57 of which have the potential to infect humans. These are divided into seven subgroups, A to G, that differ in cellular tropism (Khare et al., 2011; Lee et al., 2017). The first generation of Ad vectors derived from serotypes 2 and 5 (Campos and Barry, 2007), belonging to subtype C and associated with respiratory tract infections (Chang et al., 2008). In these vectors, the deletion of the early genes E1 and E3 results in incapacity to replicate and creates enough space for the insertion of a transgene cassette of up to 7-8 kb (Campos and Barry, 2007). Since the E1 region is necessary for virus replication, these vectors are commonly produced in the 293 cell line, human embryonic kidney cells engineered to express the E1A protein in trans (Goverdhana et al., 2005). Ad vectors can infect both proliferating and quiescent cells and their genome can persist in episomal form, limiting the risk of insertional mutagenesis (Lee et al., 2017). Several hurdles have emerged for Ad vectors gene transfer technology, including transient transgene expression (from two weeks to a few months) and in vivo toxicity, due to adaptive immune response and pro-inflammatory properties of residual viral proteins (Lowenstein and Castro, 2003; 2004; Lee et al., 2017). Subsequent generations of Ad vectors present even larger deletions of the viral genome to increase cloning capacity and reduce toxicity. The most recent vectors, known as gutless or high capacity vectors, retain from the viral genome only the internal terminal repeats (ITR) necessary for replication, and the encapsulation sequence (psi). These vectors have therefore lost all the elements necessary for replication, which are provided in trans by a helper virus, and can host 35 kb of foreign DNA (Lowenstein and Castro, 2002; Campos and Barry, 2007; Lee et al., 2017). However, separation of these vectors from the helper virus is cumbersome. Moreover, large-scale production should be implemented (Alba et al., 2005).

Ad vectors have been widely studied for the treatment of tumours (Dobbelstein, 2004; Rein et al., 2006; Sharma et al., 2009). Recently, promising advances were obtained thanks to the discovery of a transient electrostatic interaction between Ad52 and a specific type of carbohydrate overexpressed in brain and lung cancer (Lenman et al., 2018). Preclinical studies for CNS with adenoviruses have been conducted in rodent models of PD and HD by delivering GDNF or BDNF, respectively (Choi-Lundberg et al., 1998; Bemelmans et al., 1999). These studies indicate that GDNF and BDNF may have therapeutic value for PD and HD.

2.1.3 Adeno-associated vectors

Adeno-associated viruses (AAVs) are small, non-enveloped single-stranded DNA viruses belonging to the Parvoviridae family. Despite the size limitation, they are still considered as the most promising vehicle for gene therapy targeting the CNS because clinically safe, effective in transducing dividing and quiescent cells, while capable of establishing a long-term transgene expression. More than 150 clinical trials with a good safety profile and significant clinical benefit in many genetic diseases used AAV vectors (Penaud-Budloo et al., 2018). The AAV genome contains three genes, replication (*rev*), assembly (*aap*) and capsid (*cap*) (Naso et al., 2017), between two internal terminal repeats (ITRs) (McCarty et al., 2004) necessary for viral replication, integration and packaging (Berns and Giraud, 1996; Nakai et al., 1999; Musatov et al., 2002). In addition to lack of pathogenicity and immunogenicity, AAVs can persist in the host cell in an episomal state (Bouard et al., 2009). Only 10% of the AAVs integrate into the host cell genome (Naso et al., 2017). In recombinant AAV vectors, the expression cassette is placed between the two ITRs, by replacing the *rev*, *cap* and *aap* genes (Mingozzi and High, 2011).

More than 12 different AAV serotypes have been isolated (Duan, 2016), each characterized by a typical tropism for hepatocytes, myocytes and/or neuronal cells (Nakai et al., 2005; Mandel et al., 2006). The differential tissue tropisms of the different AAV serotypes depends on capsid surface proteins that ensure interaction with cell-specific surface receptors, such as sialic acid for AAVs 1, 4, 5, and 6 (Kaludov et al., 2001; Wu et al., 2006) or galactose for AAV9 (Bell et al., 2011; Shen et al., 2011). A marked neurotropism was observed in the AAV2, AAV5, AAV9 serotypes (Burger et al., 2004; Aschauer et al., 2013), while AAV8, AAV1 and AAV5 efficiently transduce both neurons and glia cells (Davidson et al., 2000; Wang et al., 2003a). Some serotypes display the ability to cross the blood-brain-barrier (BBB) after systemic delivery (Zhang et al., 2011; Yang et al., 2014). When administered intravenously, AAV9 targets preferentially neurons in the neonatal brain and astrocytes in the adult brain (Duque et al., 2009; Foust et al., 2009). The drawback of these attractive non-invasive routes of administration is the ability of AAV to effectively infect liver cells (Gregorevic et al., 2004; Inagaki et al., 2006; Zincarelli et al., 2008). Research is ongoing to identify strategies to circumvent this problem (Pulicherla et al., 2011).

Owing to the small sized genome, AAV vectors are capable of accommodating less than 5 kb of exogenous DNA (Wang et al., 2014; Chira et al., 2015), leading to exploration of feasible strategies for delivering large genes. One approach could be using truncated forms of genes and/or promoters that maintain the properties of their full-length counterpart (Wang et al., 2000; Kodippili et al., 2018; Zhang et al., 2018). However, the generation and use of this "minigene" constructs expose to the risk of failing to reach the desired levels of transgene expression and function (Harper et al., 2002). An alternative strategy has been developed taking advantage of the virus innate ability to undergo a genomic ITR-mediated intermolecular recombination, generating head-to-tail DNA concatamers in the infected cells (Yan et al., 2005). In this context, the DNA sequence of an oversized expression cassette can be splitted and packaged in two (Duan et al., 1998; Yan et al., 2000; Duan et al., 2001; Ghosh et al., 2008; Trapani et al., 2014) or even three (Maddalena et al., 2018) independent AAV vectors. Upon concomitant infection of a host cell, these multiple AAV vectors may give rise to DNA concatamers which have been shown to reconstitute the whole cassette in both in vitro and in vivo assays (Maddalena et al., 2018). The efficiency of this multiple-vector strategy is obviously significantly lower than the single-vector strategy (Duan et al., 2001), and attempts are ongoing to improve the situation (Ghosh et al., 2008).

The potential of AAV-based gene therapy has been tested in many different neurological disorder, including lysosomal storage diseases (Worgall et al., 2008; Tardieu et al., 2014), AD (Rafii et al., 2014), Batten disease (Souweidane et al., 2010), PD (Kaplitt et al., 2007; Eberling et al., 2008; Christine et al., 2009; Mittermeyer et al., 2012) and spinal muscular atrophy (Mendell et al., 2017). As an example, one of the most promising AAV studies in PD delivered glutamic acid decarboxylase (GAD) in the subthalamic nucleus of 12 PD patients, and led to a 24% improvement in the UPDRS score (Kaplitt et al., 2007). More recently, a phase I study used an AAV2 to deliver aromatic L-amino acid decarboxylase (AADC) in the striatum of 15 PD patients (NCT01973543). Primary completion date of this study is estimated on December 2019.

2.1.4 HSV based viral vectors

The first HSV viral vector derived from Herpes Simplex virus type 1 (HSV-1), belonging to the Herpesviridae family, a group of double-stranded DNA viruses (Jacobs et al., 1999). Since then, three types of HSV-1 based vectors have been developed: replication-competent, replication-defective and amplicon vectors (Artusi et al., 2018). Replication-competent vectors are widely used in oncology for their ability to complete a lithic cycle in the presence of permissive cellular environments (Ikeda et al., 2000; Todo, 2008) and as helper viruses for amplicon and AAV vector production. Replication defective and amplicon vectors are suitable as

gene transfer tools for CNS disorders (Goverdhana et al., 2005; Berges et al., 2007; Fink and Mata, 2008). HSV-1 is the major viral vector known to naturally target neurons (Berges et al., 2007). Its large genome (152kb) encodes about 80 genes, half of which can be removed to make room for more than 50kb of foreign DNA in the case of replication-defective vectors and up to 150 kb for amplicon vectors (Simonato et al., 2000). HSV-1 vectors maintain high infectivity, ability of both retrograde and anterograde transport and potential to establish a latency infection in an episomal-form. Limits in their application are residual toxicity towards the infected cells (Goverdhana et al., 2005), and the short-term expression of the transgene due to rapid silencing mechanisms. Safer HSV-1 vectors have been obtained through the elimination of expression of all immediate-early genes (Miyagawa et al., 2015; Verlengia et al., 2017). Strategies to bypass epigenetic silencing included the use of enhancers or protective regulatory sequences, and the construction of hybrid amplicon vector platforms via the incorporation of genetic elements from other viruses (Epstein, 2009b; a; Han et al., 2018b). The most recent advancement will be described more in detail in the section "New vectors for the delivery of multiple insertion cassettes".

2.2 Nonviral vectors

The simplest types of vector for gene transfer consists of naked DNA, particle based and chemical based. Non-viral vectors offer important advantages over viral vector approaches, such as reduced pathogenicity, low cost and simple production techniques, but their greatest potential lies in the cargo capacity and bio-safety (Zhang et al., 2004; Ramamoorth and Narvekar, 2015). However, DNA delivered in non-viral vectors or as naked DNA must overcome a number of extracellular and intracellular barriers, limiting the efficiency of DNA transfection (Howell et al., 2003; Matsumoto et al., 2009). First of all, the transfection efficiency is limited by the premature release of the genetic material into the bloodstream and its subsequent degradation by serum nucleases when administered intravenously, while the endocytosed DNA is in large part degraded along the endosomes/lysosomes pathway, before it reaches the nucleus (Ogris et al., 1999; Perez-Martinez et al., 2011).

Several methods have been developed to improve delivery of naked DNA to cells and tissues, which are divided in physical methods and chemical carriers. In addition to direct injection and microinjection into the nucleus, physical methods include electroporation, sonoporation, megnetofection, hydroporation and ballistic methods. Chemical carriers are based on inorganic (which includes calcium sulphate, silica, gold, magnetic compounds, quantum dots), lipid, polymer and peptide particles (Ramamoorth and Narvekar, 2015). Among these the most common non-viral vectors used in gene therapy are cationic polymers and cationic lipids. Lipid-DNA complexes, or lipoplesses, are produced by mixing the DNA with cationic derivatives of fatty acids or cholesterol, while for the preparation of polymers-DNA complexes, or polyplesses, high molecular weight polycarbonate, such as polylysine or polyethylenamine (PEI), are used (Li and Huang, 2006; Jayant et al., 2016). Lipids and cationic polymers are amphipathic molecules able to bind to the polyanionic DNA molecule trough the establishment of electrostatic interactions. This increases the affinity of the DNA for the negatively charged cell membrane, promoting the endocytosis of DNA (Mounkes et al., 1998). Polyplexes and lipoplexes can be chemically modified to obtain systems specifically oriented towards particular target tissues. This can be achieved by associating peptide ligands for cellular receptors or viral proteins, such as the tat protein of the HIV-1 virus (Frankel and Pabo, 1988) and the HSV-1 VP22 transcription factor (Elliott and O'Hare, 1997), that allow nuclear localization or specific cellular tropisms.

Efficacy of cationic lipids and polymers is dependent on cationic charge, saturation and linker stability (Jayant et al., 2016). Several strategies have been explored to increase the stability of DNA in the circulation, such as the use of hydrophilic polymers to shield the residual surface charge. Polyethylene glycol (PEG) is commonly used (Malik et al., 2000; Dufes et al., 2005; Huang et al., 2007). Another approach to this problem is the use of bioresponsive polymers that exploit the chemical-physical properties of biological microenvironments (pH, presence of reducing agents, etc.) to promote the release of the genetic material exclusively in the intracellular environment. Other tested solutions were acetyl bonds, which degrade at the pH of the endosomal environment (Knorr et al., 2007; Wolff and Rozema, 2008), or disulfide bridges, that are reduced in the cytosol (Niidome and Huang, 2002; Piest et al.,2008).

To date, 18% of gene therapy clinical trials used naked DNA, whereas cationic polymers have only been used in animal models (Ginn et al., 2018). Recently, naked plasmid DNA has been tested also in a trial for a neurological disorder, a phase I clinical trial of ex vivo gene therapy for AD (Tuszynski et al., 2005; Tuszynski et al., 2015).

3. Regulation of gene expression

As previously mentioned, precise regulation of gene expression is essential for any gene therapy approach. A good gene regulation system should: be adjustable over a broad dose range; exert no off-target effect; not affect endogenous gene expression; be region or cell specific; allow to quickly turn off and on transgene expression (Naidoo and Young, 2012). Regulation of gene expression, in terms of increasing or decreasing levels of a specific gene product or in terms of directing the information to a desired target tissue, can occur at different molecular levels. In this section we will discuss the gene regulation strategies currently used in gene therapy, e.g.: at the transcriptional level, with the use of tissue specific and inducible promoters; and at post-transcriptional level, with the use of RNA interference techniques.

3.1 Transcriptional level: tissue specific and Inducible promoters

Transcriptional regulation can be defined as the control of the amount of RNA transcribed. It results from the combined effect of structural properties (euchromatin and heterochromatin state) and the interaction of transcription factors with regulatory DNA elements, including promoters, insulators, enhancers and silencers.

3.1.1 Ubiquitous and tissue-specific promoters

Promoters are the main elements that determine the strength and cellular specificity of gene expression. When the achievement of a specific cell target is not required, i.e. transgene expression is sought in the broadest possible spectrum of cells, ubiquitous expression promoters are used. Ubiquitous and constitutive promoters are strongly active in a wide range of cells and tissues. Previous works have described the relative strength of commonly-used transcriptional regulatory elements both in vitro and in vivo (Pasleau et al., 1985; Martin-Gallardo et al., 1988; Oellig and Seliger, 1990; Yew et al., 1997) and strength differences in various tissues (Manthorpe et al., 1993; Hartikka et al., 1996). The following promoters are frequently employed to

drive exogenous DNA expression in a non-cell specific manner: cytomegalovirus (CMV) immediate-early, enhancer/chicken-β actin (CAG), human ubiquitin C (UBC), simian virus 40 early (SV40), human elongation factor 1α (EF1A) and mouse phosphoglycerate kinase 1 (PGK). A recent comparative study quantified the strength of eight commonly used promoters in different cell lines through flow cytometry. The results show that CAG, EF1α and CMV are the strongest promoters among those analysed. CMV promoter is the most variable, being very strong in some cell types and rather weak in others (Qin et al., 2010).

The use of cell-type specific promoters, driving genes selectively expressed in a certain cell type, can limit the expression of the transgene to that cell type. For neurological diseases, specifically labeling a population of neurons or glial cells would allow to achieve the therapeutic goal without incurring in off-target effects. What limits the use of these promoters are the low level of expression and their genomic size. The synapsin-1 (Syn1) and the neuron-specific enolase (NSE) promoter are used for their ability to selectively drive transgene expression in neurons (Peel et al., 1997; Kugler et al., 2001; Kugler et al., 2003; McLean et al., 2014), while the glial fibrillary acidic protein (GFAP) promoter results in astrocyte-specific expression (Smith-Arica et al., 2000; Lee et al., 2008). Transgene expression can be specifically targeted to oligodendrocytes by the myelin basic protein (MBP) (von Jonquieres et al., 2013) or the human myelin associated glycoprotein (*MAG*) promoter. Recent studies revealed that both the full-length and the trounced version of the *MAG* promoter induced more than 95% of transgene expression into oligodendrocytes (von Jonquieres et al., 2016). The immune surveillance system plays a crucial role in many CNS disorders, including AD and multiple sclerosis. The specific targeting of microglia, representing up to 10% of adult brain cells (Kettenmann et al., 2011) could be useful to suppress microglial activation and neuroinflammation (Loane and Kumar, 2016). Using the F4/80 or the human CD68 promoter enables selective targeting of microglia. The highest levels of microglial cells specificity (>95%) has been yielded by the F4/80 promoter in combination with a surface-mutated AAV6 capsid (Rosario et al., 2016).

The balance between excitatory and inhibitory signals, basically the equilibrium between glutamatergic and GABAergic neurotransmission, can be often disrupted in diseases like epilepsy. Therefore, targeting specifically GABAergic or glutamatergic neurons could represent a therapeutic approach. The phosphate-activated glutaminase (PAG) or the vesicular glutamate transporter (vGLUT) promoter ensure ∼90% glutamatergic neuron-specific expression, whereas the glutamic acid decarboxylase (GAD) promoter ensures ∼90% GABAergic neuron-specific expression (Rasmussen et al., 2007).

Promoters are not the only elements necessary for transcriptional regulation. Combining regulation elements of different kinds, such as promoters, enhancers, introns and polyadenylation signals by creating hybrid sequences allows to modulate the expression levels as desired. The levels of transgene expression may be strongly influenced by a rapid epigenetic silencing of the exogenous promoters. To protect the promoter and the whole expression cassette from heterochromatization, insulator elements have been tested for their ability to maintain transcriptionally competent whole portions of DNA, regardless of the tissue type and the integration site (Chung et al., 1993; Bell et al., 1999). As reviewed extensively elsewhere, these protective elements are divided into enhancer-blocking insulators, whose function are mediated by the CTCF-binding factor (Gaszner and Felsenfeld, 2006; Phillips and Corces, 2009) and barrier insulators, whose mechanism of action is less known (West et al., 2002; Gaszner and Felsenfeld, 2006; Raab and Kamakaka, 2010). Insulators are extracted from loci of housekeeping genes containing CpG islands, that are resistant to methylation. First well characterized vertebrate insulator derived from the chicken β-globin locus associated with a constitutive DNAse I hypersensitive site called cHS4 (Chung et al., 1993). cHS4 exhibits both enhancer-blocking activity and barrier activity (Yao et al., 2003). Many studies concerning the delivery of retroviral vectors showed that the inclusion of the cHS4 element allows to increase transgene expression (Modin et al., 2000; Rivella et al.,

2000; Emery, 2011). Others, such as ubiquitous chromatin opening element (UCOE), derived from the human HNRPA2B1-CBX3 locus (A2UCOE) shows increased stability of transgene expression, due mainly to its resistance to DNA methylation-mediated gene silencing (Zhang et al., 2010). Among other elements to be considered are enhancer elements, whose insertion significantly affects the expression levels of the transgene (Hartikka et al., 1996). Often used in genetic engineering is the CMV enhancer (eCMV), whose presence in cultured cells multiplies the expression of the transgene 8 to 67 times (Yew et al., 1997), conferring efficient neurons specific gene expression when using the PDGF-β (platelet-derived growth factor- β) promoter (Gruh et al., 2008).

3.1.2 Inducible promoters

For many applications it is necessary to modulate the expression of the transgene by switching on or off the transcriptional activity. Unregulated long-term overexpression of certain transgenes can cause side effects in the CNS, such as aberrant reorganization of the tissue and activation of compensative pathways and/or inactivation/saturation of activated pathways. A finer regulation can be achieved using inducible promoters. The use of inducible promoters is based on the idea that the expression of the therapeutic gene can be regulated by a transcription factor whose activity is inducible. These systems are obtained by incorporating in the vector (or in a separate vector) the constitutive expression cassette for a transcription factor (transactivator) able to activate or block the expression of the transgene depending on the availability of a soluble molecule that can be administered systemically.

3.1.2.1 The Tet ON/Tet OFF regulation system

A commonly used regulation system is based on the mechanism of tetracycline resistance in prokaryotes. Two variants are available (Figure 1), both relying on tetracycline to deactivate (Tet-OFF system) or activate gene expression (Tet-ON). In the Tet-OFF system, the transgene is under the transcriptional control of the tet operator (tetO), a fragment of DNA responsive to the transactivator tTA, composed of the tet-repressor (tetR) fused to the VP16 viral protein transactivation domain. The transgene is expressed only when tTA binds tetO in the absence of doxycycline, an analogue of tetracycline. Otherwise stated, the presence of tetracycline or its analog in the culture medium or in the organism reversibly induces the transactivator to detach from the operator, causing the transgene to "switch off". The Tet-ON system was developed by inducing random mutations in the tetR. One mutation resulted in a protein with opposite function, that was named reverse tet-repressor (rtetR). This mutant protein, when fused to the VP16 transactivation domain (reverse transactivator, rtTA), drives transgene expression only in the presence of doxycycline (Gossen et al.,1995).

Tetracycline-based regulatory systems hold a great potential for gene therapy applications. They ensure rapid in vivo induction or inhibition kinetics (Xiong et al., 2006) and low toxicity – tetracycline and its derivatives have been used for decades for their antimicrobial activity (Pasquale and Tan, 2005). Limitations are mainly due to high basal transgene expression, in particular when the expression is driven by a constitutive promoter. Recently, a second generation of tetracycline-regulated system containing a shortened CMV minimal promoter was found to enhance regulation efficiency and display low basal expression (Agha- Mohammadi et al., 2004). Modifications in the tetO sequence (TRE-tight1) driven by a neuron-specific enolase (NSE) was found to improve gene expression efficiency and to reduce the leaky basal transcription (Tian et al., 2009).

For CNS applications, it is necessary to obtain high concentration of doxycycline in the CNS (Nau et al., 2010). New rtTA variants containing mutations in the doxycycline contact domain enhance doxycycline sensitivity, resulting in a reduction of doxycycline concentrations required for transgene activation (Das et al., 2004;

Zhou et al., 2006). The majority of CNS applications involving the tetracycline-regulated system used viral vectors for the construct delivery, e.g. lentivirus (Georgievska et al., 2004; Pluta et al., 2005), adenovirus or AAV (Ebert et al., 2005; Lee et al., 2005; Le Guiner et al., 2014), resulting in a tightly regulated gene expression. For example, the lentivirus vector-mediated delivery of GDNF regulated by a Tet-ON system in a PD rat model resulted in a precise regulation of transgene expression and in neuroprotection of nigral DA neurons (Chen et al., 2014).

3.1.2.2 The rapamycin regulation system

The rapamycin regulation system is based on the interaction between two inactive transcription factors, a DNA binding domain and a DNA transcriptional activation domain. Each transcription factor is fused to heterologous binding domains for rapamycin. The DNA binding domain is fused to three copies of the FK-binding protein (FKBP), while the DNA activation domain is fused to a lipid kinase, FKBP12 rapamycin-associated protein (FRAP) (Rivera et al., 1996; Kang et al., 2008). Rapamycin allows their interaction, thus forming an active, heterodimeric transcription factor that drives the expression of the transgene (Figure 2).

This system holds many of the features required for clinically use. First, rapamycin is a clinically approved drug, used as an antifungal and anti-tumor molecule that can be administered orally and can cross the BBB (Dutta et al., 2014). Second, the system ensures low basal expression of the transgene in the absence of rapamycin but can be triggering by low doses of the drug (Naidoo and Young, 2012). The limitations are mainly related to the immunosuppressive properties of rapamycin, dependent on the blockade of mTOR signaling pathways. The rapamycin analogues "rapalog" (e.g. AP21967) were engineered by adding substituents that prevent the binding to mTOR (Bayle et al., 2006).

A limited number of studies tested this system in the CNS by delivering it through lentiviral (Vogel et al., 2008), AAV (Sanftner et al., 2006) and HSV-1 based vectors (Wang et al., 2003b). A dose-dependent response to rapamycin was observed after delivering into the rat striatum a rapamycin regulated AAV2-GDNF vector and evaluating GDNF biogenesis and accumulation under various rapamycin dosing regimens. In addition, chronic administration with clinically compatible regimens provided GDNF protein levels around 0.80 ng/mg, similar to those reported to be neuroprotective in PD animal models (Hadaczek et al., 2011).

3.2 Post-trascriptional gene regulation: RNA interference

Expression levels of the transgenes depend also on the mRNA stability in the cytosol. Polyadenylation (polyA) signals are necessary to stabilize transcripts, nuclear export and translation initiation (Jacobson and Peltz, 1996; Hall, 2002). Insertion of a polyA sequence allows to increase from 3- to 6.5-fold gene expression levels in different cell lines and in primary culture, independent of the promoter (Hager et al., 2008).

When speaking of post-transcriptional gene regulation, however, one generally refers to approaches in which the transgene is designed to enhance degradation or block translation of a target mRNA. The typical example is RNA interference (RNAi). RNAi is a physiological mechanism, normally present in eukaryotic cells and mainly mediated by short-interfering RNAs (siRNAs) and microRNAs (miRNAs). The main difference between these two is that siRNAs are perfectly complementary to their target mRNA, while miRNAs, that are much shorter and have lower complementarity, can interact with multiple mRNA targets. Based on RNAi, it is possible to silence gene expression by designing RNA sequences, artificial miRNAs or short hairpin RNAs (shRNA), that target coding and/or non-coding mRNA regions with perfect complementarity.

Neurodegenerative disease resulting from a single gene mutation that causes gain-of-function or an accumulation of a mutant protein are ideal candidates for gene suppression approaches. Unfortunately, RNA molecules do not cross the BBB, and the use of viral and non-viral vector is necessary for their delivery. RNAi has been widely investigated in Huntington disease (HD), an autosomal-dominant neurodegenerative disorder caused by a CAG trinucleotide repeat expansion in the HTT gene. A potential therapeutic strategy for HD is to reduce mutant HTT expression using shRNA or miRNA molecules against HTT mRNA. Several studies have achieved this goal by using AAV-mediated shRNA transfer in mouse models of HD disease, resulting in reduced HTT mRNA and improved motor and neuropathological abnormalities (Harper et al., 2005; Rodriguez-Lebron et al., 2005). Using RNAi against HTT mRNA does not imply the degradation of only the mutated protein, but also of the wild-type protein that plays an important role in neuronal survival (Reiner et al., 2003). This does not seem to cause significant site-effects up to 9 months after treatment (Boudreau et al., 2009; Drouet et al., 2009). However, other harmful effects have been observed, including the activation of a potent innate interferon response, due mainly to a first line cell defence against viral infection (Sledz et al., 2003), widespread changes in expression levels in unrelated genes, due to non-specific degradation of non-target mRNAs (Jackson et al., 2003; Persengiev et al., 2004; Scacheri et al., 2004), and saturation of endogenous Silencing Pathways (Grimm et al., 2006). To reduce off-target effects, a series of bioinformatic prediction programs based on mathematical algorithms have been developed, that identify the hypothetical target mRNAs of each specific miRNA. These computerized media, accessible on the web (www.targetscan.org, www.pictar.mdc-berlin.de), take into account target complementarity, evolutionary conservation among species and the thermodynamic stability of the heteroduplex formed by the interaction between miRNAs and mRNAs (Reynolds et al., 2004).

Anti-sense oligonucleotides (ASOs), are another silencing tool. ASOs are single-stranded DNA molecules which are complementary to targeted pre-mRNA. Following the formation of an RNA/DNA duplex, an endonuclease is recruited that will degrade the pre-mRNA. ASOs have been intensively tested for human neurodegenerative disorders. For example, ASOs that selectively decrease human tau mRNA have been shown to lead to reduced tau protein deposition and neuronal loss in a mouse model of AD (DeVos et al., 2017).

3.3 Spatiotemporal regulation tools

The complexity of the mammalian brain has no comparison: dozens of billions of interconnected neurons, with complex morphology and circuit interaction, capable of exchanging electrical signals with a precise temporal scan in the order of milliseconds (Luo et al., 2018). This complexity represents a formidable obstacle for neuroscientists to fully understanding the brain physiology and developing effective strategies to treat neurological disorders. A great challenge is the ability to control only one type of cell in the brain without affecting others. Electrical, physical, pharmacological, and genetic methods are traditionally used to manipulate cells and synapses (Carter and Shieh, 2015). All these methods lack temporal and spatial resolution and can cause stimulation, inhibition, or inactivation of off-target cells and processes. To overcome these limitations, new genetic tools referred to as “chemogenetic” and “optogenetics” have been developed.

3.3.1 Designer receptors exclusively activated by designer drug (DREADDS)

Chemogenetics is the processes in which proteins are engineered to interact specifically with a small molecule (Sternson and Roth, 2014). Different proteins involved in CNS disorders have been engineered to this aim, including kinases and other enzymes (Bishop et al., 1998; Cohen et al., 2005; Dar et al., 2012), ligand-

gated channels (Zemelman et al., 2003; Magnus et al., 2011) G protein-coupled receptors (GPCRs; (Armbruster et al., 2007; Alexander et al., 2009; Vardy et al., 2015). The latter include allele-specific GPCRs (Strader et al., 1991), Receptors Activated Solely by a Synthetic Ligand (RASSLs; (Coward et al., 1998) and Designer Receptors Exclusively Activated by Designer Drugs (DREADDs; (Armbruster et al., 2007). The first chemogenetically engineered GPCR was the β-adrenergic receptor (βAR; (Strader et al., 1991). Following mutation at the βAR binding site the responsiveness to the natural ligand failed and a new specificity was obtained to ketonic and catechol esterase agonists. Several years later, RASSLs receptors were developed, based on human κ-opioids, that lost their affinity for the endogenous peptide ligand (dynorphin) and gained specificity for small and safe drugs such as spiradoline (Coward et al., 1998). However, both these systems displayed very low affinity for the new ligands.

The development of DREADDs overcame this limitation (Armbruster et al., 2007). Together with optogenetics, the DREADDs technology is currently the most used tool for in vivo manipulation of the activity of genetically-defined neuronal populations. An example of DREADDs technology is the use of modified muscarinic receptors, hM3Dq for stimulation and hM4Di for inhibition, which have lost their affinity for endogenous acetylcholine, but can be activated by a synthetic ligand (Clozapine-N-oxide, CNO) that crosses the BBB (Armbruster et al., 2007; Alexander et al., 2009). Compared to previous techniques, chemogenetics based on DREADD confers the ability to regulate and manipulate in a non-invasive manner the activity of specific neuronal circuits. Combined with the set of gene therapy tools described above, DREADDs can be delivered and selectively expressed in the neuronal subpopulation of interest, for example serotonergic (Teissier et al., 2015; Urban et al., 2016) or glutamatergic neurons (Krashes et al., 2014; Zhu et al., 2014; Zhu et al., 2016).

DREADDs are a useful tool for basic scientific research but may also refine gene therapy approaches for neurodegenerative disorders in which changes in neuronal activity plays an important role. Neuronal hyperactivity and hyperexcitability of the cerebral cortex and hippocampus are common features of both epilepsy and AD (Badawy et al., 2009; de Haan et al., 2017). On demand attenuation of seizures was achieved after delivery of AAV vectors carrying the hM4Di receptor under the control of the *CamkIIα* promoter (Katzel et al., 2014). PD patients often present lower-body axial symptoms, including gait disorders, freezing and postural instability and upper-body axial symptoms, namely dysarthria, deglutition and respiratory function (Moreau et al., 2016). Transient cholinergic-specific stimulation led to a striking improvement in motor scores in a rodent model of PD including gait and postural abnormalities (Pienaar et al., 2015).

3.3.2 Optogenetic approaches

The term optogenetics indicates an optic methodology useful for probing and controlling genetically targeted neurons within intact neuronal circuits (Deisseroth, 2011). The idea of using the light as a tool to control neuronal function was originally put forward by the British scientist Francis Crick (Crick, 1979). In the 70', biologists discovered that some microorganisms generate proteins that, in response to visible light, regulate the flow of electric charge through membranes (Oesterhelt and Stoeckenius, 1971). These proteins, named opsins, are photosensitive trans-membrane proteins which, when illuminated, induce transmembrane ion fluxes, inducing changes in the electrical activity of the cell. There are two major classes of opsins, which differs in sensitivity to light and absorption properties, and can determine the activation or inhibition of neurons (Deisseroth, 2015):

- Channelrhodopsin (ChR): a blue light activated cation-channel from *Chlamydomonas reinhardtii*, used to excite neurons (Nagel et al., 2003);

- Halorhodopsin (NpHR): a yellow light activated chloride-pump from *Natronomonas pharaonic*, used to inhibit neurons (Chow et al., 2010).

Through viral vectors, the gene coding for an opsin can be integrated into target neurons, leading to expression of the opsin protein on the membrane. A nearby source of light, set on the right wavelength and frequency, can then interact with it, activating or inhibiting neuron activity. Introduction of mutations to existing opsin variants allowed to overcome certain problems associated with light delivery. The ChR chETA mutant displays faster channel closing and increased temporal control (Gunaydin et al., 2010). The C1V1 mutant can be excited by longer wavelengths, allowing deeper penetration of the tissue (Yizhar et al., 2011). At the same time, light delivery tools have been improved and optimized for in vivo studies (Liu et al., 2015).

The use of optogenetics as therapeutic tools for neurological disorders has been investigated in PD, AD and epilepsy (Kravitz et al., 2010; Zahedi et al., 2013; Seeger-Armbruster et al., 2015). Enhanced excitation of pyramidal neurons is a common feature of many forms of epilepsy, and its control may lead to therapeutic effects. NpHR delivery into these neurons promptly and dramatically reduced seizures upon light stimulation (Krook-Magnuson et al., 2013). Enhancing inhibitory activity of interneurons via transfection of the excitatory opsin ChR also resulted in reduced seizure frequency and severity (Krook-Magnuson et al., 2013). Optical inhibition of the subthalamic nucleus in PD models significantly improved akinesia and ameliorated levodopa-induced dyskinesia (Yoon et al., 2014; Yoon et al., 2016).

4. Genome editing

Genome editing is a gene therapy technique that allows precise and efficient genetic modifications by introducing a double strand break (DSB) within a specific genomic sequence, followed by the introduction of modifications of the same sequence during the repair mechanisms triggered by the cutting. Eukaryotic cells can repair DSBs mainly by using two mechanisms: homology directed repair (HDR) and non-homologous end Joining (NHEJ). There are many approaches aimed at modifying, inserting or eliminating pairs of nucleotides in the genomic study sequence using engineered nucleases (Gaj et al., 2016).

- **Zinc finger nuclease (ZFN)**
  ZFNs are composed of a cutting domain derived from an endonuclease subunit, often that of the restriction enzyme FokI, fused to a DNA binding domain, consisting of Cys2-His2 modules with a "zinc finger structure" (Urnov et al., 2010). Each ZF module contains 30 amino acids able to bind three adjacent nucleotides. Replacing these amino acids allows to modify the DNA binding specificity creating synthetic motifs. Since FokI is a dimeric enzyme, two ZFN should be created to ensure the cleavage of DNA. In practice, however, the creation of zinc binding domains that efficiently recognize a selected DNA sequence is a long and laborious process. The specificity of each module depends on the adjacent modules with which it is fused. This phenomenon can lead to the formation of nucleases that are not specific to the desired sequence. Furthermore, not all the possible nucleotide triplets can be recognized by the zinc finger modules and this makes the design of ZFN even more difficult.
- **Transcriptional activator-like effectors (TALEs)**
  TALEs represent another class of proteins that specifically bind DNA. In 1989, Bonas and collaborators identified an interesting family of proteins in the bacteria of genus *Xanthomonas campestrism* (Bonas

et al., 1989; Moscou and Bogdanove, 2009; Boch and Bonas, 2010). The central DNA binding domain consists of sequences of 34 tandem repeated amino acids called monomers. The sequence of each monomer is highly conserved and differs only for two amino acids that are in positions 12 and 13, namely repeat variable diresidues (RVD), capable to recognize a single nucleotide (Boch and Bonas, 2010; Mussolino and Cathomen, 2012). Similar to ZFNs, TALE modules can be bound in series to form DNA binding domains, able to recognize the DNA sequence of interest. DNA cleavage occur fusing FokI to TALEs (Mussolino and Cathomen, 2012). While compared to ZNFs, the DNA interaction of individual TALE modules is not hindered by neighbouring domains. Therefore, generating new artificial nucleases based on the TALE structure is simpler and faster (Jankele and Svoboda, 2014). TALE are able to recognize any sequence with an impressive success rate. The major limitation is their large size, that makes them difficult to deliver with viral vectors.

- **Clustered regularly interspaced short palindromic repeats/Cas (CRISPR/Cas)**
  The CRISPR/Cas9 system is the most recent system for gene editing. It was first discovered in 1987 in *Streptococcus pyogenes* bacteria, which adopt this system as protection against phage attacks and plasmid transfers. However, its use as a tool for gene editing is much more recent (Doudna and Charpentier, 2014). The system is made up of a Cas9 endonuclease combined with a 20-nt guide RNA (sgRNA), to form a functional complex that acts as an RNA-directed DNA endonuclease capable of generating a DNA double-strand break (DSB) within a specific target sequence. Cas9 specificity is dictated by sgRNA and a protospacer adjacent motif (PAM), a highly represented trinucleotide sequence (usually 5 '-NGG-3') absolutely required to initiate the sgRNA mediated DNA binding (Karvelis et al., 2015). The cut is then repaired by NHEJ, which introduces in/del mutations, or by HDR, which repairs the DSB without inserting any mutations. In the latter case, the correction can be performed trough a Donor vector (HDR Donor) carrying the correct DNA sequence that is transferred later by homologous recombination at the nick level (Ran et al., 2013). Although the CRISPR/Cas9 system is an innovative, simple and inexpensive, it presents an important limitation in that, with respect to the TALENs and ZFNs methods, it holds a higher probability to cause off-targets effects, due to a sgRNA much smaller than those used in the other two systems (Xie et al., 2014). Numerous softwares allow to design the best sgRNA for the target site and, in addition, there are countless tools that allow to search for all possible off-targets sites (Nalls et al., 2014). Further strategies proposed to reduce off-target site effects are the use of a modified version of Cas9 (D10A) capable of directly cutting a single strand of DNA; or using two mutated Cas9 (Cas9 nickase) having two sgRNAs to create a nick on a strand and one on the opposite strand, which are close enough to produce a DSB allowing the activation of HDR. It has been estimated that the double nick strategy increases 1500 times the target side specificity, decreasing the off-target effects and possible indel (Cong et al., 2013; Ran et al., 2013).

Engineered nucleases are useful tools for treating a wide variety of diseases, but also for helping to establish better cellular and animal models that more faithfully mimic human neurodegenerative diseases (Gaj et al., 2016; Maeder and Gersbach, 2016). The ZFNs system was used in HD mouse model to reduce the level of mutant HTT (mHTT), showing a 95% reduction of mutant protein and a 78% reduction of mRNA levels (Garriga-Canut et al., 2012). Striatal delivery of AAV2 encoding for an engineered ZFP transcription factor that activate the expression of the endogenous GDNF gene results in improvements in the motor function in a rat model of PD (Laganiere et al., 2010). The TALE technology was used in a recent study for allele-specific targeting of human HD fibroblasts. TALE were designed to target single-nucleotide polymorphisms (SNP) in the mutant allele, reducing mutant allele expression (Fink et al., 2016). Recently, CRISPR/Cas9 was used to suppress endogenous mHTT expression in the striatum of a mouse model of HD, resulting in complete depletion of HTT aggregates (Yang et al., 2017). Other neurodegenerative diseases could benefit from the enormous potential of the CRISPR/Cas9 technology. The possibility to use this system to cut and silence

potential neuropathological hallmark proteins involved in AD and PD can facilitate the discovery of gene variants associated with disease progression.

5. New vectors for delivering multiple expression cassettes

It is often necessary to transfer large genomic sequences or multigenic cassettes to obtain a therapeutic effect. Disorders of the CNS are often not a result of single gene mutation or of a single molecular mechanism, but have instead a multifactorial origin. As a result, the therapeutic gene(s) and/or the regulation sequence that should be delivered very often exceed the payload capacity of a viral vector (Thomas et al., 2003). HSV vectors represent an attractive solution for this issue, because of their large genomic size and capacity to host large amounts of foreign DNA. Previous generations of replication-defective HSV-1 vectors, however, display highly significant limitations, including toxicity and short-term expression of the transgenes. Many recent studies have been aimed at solving these problems.

The HSV productive cycle is characterized by a temporally regulated cascade of gene expression, during which three distinct classes of transcripts are expressed in a sequential manner. The immediate early genes (IE or α), including ICP0, ICP4, ICP22, ICP27 and ICP47 are first expressed, then early (E or β) genes and finally late (L or γ) genes. The deletion of α genes shuts off viral gene expression, with reduction of cytotoxicity (Glorioso and Fink, 2004). Deletion of two IE genes, ICP4 and ICP27, gave rise to the first (ΔICP4) and second (ΔICP4/27) generation of HSV-1 vectors (Glorioso, 2014). These early generations of vectors were able to establish a long-term expression without the ability to reactivate (Glorioso, 2014). However, these vectors were still toxic, mainly due to the presence of ICP0 (Samaniego et al., 1997). The consequent deletion of ICP0 gave rise to the third generation of HSV-1 vectors that were devoid of toxicity but displayed a limited expression of the transgene over time (Yao and Schaffer, 1995). IE genes, in particular ICP0, are required not only for establishment of a lytic reproductive cycle, but also to overcome innate immune responses, hide infected cells from immune surveillance, block cell division, block apoptosis and prevent epigenetic repression of viral gene expression. Therefore, the fourth generation of HSV-1 vectors, namely JΔNI, were engineered inserting the latency-associated promoter (LAP) in the latency locus and using insulator sequences (CTRL) (Miyagawa et al., 2015), which acted as boundary elements to shield this particular locus against epigenetic modifications (Bloom et al., 2010). This new generation of highly defective HSV vectors offered a large payload capacity, the largest available among viral vectors for gene therapy, were devoid of all viral IE genes and, for the first time, allowed transgene expression in the absence of ICP0 in both neuronal and non- neuronal cells in vitro (Miyagawa et al., 2015). Surprisingly, the expression of transgenes inserted in the ICP4 locus declined with the removal of all IE genes in non-neuronal culture, with the very notable exception of dorsal root ganglion (DRG) cells (Miyagawa et al., 2015). In vivo investigation subsequently demonstrated that delivering these new vectors into different brain regions allows to obtain a robust and persistent (up to 6 months) neuron specific expression of transgenes inserted in the ICP4 locus, without evidence of toxicity or inflammatory cell infiltration (Verlengia et al., 2017). Further modification of the viral backbone allowed to improve transgene expression through the deletion of the virion host shutoff (vhs) gene (a new backbone called JΔNI8). Vhs acts by reducing the host immune response and the recognition of infected cells (Smiley, 2004; Rivas et al., 2016). Vhs-deleted vectors displayed a robust, long-lasting and neuron-specific expression of transgenes from the ICP4 locus, without any evidence of toxicity (Miyagawa et al., 2017). These results

suggest that the insertion site is critical to achieve a sustained and prolonged expression of the transgene (Verlengia et al., 2017). Recently, in order to overcome the rapid transcriptional repression of transgenes cloned outside the ICP4 locus, the backbone was further engineered with the insertion of cellular anti-silencing elements, to prevent the formation of heterochromatin at the transgene promoter level. Different types of anti-silencing elements were evaluated, but the most effective in increasing transgene expression was A2UCOE (Han et al., 2018a). In conclusion, the JΔNI backbone seems to hold the features and the flexibility of options needed for gene therapy applications to CNS diseases.

Amplicon vectors are another promising class of HSV-1 based vectors. Amplicons maintain all structural, immunological and host range properties of the wild-type virus, but only two elements, the viral origin of replication (ori) and the capsid packaging sequence (pac) are retained from its original genome, the rest consisting in a concatemer repetition of the foreign DNA (Epstein, 2009b). The major advantage of this gene transfer tool is that the total deletion of viral genes allows the insertion of up to 150 kb of exogenous DNA. The number of concatameric repeats depends on the size of the expression cassette, i.e. short sequences allow the insertion of more copies of the gene of interest. Furthermore, the complete absence of all viral genes strongly reduces the risk of reactivation, complementation or recombination with latent HSV-1 genomes (Epstein, 2009a). The downside is that amplicon propagation becomes overly difficult, because cell lines able to complement all viral proteins in trans are not available. Therefore, first generation of amplicon vectors were propagated by transfection of amplicon plasmid into cells which were then superinfected with an HSV-1 helper virus. This led to the production of largely impure stocks which induced strong cytotoxicity upon infection. A second generation of amplicon vectors was produced using HSV-1 helper viruses defective for one or more IE genes that were complemented in trans by appropriately engineered cell lines. Unfortunately, this approach still leads to a significant (about 1%) contamination with helper virus (Pechan et al., 1996). A promising approach is the use of a helper virus (the LaL helper) in which the packaging sequence is deleted by Cre-lox specific-site recombination, preventing LaL helper encapsulation (Logvinoff and Epstein, 2000). Further deletions in the helper virus genome, e.g deletion of ICP4 gene and the virulence factor ICP34.5 (LaLΔJ helper virus) allow to produce viral stocks with contamination of 0.05 to 0.5% of helper particles that are defective and not capable of replication (Zaupa et al., 2003). Whereas amplicon vectors have been widely used for exploring the mechanisms of CNS function, only few studies have focused on their use for gene therapy (Cuchet et al., 2007). Recently, amplicons have been employed to silence BDNF expression in an animal model of epilepsy (Falcicchia et al., 2016). Unfortunately, the presence of bacterial sequences in the amplicon genome causes transgene silencing by forming inactive chromatin and, therefore, transgene expression is not long-lasting (Suzuki et al., 2006). Therefore, one main focus of the current research in the amplicon field is the development of new production techniquesthat can allow to obtain a long-term expression of the transgene.

6. Conclusions

The rapid progress of viral and non-viral vector systems has increased the probability of success of CNS gene therapy as an alternative to existing pharmacological treatments. However, all the delivery systems developed thus far have advantages and disadvantages and, therefore, the search for an ideal delivery system continues. A lesson learned from the research performed to date is that delivery tools do not necessarily

adapt to all applications, but should be chosen according to the specific situation and need. Understanding the rules of transcriptional and post-transcriptional gene regulation will allow to improve our techniques. In addition, optogenetic and chemogenetic approaches can provide a precise temporal and spatial regulation of gene expression, and the recent advent of genome-editing technologies allows the direct manipulation of the genome. Therefore, even if more work will be needed to overcome the last hurdles, gene therapy now holds a strong promise to become a safe and effective option for CNS diseases in the not too distant future.

References

Agha-Mohammadi, S., O'Malley, M., Etemad, A., Wang, Z., Xiao, X., and Lotze, M.T. (2004). Second-generation tetracycline-regulatable promoter: repositioned tet operator elements optimize transactivator synergy while shorter minimal promoter offers tight basal leakiness. *J Gene Med* 6(7)**,** 817-828. doi: 10.1002/jgm.566.

Alba, R., Bosch, A., and Chillon, M. (2005). Gutless adenovirus: last-generation adenovirus for gene therapy. *Gene Ther* 12 Suppl 1**,** S18-27. doi: 10.1038/sj.gt.3302612.

Alexander, G.M., Rogan, S.C., Abbas, A.I., Armbruster, B.N., Pei, Y., Allen, J.A., et al. (2009). Remote Control of Neuronal Activity in Transgenic Mice Expressing Evolved G Protein-Coupled Receptors. *Neuron* 63(1)**,** 27-39. doi: 10.1016/j.neuron.2009.06.014.

Armbruster, B.N., Li, X., Pausch, M.H., Herlitze, S., and Roth, B.L. (2007). Evolving the lock to fit the key to create a family of G protein-coupled receptors potently activated by an inert ligand. *Proceedings of the National Academy of Sciences of the United States of America* 104(12)**,** 5163-5168. doi: 10.1073/pnas.0700293104.

Artusi, S., Miyagawa, Y., Goins, W.F., Cohen, J.B., and Glorioso, J.C. (2018). Herpes Simplex Virus Vectors for Gene Transfer to the Central Nervous System. *Diseases* 6(3). doi: 10.3390/diseases6030074.

Aschauer, D.F., Kreuz, S., and Rumpel, S. (2013). Analysis of transduction efficiency, tropism and axonal transport of AAV serotypes 1, 2, 5, 6, 8 and 9 in the mouse brain. *PLoS One* 8(9)**,** e76310. doi: 10.1371/journal.pone.0076310.

Azzouz, M., Martin-Rendon, E., Barber, R.D., Mitrophanous, K.A., Carter, E.E., Rohll, J.B., et al. (2002). Multicistronic lentiviral vector-mediated striatal gene transfer of aromatic L-amino acid decarboxylase, tyrosine hydroxylase, and GTP cyclohydrolase I induces sustained transgene expression, dopamine production, and functional improvement in a rat model of Parkinson's disease. *J Neurosci* 22(23)**,** 10302-10312.

Badawy, R.A.B., Harvey, A.S., and MacDonell, R.A.L. (2009). Cortical hyperexcitability and epileptogenesis: Understanding the mechanisms of epilepsy - Part 2. *Journal of Clinical Neuroscience* 16(4)**,** 485-500. doi: 10.1016/j.jocn.2008.10.001.

Bartus, R.T., Baumann, T.L., Siffert, J., Herzog, C.D., Alterman, R., Boulis, N., et al. (2013). Safety/feasibility of targeting the substantia nigra with AAV2-neurturin in Parkinson patients. *Neurology* 80(18)**,** 1698-1701. doi: 10.1212/WNL.0b013e3182904faa.

Bayle, J.H., Grimley, J.S., Stankunas, K., Gestwicki, J.E., Wandless, T.J., and Crabtree, G.R. (2006). Rapamycin analogs with differential binding specificity permit orthogonal control of protein activity. *Chem Biol* 13(1)**,** 99-107. doi: 10.1016/j.chembiol.2005.10.017.

Bell, A.C., West, A.G., and Felsenfeld, G. (1999). The protein CTCF is required for the enhancer blocking activity of vertebrate insulators. *Cell* 98(3)**,** 387-396.

Bell, C.L., Vandenberghe, L.H., Bell, P., Limberis, M.P., Gao, G.P., Van Vliet, K., et al. (2011). The AAV9 receptor and its modification to improve in vivo lung gene transfer in mice. *J Clin Invest* 121(6)**,** 2427-2435. doi: 10.1172/JCI57367.

Bemelmans, A.P., Horellou, P., Pradier, L., Brunet, I., Colin, P., and Mallet, J. (1999). Brain-derived neurotrophic factor-mediated protection of striatal neurons in an excitotoxic rat model of Huntington's disease, as demonstrated by adenoviral gene transfer. *Hum Gene Ther* 10(18)**,** 2987-2997. doi: 10.1089/10430349950016393.

Berges, B.K., Wolfe, J.H., and Fraser, N.W. (2007). Transduction of brain by herpes simplex virus vectors. *Mol Ther* 15(1)**,** 20-29. doi: 10.1038/sj.mt.6300018.

Berns, K.I., and Giraud, C. (1996). Biology of adeno-associated virus. *Curr Top Microbiol Immunol* 218**,** 1-23.

Bertram, L., and Tanzi, R.E. (2005). The genetic epidemiology of neurodegenerative disease. *J Clin Invest* 115(6)**,** 1449-1457. doi: 10.1172/JCI24761.

Bishop, A.C., Shah, K., Liu, Y., Witucki, L., Kung, C.Y., and Shokat, K.M. (1998). Design of allele-specific inhibitors to probe protein kinase signaling. *Current Biology* 8(5)**,** 257-266. doi: Doi 10.1016/S0960-9822(98)70198-8.

Bloom, D.C., Giordani, N.V., and Kwiatkowski, D.L. (2010). Epigenetic regulation of latent HSV-1 gene expression. *Biochim Biophys Acta* 1799(3-4)**,** 246-256. doi: 10.1016/j.bbagrm.2009.12.001.

Boch, J., and Bonas, U. (2010). Xanthomonas AvrBs3 family-type III effectors: discovery and function. *Annu Rev Phytopathol* 48**,** 419-436. doi: 10.1146/annurev-phyto-080508-081936.

Bonas, U., Stall, R.E., and Staskawicz, B. (1989). Genetic and structural characterization of the avirulence gene avrBs3 from Xanthomonas campestris pv. vesicatoria. *Mol Gen Genet* 218(1)**,** 127-136.

Bouard, D., Alazard-Dany, D., and Cosset, F.L. (2009). Viral vectors: from virology to transgene expression. *Br J Pharmacol* 157(2)**,** 153-165. doi: 10.1038/bjp.2008.349.

Boudreau, R.L., McBride, J.L., Martins, I., Shen, S., Xing, Y., Carter, B.J., et al. (2009). Nonallele-specific silencing of mutant and wild-type huntingtin demonstrates therapeutic efficacy in Huntington's disease mice. *Mol Ther* 17(6)**,** 1053-1063. doi: 10.1038/mt.2009.17.

Bourdenx, M., Dutheil, N., Bezard, E., and Dehay, B. (2014). Systemic gene delivery to the central nervous system using Adeno-associated virus. *Front Mol Neurosci* 7**,** 50. doi: 10.3389/fnmol.2014.00050.

Brown, R.C., Lockwood, A.H., and Sonawane, B.R. (2005). Neurodegenerative diseases: an overview of environmental risk factors. *Environ Health Perspect* 113(9)**,** 1250-1256. doi: 10.1289/ehp.7567.

Budd Haeberlein, S.L., and Harris, T.J. (2015). Promising Targets for the Treatment of Neurodegenerative Diseases. *Clin Pharmacol Ther* 98(5)**,** 492-501. doi: 10.1002/cpt.195.

Burger, C., Gorbatyuk, O.S., Velardo, M.J., Peden, C.S., Williams, P., Zolotukhin, S., et al. (2004). Recombinant AAV viral vectors pseudotyped with viral capsids from serotypes 1, 2, and 5 display differential efficiency and cell tropism after delivery to different regions of the central nervous system. *Mol Ther* 10(2)**,** 302-317. doi: 10.1016/j.ymthe.2004.05.024.

Campos, S.K., and Barry, M.A. (2007). Current advances and future challenges in Adenoviral vector biology and targeting. *Curr Gene Ther* 7(3)**,** 189-204.

Carter, M., and Shieh, J. (2015). Guide to Research Techniques in Neuroscience. *Elsevier* 2nd.

Case, S.S., Price, M.A., Jordan, C.T., Yu, X.J., Wang, L., Bauer, G., et al. (1999). Stable transduction of quiescent CD34(+)CD38(-) human hematopoietic cells by HIV-1-based lentiviral vectors. *Proc Natl Acad Sci U S A* 96(6)**,** 2988-2993.

Chang, S.Y., Lee, C.N., Lin, P.H., Huang, H.H., Chang, L.Y., Ko, W., et al. (2008). A community-derived outbreak of adenovirus type 3 in children in Taiwan between 2004 and 2005. *J Med Virol* 80(1)**,** 102-112. doi: 10.1002/jmv.21045.

Chen, S.S., Yang, C., Hao, F., Li, C., Lu, T., Zhao, L.R., et al. (2014). Intrastriatal GDNF gene transfer by inducible lentivirus vectors protects dopaminergic neurons in a rat model of parkinsonism. *Exp Neurol* 261**,** 87-96. doi: 10.1016/j.expneurol.2014.06.022.

Chira, S., Jackson, C.S., Oprea, I., Ozturk, F., Pepper, M.S., Diaconu, I., et al. (2015). Progresses towards safe and efficient gene therapy vectors. *Oncotarget* 6(31)**,** 30675-30703. doi: 10.18632/oncotarget.5169.

Choi-Lundberg, D.L., Lin, Q., Schallert, T., Crippens, D., Davidson, B.L., Chang, Y.N., et al. (1998). Behavioral and cellular protection of rat dopaminergic neurons by an adenoviral vector encoding glial cell line-derived neurotrophic factor. *Exp Neurol* 154(2)**,** 261-275. doi: 10.1006/exnr.1998.6887.

Chow, B.Y., Han, X., Dobry, A.S., Qian, X., Chuong, A.S., Li, M., et al. (2010). High-performance genetically targetable optical neural silencing by light-driven proton pumps. *Nature* 463(7277)**,** 98-102. doi: 10.1038/nature08652.

Christine, C.W., Starr, P.A., Larson, P.S., Eberling, J.L., Jagust, W.J., Hawkins, R.A., et al. (2009). Safety and tolerability of putaminal AADC gene therapy for Parkinson disease. *Neurology* 73(20)**,** 1662-1669. doi: 10.1212/WNL.0b013e3181c29356.

Chung, J.H., Whiteley, M., and Felsenfeld, G. (1993). A 5' element of the chicken beta-globin domain serves as an insulator in human erythroid cells and protects against position effect in Drosophila. *Cell* 74(3)**,** 505-514.

Cohen, M.S., Zhang, C., Shokat, K.M., and Taunton, J. (2005). Structural bioinformatics-based design of selective, irreversible kinase inhibitors. *Science* 308(5726)**,** 1318-1321. doi: 10.1126/science1108367.

Cong, L., Ran, F.A., Cox, D., Lin, S., Barretto, R., Habib, N., et al. (2013). Multiplex genome engineering using CRISPR/Cas systems. *Science* 339(6121)**,** 819-823. doi: 10.1126/science.1231143.

Cooray, S., Howe, S.J., and Thrasher, A.J. (2012). Retrovirus and lentivirus vector design and methods of cell conditioning. *Methods Enzymol* 507**,** 29-57. doi: 10.1016/B978-0-12-386509-0.00003-X.

Coward, P., Wada, H.G., Falk, M.S., Chan, S.D.H., Meng, F., Akil, H., et al. (1998). Controlling signaling with a specifically designed G(i)-coupled receptor. *Proceedings of the National Academy of Sciences of the United States of America* 95(1)**,** 352-357. doi: DOI 10.1073/pnas.95.1.352.

Crick, F.H. (1979). Thinking about the brain. *Sci Am* 241(3)**,** 219-232.

Cuchet, D., Potel, C., Thomas, J., and Epstein, A.L. (2007). HSV-1 amplicon vectors: a promising and versatile tool for gene delivery. *Expert Opin Biol Ther* 7(7)**,** 975-995. doi: 10.1517/14712598.7.7.975.

Cummings, J., Lee, G., Mortsdorf, T., Ritter, A., and Zhong, K. (2017). Alzheimer's disease drug development pipeline: 2017. *Alzheimers Dement (N Y)* 3(3)**,** 367-384. doi: 10.1016/j.trci.2017.05.002.

Dar, A.C., Das, T.K., Shokat, K.M., and Cagan, R.L. (2012). Chemical genetic discovery of targets and anti-targets for cancer polypharmacology. *Nature* 486(7401)**,** 80-U101. doi: 10.1038/nature11127.

Das, A.T., Zhou, X., Vink, M., Klaver, B., Verhoef, K., Marzio, G., et al. (2004). Viral evolution as a tool to improve the tetracycline-regulated gene expression system. *J Biol Chem* 279(18)**,** 18776-18782. doi: 10.1074/jbc.M313895200.

Davidson, B.L., Stein, C.S., Heth, J.A., Martins, I., Kotin, R.M., Derksen, T.A., et al. (2000). Recombinant adeno-associated virus type 2, 4, and 5 vectors: transduction of variant cell types and regions in the mammalian central nervous system. *Proc Natl Acad Sci U S A* 97(7)**,** 3428-3432. doi: 10.1073/pnas.050581197.

de Haan, W., van Straaten, E.C.W., Gouw, A.A., and Stam, C.J. (2017). Altering neuronal excitability to preserve network connectivity in a computational model of Alzheimer's disease. *Plos Computational Biology* 13(9). doi: ARTN e100570710.1371/journal.pcbi.1005707.

Deisseroth, K. (2011). Optogenetics. *Nat Methods* 8(1)**,** 26-29. doi: 10.1038/nmeth.f.324.

Deisseroth, K. (2015). Optogenetics: 10 years of microbial opsins in neuroscience. *Nat Neurosci* 18(9)**,** 1213-1225. doi: 10.1038/nn.4091.

DeVos, S.L., Miller, R.L., Schoch, K.M., Holmes, B.B., Kebodeaux, C.S., Wegener, A.J., et al. (2017). Tau reduction prevents neuronal loss and reverses pathological tau deposition and seeding in mice with tauopathy. *Sci Transl Med* 9(374). doi: 10.1126/scitranslmed.aag0481.

Dobbelstein, M. (2004). Replicating adenoviruses in cancer therapy. *Curr Top Microbiol Immunol* 273**,** 291-334.

Doudna, J.A., and Charpentier, E. (2014). Genome editing. The new frontier of genome engineering with CRISPR-Cas9. *Science* 346(6213)**,** 1258096. doi: 10.1126/science.1258096.

Drouet, V., Perrin, V., Hassig, R., Dufour, N., Auregan, G., Alves, S., et al. (2009). Sustained effects of nonallele-specific Huntingtin silencing. *Ann Neurol* 65(3)**,** 276-285. doi: 10.1002/ana.21569.

Duan, D. (2016). Systemic delivery of adeno-associated viral vectors. *Curr Opin Virol* 21**,** 16-25. doi: 10.1016/j.coviro.2016.07.006.

Duan, D., Sharma, P., Yang, J., Yue, Y., Dudus, L., Zhang, Y., et al. (1998). Circular intermediates of recombinant adeno-associated virus have defined structural characteristics responsible for long-term episomal persistence in muscle tissue. *J Virol* 72(11)**,** 8568-8577.

Duan, D., Yue, Y., and Engelhardt, J.F. (2001). Expanding AAV packaging capacity with trans-splicing or overlapping vectors: a quantitative comparison. *Mol Ther* 4(4)**,** 383-391. doi: 10.1006/mthe.2001.0456.

Dufes, C., Uchegbu, I.F., and Schatzlein, A.G. (2005). Dendrimers in gene delivery. *Adv Drug Deliv Rev* 57(15)**,** 2177-2202. doi: 10.1016/j.addr.2005.09.017.

Duque, S., Joussemet, B., Riviere, C., Marais, T., Dubreil, L., Douar, A.M., et al. (2009). Intravenous administration of self-complementary AAV9 enables transgene delivery to adult motor neurons. *Mol Ther* 17(7)**,** 1187-1196. doi: 10.1038/mt.2009.71.

Dutta, S., Basak, B., Bhunia, B., Chakraborty, S., and Dey, A. (2014). Kinetics of rapamycin production by Streptomyces hygroscopicus MTCC 4003. *3 Biotech* 4(5)**,** 523-531. doi: 10.1007/s13205-013-0189-2.

Eberling, J.L., Jagust, W.J., Christine, C.W., Starr, P., Larson, P., Bankiewicz, K.S., et al. (2008). Results from a phase I safety trial of hAADC gene therapy for Parkinson disease. *Neurology* 70(21)**,** 1980-1983. doi: 10.1212/01.wnl.0000312381.29287.ff.

Ebert, A.D., Chen, F., He, X., Cryns, V.L., and Bohn, M.C. (2005). A tetracycline-regulated adenovirus encoding dominant-negative caspase-9 is regulated in rat brain and protects against neurotoxin-induced cell death in vitro, but not in vivo. *Exp Neurol* 191 Suppl 1**,** S80-94. doi: 10.1016/j.expneurol.2004.08.024.

Elliott, G., and O'Hare, P. (1997). Intercellular trafficking and protein delivery by a herpesvirus structural protein. *Cell* 88(2)**,** 223-233.

Emery, D.W. (2011). The use of chromatin insulators to improve the expression and safety of integrating gene transfer vectors. *Hum Gene Ther* 22(6)**,** 761-774. doi: 10.1089/hum.2010.233.

Epstein, A.L. (2009a). HSV-1-derived amplicon vectors: recent technological improvements and remaining difficulties - A Review. *Memorias Do Instituto Oswaldo Cruz* 104(3)**,** 399-410. doi: Doi 10.1590/S0074-02762009000300002.

Epstein, A.L. (2009b). Progress and prospects: biological properties and technological advances of herpes simplex virus type 1-based amplicon vectors. *Gene Ther* 16(6)**,** 709-715. doi: 10.1038/gt.2009.42.

Escors, D., and Breckpot, K. (2010). Lentiviral vectors in gene therapy: their current status and future potential. *Arch Immunol Ther Exp (Warsz)* 58(2)**,** 107-119. doi: 10.1007/s00005-010-0063-4.

Eslamboli, A., Georgievska, B., Ridley, R.M., Baker, H.F., Muzyczka, N., Burger, C., et al. (2005). Continuous low-level glial cell line-derived neurotrophic factor delivery using recombinant adeno-associated viral vectors provides neuroprotection and induces behavioral recovery in a primate model of Parkinson's disease. *J Neurosci* 25(4)**,** 769-777. doi: 10.1523/JNEUROSCI.4421-04.2005.

Falcicchia, C., Trempat, P., Binaschi, A., Perrier-Biollay, C., Roncon, P., Soukupova, M., et al. (2016). Silencing Status Epilepticus-Induced BDNF Expression with Herpes Simplex Virus Type-1 Based Amplicon Vectors. *PLoS One* 11(3)**,** e0150995. doi: 10.1371/journal.pone.0150995.

Fink, D.J., and Mata, M. (2008). HSV gene transfer in the treatment of chronic pain. *Sheng Li Xue Bao* 60(5)**,** 610-616.

Fink, K.D., Deng, P., Gutierrez, J., Anderson, J.S., Torrest, A., Komarla, A., et al. (2016). Allele-Specific Reduction of the Mutant Huntingtin Allele Using Transcription Activator-Like Effectors in Human Huntington's Disease Fibroblasts. *Cell Transplant* 25(4)**,** 677-686. doi: 10.3727/096368916X690863.

Foust, K.D., Nurre, E., Montgomery, C.L., Hernandez, A., Chan, C.M., and Kaspar, B.K. (2009). Intravascular AAV9 preferentially targets neonatal neurons and adult astrocytes. *Nat Biotechnol* 27(1)**,** 59-65. doi: 10.1038/nbt.1515.

Frankel, A.D., and Pabo, C.O. (1988). Cellular uptake of the tat protein from human immunodeficiency virus. *Cell* 55(6)**,** 1189-1193.

Fukuchi, K., Tahara, K., Kim, H.D., Maxwell, J.A., Lewis, T.L., Accavitti-Loper, M.A., et al. (2006). Anti-Abeta single-chain antibody delivery via adeno-associated virus for treatment of Alzheimer's disease. *Neurobiol Dis* 23(3)**,** 502-511. doi: 10.1016/j.nbd.2006.04.012.

Gaj, T., Sirk, S.J., Shui, S.L., and Liu, J. (2016). Genome-Editing Technologies: Principles and Applications. *Cold Spring Harb Perspect Biol* 8(12). doi: 10.1101/cshperspect.a023754.

Garriga-Canut, M., Agustin-Pavon, C., Herrmann, F., Sanchez, A., Dierssen, M., Fillat, C., et al. (2012). Synthetic zinc finger repressors reduce mutant huntingtin expression in the brain of R6/2 mice. *Proc Natl Acad Sci U S A* 109(45)**,** E3136-3145. doi: 10.1073/pnas.1206506109.

Gasmi, M., Brandon, E.P., Herzog, C.D., Wilson, A., Bishop, K.M., Hofer, E.K., et al. (2007). AAV2-mediated delivery of human neurturin to the rat nigrostriatal system: long-term efficacy and tolerability of CERE-120 for Parkinson's disease. *Neurobiol Dis* 27(1)**,** 67-76. doi: 10.1016/j.nbd.2007.04.003.

Gaszner, M., and Felsenfeld, G. (2006). Insulators: exploiting transcriptional and epigenetic mechanisms. *Nat Rev Genet* 7(9), 703-713. doi: 10.1038/nrg1925.

Georgievska, B., Jakobsson, J., Persson, E., Ericson, C., Kirik, D., and Lundberg, C. (2004). Regulated delivery of glial cell line-derived neurotrophic factor into rat striatum, using a tetracycline-dependent lentiviral vector. *Hum Gene Ther* 15(10), 934-944. doi: 10.1089/hum.2004.15.934.

Ghosh, A., Yue, Y., Lai, Y., and Duan, D. (2008). A hybrid vector system expands adeno-associated viral vector packaging capacity in a transgene-independent manner. *Mol Ther* 16(1), 124-130. doi: 10.1038/sj.mt.6300322.

Ginn, S.L., Amaya, A.K., Alexander, I.E., Edelstein, M., and Abedi, M.R. (2018). Gene therapy clinical trials worldwide to 2017: An update. *Journal of Gene Medicine* 20(5). doi: ARTN e3015

10.1002/jgm.3015.

Glorioso, J.C. (2014). Herpes simplex viral vectors: late bloomers with big potential. *Hum Gene Ther* 25(2), 83-91. doi: 10.1089/hum.2014.2501.

Glorioso, J.C., and Fink, D.J. (2004). Herpes vector-mediated gene transfer in treatment of diseases of the nervous system. *Annu Rev Microbiol* 58, 253-271. doi: 10.1146/annurev.micro.58.030603.123709.

Gossen, M., Freundlieb, S., Bender, G., Muller, G., Hillen, W., and Bujard, H. (1995). Transcriptional activation by tetracyclines in mammalian cells. *Science* 268(5218), 1766-1769.

Goverdhana, S., Puntel, M., Xiong, W., Zirger, J.M., Barcia, C., Curtin, J.F., et al. (2005). Regulatable gene expression systems for gene therapy applications: progress and future challenges. *Mol Ther* 12(2), 189-211. doi: 10.1016/j.ymthe.2005.03.022.

Gregorevic, P., Blankinship, M.J., Allen, J.M., Crawford, R.W., Meuse, L., Miller, D.G., et al. (2004). Systemic delivery of genes to striated muscles using adeno-associated viral vectors. *Nat Med* 10(8), 828-834. doi: 10.1038/nm1085.

Grimm, D., Streetz, K.L., Jopling, C.L., Storm, T.A., Pandey, K., Davis, C.R., et al. (2006). Fatality in mice due to oversaturation of cellular microRNA/short hairpin RNA pathways. *Nature* 441(7092), 537-541. doi: 10.1038/nature04791.

Gruh, I., Wunderlich, S., Winkler, M., Schwanke, K., Heinke, J., Blomer, U., et al. (2008). Human CMV immediate-early enhancer: a useful tool to enhance cell-type-specific expression from lentiviral vectors. *J Gene Med* 10(1), 21-32. doi: 10.1002/jgm.1122.

Gunaydin, L.A., Yizhar, O., Berndt, A., Sohal, V.S., Deisseroth, K., and Hegemann, P. (2010). Ultrafast optogenetic control. *Nat Neurosci* 13(3), 387-392. doi: 10.1038/nn.2495.

Hadaczek, P., Beyer, J., Kells, A., Narrow, W., Bowers, W., Federoff, H.J., et al. (2011). Evaluation of an AAV2-based rapamycin-regulated glial cell line-derived neurotrophic factor (GDNF) expression vector system. *PLoS One* 6(11), e27728. doi: 10.1371/journal.pone.0027728.

Hager, S., Frame, F.M., Collins, A.T., Burns, J.E., and Maitland, N.J. (2008). An internal polyadenylation signal substantially increases expression levels of lentivirus-delivered transgenes but has the potential to reduce viral titer in a promoter-dependent manner. *Hum Gene Ther* 19(8), 840-850. doi: 10.1089/hum.2007.165.

Hall, T.M. (2002). Poly(A) tail synthesis and regulation: recent structural insights. *Curr Opin Struct Biol* 12(1), 82-88.

Han, F., Miyagawa, Y., Verlengia, G., Ingusci, S., Soukupova, M., Simonato, M., et al. (2018a). Cellular Antisilencing Elements Support Transgene Expression from Herpes Simplex Virus Vectors in the Absence of Immediate Early Gene Expression. *Journal of Virology* 92(17). doi: ARTN e00536-1810.1128/JVI.00536-18.

Han, F., Miyagawa, Y., Verlengia, G., Ingusci, S., Soukupova, M., Simonato, M., et al. (2018b). Cellular Antisilencing Elements Support Transgene Expression from Herpes Simplex Virus Vectors in the Absence of Immediate Early Gene Expression. *J Virol* 92(17). doi: 10.1128/JVI.00536-18.

Harper, S.Q., Hauser, M.A., DelloRusso, C., Duan, D., Crawford, R.W., Phelps, S.F., et al. (2002). Modular flexibility of dystrophin: implications for gene therapy of Duchenne muscular dystrophy. *Nat Med* 8(3), 253-261. doi: 10.1038/nm0302-253.

Harper, S.Q., Staber, P.D., He, X., Eliason, S.L., Martins, I.H., Mao, Q., et al. (2005). RNA interference improves motor and neuropathological abnormalities in a Huntington's disease mouse model. *Proc Natl Acad Sci U S A* 102(16)**,** 5820-5825. doi: 10.1073/pnas.0501507102.

Hartikka, J., Sawdey, M., Cornefert-Jensen, F., Margalith, M., Barnhart, K., Nolasco, M., et al. (1996). An improved plasmid DNA expression vector for direct injection into skeletal muscle. *Hum Gene Ther* 7(10)**,** 1205-1217. doi: 10.1089/hum.1996.7.10-1205.

Hebert, L.E., Weuve, J., Scherr, P.A., and Evans, D.A. (2013). Alzheimer disease in the United States (2010-2050) estimated using the 2010 census. *Neurology* 80(19)**,** 1778-1783. doi: 10.1212/WNL.0b013e31828726f5.

Howell, D.P., Krieser, R.J., Eastman, A., and Barry, M.A. (2003). Deoxyribonuclease II is a lysosomal barrier to transfection. *Mol Ther* 8(6)**,** 957-963.

Huang, R.Q., Qu, Y.H., Ke, W.L., Zhu, J.H., Pei, Y.Y., and Jiang, C. (2007). Efficient gene delivery targeted to the brain using a transferrin-conjugated polyethyleneglycol-modified polyamidoamine dendrimer. *FASEB J* 21(4)**,** 1117-1125. doi: 10.1096/fj.06-7380com.

Ikeda, K., Wakimoto, H., Ichikawa, T., Jhung, S., Hochberg, F.H., Louis, D.N., et al. (2000). Complement depletion facilitates the infection of multiple brain tumors by an intravascular, replication-conditional herpes simplex virus mutant. *J Virol* 74(10)**,** 4765-4775.

Inagaki, K., Fuess, S., Storm, T.A., Gibson, G.A., McTiernan, C.F., Kay, M.A., et al. (2006). Robust systemic transduction with AAV9 vectors in mice: efficient global cardiac gene transfer superior to that of AAV8. *Mol Ther* 14(1)**,** 45-53. doi: 10.1016/j.ymthe.2006.03.014.

Jackson, A.L., Bartz, S.R., Schelter, J., Kobayashi, S.V., Burchard, J., Mao, M., et al. (2003). Expression profiling reveals off-target gene regulation by RNAi. *Nat Biotechnol* 21(6)**,** 635-637. doi: 10.1038/nbt831.

Jacobs, A., Breakefield, X.O., and Fraefel, C. (1999). HSV-1-based vectors for gene therapy of neurological diseases and brain tumors: part II. Vector systems and applications. *Neoplasia* 1(5)**,**402-416.

Jacobson, A., and Peltz, S.W. (1996). Interrelationships of the pathways of mRNA decay and translation in eukaryotic cells. *Annu Rev Biochem* 65**,** 693-739. doi: 10.1146/annurev.bi.65.070196.003401.

Jankele, R., and Svoboda, P. (2014). TAL effectors: tools for DNA targeting. *Brief Funct Genomics* 13(5)**,** 409-419. doi: 10.1093/bfgp/elu013.

Jarraya, B., Boulet, S., Ralph, G.S., Jan, C., Bonvento, G., Azzouz, M., et al. (2009). Dopamine gene therapy for Parkinson's disease in a nonhuman primate without associated dyskinesia. *Sci Transl Med* 1(2)**,** 2ra4. doi: 10.1126/scitranslmed.3000130.

Jayant, R.D., Sosa, D., Kaushik, A., Atluri, V., Vashist, A., Tomitaka, A., et al. (2016). Current status of non-viral gene therapy for CNS disorders. *Expert Opin Drug Deliv* 13(10)**,** 1433-1445. doi: 10.1080/17425247.2016.1188802.

Kaludov, N., Brown, K.E., Walters, R.W., Zabner, J., and Chiorini, J.A. (2001). Adeno-associated virus serotype 4 (AAV4) and AAV5 both require sialic acid binding for hemagglutination and efficient transduction but differ in sialic acid linkage specificity. *J Virol* 75(15)**,** 6884-6893. doi: 10.1128/JVI.75.15.6884-6893.2001.

Kang, C.B., Hong, Y., Dhe-Paganon, S., and Yoon, H.S. (2008). FKBP family proteins: immunophilins with versatile biological functions. *Neurosignals* 16(4)**,** 318-325. doi: 10.1159/000123041.

Kaplitt, M.G., Feigin, A., Tang, C., Fitzsimons, H.L., Mattis, P., Lawlor, P.A., et al. (2007). Safety and tolerability of gene therapy with an adeno-associated virus (AAV) borne GAD gene for Parkinson's disease: an open label, phase I trial. *Lancet* 369(9579)**,** 2097-2105. doi: 10.1016/S0140-6736(07)60982-9.

Karvelis, T., Gasiunas, G., Young, J., Bigelyte, G., Silanskas, A., Cigan, M., et al. (2015). Rapid characterization of CRISPR-Cas9 protospacer adjacent motif sequence elements. *Genome Biol* 16**,** 253. doi: 10.1186/s13059-015-0818-7.

Katsouri, L., Lim, Y.M., Blondrath, K., Eleftheriadou, I., Lombardero, L., Birch, A.M., et al. (2016). PPARgamma-coactivator-1alpha gene transfer reduces neuronal loss and amyloid-beta generation by reducing beta-secretase in an Alzheimer's disease model. *Proc Natl Acad Sci U S A* 113(43)**,** 12292-12297. doi: 10.1073/pnas.1606171113.

Katzel, D., Nicholson, E., Schorge, S., Walker, M.C., and Kullmann, D.M. (2014). Chemical-genetic attenuation of focal neocortical seizures. *Nature Communications* 5. doi: ARTN 384710.1038/ncomms4847.

Kettenmann, H., Hanisch, U.K., Noda, M., and Verkhratsky, A. (2011). Physiology of microglia. *Physiol Rev* 91(2)**,** 461-553. doi: 10.1152/physrev.00011.2010.

Khare, R., Chen, C.Y., Weaver, E.A., and Barry, M.A. (2011). Advances and future challenges in adenoviral vector pharmacology and targeting. *Curr Gene Ther* 11(4)**,** 241-258.

Kim, V.N., Mitrophanous, K., Kingsman, S.M., and Kingsman, A.J. (1998). Minimal requirement for a lentivirus vector based on human immunodeficiency virus type 1. *J Virol* 72(1)**,** 811-816.

Knorr, V., Allmendinger, L., Walker, G.F., Paintner, F.F., and Wagner, E. (2007). An acetal-based PEGylation reagent for pH-Sensitive shielding of DNA polyplexes. *Bioconjugate Chemistry* 18(4)**,** 1218-1225. doi: 10.1021/bc060327a.

Kodippili, K., Hakim, C.H., Pan, X., Yang, H.T., Yue, Y., Zhang, Y., et al. (2018). Dual AAV Gene Therapy for Duchenne Muscular Dystrophy with a 7-kb Mini-Dystrophin Gene in the Canine Model. *Hum Gene Ther* 29(3)**,** 299-311. doi: 10.1089/hum.2017.095.

Kordower, J.H., Herzog, C.D., Dass, B., Bakay, R.A., Stansell, J., 3rd, Gasmi, M., et al. (2006). Delivery of neurturin by AAV2 (CERE-120)-mediated gene transfer provides structural and functional neuroprotection and neurorestoration in MPTP-treated monkeys. *Ann Neurol* 60(6)**,** 706-715. doi: 10.1002/ana.21032.

Krashes, M.J., Shah, B.P., Madara, J.C., Olson, D.P., Strochlic, D.E., Garfield, A.S., et al. (2014). An excitatory paraventricular nucleus to AgRP neuron circuit that drives hunger. *Nature* 507(7491)**,** 238-+. doi: 10.1038/nature12956.

Kravitz, A.V., Freeze, B.S., Parker, P.R.L., Kay, K., Thwin, M.T., Deisseroth, K., et al. (2010). Regulation of parkinsonian motor behaviours by optogenetic control of basal ganglia circuitry. *Nature* 466(7306)**,** 622-U627. doi: 10.1038/nature09159.

Krook-Magnuson, E., Armstrong, C., Oijala, M., and Soltesz, I. (2013). On-demand optogenetic control of spontaneous seizures in temporal lobe epilepsy. *Nature Communications* 4. doi: ARTN 137610.1038/ncomms2376.

Kugler, S., Kilic, E., and Bahr, M. (2003). Human synapsin 1 gene promoter confers highly neuron-specific long-term transgene expression from an adenoviral vector in the adult rat brain depending on the transduced area. *Gene Ther* 10(4)**,** 337-347. doi: 10.1038/sj.gt.3301905.

Kugler, S., Meyn, L., Holzmuller, H., Gerhardt, E., Isenmann, S., Schulz, J.B., et al. (2001). Neuron-specific expression of therapeutic proteins: evaluation of different cellular promoters in recombinant adenoviral vectors. *Mol Cell Neurosci* 17(1)**,** 78-96. doi: 10.1006/mcne.2000.0929.

Laganiere, J., Kells, A.P., Lai, J.T., Guschin, D., Paschon, D.E., Meng, X., et al. (2010). An engineered zinc finger protein activator of the endogenous glial cell line-derived neurotrophic factor gene provides functional neuroprotection in a rat model of Parkinson's disease. *J Neurosci* 30(49)**,** 16469-16474. doi: 10.1523/JNEUROSCI.2440-10.2010.

Lang, A.E., Gill, S., Patel, N.K., Lozano, A., Nutt, J.G., Penn, R., et al. (2006). Randomized controlled trial of intraputamenal glial cell line-derived neurotrophic factor infusion in Parkinson disease. *Ann Neurol* 59(3)**,** 459-466. doi: 10.1002/ana.20737.

Le Guiner, C., Stieger, K., Toromanoff, A., Guilbaud, M., Mendes-Madeira, A., Devaux, M., et al. (2014). Transgene regulation using the tetracycline-inducible TetR-KRAB system after AAV-mediated gene transfer in rodents and nonhuman primates. *PLoS One* 9(9)**,** e102538. doi: 10.1371/journal.pone.0102538.

Lee, Y., Messing, A., Su, M., and Brenner, M. (2008). GFAP promoter elements required for region-specific and astrocyte-specific expression. *Glia* 56(5)**,** 481-493. doi: 10.1002/glia.20622.

Lee, Y.B., Cosgrave, A.S., Glover, C.P., Bienemann, A., Heywood, D., Hobson, R.J., et al. (2005). Increased utility in the CNS of a powerful neuron-specific tetracycline-regulatable adenoviral system developed using a post-transcriptional enhancer. *J Gene Med* 7(5)**,** 576-583. doi: 10.1002/jgm.694.

Lee, C.S., Bishop, R. Zhang, X. Yu, E.M. Farina, S. Yan, et al. (2017). Adenovirus-Mediated Gene Delivery: Potential Applications for Gene and Cell-Based Therapies in the New Era of Personalized Medicine. *Genes Dis* (4), 43-63. doi: 10.1016/j.gendis.2017.04.001.

Lenman, A., Liaci, A.M., Liu, Y., Frangsmyr, L., Frank, M., Blaum, B.S., et al. (2018). Polysialic acid is a cellular receptor for human adenovirus 52. *Proc Natl Acad Sci U S A* 115(18)**,** E4264-E4273. doi: 10.1073/pnas.1716900115.

Li, S.D., and Huang, L. (2006). Gene therapy progress and prospects: non-viral gene therapy by systemic delivery. *Gene Ther* 13(18)**,** 1313-1319. doi: 10.1038/sj.gt.3302838.

Liu, Y., Jacques, S.L., Azimipour, M., Rogers, J.D., Pashaie, R., and Eliceiri, K.W. (2015). OptogenSIM: a 3D Monte Carlo simulation platform for light delivery design in optogenetics. *Biomed Opt Express* 6(12)**,** 4859-4870. doi: 10.1364/BOE.6.004859.

Loane, D.J., and Kumar, A. (2016). Microglia in the TBI brain: The good, the bad, and the dysregulated. *Exp Neurol* 275 Pt 3**,** 316-327. doi: 10.1016/j.expneurol.2015.08.018.

Logvinoff, C., and Epstein, A.L. (2000). Genetic engineering of herpes simplex virus and vector genomes carrying loxP sites in cells expressing Cre recombinase. *Virology* 267(1)**,** 102-110. doi: 10.1006/viro.1999.0108.

Lombardo, A., Genovese, P., Beausejour, C.M., Colleoni, S., Lee, Y.L., Kim, K.A., et al. (2007). Gene editing in human stem cells using zinc finger nucleases and integrase-defective lentiviral vector delivery. *Nat Biotechnol* 25(11)**,** 1298-1306. doi: 10.1038/nbt1353.

Lowenstein, P.R., and Castro, M.G. (2002). Progress and challenges in viral vector-mediated gene transfer to the brain. *Curr Opin Mol Ther* 4(4)**,** 359-371.

Lowenstein, P.R., and Castro, M.G. (2003). Inflammation and adaptive immune responses to adenoviral vectors injected into the brain: peculiarities, mechanisms, and consequences. *Gene Ther* 10(11)**,** 946-954. doi: 10.1038/sj.gt.3302048.

Lowenstein, P.R., and Castro, M.G. (2004). Recent advances in the pharmacology of neurological gene therapy. *Curr Opin Pharmacol* 4(1)**,** 91-97. doi: 10.1016/j.coph.2003.10.005.

Luo, L.Q., Callaway, E.M., and Svoboda, K. (2018). Genetic Dissection of Neural Circuits: A Decade of Progress (vol 98, pg 256, 2018). *Neuron* 98(4)**,** 865-865. doi: 10.1016/j.neuron.2018.05.004.

Maddalena, A., Tornabene, P., Tiberi, P., Minopoli, R., Manfredi, A., Mutarelli, M., et al. (2018). Triple Vectors Expand AAV Transfer Capacity in the Retina. *Mol Ther* 26(2)**,** 524-541. doi: 10.1016/j.ymthe.2017.11.019.

Maeder, M.L., and Gersbach, C.A. (2016). Genome-editing Technologies for Gene and Cell Therapy. *Mol Ther* 24(3)**,** 430-446. doi: 10.1038/mt.2016.10.

Maetzig, T., Galla, M., Baum, C., and Schambach, A. (2011). Gammaretroviral vectors: biology, technology and application. *Viruses* 3(6)**,** 677-713. doi: 10.3390/v3060677.

Magnus, C.J., Lee, P.H., Atasoy, D., Su, H.H., Looger, L.L., and Sternson, S.M. (2011). Chemical and Genetic Engineering of Selective Ion Channel-Ligand Interactions. *Science* 333(6047)**,** 1292-1296. doi: 10.1126/science.1206606.

Malik, N., Wiwattanapatapee, R., Klopsch, R., Lorenz, K., Frey, H., Weener, J.W., et al. (2000). Dendrimers: relationship between structure and biocompatibility in vitro, and preliminary studies on the biodistribution of 125I-labelled polyamidoamine dendrimers in vivo. *J Control Release* 65(1-2)**,** 133-148.

Mandel, R.J. (2010). CERE-110, an adeno-associated virus-based gene delivery vector expressing human nerve growth factor for the treatment of Alzheimer's disease. *Curr Opin Mol Ther* 12(2)**,** 240-247.

Mandel, R.J., Manfredsson, F.P., Foust, K.D., Rising, A., Reimsnider, S., Nash, K., et al. (2006). Recombinant adeno-associated viral vectors as therapeutic agents to treat neurological disorders. *Mol Ther* 13(3)**,** 463-483. doi: 10.1016/j.ymthe.2005.11.009.

Manthorpe, M., Cornefert-Jensen, F., Hartikka, J., Felgner, J., Rundell, A., Margalith, M., et al. (1993). Gene therapy by intramuscular injection of plasmid DNA: studies on firefly luciferase gene expression in mice. *Hum Gene Ther* 4(4)**,** 419-431. doi: 10.1089/hum.1993.4.4-419.

Marks, W.J., Jr., Bartus, R.T., Siffert, J., Davis, C.S., Lozano, A., Boulis, N., et al. (2010). Gene delivery of AAV2-neurturin for Parkinson's disease: a double-blind, randomised, controlled trial. *Lancet Neurol* 9(12)**,** 1164-1172. doi: 10.1016/S1474-4422(10)70254-4.

Marks, W.J., Jr., Baumann, T.L., and Bartus, R.T. (2016). Long-Term Safety of Patients with Parkinson's Disease Receiving rAAV2-Neurturin (CERE-120) Gene Transfer. *Hum Gene Ther* 27(7)**,** 522-527. doi: 10.1089/hum.2015.134.

Marks, W.J., Jr., Ostrem, J.L., Verhagen, L., Starr, P.A., Larson, P.S., Bakay, R.A., et al. (2008). Safety and tolerability of intraputaminal delivery of CERE-120 (adeno-associated virus serotype 2-neurturin) to patients with idiopathic Parkinson's disease: an open-label, phase I trial. *Lancet Neurol* 7(5)**,** 400-408. doi: 10.1016/S1474-4422(08)70065-6.

Martin-Gallardo, A., Montoya-Zavala, M., Kelder, B., Taylor, J., Chen, H., Leung, F.C., et al. (1988). A comparison of bovine growth-hormone gene expression in mouse L cells directed by the Moloney murine-leukemia virus long terminal repeat, simian virus-40 early promoter or cytomegalovirus immediate-early promoter. *Gene* 70(1)**,** 51-56.

Matsumoto, Y., Itaka, K., Yamasoba, T., and Kataoka, K. (2009). Intranuclear fluorescence resonance energy transfer analysis of plasmid DNA decondensation from nonviral gene carriers. *J Gene Med* 11(7)**,** 615-623. doi: 10.1002/jgm.1338.

Maurice, M., Verhoeyen, E., Salmon, P., Trono, D., Russell, S.J., and Cosset, F.L. (2002). Efficient gene transfer into human primary blood lymphocytes by surface-engineered lentiviral vectors that display a T cell-activating polypeptide. *Blood* 99(7)**,** 2342-2350.

McCarty, D.M., Young, S.M., Jr., and Samulski, R.J. (2004). Integration of adeno-associated virus (AAV) and recombinant AAV vectors. *Annu Rev Genet* 38**,** 819-845. doi: 10.1146/annurev.genet.37.110801.143717.

McLean, J.R., Smith, G.A., Rocha, E.M., Hayes, M.A., Beagan, J.A., Hallett, P.J., et al. (2014). Widespread neuron-specific transgene expression in brain and spinal cord following synapsin promoter-driven AAV9 neonatal intracerebroventricular injection. *Neurosci Lett* 576**,** 73-78. doi: 10.1016/j.neulet.2014.05.044.

Mendell, J.R., Al-Zaidy, S., Shell, R., Arnold, W.D., Rodino-Klapac, L.R., Prior, T.W., et al. (2017). Single-Dose Gene-Replacement Therapy for Spinal Muscular Atrophy. *N Engl J Med* 377(18)**,** 1713-1722. doi: 10.1056/NEJMoa1706198.

Mingozzi, F., and High, K.A. (2011). Therapeutic in vivo gene transfer for genetic disease using AAV: progress and challenges. *Nat Rev Genet* 12(5)**,** 341-355. doi: 10.1038/nrg2988.

Mittermeyer, G., Christine, C.W., Rosenbluth, K.H., Baker, S.L., Starr, P., Larson, P., et al. (2012). Long-term evaluation of a phase 1 study of AADC gene therapy for Parkinson's disease. *Hum Gene Ther* 23(4)**,** 377-381. doi: 10.1089/hum.2011.220.

Miyagawa, Y., Marino, P., Verlengia, G., Uchida, H., Goins, W.F., Yokota, S., et al. (2015). Herpes simplex viral-vector design for efficient transduction of nonneuronal cells without cytotoxicity. *Proc Natl Acad Sci U S A* 112(13)**,** E1632-1641. doi: 10.1073/pnas.1423556112.

Miyagawa, Y., Verlengia, G., Reinhart, B., Han, F., Uchida, H., Zucchini, S., et al. (2017). Deletion of the Virion Host Shut-off Gene Enhances Neuronal-Selective Transgene Expression from an HSV Vector Lacking Functional IE Genes. *Mol Ther Methods Clin Dev* 6**,** 79-90. doi: 10.1016/j.omtm.2017.06.001.

Modin, C., Pedersen, F.S., and Duch, M. (2000). Lack of shielding of primer binding site silencer-mediated repression of an internal promoter in a retrovirus vector by the putative insulators scs, BEAD-1, and HS4. *J Virol* 74(24)**,** 11697-11707.

Moreau, C., Devos, D., Baille, G., Delval, A., Tard, C., Perez, T., et al. (2016). Are Upper-Body Axial Symptoms a Feature of Early Parkinson's Disease? *Plos One* 11(9). doi: ARTN e0162904

10.1371/journal.pone.0162904.

Moscou, M.J., and Bogdanove, A.J. (2009). A simple cipher governs DNA recognition by TAL effectors. *Science* 326(5959)**,** 1501. doi: 10.1126/science.1178817.

Mounkes, L.C., Zhong, W., Cipres-Palacin, G., Heath, T.D., and Debs, R.J. (1998). Proteoglycans mediate cationic liposome-DNA complex-based gene delivery in vitro and in vivo. *J Biol Chem* 273(40)**,** 26164-26170.

Mueller, S.G., Schuff, N., and Weiner, M.W. (2006). Evaluation of treatment effects in Alzheimer's and other neurodegenerative diseases by MRI and MRS. *NMR Biomed* 19(6), 655-668. doi: 10.1002/nbm.1062.

Musatov, S., Roberts, J., Pfaff, D., and Kaplitt, M. (2002). A cis-acting element that directs circular adeno-associated virus replication and packaging. *J Virol* 76(24), 12792-12802.

Mussolino, C., and Cathomen, T. (2012). TALE nucleases: tailored genome engineering made easy. *Curr Opin Biotechnol* 23(5), 644-650. doi: 10.1016/j.copbio.2012.01.013.

Nagel, G., Szellas, T., Huhn, W., Kateriya, S., Adeishvili, N., Berthold, P., et al. (2003). Channelrhodopsin-2, a directly light-gated cation-selective membrane channel. *Proc Natl Acad Sci U S A* 100(24), 13940-13945. doi: 10.1073/pnas.1936192100.

Naidoo, J., and Young, D. (2012). Gene regulation systems for gene therapy applications in the central nervous system. *Neurol Res Int* 2012, 595410. doi: 10.1155/2012/595410.

Nakai, H., Fuess, S., Storm, T.A., Muramatsu, S., Nara, Y., and Kay, M.A. (2005). Unrestricted hepatocyte transduction with adeno-associated virus serotype 8 vectors in mice. *J Virol* 79(1), 214-224. doi: 10.1128/JVI.79.1.214-224.2005.

Nakai, H., Iwaki, Y., Kay, M.A., and Couto, L.B. (1999). Isolation of recombinant adeno-associated virus vector-cellular DNA junctions from mouse liver. *J Virol* 73(7), 5438-5447.

Nalls, M.A., Pankratz, N., Lill, C.M., Do, C.B., Hernandez, D.G., Saad, M., et al. (2014). Large-scale meta-analysis of genome-wide association data identifies six new risk loci for Parkinson's disease. *Nat Genet* 46(9), 989-993. doi: 10.1038/ng.3043.

Naso, M.F., Tomkowicz, B., Perry, W.L., 3rd, and Strohl, W.R. (2017). Adeno-Associated Virus (AAV) as a Vector for Gene Therapy. *BioDrugs* 31(4), 317-334. doi: 10.1007/s40259-017-0234-5.

Nau, R., Sorgel, F., and Eiffert, H. (2010). Penetration of drugs through the blood-cerebrospinal fluid/blood-brain barrier for treatment of central nervous system infections. *Clin Microbiol Rev* 23(4), 858-883. doi: 10.1128/CMR.00007-10.

Niidome, T., and Huang, L. (2002). Gene therapy progress and prospects: Nonviral vectors. *Gene Therapy* 9(24), 1647-1652. doi: DOI 10.1038/sj.gt.3301923.

Oellig, C., and Seliger, B. (1990). Gene transfer into brain tumor cell lines: reporter gene expression using various cellular and viral promoters. *J Neurosci Res* 26(3), 390-396. doi: 10.1002/jnr.490260317.

Oesterhelt, D., and Stoeckenius, W. (1971). Rhodopsin-like protein from the purple membrane of Halobacterium halobium. *Nat New Biol* 233(39), 149-152.

Ogris, M., Brunner, S., Schuller, S., Kircheis, R., and Wagner, E. (1999). PEGylated DNA/transferrin-PEI complexes: reduced interaction with blood components, extended circulation in blood and potential for systemic gene delivery. *Gene Ther* 6(4), 595-605. doi: 10.1038/sj.gt.3300900.

Page, K.A., Landau, N.R., and Littman, D.R. (1990). Construction and use of a human immunodeficiency virus vector for analysis of virus infectivity. *J Virol* 64(11), 5270-5276.

Palfi, S., Gurruchaga, J.M., Lepetit, H., Howard, K., Ralph, G.S., Mason, S., et al. (2018). Long-Term Follow-Up of a Phase I/II Study of ProSavin, a Lentiviral Vector Gene Therapy for Parkinson's Disease. *Hum Gene Ther Clin Dev* 29(3), 148-155. doi: 10.1089/humc.2018.081.

Palfi, S., Gurruchaga, J.M., Ralph, G.S., Lepetit, H., Lavisse, S., Buttery, P.C., et al. (2014). Long-term safety and tolerability of ProSavin, a lentiviral vector-based gene therapy for Parkinson's disease: a dose escalation, open-label, phase 1/2 trial. *Lancet* 383(9923), 1138-1146. doi: 10.1016/S0140-6736(13)61939-X.

Pascual-Lucas, M., Viana da Silva, S., Di Scala, M., Garcia-Barroso, C., Gonzalez-Aseguinolaza, G., Mulle, C., et al. (2014). Insulin-like growth factor 2 reverses memory and synaptic deficits in APP transgenic mice. *EMBO Mol Med* 6(10), 1246-1262. doi: 10.15252/emmm.201404228.

Pasleau, F., Tocci, M.J., Leung, F., and Kopchick, J.J. (1985). Growth hormone gene expression in eukaryotic cells directed by the Rous sarcoma virus long terminal repeat or cytomegalovirus immediate-early promoter. *Gene* 38(1-3), 227-232.

Pasquale, T.R., and Tan, J.S. (2005). Nonantimicrobial effects of antibacterial agents. *Clin Infect Dis* 40(1)**,** 127-135. doi: 10.1086/426545.

Pechan, P.A., Fotaki, M., Thompson, R.L., Dunn, R., Chase, M., Chiocca, E.A., et al. (1996). A novel 'piggyback' packaging system for herpes simplex virus amplicon vectors. *Hum Gene Ther* 7(16)**,** 2003-2013. doi: 10.1089/hum.1996.7.16-2003.

Peel, A.L., Zolotukhin, S., Schrimsher, G.W., Muzyczka, N., and Reier, P.J. (1997). Efficient transduction of green fluorescent protein in spinal cord neurons using adeno-associated virus vectors containing cell type-specific promoters. *Gene Ther* 4(1)**,** 16-24. doi: 10.1038/sj.gt.3300358.

Penaud-Budloo, M., Francois, A., Clement, N., and Ayuso, E. (2018). Pharmacology of Recombinant Adeno-associated Virus Production. *Mol Ther Methods Clin Dev* 8**,** 166-180. doi: 10.1016/j.omtm.2018.01.002.

Perez-Martinez, F.C., Guerra, J., Posadas, I., and Cena, V. (2011). Barriers to non-viral vector-mediated gene delivery in the nervous system. *Pharm Res* 28(8)**,** 1843-1858. doi: 10.1007/s11095-010-0364-7.

Persengiev, S.P., Zhu, X., and Green, M.R. (2004). Nonspecific, concentration-dependent stimulation and repression of mammalian gene expression by small interfering RNAs (siRNAs). *RNA* 10(1)**,** 12-18.

Phillips, J.E., and Corces, V.G. (2009). CTCF: master weaver of the genome. *Cell* 137(7)**,** 1194-1211. doi: 10.1016/j.cell.2009.06.001.

Pienaar, I.S., Gartside, S.E., Sharma, P., De Paola, V., Gretenkord, S., Withers, D., et al. (2015). Pharmacogenetic stimulation of cholinergic pedunculopontine neurons reverses motor deficits in a rat model of Parkinson's disease. *Molecular Neurodegeneration* 10. doi: ARTN 47

10.1186/s13024-015-0044-5.

Piest, M., Lin, C., Mateos-Timoneda, M.A., Lok, M.C., Hennink, W.E., Feijen, J., et al. (2008). Novel poly(amido amine)s with bioreducible disulfide linkages in their diamino-units: Structure effects and in vitro gene transfer properties. *Journal of Controlled Release* 132(3)**,** E12-E13. doi: 10.1016/j.jconrel.2008.09.047.

Pluta, K., Luce, M.J., Bao, L., Agha-Mohammadi, S., and Reiser, J. (2005). Tight control of transgene expression by lentivirus vectors containing second-generation tetracycline-responsive promoters. *J Gene Med* 7(6)**,** 803-817. doi: 10.1002/jgm.712.

Prince, M., Bryce, R., Albanese, E., Wimo, A., Ribeiro, W., and Ferri, C.P. (2013). The global prevalence of dementia: a systematic review and metaanalysis. *Alzheimers Dement* 9(1)**,** 63-75 e62. doi: 10.1016/j.jalz.2012.11.007.

Pulicherla, N., Shen, S., Yadav, S., Debbink, K., Govindasamy, L., Agbandje-McKenna, M., et al. (2011). Engineering liver-detargeted AAV9 vectors for cardiac and musculoskeletal gene transfer. *Mol Ther* 19(6)**,** 1070-1078. doi: 10.1038/mt.2011.22.

Qin, J.Y., Zhang, L., Clift, K.L., Hulur, I., Xiang, A.P., Ren, B.Z., et al. (2010). Systematic comparison of constitutive promoters and the doxycycline-inducible promoter. *PLoS One* 5(5)**,** e10611. doi: 10.1371/journal.pone.0010611.

Raab, J.R., and Kamakaka, R.T. (2010). Insulators and promoters: closer than we think. *Nat Rev Genet* 11(6)**,** 439-446. doi: 10.1038/nrg2765.

Rafii, M.S., Baumann, T.L., Bakay, R.A., Ostrove, J.M., Siffert, J., Fleisher, A.S., et al. (2014). A phase1 study of stereotactic gene delivery of AAV2-NGF for Alzheimer's disease. *Alzheimers Dement* 10(5)**,** 571-581. doi: 10.1016/j.jalz.2013.09.004.

Ramamoorth, M., and Narvekar, A. (2015). Non viral vectors in gene therapy- an overview. *J Clin Diagn Res* 9(1)**,** GE01-06. doi: 10.7860/JCDR/2015/10443.5394.

Ran, F.A., Hsu, P.D., Lin, C.Y., Gootenberg, J.S., Konermann, S., Trevino, A.E., et al. (2013). Double nicking by RNA-guided CRISPR Cas9 for enhanced genome editing specificity. *Cell* 154(6)**,** 1380-1389. doi: 10.1016/j.cell.2013.08.021.

Rasmussen, M., Kong, L., Zhang, G.R., Liu, M., Wang, X., Szabo, G., et al. (2007). Glutamatergic or GABAergic neuron-specific, long-term expression in neocortical neurons from helper virus-free HSV-1 vectors containing the phosphate-activated glutaminase, vesicular glutamate transporter-1, or glutamic acid decarboxylase promoter. *Brain Res* 1144**,** 19-32. doi: 10.1016/j.brainres.2007.01.125.

Rein, D.T., Breidenbach, M., and Curiel, D.T. (2006). Current developments in adenovirus-based cancer gene therapy. *Future Oncol* 2(1)**,** 137-143. doi: 10.2217/14796694.2.1.137.

Reiner, A., Dragatsis, I., Zeitlin, S., and Goldowitz, D. (2003). Wild-type huntingtin plays a role in brain development and neuronal survival. *Mol Neurobiol* 28(3)**,** 259-276. doi: 10.1385/MN:28:3:259.

Reynolds, A., Leake, D., Boese, Q., Scaringe, S., Marshall, W.S., and Khvorova, A. (2004). Rational siRNA design for RNA interference. *Nat Biotechnol* 22(3)**,** 326-330. doi: 10.1038/nbt936.

Rivas, H.G., Schmaling, S.K., and Gaglia, M.M. (2016). Shutoff of Host Gene Expression in Influenza A Virus and Herpesviruses: Similar Mechanisms and Common Themes. *Viruses* 8(4)**,** 102. doi: 10.3390/v8040102.

Rivella, S., Callegari, J.A., May, C., Tan, C.W., and Sadelain, M. (2000). The cHS4 insulator increases the probability of retroviral expression at random chromosomal integration sites. *J Virol* 74(10)**,** 4679-4687.

Rivera, V.M., Clackson, T., Natesan, S., Pollock, R., Amara, J.F., Keenan, T., et al. (1996). A humanized system for pharmacologic control of gene expression. *Nat Med* 2(9)**,** 1028-1032.

Rodriguez-Lebron, E., Denovan-Wright, E.M., Nash, K., Lewin, A.S., and Mandel, R.J. (2005). Intrastriatal rAAV-mediated delivery of anti-huntingtin shRNAs induces partial reversal of disease progression in R6/1 Huntington's disease transgenic mice. *Mol Ther* 12(4)**,** 618-633. doi: 10.1016/j.ymthe.2005.05.006.

Rosario, A.M., Cruz, P.E., Ceballos-Diaz, C., Strickland, M.R., Siemienski, Z., Pardo, M., et al. (2016). Microglia-specific targeting by novel capsid-modified AAV6 vectors. *Mol Ther Methods Clin Dev* 3**,** 16026. doi: 10.1038/mtm.2016.26.

Ryan, D.A., Mastrangelo, M.A., Narrow, W.C., Sullivan, M.A., Federoff, H.J., and Bowers, W.J. (2010). Abeta-directed single-chain antibody delivery via a serotype-1 AAV vector improves learning behavior and pathology in Alzheimer's disease mice. *Mol Ther* 18(8)**,** 1471-1481. doi: 10.1038/mt.2010.111.

Sakuma, T., Barry, M.A., and Ikeda, Y. (2012). Lentiviral vectors: basic to translational. *Biochem J* 443(3)**,** 603-618. doi: 10.1042/BJ20120146.

Samaniego, L.A., Wu, N., and DeLuca, N.A. (1997). The herpes simplex virus immediate-early protein ICP0 affects transcription from the viral genome and infected-cell survival in the absence of ICP4 and ICP27. *J Virol* 71(6)**,** 4614-4625.

Sanftner, L.M., Rivera, V.M., Suzuki, B.M., Feng, L., Berk, L., Zhou, S., et al. (2006). Dimerizer regulation of AADC expression and behavioral response in AAV-transduced 6-OHDA lesioned rats. *Mol Ther* 13(1)**,** 167-174. doi: 10.1016/j.ymthe.2005.06.480.

Scacheri, P.C., Rozenblatt-Rosen, O., Caplen, N.J., Wolfsberg, T.G., Umayam, L., Lee, J.C., et al. (2004). Short interfering RNAs can induce unexpected and divergent changes in the levels of untargeted proteins in mammalian cells. *Proc Natl Acad Sci U S A* 101(7)**,** 1892-1897. doi: 10.1073/pnas.0308698100.

Seeger-Armbruster, S., Bosch-Bouju, C., Little, S.T., Smither, R.A., Hughes, S.M., Hyland, B.I., et al. (2015). Patterned, but not tonic, optogenetic stimulation in motor thalamus improves reaching in acute drug-induced Parkinsonian rats. *J Neurosci* 35(3)**,** 1211-1216. doi: 10.1523/JNEUROSCI.3277-14.2015.

Sharma, A., Tandon, M., Bangari, D.S., and Mittal, S.K. (2009). Adenoviral vector-based strategies for cancer therapy. *Curr Drug ther* 4(2)**,** 117-138.

Shen, S., Bryant, K.D., Brown, S.M., Randell, S.H., and Asokan, A. (2011). Terminal N-linked galactose is the primary receptor for adeno-associated virus 9. *J Biol Chem* 286(15)**,** 13532-13540. doi: 10.1074/jbc.M110.210922.

Shimada, M., Abe, S., Takahashi, T., Shiozaki, K., Okuda, M., Mizukami, H., et al. (2013). Prophylaxis and treatment of Alzheimer's disease by delivery of an adeno-associated virus encoding a monoclonal antibody targeting the amyloid Beta protein. *PLoS One* 8(3)**,** e57606. doi: 10.1371/journal.pone.0057606.

Simonato, M., Bennett, J., Boulis, N.M., Castro, M.G., Fink, D.J., Goins, W.F., et al. (2013). Progress in gene therapy for neurological disorders. *Nat Rev Neurol* 9(5)**,** 277-291. doi: 10.1038/nrneurol.2013.56.

Simonato, M., Manservigi, R., Marconi, P., and Glorioso, J. (2000). Gene transfer into neurones for the molecular analysis of behaviour: focus on herpes simplex vectors. *Trends Neurosci* 23(5)**,** 183-190.

Sinclair, A.M., Agrawal, Y.P., Elbar, E., Agrawal, R., Ho, A.D., and Levine, F. (1997). Interaction of vesicular stomatitis virus-G pseudotyped retrovirus with CD34+ and CD34+ CD38- hematopoietic progenitor cells. *Gene Ther* 4(9)**,** 918-927. doi: 10.1038/sj.gt.3300479.

Sledz, C.A., Holko, M., de Veer, M.J., Silverman, R.H., and Williams, B.R. (2003). Activation of the interferon system by short-interfering RNAs. *Nat Cell Biol* 5(9)**,** 834-839. doi: 10.1038/ncb1038.

Smiley, J.R. (2004). Herpes simplex virus virion host shutoff protein: immune evasion mediated by a viral RNase? *J Virol* 78(3)**,** 1063-1068.

Smith-Arica, J.R., Morelli, A.E., Larregina, A.T., Smith, J., Lowenstein, P.R., and Castro, M.G. (2000). Cell-type-specific and regulatable transgenesis in the adult brain: adenovirus-encoded combined transcriptional targeting and inducible transgene expression. *Mol Ther* 2(6)**,** 579-587. doi: 10.1006/mthe.2000.0215.

Souweidane, M.M., Fraser, J.F., Arkin, L.M., Sondhi, D., Hackett, N.R., Kaminsky, S.M., et al. (2010). Gene therapy for late infantile neuronal ceroid lipofuscinosis: neurosurgical considerations. *J Neurosurg Pediatr* 6(2)**,** 115-122. doi: 10.3171/2010.4.PEDS09507.

Sternson, S.M., and Roth, B.L. (2014). Chemogenetic Tools to Interrogate Brain Functions. *Annual Review of Neuroscience, Vol 37* 37. doi: 10.1146/annurev-neuro-071013-014048.

Strader, C.D., Gaffney, T., Sugg, E.E., Candelore, M.R., Keys, R., Patchett, A.A., et al. (1991). Allele-Specific Activation of Genetically Engineered Receptors. *Journal of Biological Chemistry* 266(1)**,** 5-8.

Sutton, R.E., Reitsma, M.J., Uchida, N., and Brown, P.O. (1999). Transduction of human progenitor hematopoietic stem cells by human immunodeficiency virus type 1-based vectors is cell cycle dependent. *J Virol* 73(5)**,** 3649-3660.

Suzuki, M., Kasai, K., and Saeki, Y. (2006). Plasmid DNA sequences present in conventional herpes simplex virus amplicon vectors cause rapid transgene silencing by forming inactive chromatin. *J Virol* 80(7)**,** 3293-3300. doi: 10.1128/JVI.80.7.3293-3300.2006.

Tardieu, M., Zerah, M., Husson, B., de Bournonville, S., Deiva, K., Adamsbaum, C., et al. (2014). Intracerebral administration of adeno-associated viral vector serotype rh.10 carrying human SGSH and SUMF1 cDNAs in children with mucopolysaccharidosis type IIIA disease: results of a phase I/II trial. *Hum Gene Ther* 25(6)**,** 506-516. doi: 10.1089/hum.2013.238.

Teissier, A., Chemiakine, A., Inbar, B., Bagchi, S., Ray, R.S., Palmiter, R.D., et al. (2015). Activity of Raphe Serotonergic Neurons Controls Emotional Behaviors. *Cell Reports* 13(9)**,** 1965-1976. doi: 10.1016/j.celrep.2015.10.061.

Teschemacher, A.G., Wang, S., Lonergan, T., Duale, H., Waki, H., Paton, J.F., et al. (2005). Targeting specific neuronal populations using adeno- and lentiviral vectors: applications for imaging and studies of cell function. *Exp Physiol* 90(1)**,** 61-69. doi: 10.1113/expphysiol.2004.028191.

Thomas, C.E., Ehrhardt, A., and Kay, M.A. (2003). Progress and problems with the use of viral vectors for gene therapy. *Nat Rev Genet* 4(5)**,** 346-358. doi: 10.1038/nrg1066.

Tian, X., Wang, G., Xu, Y., Wang, P., Chen, S., Yang, H., et al. (2009). An improved tet-on system for gene expression in neurons delivered by a single lentiviral vector. *Hum Gene Ther* 20(2)**,** 113-123. doi: 10.1089/hum.2008.018.

Todo, T. (2008). "Armed" oncolytic herpes simplex viruses for brain tumor therapy. *Cell Adh Migr* 2(3)**,** 208-213.

Trapani, I., Colella, P., Sommella, A., Iodice, C., Cesi, G., de Simone, S., et al. (2014). Effective delivery of large genes to the retina by dual AAV vectors. *EMBO Mol Med* 6(2)**,** 194-211. doi: 10.1002/emmm.201302948.

Tuszynski, M.H., Thal, L., Pay, M., Salmon, D.P., Sang, U.H., Bakay, R., et al. (2005). A phase 1 clinical trial of nerve growth factor gene therapy for Alzheimer disease. *Nature Medicine* 11(5)**,** 551-555. doi: 10.1038/nm1239.

Tuszynski, M.H., Yang, J.H., Barba, D., Hoi-Sang, U., Bakay, R.A.E., Pay, M.M., et al. (2015). Nerve Growth Factor Gene Therapy Activation of Neuronal Responses in Alzheimer Disease. *Jama Neurology* 72(10)**,** 1139-1147. doi: 10.1001/jamaneurol.2015.1807.

Urban, D.J., Zhu, H., Marcinkiewcz, C.A., Michaelides, M., Oshibuchi, H., Rhea, D., et al. (2016). Elucidation of The Behavioral Program and Neuronal Network Encoded by Dorsal Raphe Serotonergic Neurons. *Neuropsychopharmacology* 41(5)**,** 1404-1415. doi: 10.1038/npp.2015.293.

Urnov, F.D., Rebar, E.J., Holmes, M.C., Zhang, H.S., and Gregory, P.D. (2010). Genome editing with engineered zinc finger nucleases. *Nat Rev Genet* 11(9)**,** 636-646. doi: 10.1038/nrg2842.

Van Deerlin, V.M. (2012). The genetics and neuropathology of neurodegenerative disorders: perspectives and implications for research and clinical practice. *Acta Neuropathol* 124(3)**,** 297-303. doi: 10.1007/s00401-012-1032-2.

Vardy, E., Robinson, J.E., Li, C., Olsen, R.H.J., DiBerto, J.F., Giguere, P.M., et al. (2015). A New DREADD Facilitates the Multiplexed Chemogenetic Interrogation of Behavior. *Neuron* 86(4)**,** 936-946. doi: 10.1016/j.neuron.2015.03.065.

Verhoeyen, E., Dardalhon, V., Ducrey-Rundquist, O., Trono, D., Taylor, N., and Cosset, F.L. (2003). IL-7 surface-engineered lentiviral vectors promote survival and efficient gene transfer in resting primary T lymphocytes. *Blood* 101(6)**,** 2167-2174. doi: 10.1182/blood-2002-07-2224.

Verlengia, G., Miyagawa, Y., Ingusci, S., Cohen, J.B., Simonato, M., and Glorioso, J.C. (2017). Engineered HSV vector achieves safe long-term transgene expression in the central nervous system. *Sci Rep* 7(1)**,** 1507. doi: 10.1038/s41598-017-01635-1.

Vogel, R., Mammeri, H., and Mallet, J. (2008). Lentiviral vectors mediate nonimmunosuppressive rapamycin analog-induced production of secreted therapeutic factors in the brain: regulation at the level of transcription and exocytosis. *Hum Gene Ther* 19(2)**,** 167-178. doi: 10.1089/hum.2007.125.

von Jonquieres, G., Frohlich, D., Klugmann, C.B., Wen, X., Harasta, A.E., Ramkumar, R., et al. (2016). Recombinant Human Myelin-Associated Glycoprotein Promoter Drives Selective AAV-Mediated Transgene Expression in Oligodendrocytes. *Front Mol Neurosci* 9**,** 13. doi: 10.3389/fnmol.2016.00013.

von Jonquieres, G., Mersmann, N., Klugmann, C.B., Harasta, A.E., Lutz, B., Teahan, O., et al. (2013). Glial promoter selectivity following AAV-delivery to the immature brain. *PLoS One* 8(6)**,** e65646. doi: 10.1371/journal.pone.0065646.

Wang, B., Li, J., and Xiao, X. (2000). Adeno-associated virus vector carrying human minidystrophin genes effectively ameliorates muscular dystrophy in mdx mouse model. *Proc Natl Acad Sci U S A* 97(25)**,** 13714-13719. doi: 10.1073/pnas.240335297.

Wang, C., Wang, C.M., Clark, K.R., and Sferra, T.J. (2003a). Recombinant AAV serotype 1 transduction efficiency and tropism in the murine brain. *Gene Ther* 10(17)**,** 1528-1534. doi: 10.1038/sj.gt.3302011.

Wang, D., Zhong, L., Nahid, M.A., and Gao, G. (2014). The potential of adeno-associated viral vectors for gene delivery to muscle tissue. *Expert Opin Drug Deliv* 11(3)**,** 345-364. doi: 10.1517/17425247.2014.871258.

Wang, L., Muramatsu, S., Lu, Y., Ikeguchi, K., Fujimoto, K., Okada, T., et al. (2002). Delayed delivery of AAV-GDNF prevents nigral neurodegeneration and promotes functional recovery in a rat model of Parkinson's disease. *Gene Ther* 9(6)**,** 381-389. doi: 10.1038/sj.gt.3301682.

Wang, S., Petravicz, J., and Breakefield, X.O. (2003b). Single HSV-amplicon vector mediates drug-induced gene expression via dimerizer system. *Mol Ther* 7(6)**,** 790-800.

West, A.G., Gaszner, M., and Felsenfeld, G. (2002). Insulators: many functions, many mechanisms. *Genes Dev* 16(3)**,** 271-288. doi: 10.1101/gad.954702.

Wolff, J.A., and Rozema, D.B. (2008). Breaking the bonds: Non-viral vectors become chemically dynamic. *Molecular Therapy* 16(1)**,** 8-15. doi: DOI 10.1038/sj.mt.6300326.

Worgall, S., Sondhi, D., Hackett, N.R., Kosofsky, B., Kekatpure, M.V., Neyzi, N., et al. (2008). Treatment of late infantile neuronal ceroid lipofuscinosis by CNS administration of a serotype 2 adeno-associated virus expressing CLN2 cDNA. *Hum Gene Ther* 19(5)**,** 463-474. doi: 10.1089/hum.2008.022.

Wu, Z., Miller, E., Agbandje-McKenna, M., and Samulski, R.J. (2006). Alpha2,3 and alpha2,6 N-linked sialic acids facilitate efficient binding and transduction by adeno-associated virus types 1 and 6. *J Virol* 80(18)**,** 9093-9103. doi: 10.1128/JVI.00895-06.

Xie, S., Shen, B., Zhang, C., Huang, X., and Zhang, Y. (2014). sgRNAcas9: a software package for designing CRISPR sgRNA and evaluating potential off-target cleavage sites. *PLoS One* 9(6), e100448. doi: 10.1371/journal.pone.0100448.

Xiong, W., Goverdhana, S., Sciascia, S.A., Candolfi, M., Zirger, J.M., Barcia, C., et al. (2006). Regulatable gutless adenovirus vectors sustain inducible transgene expression in the brain in the presence of an immune response against adenoviruses. *J Virol* 80(1), 27-37. doi: 10.1128/JVI.80.1.27-37.2006.

Yan, Z., Zak, R., Zhang, Y., and Engelhardt, J.F. (2005). Inverted terminal repeat sequences are important for intermolecular recombination and circularization of adeno-associated virus genomes. *J Virol* 79(1), 364-379. doi: 10.1128/JVI.79.1.364-379.2005.

Yan, Z., Zhang, Y., Duan, D., and Engelhardt, J.F. (2000). Trans-splicing vectors expand the utility of adeno-associated virus for gene therapy. *Proc Natl Acad Sci U S A* 97(12), 6716-6721.

Yang, B., Li, S., Wang, H., Guo, Y., Gessler, D.J., Cao, C., et al. (2014). Global CNS transduction of adult mice by intravenously delivered rAAVrh.8 and rAAVrh.10 and nonhuman primates by rAAVrh.10. *Mol Ther* 22(7), 1299-1309. doi: 10.1038/mt.2014.68.

Yang, S., Chang, R., Yang, H., Zhao, T., Hong, Y., Kong, H.E., et al. (2017). CRISPR/Cas9-mediated gene editing ameliorates neurotoxicity in mouse model of Huntington's disease. *J Clin Invest* 127(7), 2719-2724. doi: 10.1172/JCI92087.

Yao, F., and Schaffer, P.A. (1995). An activity specified by the osteosarcoma line U2OS can substitute functionally for ICP0, a major regulatory protein of herpes simplex virus type 1. *J Virol* 69(10), 6249-6258.

Yao, S., Osborne, C.S., Bharadwaj, R.R., Pasceri, P., Sukonnik, T., Pannell, D., et al. (2003). Retrovirus silencer blocking by the cHS4 insulator is CTCF independent. *Nucleic Acids Res* 31(18), 5317-5323.

Yee, J.K., Miyanohara, A., LaPorte, P., Bouic, K., Burns, J.C., and Friedmann, T. (1994). A general method for the generation of high-titer, pantropic retroviral vectors: highly efficient infection of primary hepatocytes. *Proc Natl Acad Sci U S A* 91(20), 9564-9568.

Yew, N.S., Wysokenski, D.M., Wang, K.X., Ziegler, R.J., Marshall, J., McNeilly, D., et al. (1997). Optimization of plasmid vectors for high-level expression in lung epithelial cells. *Hum Gene Ther* 8(5), 575-584. doi: 10.1089/hum.1997.8.5-575.

Yizhar, O., Fenno, L.E., Davidson, T.J., Mogri, M., and Deisseroth, K. (2011). Optogenetics in neural systems. *Neuron* 71(1), 9-34. doi: 10.1016/j.neuron.2011.06.004.

Yoon, H.H., Min, J., Hwang, E., Lee, C.J., Suh, J.K., Hwang, O., et al. (2016). Optogenetic Inhibition of the Subthalamic Nucleus Reduces Levodopa-Induced Dyskinesias in a Rat Model of Parkinson's Disease. *Stereotact Funct Neurosurg* 94(1), 41-53. doi: 10.1159/000442891.

Yoon, H.H., Park, J.H., Kim, Y.H., Min, J., Hwang, E., Lee, C.J., et al. (2014). Optogenetic inactivation of the subthalamic nucleus improves forelimb akinesia in a rat model of Parkinson disease. *Neurosurgery* 74(5), 533-540; discussion 540-531. doi: 10.1227/NEU.0000000000000297.

Zahedi, A., Defea, K., and Ethell, I. (2013). Optogenetics to Target Actin-Mediated Synaptic Loss in Alzheimer's. *Optogenetics: Optical Methods for Cellular Control* 8586. doi: Artn 85860s

10.1117/12.2000480.

Zaupa, C., Revol-Guyot, V., and Epstein, A.L. (2003). Improved packaging system for generation of high-level noncytotoxic HSV-1 amplicon vectors using Cre-loxP site-specific recombination to delete the packaging signals of defective helper genomes. *Hum Gene Ther* 14(11), 1049-1063. doi: 10.1089/104303403322124774.

Zemelman, B.V., Nesnas, N., Lee, G.A., and Miesenbock, G. (2003). Photochemical gating of heterologous ion channels: Remote control over genetically designated populations of neurons. *Proceedings of the National Academy of Sciences of the United States of America* 100(3), 1352-1357. doi: 10.1073/pnas.242738899.

Zhang, F., Frost, A.R., Blundell, M.P., Bales, O., Antoniou, M.N., and Thrasher, A.J. (2010). A ubiquitous chromatin opening element (UCOE) confers resistance to DNA methylation-mediated silencing of lentiviral vectors. *Mol Ther* 18(9), 1640-1649. doi: 10.1038/mt.2010.132.

Zhang, H., Yang, B., Mu, X., Ahmed, S.S., Su, Q., He, R., et al. (2011). Several rAAV vectors efficiently cross the blood-brain barrier and transduce neurons and astrocytes in the neonatal mouse central nervous system. *Mol Ther* 19(8)**,** 1440-1448. doi: 10.1038/mt.2011.98.

Zhang, S., Xu, Y., Wang, B., Qiao, W., Liu, D., and Li, Z. (2004). Cationic compounds used in lipoplexes and polyplexes for gene delivery. *J Control Release* 100(2)**,** 165-180. doi: 10.1016/j.jconrel.2004.08.019.

Zhang, W., Li, L., Su, Q., Gao, G., and Khanna, H. (2018). Gene Therapy Using a miniCEP290 Fragment Delays Photoreceptor Degeneration in a Mouse Model of Leber Congenital Amaurosis. *Hum Gene Ther* 29(1)**,** 42-50. doi: 10.1089/hum.2017.049.

Zhao, J., and Lever, A.M. (2007). Lentivirus-mediated gene expression. *Methods Mol Biol* 366**,** 343-355. doi: 10.1007/978-1-59745-030-0_20.

Zhou, X., Vink, M., Klaver, B., Berkhout, B., and Das, A.T. (2006). Optimization of the Tet-On system for regulated gene expression through viral evolution. *Gene Ther* 13(19)**,** 1382-1390. doi: 10.1038/sj.gt.3302780.

Zhu, H., Pleil, K.E., Urban, D.J., Moy, S.S., Kash, T.L., and Roth, B.L. (2014). Chemogenetic Inactivation of Ventral Hippocampal Glutamatergic Neurons Disrupts Consolidation of Contextual Fear Memory. *Neuropsychopharmacology* 39(8)**,** 1880-1892. doi: 10.1038/npp.2014.35.

Zhu, Y.J., Wienecke, C.F.R., Nachtrab, G., and Chen, X.K. (2016). A thalamic input to the nucleus accumbens mediates opiate dependence. *Nature* 530(7589)**,** 219-+. doi: 10.1038/nature16954.

Zincarelli, C., Soltys, S., Rengo, G., and Rabinowitz, J.E. (2008). Analysis of AAV serotypes 1-9 mediated gene expression and tropism in mice after systemic injection. *Mol Ther* 16(6)**,** 1073-1080. doi: 10.1038/mt.2008.76.

Figures

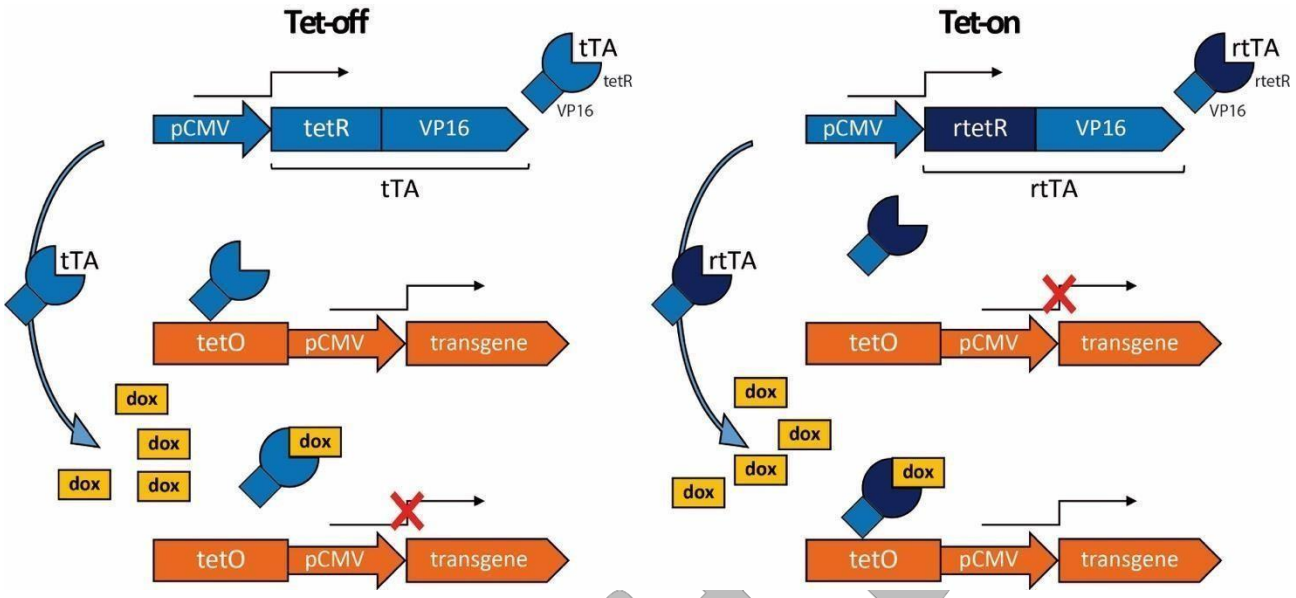

Figure 1. Tetracycline regulation system. In this example, the constitutively active human cytomegalovirus promoter (pCMV) drives the expression of the tetracycline transactivator (tTA) or of the tetracycline reverse transactivator (rtTA), consisting respectively of the tet-repressor (tetR) or reverse tet-repressor (rtetR) fused to the VP16 transactivation domain. **Tet-off**: tTA binds the tet operator (tetO) to drive transgene expression in the absence, but not in the presence of doxycycline (dox). **Tet-on**: rtTA binds to tetO and drivestransgene expression in the presence, but not in the absence ofdox.

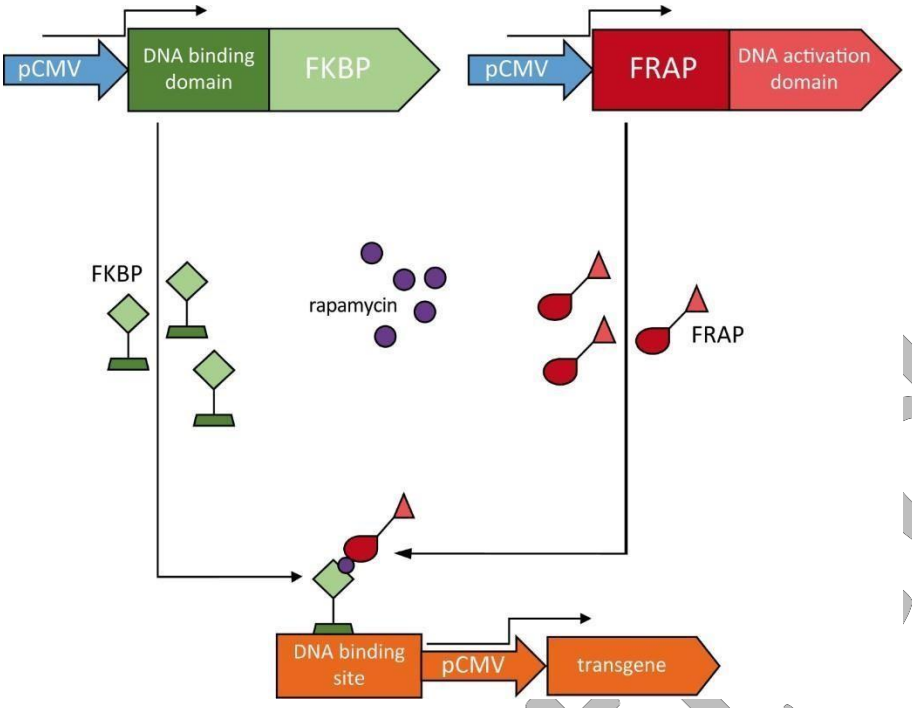

Figure 2. Rapamycin regulation system. In this example, the constitutively active human cytomegalovirus promoter (pCMV) drives the expression of two transcription factors, one consisting of the FK-binding protein (FKBP) fused to a DNA binding domain (in green), the other consisting of a FKBP12 rapamycin-associated protein (FRAP) fused to a DNA activation domain (in red). Rapamycin enables dimerization of the transcription factors and the resulting heterodimer is able to drive expression of the transgene ofinterest.

1.2 A matter of genes: the hurdles of gene therapy for epilepsy

A matter of genes:

the hurdles of gene therapy for epilepsy

Selene Ingusci[1], Stefano Cattaneo[2], Gianluca Verlengia[1,2], Silvia Zucchini[1,3], Michele Simonato[1,2]

[1] Department of Medical Sciences and National Institute of Neuroscience, University of Ferrara, Ferrara, Italy

[2] University Vita-Salute San Raffaele, Milan, Italy

[3] Technopole of Ferrara, LTTA Laboratory for Advanced Therapies, Ferrara, Italy

Short title:

Gene therapy for epilepsy

Corresponding author:

Michele Simonato, MD

Dept. Medical Sciences, University of Ferrara

44121 Ferrara, Italy

Email: michele.simonato@unife.it

School of Medicine, University Vita-Salute San Raffaele

20132 Milan, Italy

Email: simonato.michele@hsr.it

Summary

Gene therapy has recently advanced to the level of standard of care for several diseases. However, its application to neurological disorders is still in the experimental phase. In this review, we discuss recent advancements in the field that provide optimism on the possibility to have first-in-human studies for gene therapy of some forms of epilepsy in the not so distant future.

Introduction

As is well known, current therapies for epilepsy are largely unsatisfactory (1). In spite of the many available antiepileptic drugs and of other therapeutic approaches (surgery, brain stimulation, ketogenic diet, etc.), about a third of the patients do not get control of their seizures. We do not have any treatment able to prevent epilepsy development in at-risk individuals. We do not have adequate control of epilepsy co-morbidities that heavily affect the quality of life of patients. Many devastating forms of epilepsy are resistant to any treatment. And the list could continue.

Within this scenario, the search for new, alternative therapeutic approaches is always a priority, and gene therapy is often a consideration. In principle, the idea is simple: use some kind of vector to transfer the DNA encoding some "therapeutic" protein(s) into the diseased cells, in order to permanently heal them. There are different types of DNA that one could desire to transfer, reflecting different therapeutic strategies. The most obvious is the healthy variant of a defective gene, which could be an option in some genetic forms of epilepsy. But it would also be possible to attempt healing the defective gene using gene editing technologies, including clustered regularly interspaced short palindromic repeats (CRISPR)-Cas9-mediated genetic modification, and gene activation or inhibition (CRISPRa or CRISPRi). Another option could be to transfer genes that can modify cell (or circuit) function and control hyperexcitability, like channels, neurotransmitters, or receptors. Finally, one could transfer genes encoding proteins that render the cell sensitive to specific drugs (chemogenetics) or to light stimulation (optogenetics).

In sum, there are multiple, diverse options and strategies on stage. But are these doable? Can they be applied to all forms of epilepsy? Which forms of epilepsy may represent low hanging fruit for starting a program of clinical translation? Answering the first question means having at hand systems of gene transfer (vectors) that are safe, allow transfer of a sufficiently large DNA cargo, and ensure robust, lasting and regulated expression of the therapeutic gene(s) in a specific target cell. The other questions underlie other key problems, for example the fact that, for focal epilepsies, it may be sufficient to inject the vector and express the therapeutic gene(s) in a relatively restricted brain area, whereas in generalized epilepsies there could be a need to obtain widespread expression in the whole brain.

Below, we will briefly summarize the state of the art of vector development for gene therapy and the results of preclinical studies in epilepsy models. We will then describe some recent advances that may be implemented in epileptology, moving the field closer to a much awaited clinical application.

Viral vectors for the central nervous system (CNS)

There are two main classes of gene delivery-tools, non-viral and viral vectors, each endowed with specific advantages and disadvantages. Compared with viral vectors, non-viral vectors tend to have lower immunogenicity, due to the absence of pre-existing immunity, larger payload capacity and easier production techniques (2, 3). However, their major drawback is the low transduction efficiency.

In contrast, viral vectors exploit the viruses' highly evolved strategies for efficient transfer of foreign DNA into eukaryotic cells. Among different viruses engineered and tested for gene therapy, the most promising candidates for CNS applications seem to be adeno-associated, lenti- and herpes viruses (Table 1). Adeno-associated viruses (AAV) are small single-stranded DNA viruses (4, 5). In spite of their limited cargo capacity (4.5 kb), AAV vectors are the most commonly used in clinical trials for CNS gene therapy (6) because they exhibit low immunogenicity, no pathogenicity and long-lasting transgene expression in both dividing and non-dividing cells (7). Several AAV serotypes have been identified and developed, based on capsid variants that confer different tropisms, antigenic profiles (8) and transduction efficiency (9, 10). For example, the AAV1, AAV2, AAV5 and AAV8 serotypes display a marked neuronal tropism (11-13), whereas the AAV9 serotype can cross the blood-brain barrier (BBB) after peripheral administration (14). A tropism

shift from neurons to glia is observed in the mature brain (15), indicating that brain development should be considered for therapeutic applications. All these features can be modulated and improved by combining two or more different serotypes (8), by mutation of capsid tyrosine residues (16) or by fusing peptides to capsid proteins (6). One major problem with AAV vectors is the inactivation by neutralizing antibodies. However, chemical compounds (8) or association with exosomes (17) have been tested to shield the capsid from neutralizing antibodies.

Lentiviruses (LV) are integrating single stranded RNA viruses, capable of transducing non-dividing and dividing cells (18). Most LV vectors derive from human immunodeficiency virus (HIV) and have a transgene payload capacity of about 9 kb (19). Pseudotyping their envelope with glycoproteins derived from herpes simplex (HSV), rabies or vesicular stomatitis virus allows one to modify, improve and refine cellular tropism and transduction efficiency (20-24). Insertional mutagenesis is a potential risk. Non-integrating LV vectors have been developed by introducing mutations in the integrase gene, such that the viral genome persists in the host cell mostly (even if not exclusively) in an episomal form (25).

HSV vectors are double-stranded DNA viruses that can be divided in three main categories: replication-competent (employed in cancer), replication-defective, and amplicon vectors, carrying a DNA plasmid instead of the viral genome (26). Both replication-defective and amplicon vectors display natural neuronal tropism and high payload capacity, up to 50 and 150 kb (27), respectively, which allows the insertion of large transgenes and regulation systems. These features, together with a high transduction efficiency, the ability of both anterograde and retrograde transport and the episomal non-integrating genome, makes HSV vectors an attractive tool for CNS disorders (26-28). Their downsides are the residual toxicity and a relatively transient transgene expression (27). In addition, preparations of amplicon vectors remain contaminated by a small percentage of helper virus (28). However, new generation vectors seem to overcome these problems (Table 1 and see below).

Gene therapy approaches in animal models of epilepsy

All work on gene therapy for epilepsy thus far has been performed in animal models and by focal administration of vectors. In most cases, the focus has been on post-status epilepticus (SE) models. One study explored the antiepileptogenic effect of HSV vector-mediated delivery of the neurotrophic factors FGF-2 and BDNF in the pilocarpine model (29). Injection of this vector in the hippocampus during the latent period (3 days after SE) attenuated seizure-induced damage, favored a more physiological neurogenesis and highly reduced the occurrence of spontaneous recurrent seizures (SRSs).

All other studies focused on the chronic period, when animals were experiencing SRSs, and used seizure frequency as the primary outcome measure. This approach has greater translational potential, as it may be offered to individuals with drug-resistant focal seizures that cannot be treated surgically. Overall, the aim of all these studies was to increase inhibition in the epileptogenic area, but strategies were diverse. For example, some used AAV vectors to down-regulate excitatory receptor function (by transferring antisense NR1, an essential subunit of the NMDA receptors) or to up-regulate inhibitory receptor function (by transferring the alpha-1 subunit of the $GABA_A$ receptor) (30, 31). Others used LV vectors to overexpress potassium channels or halorhodopsin for inhibitory optogenetic stimulation (32). Or, using AAV vectors, one group expressed a modified muscarinic receptor (hM4Di) to obtain seizure suppression by systemic administration of the hM4Di selective, normally inactive agonist clozapine-N-oxide (33). Yet another strategy was to express a genetically-modified glutamate-gated Cl^- channel (34).

All these strategies proved effective. However, a common challenge is the ability to express the transgene in a specific cell population, because inhibiting inhibitory neurons would favor the occurrence of seizures (30). To avoid this problem, therefore, these authors drove expression of their transgenes by promoters specifically active in excitatory neurons, in an attempt to bias expression towards (and thereby

preferentially inhibit) excitatory neurons. As discussed below, this is a reasonable but imperfect solution.

One alternative strategy is the expression of a soluble inhibitory factor that can be secreted by the transduced cells: in this case, seizure control may be achieved without targeting specific cells, provided that the receptors for that factor are found in the injected area (35). Several studies have demonstrated that overexpression in the hippocampus of inhibitory neuropeptides (NPY, galanin, or somatostatin) exerts antiseizure effects in epilepsy models (data on NPY and galanin reviewed in (35-37); for somatostatin see (38)). Among these neuropeptides, NPY seems the most promising translationally, because it is the most effective in suppressing seizure-like activity in slices from the human epileptic hippocampus (39). However, a complication (and an opportunity) for NPY is that its effects are mediated by multiple receptors, some pro-epileptic (the Y1 subtype), others (Y2 and Y5) anti-epileptic (40). A combined administration of an AAV vector expressing NPY with one expressing the Y2 or one expressing the Y5 receptor produced much stronger reductions in seizure frequency than NPY alone (41, 42).

Looking forward

Altogether, the results of preclinical studies in epilepsy models suggest optimism as to the possibility of translation in humans. This optimism is sustained by recent advancements in clinical experimentation for other CNS diseases, in vector design and in targeting and regulation strategies.

Advancements in clinical experimentation for CNS diseases. The main obstacles on the way to human translation are the complexity and heterogeneity of the target tissue, the presence of the BBB and the safety of viral vectors. However, successful reports from experimentation for other CNS diseases are helping to concretely chart out a roadmap toward the first-in-man gene therapy for intractable epilepsy (43-45).

The direct intraparenchymal infusion of viral vectors has been successfully explored in a number of clinical studies for neurological disorders (36). One of the most promising envisaged the bilateral injection in the subthalamic nucleus of patients affected by medically refractory Parkinson's disease with a mix of recombinant AAVs encoding GABA synthesizing enzymes (GAD65 or GAD67). Upon assessment of safety and tolerability (46), this study became the first double-blinded and randomized trial of gene therapy for the CNS (47), showing beneficial effects on motor function that persisted up to 12 months (48).

A more recent study explored the use of a LV gene therapy vector for the simultaneous delivery into the striatum of three key enzymes for dopamine biosynthesis, providing a local and sustained novel source of dopamine from non-dopaminergic transduced cells. A first trial positively verified the safety profile of this treatment (49), which was subsequently confirmed in an 8-year follow-up along with a moderate improvement of motor function (50).

Another major advancement was the discovery of the ability of the AAV9 serotype to cross the BBB, which makes it potentially usable to treat genetic neurological diseases by transferring the healthy allele to the brain in a widespread manner. In a phase-1 clinical study (51), a group of patients affected by spinal muscular atrophy type 1 (SMA1), a monogenic disorder caused by mutation of the survival motor neuron 1 (SMN1) gene, has been successfully treated by a single, systemic dose of a recombinant AAV9 vector carrying the SMN1 gene. In principle, this approach may be used for some monogenetic forms of epilepsy, like Dravet syndrome (DS). Similar to SMA1, DS is generally caused by heterozygous mutations of the gene encoding the voltage-gated sodium channel alpha1 subunit (SCN1A). Unfortunately, however, neither the AAV or LV vectors can accommodate the entire SCN1A expression cassette in a single vector. To overcome this hurdle, the AAV packaging capacity may be increased by harnessing the virus natural propensity to generate head-to-tail DNA concatamers in the infected cells (52, 53). This feature has been exploited to

split and package large transgene cassettes in two (54-56) or three (57) separate AAV viral particles. The full-length cassette can then be recovered in cells that are concomitantly infected by the whole set of vectors, which, however, significantly reduces the efficiency of gene transfer (55). Efforts are ongoing to mitigate this problem (56, 57).

Advances in vector design. Vectors for CNS gene therapy should be highly refined, in order to ensure delivery to specific cell types, efficacy of transgene expression, capacity to host large and/or multiple inserts, safety, lasting transgene expression, and mechanisms to regulate expression. As described above, AAV and LV vectors do not combine all these features, while HSV vectors have been relatively overlooked so far because of concerns about cytotoxicity, immunogenicity, and difficulty in achieving persistent expression in the CNS. However, we have recently developed a new generation of HSV vectors that overcome these problems (Table 1). These are highly replication-defective vectors, devoid of all viral immediately early genes, in which viral gene expression is virtually absent (58). We found that inserting an expression cassette in a specific locus of the genome (the ICP4 locus) permits robust and long-term reporter gene expression in a diversity of neurons following stereotactic injection in the brain (59). Virus infection did not cause any neurotoxicity or inflammatory infiltrates. Therefore, these are high capacity vectors capable of safe, long-term transgene expression in the brain, opening up the possibility for therapeutic intervention into CNS diseases that require transfer of large amounts of DNA.

Advances in cell targeting and in regulation strategies. Other key advances were recently made for achieving a robust expression of the transgenes in a cell-specific manner, avoiding the risk of off-target effects. As mentioned above, the "classic" approach is to drive transgene expression through promoters that are active only in the desired cell type (60). For example, candidates to restrict gene expression in inhibitory neurons are the GAD65 or GAD67 promoters, that code for the enzyme that catalyzes the transformation of glutamate into GABA. However, this procedure does not completely ensure selectivity of expression and, in addition, the size of many full-length promoters is too large for most viral vectors. An alternative and more efficient strategy was recently proposed, based on the encoding of microRNA target motifs downstream of the transgene. The introduction of multiple target motifs for microRNAs expressed in off-target cells silenced transgene expression in these cells, thereby achieving highly specific expression in the desired cell type (61).

Another important advance involves the regulation of gene expression. Mechanisms of autoregulation are important requirements for clinical translation because they reduce the risk of negative effects on physiological brain circuitries. Lieb et al. (34) cloned into a LV vector an optimized sequence encoding a glutamate-gated chloride channel (GluCl) with an EC_{50} for glutamate of about 10 μM, i.e. high concentrations that would be reached at extrasynaptic levels only during seizures. When injected in the rat neocortex, this vector led to a potent attenuation of evoked and spontaneous seizures, in the absence of alterations in normal brain function.

Conclusions

Although gene therapy is becoming an established approach for an increasing number of diseases, its application to CNS disorders still poses formidable challenges that are not yet completely overcome. While it will be essential to sort out all possible problems before clinical testing, the good news is that the field is progressing rapidly, and it seems plausible that the time for a first-in-man gene therapy for epilepsy is not too far anymore.

Table 1. Viral vectors.

	Adeno-associated vectors	Lentiviral vectors	"Classic" Herpes virus vectors	"New" Herpes virus vectors
Family of wild-type virus	Parvoviridae	Retroviridae	Herpesviridae	Herpesviridae
Infection/tropism	Dividing and non-dividing cells	Dividing and non-dividing cells	Dividing and non-dividing cells	Dividing and non-dividing cells
Genetic material	ssDNA	ssRNA	dsDNA	dsDNA
Host genome interaction	No*	Yes	No	No
Packaging capacity	4.5 kb**	9 kb	50-150 kb	50 kb
Toxicity	Low	Low	Moderate	Low
Transgene expression	Long-lasting	Long-lasting	Transient	Long-lasting
Main limitation	Very small packaging capacity	Small packaging capacity Integration	Inflammation Transient transgene expression	Not yet clinically tested
Main advantages	Non-inflammatory Non-pathogenic	Persistent transgene expression	Large payload capacity	Large payload capacity

* Some integration at very low frequency.

** Packaging capacity may be increased by splitting the transgene cassette in 2-3 viruses.

References

1 Simonato M, Brooks-Kayal AR, Engel J, Jr., Galanopoulou AS, Jensen FE, Moshe SL, O'Brien TJ, Pitkanen A, Wilcox KS and French JA. The challenge and promise of anti-epileptic therapy development in animal models. *Lancet Neurol* 2014;**13**(9):949-60.

2 Pack DW, Hoffman AS, Pun S and Stayton PS. Design and development of polymers for gene delivery. *Nat Rev Drug Discov* 2005;**4**(7):581-93.

3 Mintzer MA and Simanek EE. Nonviral vectors for gene delivery. *Chem Rev*2009;**109**(2):259-302.

4 Kaplitt MG, Leone P, Samulski RJ, Xiao X, Pfaff DW, O'Malley KL and During MJ. Long-term gene expression and phenotypic correction using adeno-associated virus vectors in the mammalian brain. *Nat Genet* 1994;**8**(2):148-54.

5 McCown TJ, Xiao X, Li J, Breese GR and Samulski RJ. Differential and persistent expression patterns of CNS gene transfer by an adeno-associated virus (AAV) vector. *Brain Res* 1996;**713**(1-2):99-107.

6 Choudhury SR, Harris AF, Cabral DJ, Keeler AM, Sapp E, Ferreira JS, Gray-Edwards HL, Johnson JA, Johnson AK, Su Q, Stoica L, DiFiglia M, Aronin N, Martin DR, Gao G and Sena-Esteves M. Widespread Central Nervous System Gene Transfer and Silencing After Systemic Delivery of Novel AAV-AS Vector. *Molecular therapy : the journal of the American Society of Gene Therapy* 2016;**24**(4):726-35.

7 Kaeppel C, Beattie SG, Fronza R, van Logtenstein R, Salmon F, Schmidt S, Wolf S, Nowrouzi A, Glimm H, von Kalle C, Petry H, Gaudet D and Schmidt M. A largely random AAV integration profile after LPLD gene therapy. *Nat Med* 2013;**19**(7):889-91.

8 Castle MJ, Turunen HT, Vandenberghe LH and Wolfe JH. Controlling AAV Tropism in the Nervous System with Natural and Engineered Capsids. *Methods Mol Biol*2016;**1382**:133-49.

9 Harding TC, Dickinson PJ, Roberts BN, Yendluri S, Gonzalez-Edick M, Lecouteur RA and Jooss KU. Enhanced gene transfer efficiency in the murine striatum and an orthotopic glioblastoma tumor model, using AAV-7- and AAV-8-pseudotyped vectors. *Hum Gene Ther*2006;**17**(8):807-20.

10 Weinberg MS, Blake BL, Samulski RJ and McCown TJ. The influence of epileptic neuropathology and prior peripheral immunity on CNS transduction by rAAV2 and rAAV5. *Gene Ther*2011;**18**(10):961-8.

11 Dodiya HB, Bjorklund T, Stansell J, 3rd, Mandel RJ, Kirik D and Kordower JH. Differential transduction following basal ganglia administration of distinct pseudotyped AAV capsid serotypes in nonhuman primates. *Molecular therapy : the journal of the American Society of Gene Therapy* 2010;**18**(3):579-87.

12 Burger C, Gorbatyuk OS, Velardo MJ, Peden CS, Williams P, Zolotukhin S, Reier PJ, Mandel RJ and Muzyczka N. Recombinant AAV viral vectors pseudotyped with viral capsids from serotypes 1, 2, and 5 display differential efficiency and cell tropism after delivery to different regions of the central nervous system. *Molecular therapy : the journal of the American Society of Gene Therapy* 2004;**10**(2):302-17.

13 Davidson BL, Stein CS, Heth JA, Martins I, Kotin RM, Derksen TA, Zabner J, Ghodsi A and Chiorini JA. Recombinant adeno-associated virus type 2, 4, and 5 vectors: transduction of variant cell types and regions in the mammalian central nervous system. *Proceedings of the National Academy of Sciences of the United States of America* 2000;**97**(7):3428-32.

14 Klein RL, Dayton RD, Tatom JB, Henderson KM and Henning PP. AAV8, 9, Rh10, Rh43 vector gene transfer in the rat brain: effects of serotype, promoter and purification method. *Molecular therapy : the journal of the American Society of Gene Therapy* 2008;**16**(1):89-96.

15 Foust KD, Nurre E, Montgomery CL, Hernandez A, Chan CM and Kaspar BK. Intravascular AAV9 preferentially targets neonatal neurons and adult astrocytes. *Nat Biotechnol*2009;**27**(1):59-65.

16 Kanaan NM, Sellnow RC, Boye SL, Coberly B, Bennett A, Agbandje-McKenna M, Sortwell CE, Hauswirth WW, Boye SE and Manfredsson FP. Rationally Engineered AAV Capsids Improve Transduction and Volumetric Spread in the CNS. *Mol Ther Nucleic Acids*2017;**8**:184-197.

17 Hudry E, Martin C, Gandhi S, Gyorgy B, Scheffer DI, Mu D, Merkel SF, Mingozzi F, Fitzpatrick Z, Dimant H, Masek M, Ragan T, Tan S, Brisson AR, Ramirez SH, Hyman BT and Maguire CA. Exosome-associated AAV vector as a robust and convenient neuroscience tool. *Gene Ther* 2016;**23**(11):819.

18 Bukrinsky MI, Haggerty S, Dempsey MP, Sharova N, Adzhubel A, Spitz L, Lewis P, Goldfarb D, Emerman M and Stevenson M. A nuclear localization signal within HIV-1 matrix protein that governs infection of non-dividing cells. *Nature* 1993;**365**(6447):666-9.
19 Liu YP and Berkhout B. HIV-1-based lentiviral vectors. *Methods Mol Biol*2014;**1087**:273-84.
20 Wong LF, Azzouz M, Walmsley LE, Askham Z, Wilkes FJ, Mitrophanous KA, Kingsman SM and Mazarakis ND. Transduction patterns of pseudotyped lentiviral vectors in the nervous system. *Molecular therapy : the journal of the American Society of Gene Therapy* 2004;**9**(1):101-11.
21 Mazarakis ND, Azzouz M, Rohll JB, Ellard FM, Wilkes FJ, Olsen AL, Carter EE, Barber RD, Baban DF, Kingsman SM, Kingsman AJ, O'Malley K and Mitrophanous KA. Rabies virus glycoprotein pseudotyping of lentiviral vectors enables retrograde axonal transport and access to the nervous system after peripheral delivery. *Hum Mol Genet* 2001;**10**(19):2109-21.
22 Kato S, Inoue K, Kobayashi K, Yasoshima Y, Miyachi S, Inoue S, Hanawa H, Shimada T, Takada M and Kobayashi K. Efficient gene transfer via retrograde transport in rodent and primate brains using a human immunodeficiency virus type 1-based vector pseudotyped with rabies virus glycoprotein. *Hum Gene Ther* 2007;**18**(11):1141-51.
23 Trabalza A, Eleftheriadou I, Sgourou A, Liao TY, Patsali P, Lee H and Mazarakis ND. Enhanced central nervous system transduction with lentiviral vectors pseudotyped with RVG/HIV-1gp41 chimeric envelope glycoproteins. *Journal of virology* 2014;**88**(5):2877-90.
24 Carpentier DC, Vevis K, Trabalza A, Georgiadis C, Ellison SM, Asfahani RI and Mazarakis ND. Enhanced pseudotyping efficiency of HIV-1 lentiviral vectors by a rabies/vesicular stomatitis virus chimeric envelope glycoprotein. *Gene Ther* 2012;**19**(7):761-74.
25 Berges BK, Wolfe JH and Fraser NW. Transduction of brain by herpes simplex virusvectors. *Molecular therapy : the journal of the American Society of Gene Therapy* 2007;**15**(1):20-9.
26 Diefenbach RJ, Miranda-Saksena M, Douglas MW and Cunningham AL. Transport and egress of herpes simplex virus in neurons. *Rev Med Virol* 2008;**18**(1):35-51.
27 Goverdhana S, Puntel M, Xiong W, Zirger JM, Barcia C, Curtin JF, Soffer EB, Mondkar S, King GD, Hu J, Sciascia SA, Candolfi M, Greengold DS, Lowenstein PR and Castro MG. Regulatable gene expression systems for gene therapy applications: progress and future challenges. *Molecular therapy : the journal of the American Society of Gene Therapy*2005;**12**(2):189-211.
28 Epstein AL. Progress and prospects: biological properties and technological advances of herpes simplex virus type 1-based amplicon vectors. *Gene Ther* 2009;**16**(6):709-15.
29 Paradiso B, Marconi P, Zucchini S, Berto E, Binaschi A, Bozac A, Buzzi A, Mazzuferi M, Magri E, Navarro Mora G, Rodi D, Su T, Volpi I, Zanetti L, Marzola A, Manservigi R, Fabene PF andSimonato M. Localized delivery of fibroblast growth factor-2 and brain-derived neurotrophic factor reduces spontaneous seizures in an epilepsy model. *Proceedings of the National Academy of Sciences of the United States of America* 2009;**106**(17):7191-6.
30 Haberman R, Criswell H, Snowdy S, Ming Z, Breese G, Samulski R and McCown T. Therapeutic liabilities of in vivo viral vector tropism: adeno-associated virus vectors, NMDAR1 antisense, and focal seizure sensitivity. *Molecular therapy : the journal of the American Society of Gene Therapy* 2002;**6**(4):495-500.
31 Raol YH, Lund IV, Bandyopadhyay S, Zhang G, Roberts DS, Wolfe JH, Russek SJ and Brooks-Kayal AR. Enhancing GABA(A) receptor alpha 1 subunit levels in hippocampal dentate gyrus inhibits epilepsy development in an animal model of temporal lobe epilepsy. *The Journal of neuroscience : the official journal of the Society for Neuroscience* 2006;**26**(44):11342-6.
32 Wykes RC, Heeroma JH, Mantoan L, Zheng K, MacDonald DC, Deisseroth K, Hashemi KS, Walker MC, Schorge S and Kullmann DM. Optogenetic and potassium channel gene therapy in a rodent model of focal neocortical epilepsy. *Sci Transl Med* 2012;**4**(161):161ra152.
33 Katzel D, Nicholson E, Schorge S, Walker MC and Kullmann DM. Chemical-genetic attenuation of focal neocortical seizures. *Nature communications* 2014;**5**:3847.
34 Lieb A, Qiu Y, Dixon CL, Heller JP, Walker MC, Schorge S and Kullmann DM. Biochemical autoregulatory gene therapy for focal epilepsy. *Nat Med*2018;**24**(9):1324-1329.
35 Simonato M. Gene therapy for epilepsy. *Epilepsy & behavior : E&B*2014;**38**:125-30.

36 Simonato M, Bennett J, Boulis NM, Castro MG, Fink DJ, Goins WF, Gray SJ, Lowenstein PR, Vandenberghe LH, Wilson TJ, Wolfe JH and Glorioso JC. Progress in gene therapy for neurological disorders. *Nature reviews Neurology* 2013;**9**(5):277-91.
37 Kullmann DM, Schorge S, Walker MC and Wykes RC. Gene therapy in epilepsy-is it time for clinical trials? *Nature reviews Neurology* 2014;**10**(5):300-4.
38 Natarajan G, Leibowitz JA, Zhou J, Zhao Y, McElroy JA, King MA, Ormerod BK and Carney PR. Adeno-associated viral vector-mediated preprosomatostatin expression suppresses induced seizures in kindled rats. *Epilepsy research* 2017;**130**:81-92.
39 Ledri M, Sorensen AT, Madsen MG, Christiansen SH, Ledri LN, Cifra A, Bengzon J, Lindberg E, Pinborg LH, Jespersen B, Gotzsche CR, Woldbye DP, Andersson M and Kokaia M. Differential Effect of Neuropeptides on Excitatory Synaptic Transmission in Human Epileptic Hippocampus. *The Journal of neuroscience : the official journal of the Society for Neuroscience* 2015;**35**(26):9622-31.
40 Vezzani A, Sperk G and Colmers WF. Neuropeptide Y: emerging evidence for a functional role in seizure modulation. *Trends in neurosciences* 1999;**22**(1):25-30.
41 Woldbye DP, Angehagen M, Gotzsche CR, Elbrond-Bek H, Sorensen AT, Christiansen SH, Olesen MV, Nikitidou L, Hansen TV, Kanter-Schlifke I and Kokaia M. Adeno-associated viral vector-induced overexpression of neuropeptide Y Y2 receptors in the hippocampus suppresses seizures. *Brain : a journal of neurology* 2010;**133**(9):2778-88.
42 Gotzsche CR, Nikitidou L, Sorensen AT, Olesen MV, Sorensen G, Christiansen SH, Angehagen M, Woldbye DP and Kokaia M. Combined gene overexpression of neuropeptide Y and its receptor Y5 in the hippocampus suppresses seizures. *Neurobiology of disease* 2012;**45**(1):288-96.
43 Muramatsu S, Fujimoto K, Kato S, Mizukami H, Asari S, Ikeguchi K, Kawakami T, Urabe M, Kume A, Sato T, Watanabe E, Ozawa K and Nakano I. A phase I study of aromatic L-amino acid decarboxylase gene therapy for Parkinson's disease. *Molecular therapy : the journal of the American Society of Gene Therapy* 2010;**18**(9):1731-5.
44 Christine CW, Starr PA, Larson PS, Eberling JL, Jagust WJ, Hawkins RA, VanBrocklin HF, Wright JF, Bankiewicz KS and Aminoff MJ. Safety and tolerability of putaminal AADC gene therapy for Parkinson disease. *Neurology* 2009;**73**(20):1662-9.
45 Eberling JL, Jagust WJ, Christine CW, Starr P, Larson P, Bankiewicz KS and Aminoff MJ. Results from a phase I safety trial of hAADC gene therapy for Parkinson disease. *Neurology*2008;**70**(21):1980-3.
46 Kaplitt MG, Feigin A, Tang C, Fitzsimons HL, Mattis P, Lawlor PA, Bland RJ, Young D, Strybing K, Eidelberg D and During MJ. Safety and tolerability of gene therapy with an adeno-associated virus (AAV) borne GAD gene for Parkinson's disease: an open label, phase I trial. *Lancet* 2007;**369**(9579):2097-105.
47 LeWitt PA, Rezai AR, Leehey MA, Ojemann SG, Flaherty AW, Eskandar EN, Kostyk SK, Thomas K, Sarkar A, Siddiqui MS, Tatter SB, Schwalb JM, Poston KL, Henderson JM, Kurlan RM, Richard IH, Van Meter L, Sapan CV, During MJ, Kaplitt MG and Feigin A. AAV2-GAD gene therapy for advanced Parkinson's disease: a double-blind, sham-surgery controlled, randomised trial. *Lancet Neurol* 2011;**10**(4):309-19.
48 Niethammer M, Tang CC, LeWitt PA, Rezai AR, Leehey MA, Ojemann SG, Flaherty AW, Eskandar EN, Kostyk SK, Sarkar A, Siddiqui MS, Tatter SB, Schwalb JM, Poston KL, Henderson JM, Kurlan RM, Richard IH, Sapan CV, Eidelberg D, During MJ, Kaplitt MG and Feigin A. Long-term follow-up of a randomized AAV2-GAD gene therapy trial for Parkinson's disease. *JCI Insight*2017;**2**(7):e90133.
49 Palfi S, Gurruchaga JM, Ralph GS, Lepetit H, Lavisse S, Buttery PC, Watts C, Miskin J, Kelleher M, Deeley S, Iwamuro H, Lefaucheur JP, Thiriez C, Fenelon G, Lucas C, Brugieres P, Gabriel I, Abhay K, Drouot X, Tani N, Kas A, Ghaleh B, Le Corvoisier P, Dolphin P, Breen DP, Mason S, Guzman NV, Mazarakis ND, Radcliffe PA, Harrop R, Kingsman SM, Rascol O, Naylor S, Barker RA, Hantraye P, Remy P, Cesaro P and Mitrophanous KA. Long-term safety and tolerability of ProSavin, a lentiviral vector-based gene therapy for Parkinson's disease: a dose escalation, open-label, phase 1/2 trial. *Lancet* 2014;**383**(9923):1138-46.
50 Palfi S, Gurruchaga JM, Lepetit H, Howard K, Ralph GS, Mason S, Gouello G, Domenech P, Buttery PC, Hantraye P, Tuckwell NJ, Barker RA and Mitrophanous KA. Long-Term Follow-Up of a PhaseI/II

Study of ProSavin, a Lentiviral Vector Gene Therapy for Parkinson's Disease. *Hum Gene Ther Clin Dev* 2018;**29**(3):148-155.

51 Mendell JR, Al-Zaidy S, Shell R, Arnold WD, Rodino-Klapac LR, Prior TW, Lowes L, Alfano L, Berry K, Church K, Kissel JT, Nagendran S, L'Italien J, Sproule DM, Wells C, Cardenas JA, Heitzer MD, Kaspar A, Corcoran S, Braun L, Likhite S, Miranda C, Meyer K, Foust KD, Burghes AHM and Kaspar BK. Single-Dose Gene-Replacement Therapy for Spinal Muscular Atrophy. *N Engl J Med* 2017;**377**(18):1713-1722.

52 Duan D, Sharma P, Yang J, Yue Y, Dudus L, Zhang Y, Fisher KJ and Engelhardt JF. Circular intermediates of recombinant adeno-associated virus have defined structural characteristics responsible for long-term episomal persistence in muscle tissue. *Journal of virology* 1998;**72**(11):8568-77.

53 Duan D, Yan Z, Yue Y and Engelhardt JF. Structural analysis of adeno-associated virus transduction circular intermediates. *Virology* 1999;**261**(1):8-14.

54 Yan Z, Zhang Y, Duan D and Engelhardt JF. Trans-splicing vectors expand the utility of adeno-associated virus for gene therapy. *Proceedings of the National Academy of Sciences of the United States of America* 2000;**97**(12):6716-21.

55 Duan D, Yue Y and Engelhardt JF. Expanding AAV packaging capacity with trans-splicing or overlapping vectors: a quantitative comparison. *Molecular therapy : the journal of the American Society of Gene Therapy* 2001;**4**(4):383-91.

56 Ghosh A, Yue Y, Lai Y and Duan D. A hybrid vector system expands adeno-associated viral vector packaging capacity in a transgene-independent manner. *Molecular therapy : the journal of the American Society of Gene Therapy* 2008;**16**(1):124-30.

57 Maddalena A, Tornabene P, Tiberi P, Minopoli R, Manfredi A, Mutarelli M, Rossi S, Simonelli F, Naggert JK, Cacchiarelli D and Auricchio A. Triple Vectors Expand AAV Transfer Capacity in the Retina. *Molecular therapy : the journal of the American Society of Gene Therapy* 2018;**26**(2):524-541.

58 Miyagawa Y, Marino P, Verlengia G, Uchida H, Goins WF, Yokota S, Geller DA, Yoshida O, Mester J, Cohen JB and Glorioso JC. Herpes simplex viral-vector design for efficient transduction of nonneuronal cells without cytotoxicity. *Proceedings of the National Academy of Sciences of the United States of America* 2015;**112**(13):E1632-41.

59 Verlengia G, Miyagawa Y, Ingusci S, Cohen JB, Simonato M and Glorioso JC. Engineered HSV vector achieves safe long-term transgene expression in the central nervous system. *Sci Rep* 2017;**7**(1):1507.

60 Nathanson JL, Jappelli R, Scheeff ED, Manning G, Obata K, Brenner S and Callaway EM. Short Promoters in Viral Vectors Drive Selective Expression in Mammalian Inhibitory Neurons, but do not Restrict Activity to Specific Inhibitory Cell-Types. *Front Neural Circuits* 2009;**3**:19.

61 Keaveney MK, Tseng HA, Ta TL, Gritton HJ, Man HY and Han X. A MicroRNA-Based Gene-Targeting Tool for Virally Labeling Interneurons in the Rodent Cortex. *Cell Rep* 2018;**24**(2):294-303.

1.3 Herpes viruses

1.3 Herpes viruses

1.3.1 Herpesviridae classification:

Herpes viruses are a large family of DNA viruses (Herpes-viridae) that can infect both humans and different animal species. Currently, more than 100 viruses belonging to this family have been characterized. Members of this family with human tropism are classified in 8 different subtypes. Herpes simplex type 1 (HSV-1), Herpes simplex type 2 (HSV-2), Varicella-zoster virus (HHV-3 or VZV), Epstein-Barr virus (HHV-4 or EBV), Human cytomegalovirus (HCMV), Human Herpes virus 6 (HHV-6), Human Herpes virus 7 (HHV-7) and Kaposi's sarcoma-associated herpesvirus (KSHV or HHV8) [1]. Herpesviruses have been grouped into three subfamilies: Alphaherpesviruses (α), Betaherpesviruses (β) and Gammaherpesviruses (γ), diversified according to the genome structure, tissue tropism, cytopathology and the site of latent infection. All herpes viruses have common biological characteristics such as:

- ability to encode a large number of enzymes involved in the metabolism of nucleic acids, in DNA synthesis, in post-transcriptional synthesis and in proteins modification;

- viral DNA synthesis and capsid assembly occurring into the cell nucleus; tegument association and envelope acquisition taking place in the cytoplasm;

-ability to establish latent infection during which the viral genome takes the form of a circular molecule (episomal state) and only part of the viral genes are expressed; the latent genome can be reactivated by various stimuli to enter in the lytic cycle, in which the end point is lysis of the infected cell.

Members of the Alphaherpesvirus subfamily are characterized by a broad spectrum of infection, a relatively short lytic cycle, rapid propagation in culture and efficient destruction of infected cells. They can also effectively invade the peripheral nervous system, moving from infected epithelial cells to spinal and cervical ganglionic neurons by retrograde transport of the viral capsid [2]. The virus then persists in a latent state in the nervous system of the host, where the viral genome remains in an episomal form [3].

Betaherpesvirinae have a limited spectrum of infection and longer replication cycle in infected cells. They are able to establish latency in the secretory glands, in the lymph-reticular cells, in the kidneys and in other tissues.

Gammaherpesvirinae are usually replicated in lympho-blastoid cells, especially in T or B lymphocytes and establish latency in the lymphnodes.

1.3.2 Genomic structure and organization of a herpes simplex virus:

Herpes viruses are among the largest and most complex animal viruses. The viral particles of the HSVs consist of four basic morphological elements, represented from the outside towards the inside by [4]:

- An envelope which constitutes the external liner, and is composed of a double lipid layer, deriving from the cellular membrane, in which various viral glycoproteins are inserted, responsible for binding to specific cell receptors and for penetration of the virus into the cytoplasm;
- The tegument that is composed of a protein matrix of 12 viral proteins, some of which responsible for the induction of viral genes, especially during the very first stages ofinfection;
- The capside which presents a symmetrical icosahedral structure formed by 162 capsomers (150 exons and 12 pentons), surrounded by the tegument and containing the"core";

- The core, displaying a central protein structure associated with the viral genome consisting of double helix DNA (dsDNA).

1.3.3 HSV-1 genome:

The HSV genome (Figure 1) consists of a linear molecule of a double-stranded DNA about 152Kb long and with a molecular weight of $96x10^6$ DA, which becomes circular when enters the nucleus. The genome is composed of two unique regions, one long and one short, termed UL and US (Unique Long and Unique Short). These regions are flanked and separated by inverted repeat sequences: two internal repeated sequences, called IRL and IRS (Internal Repeats long and short), that together give rise to the so called "JOINT" region and two terminal repeated sequences placed at the 5 'and 3' end of the genome, namely TRL and TRS (Terminal Repeats long and short), which interact with each other at the time of the genome circularization [5]. The genome includes at least 84 genes, of which Infected cell protein (ICP) 0, 4, 34.5 and latency associated transcripts (LAT) are localized into repeated sequences and are present in duplicate. Among the 84 genes 38 are "essential" for viral replication and 46 are "accessory" or non-essential for a productive virus replication cycle [6]. The HSV-1 replication cycle is strictly regulated in a sequential manner: three gene classes, known as the immediate early genes (α-genes), the early genes (β-genes) and the late genes (γ), are coordinately expressed following the transcriptional regulation of viral and host cell proteins [7]. The α genes products reach the peak of synthesis from 2 to 4 hours post-infection (hpi), whereas beta genes are activated shortly after and reach the peak at 6-12 hpi. α genes do not require the synthesis of any viral protein to be expressed, but request only a cis-regulatory site (alpha TIC), which is located in the promoter-regulatory domains of the α genes; the products of these genes are involved in the regulation of β and γ genes transcription and they can also operate a positive or negative feedback regulation of α genes, although the mechanism that regulates these processes has not yet been clarified[8].

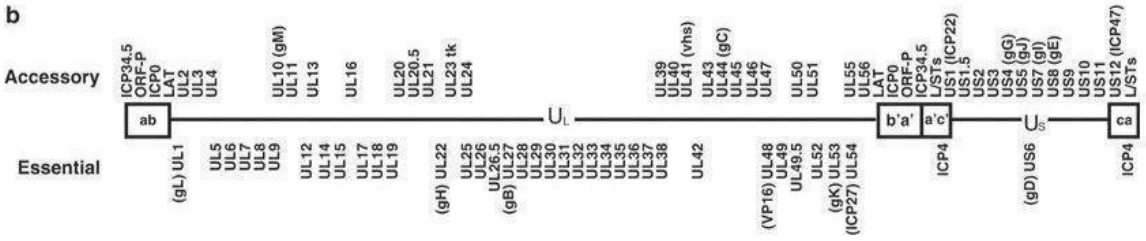

Figure 1: HSV-1 genome [2].

1.3.4 HSV-1 nucleocapsid:

The HSV genome is wrapped within an icosahedral protein shell, called nucleocapsid or simply capsid, whose total molecular mass is 0.2 billion Daltons. The capsid is composed of 162 capsomers consisting of 4 viral proteins: VP5, VP26, VP23, VP19 [9]. Within the envelope, the capside occupies about 1/3 of the volume, while the tegument occupies the remaining 2/3. The encapsidation and the release of the viral DNA take place through an opening in the capsid, due to the pUL6 protein [10].

1.3.5 HSV-1 tegument:

The capsid is surrounded by a layer of proteinaceous material called tegument. The HSV-1 tegument is involved in transcription regulation of viral α genes and in the regulation of host cell transcription (viron host-shutoff genes) [11]. The tegument contains at least 20 viral encoded proteins; some of these, including VP16, are responsible for the activation of viral α gene expression [12; 13]. Others contribute to create a more favorable environment for virus replication in infected cells, such as the VHS protein that degrades cellular mRNAs to increase the efficiency of viral protein translation [14] or the protein encoded by US11 that inhibits the activation of protein-kinase R, responsible for blocking transduction of viral transcripts in the host cell [15]. The tegument also includes the VP22 protein which acts as a stabilizer of important viral proteins such as gE, gD, and ICP0 [16] and is involved in viral dissemination during lytic infection.

1.3.6 HSV-1 Envelope:

The tegument is enclosed in an envelope originated from the cytoplasmic membranes of previously infected cells. The envelope consists of a lipidic trilaminar membrane, containing viral proteins and different glycoproteins of cellular origin; among these only 5 (gB, gC, gD, gH and gL) are important for cell adhesion, fusion and internalization of the virus (Figure 2) [17].

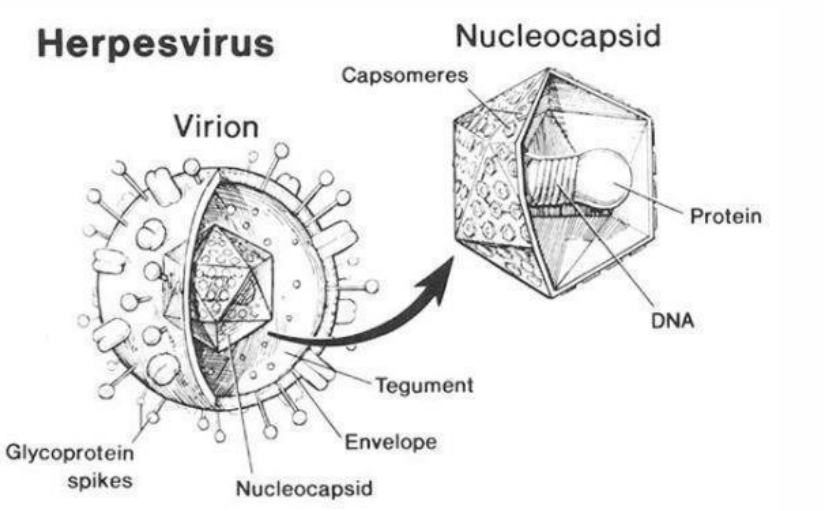

Figure 2: HSV-1 structure [4].

1.3.7 HSV-1 infection:

The virion adheres to the host cell surface thanks to the presence of the envelope glycoproteins gB and gC, which bind glycosaminoglycans (GAGs) that are general linked to protein residues to form proteoglycans which, as bristles, modulate the interaction of external molecules with cell receptors [18; 19]. This nonspecific binding follows the interaction between gD glycoprotein and three cellular receptors called nectin-1 (HveC), the Herpesvirus entry mediator (HVEM) and 3-O-sulfated heparan sulfate (3-OS HS) [20]. Following the binding of gD with its receptors, a series of conformational changes in the gH/gL glycoprotein pair leads to the definitive activation of gB, which allows fusion of the envelope with the cell membrane [21]. Following the adsorption of HSV-1, VP1 and VP2, products of the UL36 gene, localize to the nuclear pore,

mediating DNA translocation into the nucleus [22]. The nucleocapsid is transported to the nuclear pores, where the viral DNA is released and accesses the nucleus where it will circulate [23; 24].

Meanwhile, the preformed tegument proteins are released into the host cell: VHS produced by the UL41 gene, localized in the cytoplasm; VP16, produced by UL48 instead directs itself to the nucleus independently of the capsid. The function of VHS will be to inhibit host protein synthesis, to benefit viral proteins translation into host ribosomes [25]. VP16 will form a complex with TF Oct-1 and the cell proliferation factor HCF-1. The complex acts as alpha-TIF (alpha transcription initiation factor), initiating the transcription of alpha/IE-genes [26; 27]. The products of these precocious genes will activate, as we have seen, a transcriptional cascade and will inactivate nuclear mechanisms for cell cycle control. Following α genes expression, beta genes are activated, involved in the replication of viral DNA and in the induction of gamma genes, which encode for the virus structural proteins. The capsid proteins synthesized in the cytosol return to the nucleus where they will be assembled in icosahedral complexes containing the previously replicated DNA (Figure 3).

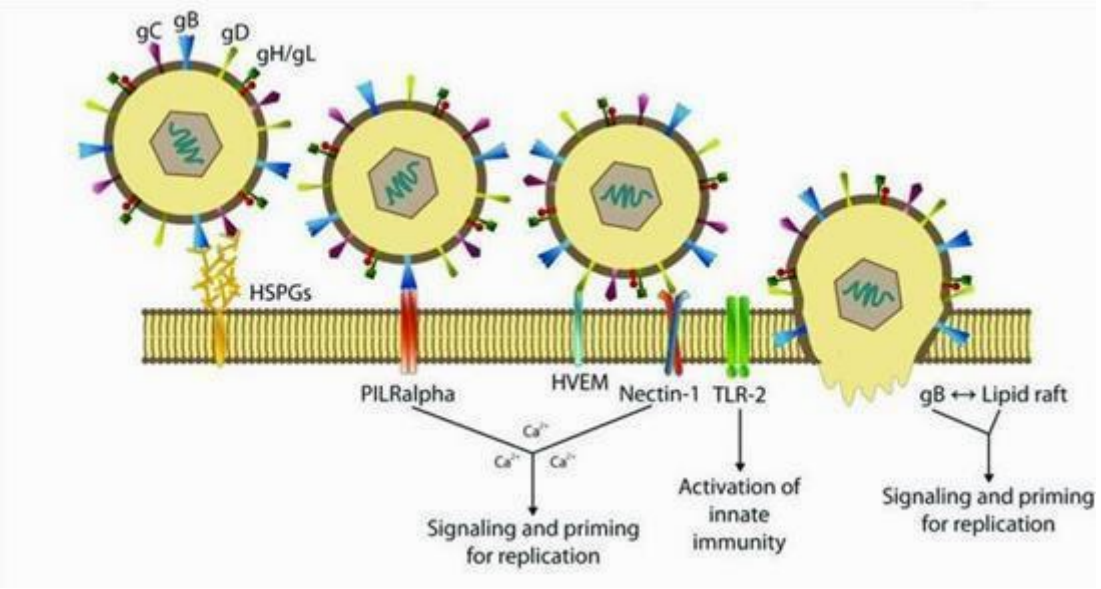

Figure 3: Mechanism of HSV-1 entry into the host cell [6].

1.3.8 Some proteins in detail:

We will now analyze some proteins in detail for the complexity of their action, their importance within the virus life cycle and, consequently, the weight that their editing takes on HSV-1 vector design and construction.

ICP0: Infected cell polypeptide 0 (ICP0) is a multi-function protein belonging to the alpha/IE group. ICP0 is a 100kDa protein encoded by the α0 gene located in the repeated inverted sequences that flank the unique long sequence of the viral genome [28]. During the first 6 hpi, ICP0 accumulates in the nucleus and then localize into the cytoplasm, where its action has not yet been fully elucidated. In the nucleus, ICP0 acts as a transactivator of beta genes transcription, allowing an efficient induction of the lytic cycle and enhancing the function of ICP4 [29]. Moreover, ICP0 is essential for viral evasion of the innate interferon response [30].

Due to its nuclear localization signal (NLS) and its E3 ubiquitin ligase domain, ICP0 localizes in the nucleus early during viral replication, accumulating initially near the nuclear bodies PML (pro-myelocytic leukemia), leading to their dispersion during the initial phase of infection and contributing to the formation of adjacent compartments for sub-nuclear replication [31]. ICP0 is able to block the epigenetic silencing acted by the host histone-deacetylase class II (HDACs) enzyme [32]. Although ICP0 is not essential for viral replication in the host cell, the ICP0-deleting mutant virus presents a 10-100-fold reduction in viral titers compared to wild-type.

ICP4: ICP4 is an α-protein with a molecular weight of 175kDa, encoded by two copies of the α4 gene localized on TRs and IRs. ICP4 is the master viral transactivator: it regulates the transcription of the majority of HSV-1 genes, inducing the expression of beta and gamma genes and suppressing the expression of α genes, in particular acting on itself and on ICP0. During viral DNA replication, ICP4 is localized in the nucleus, where it exists as homodimer. Its structure consists of a DNA binding domain, a nuclear localization domain and two transactivation regions [33]. ICP4 physically interacts with host transcription factors, such as the TATA-binding protein, TFIIB, TFIID, and TAF250. These interactions are crucial to stimulate the transcription of viral promoters that contain the cis-acting recognition site of ICP4 [34].

ICP22: ICP22 is a 68 kDa protein, encoded by α22 gene, localized in the unique short region of the viral genome. ICP22 is useful to regulate beta and gamma genes expression by altering the RNApolII phosphorylation status. This consequently results in blocking host cell genome transcription, the arrest of the cell cycle and the reduction of anti-viral response [35; 36].

ICP27: alpha-protein, encoded by UL54 which is found in the unique long sequence of the HSV genome. ICP27 shows a range of activities including regulation of gene expression, mRNA stabilization, spliceosome disruption and efficient export of viral mRNAs from the nucleus to the cytoplasm [37].

ICP47: It is the only product of an α gene (hosted in the US12 region) not involved in the regulation of gene expression, but in the modulation of the host's immune response to infection. By binding to the carriers associated with antigen processing (transporter associated with antigen processing, TAP), ICP47 is able to interfere with the loading of exogenous peptide fragments that the cell normally exposes on its surface on the MHC class I molecules to subject them to cytotoxic T lymphocytes (CTL) screening [38].

ICP34.5: gamma gene located in duplicate in the JOINT region within the TRL, together with LAT and ICP0, contributes to resistance to interferons and acts as a neurovirulence factor [39]. Recent data suggest that ICP34.5 and no-ICP0 would play a fundamental and necessary role in the reactivation of HSV-1 from latency [40].

VHS: Encoded by the UL41 gene, virion-associated host shutoff (VHS) is a tegument protein capable of suppressing cellular host protein synthesis degrading mRNAs [25].

1.3.9 Latency-associated transcript:

An important issue in HSV biology is the mechanism by which the virus establishes a latent infection in sensory neurons. During latency, the viral genome persists in the form of histone-associated circular episome [41; 42] and the expression of most of the HSV genome is silenced. However, a part of the unique long repeated region of the viral genome, known as LAT locus, is actively transcribed, due to the presence of promoter associated with latency (latency associated promoter, LAP) that remains active and determines the synthesis of specific non-coding RNA latency-associated transcripts (LATs) [43]. The mRNAs encoded by the LAT locus help maintain latency by acting mainly through RNA interference against ICP0, ICP4 and ICP34.5 [44; 45; 46]. LATs regulate not only viral genes, but also the host cell genome, blocking cellular signal pathways involved in cell proliferation and apoptotic mechanisms [44; 47; 48]. Recent studies have shown

that there are epigenetic components involved in HSV-1 latency and in reactivation [49; 50]. In particular, the LAT region is rich in H3K9 and H3K14 acetylated histones, while the surrounding regions, such as the ICP0 lytic gene, contain deacetylated and methylated histones [51]. These findings provide evidence that HSV-1 latency is established and maintained, at least in part, by complex epigenetic mechanisms.

1.3.10 HSV-1 epigenetic mechanisms:

Previous studies have shown that distinct heterochromatic and euchromatic chromatin domains are likely established within the latent genome. As described above, the HSV-1 latent genome is organized into histone H3 (K9, K14) hyperacetylated and hypoacetylated regions. This configuration of transcriptionally permissive and transcriptionally repressed chromatin during latency implies the presence of functional barriers within the HSV-1 genome [52]. The most common barriers against epigenetic mechanisms are chromatin insulator elements, which would have the capability of preventing inappropriate gene activation and/or silencing by nearby chromatin domains during latency [52; 53]. Chromatin insulators are cis-acting DNA sequence elements that can protect a given transcriptional domain from inappropriate signals from its surroundings [54]. Insulator elements have been extensively studied and classified into two main classes: enhancer blockers, which limit the action of enhancer element on the activation of genes distal to the insulator [55] and barrier elements, which prevent the extension of heterochromatin to areas of euchromatin by recruiting histone-modifying enzymes [56]. The CCCTC-binding factor (CTCF) is the most conserved and ubiquitous insulator protein, that regulates transcriptional domains by activation, repression, silencing and barrier activity [54]. In addition, some insulators are associated with gene silencing activities [57; 58].

CTCF is a multifunctional 11-zinc-finger transcriptional factor that binds to pentanucleotide motifs, such as CCCTC and CTCCC, and act as a transcriptional activator, a repressor or an insulator protein [59; 60]. There are seven conserved CTCF-binding domains in the HSV-1 genome (Figure 4) [52]. These CTCF-binding sites individually flank the latency-associated transcript (LAT) and the immediate early gene regions: CTRL2, located within the region encoding the LAT intron and containing nine copies of the CTCF motif “CTCCC”; CTRL1, located upstream of the LAT promoter near the unique long region with 23 copies of the CTCF motif; Cta′*m*, CTRS1, CTRS2, and CTRS3 located in the internal repeated sequences and CTUS1 located within the unique short region [52]. Each of these insulators is independently regulated and three of these CTCF-binding sites are occupied by CTCF during latency [61]. All together, these findings indicate that HSV-1 endogenous insulators are probably essential for preventing the rapid silencing of an ectopic promoter and must be taken into account during vector engineering.

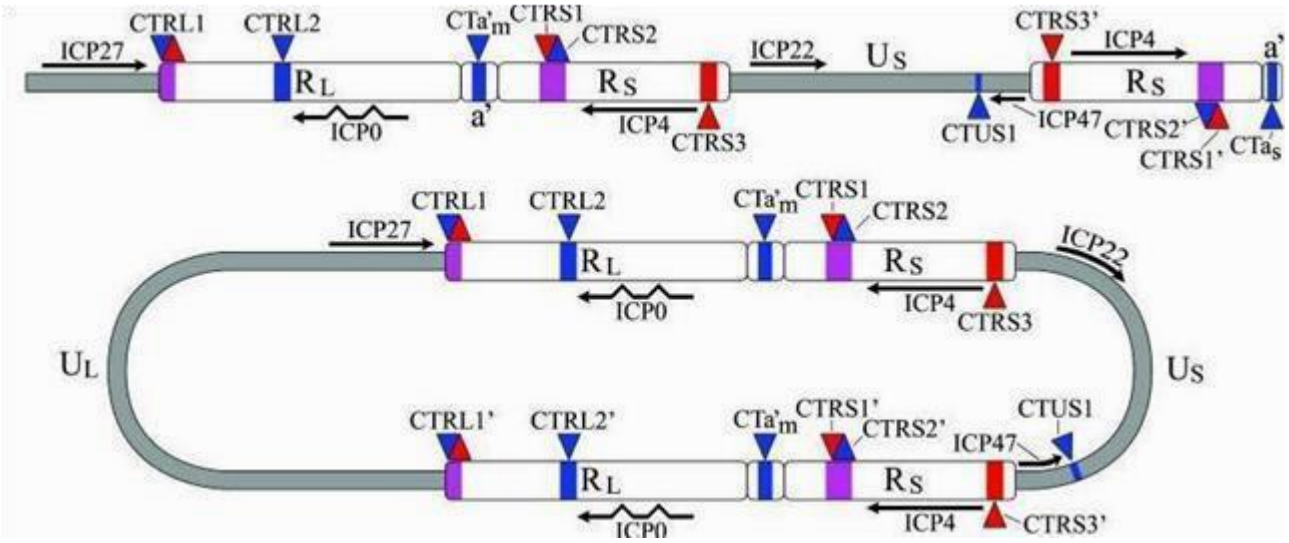

Figure 4: schematic representation of the CTCF-binding domains [52].

1.3.11 HSV-1 based viral vectors:

The manipulation of different classes of HSV-1 viral genes has led to the creation of three types of HSV-based vectors: amplicons, replication-defective vectors and replication-competent vectors (Figure 5) [62].

- **Amplicon vectors:** are HSV-1 virions carrying a concatameric plasmid DNA instead of the viral genome, which retains from wild-type HSV-1 virus the structural and the immunological features but also the infection spectrum. Amplicon vectors contain the *Escherichia coli (E.coli)* plasmid which typically includes: a HSV-1 origin for DNA replication (ori) and viral packing signals (pac); a bacterial origin of replication and antibiotic-resistance gene for propagation in *E.coli;* a fluorescence marker gene; and the transgene(s) of interest [63]. The almost total deletion of viral genes allows the insertion of up to 150 kb of foreign DNA. Amplicons are usually propagated in cells transfected with the plasmid and infected with HSV-1 helper virus, which provides the entire set of proteins to amplify and package the amplicon DNA in HSV-1 particles. Since the helper virus used is generally a non- replicative HSV-1 mutant, amplicon stocks are produced in trans-complemented cell lines [64]. However, the use of HSV-1 helpers determines the production of vector stocks contaminated by the helper virus, and the contaminating particles, even if defective, could have a significant cytotoxic effect and lead to the activation of the inflammatory response [65]. In vivo studies show that HSV amplicons released in the CNS can express their transgene for few weeks depending on the type of promoter. The expression is typically limited to a reduced number of cells [66;67].
- **Replication-defective vectors:** defective or non-replicative HSV-1 vectors are obtained by functional deletion of the α genes coding for the ICP proteins. In this case, virions are unable to start a productive lytic replication cycle both in vivo and in vitro. Replication-defective vectors are usually propagated in complementary cell lines that encode for the deleted genes. To date, there are several replication-defective vectors in which α genes are deleted in different combinations [68]. However, vectors stocks should be checked periodically, as there is a low but existing possibility that they can reacquire viral genes from complementary cells following homologous recombination.

- **Replication-competent vectors:** in this case the vectors are obtained by the deletion of non-essential genes or from their mutation, in order to make them conditionally active, e.g. responsive to drugs. In this way the virus will not be able to complete the lytic cycle unless in permissive cellular environments, such as that of the tumor cells. The removal of one or more non-essential genes significantly reduces pathogenicity. Their main use is in anti-tumor therapy where they act as oncolytic vectors [69].

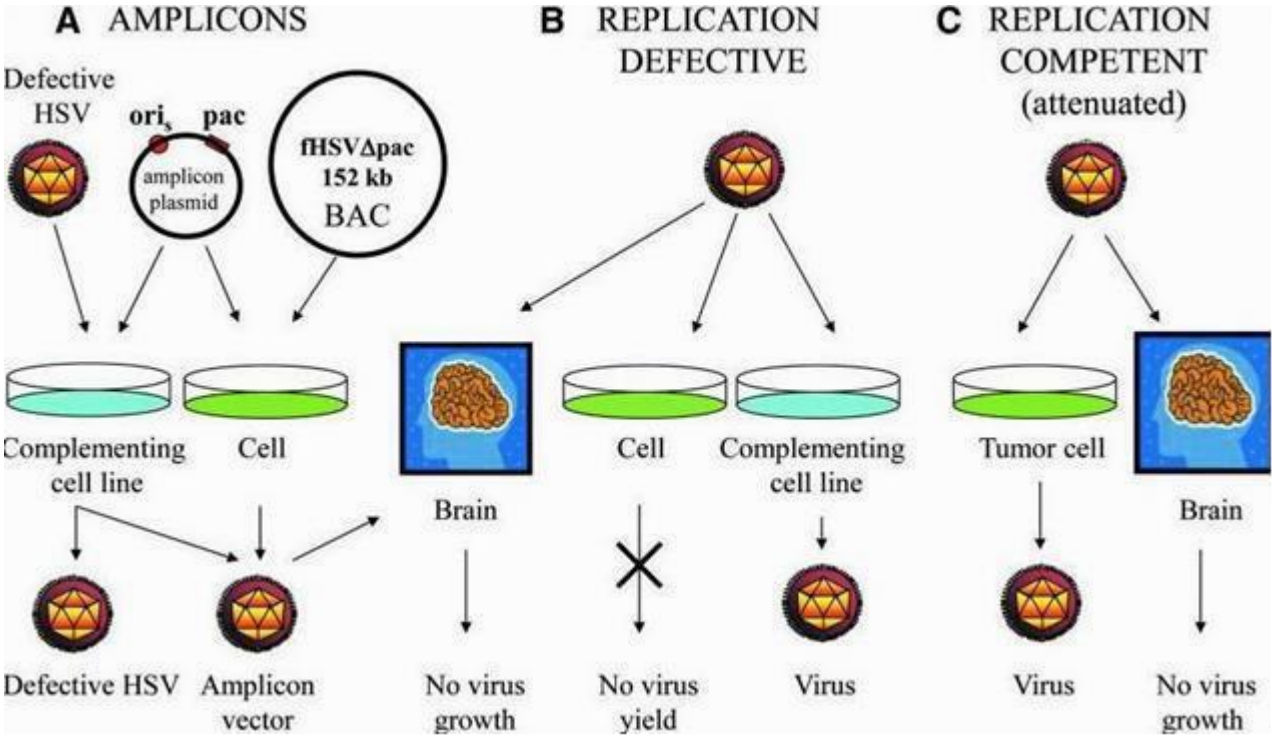

Figure 5: HSV vector design strategies [62].

Aims

This PhD project aimed at developing gene therapy tools close to readiness for clinical application in diseases of the central nervous system (CNS). CNS diseases represent an enormous unmet therapeutic need, not least because of the ageing population and because conventional pharmacological approaches are largely insufficient. Gene therapies provide a potential alternative. However, the currently used vectors present a series of drawbacks that limit their potential, including the possibility of insertional mutagenesis, or the small size of the viral genome that allows the introduction of only a single therapeutic gene per viral particle.

We focused our attention on vectors derived from Herpes Simplex type 1 for their enormous potential (described in the Introduction). Replication-defective vectors were developed in collaboration with Prof. Glorioso of the University of Pittsburgh, amplicon vectors in collaboration with BioViron (Lyon, France). We characterized these vectors considering all the key features that an optimal vector for CNS therapies should possess, namely:

- Efficacy of transgene expression
- Capacity to host large and/or multiple inserts
- Safety
- Lasting transgene expression
- Mechanisms to regulate expression

These essential features have been evaluated in the three works here presented.

a) Development of replication-defective HSV vectors that are totally replication defective, nontoxic and capable of long-term transgene expression in different brain regions.
b) Modulation of transgene expression in replication-defective HSV vectors by gene regulation elements.
c) Characterization and evaluation of four amplicon vectors in which transgenes are driven by different promoters.

3.1 Engineered HSV vector achieves safe long-term transgene expression in the central nervous system

SCIENTIFIC REPORTS

OPEN

Engineered HSV vector achieves safe long-term transgene expression in the central nervous system

Received: 7 December 2016
Accepted: 31 March 2017
Published online: 04 May 2017

Gianluca Verlengia[1,2], Yoshitaka Miyagawa[3,4], Selene Ingusci[1], Justus B. Cohen[3], Michele Simonato[1,2] & Joseph C. Glorioso[3]

Previously we reported a new series of highly defective herpes simplex virus type 1 (HSV-1) vectors that were functionally devoid of all viral immediately early (IE) genes, resulting in virtual absence of viral gene expression. Nevertheless, a reporter gene cassette inserted into the vector flanked by boundary elements from the viral latency locus showed high, persistent reporter gene activity in non-neuronal cells while an independent expression cassette inserted into a deleted ICP4 locus remained almost silent. In contrast to non-neuronal cells, we show here that the ICP4 locus cassette permitted robust reporter gene expression in a diversity of neurons following stereotactic injection of different rat brain regions; transgene expression in the hippocampus lasted up to 6 months and was essentially restricted to neurons. No evidence of neuronal cell toxicity or induction of inflammatory cell infiltrates was observed. An independent reporter gene cassette located in an intergenic region remained silent, indicating that the transgene promoter and/or insertion site are critical for sustained expression. These findings suggest the suitability of this vector for therapeutic intervention into diseases of the central nervous system that require the expression of large and/or multiple therapeutic transgenes.

Neurological diseases have an enormous medical and social impact and are without effective treatments. Gene therapies provide a potential means of genetic intervention but, in most cases, treatment requires the availability of high capacity non-integrating gene transfer tools that provide durable, regulated expression of large or multi-gene cassettes in specific neuronal cell subpopulations[1]. In addition, many diseases are autosomal dominant requiring either knock out or knock down of the mutant gene product and either repair or complement- ing gene addition. We suggest that HSV vectors provide the best opportunity to meet these complex demands since HSV vectors can accommodate large inserts and are well adapted for life-long persistence in neurons as non-integrating, circular episomes.

We recently created a safe, high capacity recombinant HSV vector that is highly stable, unable to replicate, but capable of persisting in human primary cells without evidence of cytotoxicity at very high multiplicities of infection[2]. This vector expresses extremely low levels of viral lytic genes that can be detected only by RT-PCR, a result of functional deletion of all immediate early (IE) genes. The reiterated joint region separating the unique long (U_L) and unique short (U_S) genome components is also removed, providing a total of ~25 kb of space for transgene insertion. The challenge has been to further engineer this vector to provide durable transgene expression in both neuronal and non-neuronal cell types since transgenes are rapidly silenced in the absence of expression of one of the IE genes, ICP0, due to heterochromatin formation[3,4]. We have recently overcome genome silencing through the application of moveable genetic elements from the latency-associated transcript (LAT) locus. These LAT locus-associated elements allow expression of non-viral transgene cassettes from the LAT or intergenic loci in non-neuronal cells without global activation of the viral genome[2].

[1]Section of Pharmacology, Department of Medical Sciences, and National Institute of Neuroscience, University of Ferrara, 44121, Ferrara, Italy. [2]Division of Neuroscience, University Vita-Salute San Raffaele, 20132, Milan, Italy. [3]Department of Microbiology and Molecular Genetics, University of Pittsburgh School of Medicine, Pittsburgh, PA, 15219, USA. [4]Present address: Department of Biochemistry and Molecular Biology, Nippon Medical School, Tokyo, Japan. Gianluca Verlengia andYoshitaka Miyagawa contributed equally to this work. Correspondence and requests for materials should be addressed to M.S. (email: michele.simonato@unife.it) or J.C.G. (email: glorioso@pitt.edu)

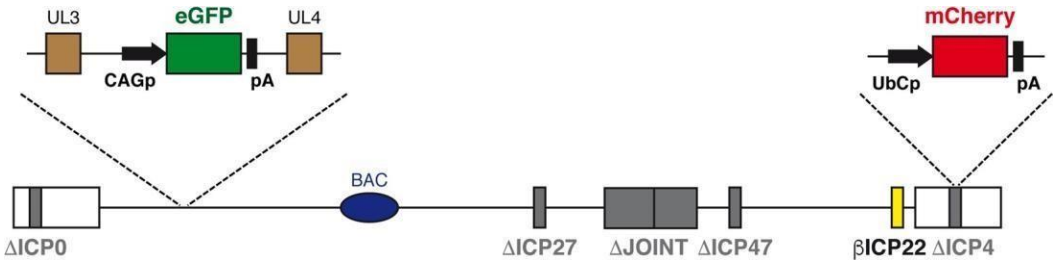

Figure 1. Graphic map of the JΔNI6 vector genome. The vector is deleted for the joint region, including the ICP47 promoter and translation initiation codon, and for the ICP0, ICP4 and ICP27 IE genes (Δ; gray boxes). Additionally, the ICP22 IE gene is converted to early-expression kinetics (β; yellow) by promoter TAATGARAT deletion. The vector hosts two expression cassettes for reporter genes: eGFP (green) between the U_L3 and U_L4 genes and mCherry (red) in the deleted terminal ICP4 locus. The eGFP gene is driven by the CAG promoter (CAGp), while the mCherry gene is driven by the ubiquitin promoter (UbCp). The BAC elements, including a chloramphenicol-resistance gene and β-galactosidase expression cassette, are located between *loxP* sites in the U_L37-U_L38 intergenic region.

Here, we report on a vector design that allows robust long-term transgene expression in neurons of the brain from a non-latency-related locus. Transgene cassette replacement of the essential ICP4 IE gene provided transgene expression for at least 6 months in rat hippocampus and transgene activity was readily documented in a variety of other brain regions that included caudate putamen, substantia nigra, and cortex. While this genomic region is normally transcriptionally silent in neurons, changes in vector genome organization and the use of a foreign promoter appeared to contribute to high transcriptional activity at this site. Vector inoculation at high doses in multiple brain regions did not induce neuronal damage or attract an inflammatory infiltrate. This is the first HSV vector capable of long-term innocuous transgene expression in the brain and offers a new, highly engineered prototype vector that can now be applied to brain gene therapies where large or multiple transgene cassettes are required to achieve a therapeutic outcome.

Results

Vector design. The genome structure of the previously described JΔNI6GFP vector employed in this study, referred to here as JΔNI6, is shown in Fig. 1 [2]. In this vector, the joint region, the ICP0, ICP4 and ICP27 IE genes, and the promoter and start codon of the ICP47 IE gene are deleted. In addition, the ICP22 IE gene is converted to early (β) expression kinetics by deletion of VP16-responsive promoter elements. The vector contains two expression cassettes for reporter genes: the enhanced green fluorescence protein (eGFP) gene inserted between the U_L3 and U_L4 genes under control of the CAG promoter, a strong synthetic promoter frequently used to drive high levels of transgene expression in mammalian cells; and the mCherry gene driven by the ubiquitin C (UbC) promoter inserted into the deleted ICP4 locus in the right terminal repeat. Bacterial artificial chromosome (BAC) genes allowing viral genome replication in bacteria, a chloramphenicol-resistance gene, and a β-galactosidase expression cassette are located between *loxP* sites in the U_L37-U_L38 intergenic region (Fig. 1). The genome also contains 2 mutations in the glycoprotein B (gB) gene previously shown to accelerate infection[5].

Transgene expression. We first monitored transgene expression *in vivo* following injection of the dentate gyrus of the dorsal hippocampus with 2 μl of a solution containing 1×10^5 plaque-forming units (pfu) of JΔNI6, corresponding to ~2.5×10^8 genome copies (gc) (Fig. 2A,B). Diffusion of the vector was estimated by analyzing the presence of mCherry-positive cells in a broad span of coronal sections prepared at multiple levels, anterior to posterior of the injection site, from animals sacrificed 2 months after vector injection. We detected mCherry fluorescence in a range of more than 3 mm (Fig. 2C). It is likely that this is an underestimation of vector diffusion, because (i) transgene expression may occur in only a subset of infected cells and (ii), more importantly, we examined in this experiment intrinsic mCherry fluorescence, which can be detected only in cells producing relatively high levels of the reporter protein (see below and Fig. 4). Together, these data show that the vector can spread, infect cells, and induce robust transgene expression in an area of more than 3 mm in diameter. This is consistent with data reported by others for smaller vectors such as those based on adeno-associated virus (AAV)[6].

To determine the time-course of transgene expression, JΔNI6 was injected into the hippocampus as above and animals were killed at different time points to examine eGFP and mCherry fluorescence (Fig. 3). We observed essentially no eGFP fluorescence. This was not due to loss of signal caused by the fixation procedure, because eGFP was easily detected after injection of other backbones and identical fixing procedures. In contrast, mCherry fluorescence was robust, peaking at 2 weeks post injection and remaining high for at least 6 months, the final time-point of the analysis (Fig. 3). A distinct mCherry signal was observed not only in cell bodies, but also in dendrites and axon terminals (Fig. 3C–E). This pattern of expression gradually subsided after 2 weeks, becoming apparently restricted to dentate gyrus cell bodies and proximal dendrites at 6 months.

A decline in expression levels may be due to vector toxicity (causing death of infected cells) or to reduced levels of transgene expression. In order to address this question and maximize the sensitivity of mCherry detection, we used brain sections from animals sacrificed 4 weeks or 6 months after JΔNI6 injection to compare the pattern of intrinsic mCherry fluorescence with that of mCherry immuno-fluorescence (IF). As expected, the IF signal was greater than the intrinsic signal. However, whereas only a slightly greater signal was observed at 4 weeks, a

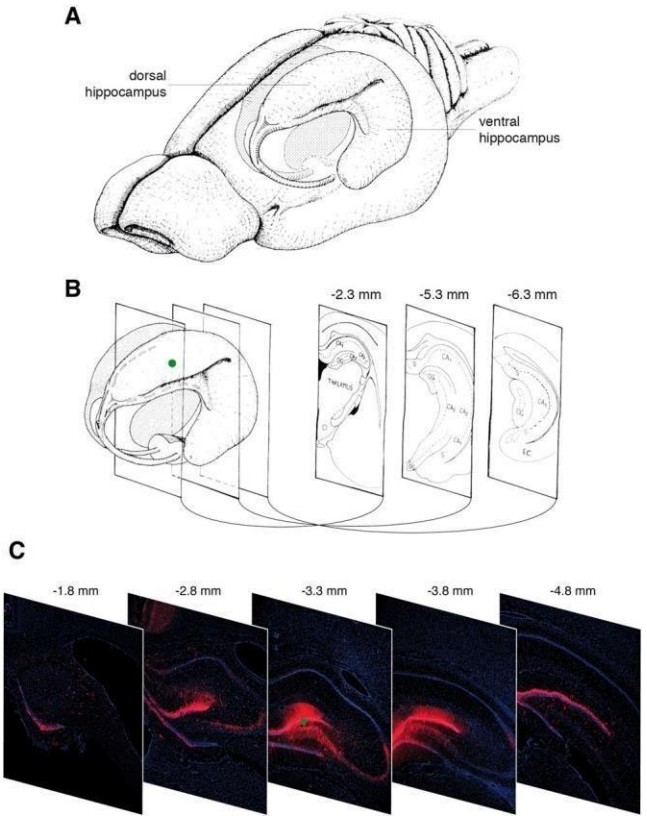

Figure 2. Distribution of cells expressing the mCherry reporter gene. (**A**) Drawing of the rat brain showing the three-dimensional organization of the hippocampus. (**B**) Coronal sections across the hippocampus. Three coronal sections through the hippocampus are shown at the right, including their anteroposterior coordinates relative to bregma. At the left, the green dot indicates the site of JΔNI6 injection. (**C**) Representative images of coronal sections from animals killed 2 months after JΔNI6 injection. Five coronal sections through the hippocampus are shown with their anteroposterior coordinates relative to bregma. Native mCherry fluorescence in red; nucleistained with DAPI in blue. The green dot in the central image indicates the site of JΔNI6 injection. Panels A and B are adapted from Fig.1 of Amaral and Witter[23] with permission from Elsevier.

substantially greater signal was observed at 6 months (Fig. 4A,B). Quantification revealed that the IF signal was approximately 60% greater than the intrinsic signal at 4 weeks, but some 5 times (500%) greater at 6 months (Fig. 4C). Whereas the decay of the intrinsic signal between 4 weeks and 6 months was approximately 85%, the IF signal declined by less than 50% in this interval (Fig. 4D). These data suggest that the reduction in nativemCherry fluorescence over time observed earlier was due to reduced levels of transgene expression rather than cell death. Toidentify the cell types in which the vector could induce transgene expression, we performed double staining with NeuroTrace, a method for visualizing nuclei and soma of neurons based on a fluorescent dye selective for the Nissl substance of neurons. In sections prepared from animals killed 2 months after JΔNI6 injection into the dorsal hippocampus, we observed overlapping mCherry and NeuroTrace signal in granule cells but not in CA3, where mCherry was in granule cell terminal axons (the mossy fibers) but not in pyramidal cell somas (Fig. 5). Essentially all mCherry-positive cells were NeuroTrace positive, indicating that neurons were the prevalent cell type expressing the transgene (Supplementary Fig. S1).

Finally, we analyzed mCherry expression following injection of JΔNI6 in other brain areas. We chose areas that are thought to play key roles in neurological and psychiatric disorders: the prefrontal cortex (schizophrenia, Alzheimer's disease), striatum (Huntington's and Parkinson's disease), Maynert nucleus (Alzheimer's disease) and substantia nigra (Parkinson's disease). Robust transgene expression was observed in each of these areas (Fig. 6), indicating that the JΔNI6 backbone may have utility for multiple disease conditions.

Safety. Since previous generations of HSV vectors were hampered by immunogenicity and toxicity to infected cells, we evaluated these responses to JΔNI6 inoculation. It is well documented that ICP0 is a leading cause of replication-defective HSV-1 cytotoxicity[7,8], and we therefore rescued ICP0 in a closely related vector without eGFP gene (JΔNI5)[2] to serve as a positive experimental control for the detection of vector toxicity (JΔNI5R0 vector). We tested lymphocyte infiltration, oxidative stress and apoptosis in animals killed one week after vector injection by staining for appropriate markers, respectively CD45, inducible nitric oxide synthase (iNOS or NOS-2) and activated caspase 3. This early time-point was chosen because these different adverse events tend to become less pronounced during the second week after injection of previous-generation vectors[9], observations

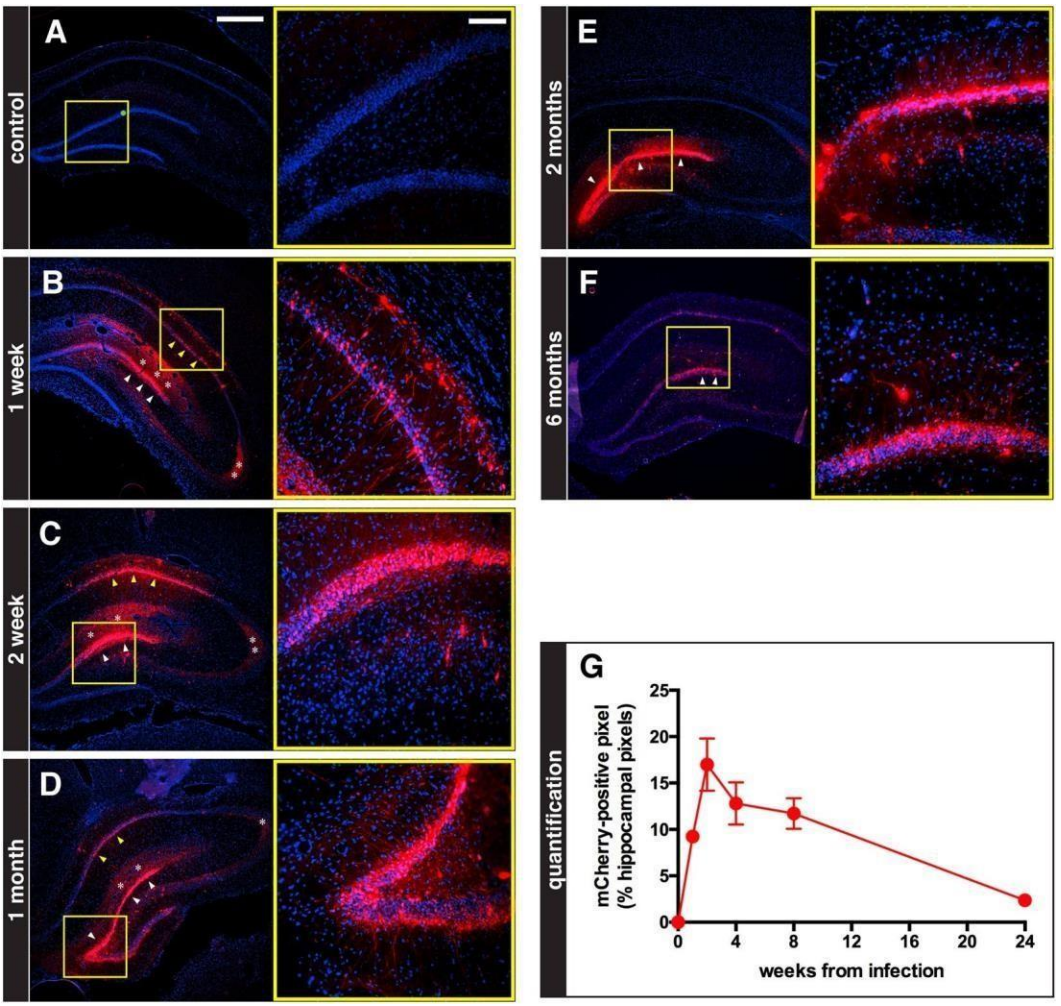

Figure 3. Time course of mCherry expression in the hippocampus. (**A**–**F**) Representative images (5 sections/animal, 4 animals/group) of coronal sections from animals killed at the indicated time-points after JΔNI6 injection into the right hippocampus (see Materials and Methods for details). Left panels show low magnification images, right panels higher magnifications of the areas framed in yellow in the left panels. These sections were at an antero-posterior level immediately adjacent to the site of injection near the upper blade of the dentate gyrus granular layer (needle tip always located at the green spot shown in the left panel of (A). Native mCherry fluorescence in red; nuclei stained in blue with DAPI. Robust mCherry fluorescence is seen in dentate gyrus cells (white arrowheads) and in CA1 neurons (yellow arrowheads); a distinct mCherry signal can be observed in dendrites and axon terminals (white asterisks indicate dentate gyrus granule cell dendrites and terminals). Horizontal bar in (**A**) left panel (for all left panels) = 500 μm; horizontal bar in (**A**) right panel (for all right panels) = 100 μm. (**G**) Quantification of the time-course of native mCherry signal in the hippocampus. Data are the means ± s.e.m. of 4 animals per group.

that we confirmed in preliminary experiments with the JΔNI5R0 vector. Our results at 1 week post vector injection showed many marker-positive cells in brains injected with JΔNI5R0, whereas brains injected with JΔNI6 were almost completely negative (Fig. 7A–C). In addition, we examined neuroinflammatory effects by analyzing microglia activation using Iba1 immunostaining. Microglia activation was observed 1 week post JΔNI5R0 injection, but not after injection of JΔNI6 (Supplementary Fig. S2). Activation was no longer observed at 1 month.

Finally, we explored neuronal damage using fluoro-jade C (FJC), a fluorescent dye that labels degenerating neurons. Again, these experiments were performed in animals killed one week after vector injection into the hippocampus and in comparison with JΔNI5R0. Of note, the JΔNI5R0 virus in this and the previous experiment was deleted for the BAC region while JΔNI6 was not; we previously reported that removal of the BAC region eliminated residual toxicity of our IE gene-depleted vectors for human fibroblasts in culture[2]. Whereas many FJC-positive cells were observed in brains injected with JΔNI5R0, virtually none were detected in JΔNI6-injected brains (Fig. 7D,E). We cannot fully explain the observation of FJC-positive cells and elongations that were not mCherry positive, but these may reflect indirect damage by JΔNI5R0 caused by lymphocyte infil- tration or oxidative stress. In time, neuronal damage induced by JΔNI5R0 resulted in a dramatic cell loss with obvious hippocampal degeneration at 1 month, whereas no hippocampal shrinkage was observed with JΔNI6

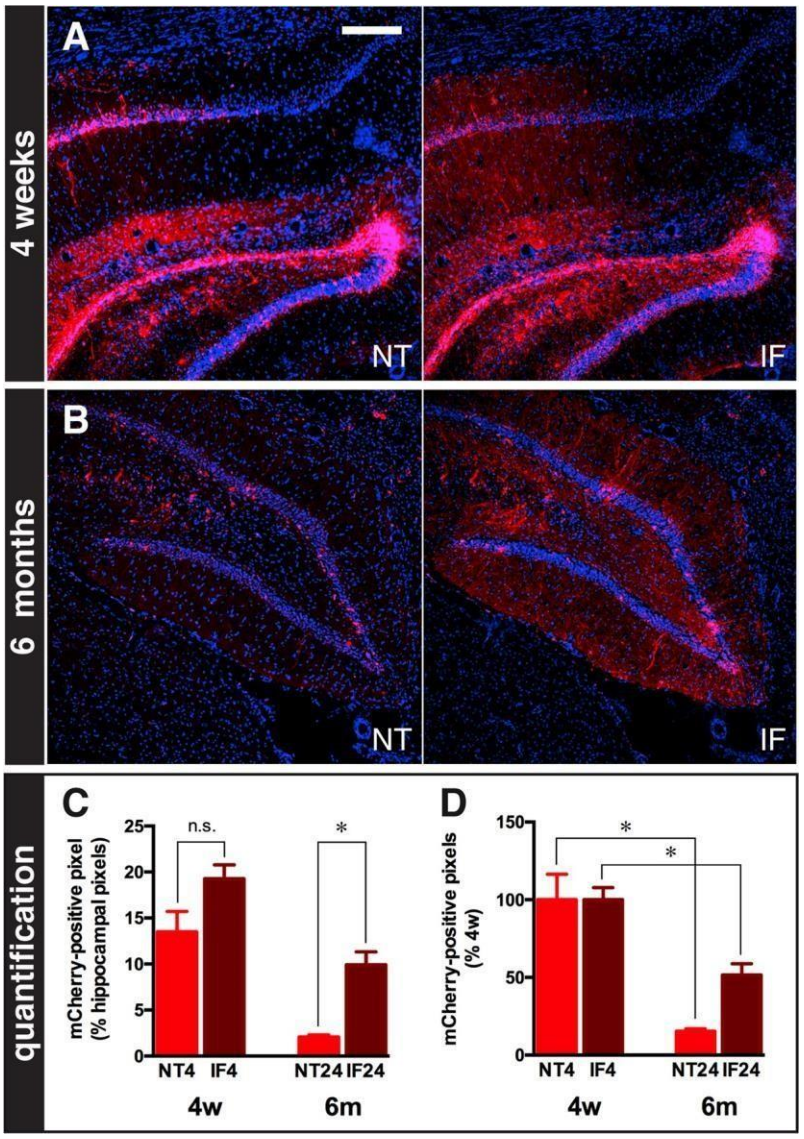

Figure 4. Comparison of native (NT) and immune-fluorescence (IF) mCherry signals. (**A**,**B**) Representative images (5 sections/animal, 4 animals/group) of coronal sections from animals killed 4 weeks (**A**) or 6 months (B) after JΔNI6 injection. NT and IF signals, both in red, are shown for the same fields. Nuclei are stained in blue with DAPI. Size bar (all panels) = 100 μm. (**C**) Quantification of NT (bright red) and IF (dark red) mCherry signals at 4 weeks (4 w) and 6 months (6 m). **(D)** Relative decay of NT (bright red) and IF (dark red) mCherry signals between 4 weeks (4 w) and 6 months (6 m). Data are the means ± s.e.m. of 4 animals per group. n.s., not significant; *$P < 0.05$, Mann-Whitney U test.

(Supplementary Fig. S3). Together, these data support the notion that JΔNI6, even with an intact BAC region, is devoid of detectable immunogenicity and toxicity to infected cells.

Discussion

Several hurdles must be overcome before gene therapy becomes a standard procedure for the treatment of neurological diseases. Indeed, while therapeutic gene transfer with AAV and lentivirus (LV) vectors has recentlyenjoyed considerable success for the treatment of peripheral diseases, to the point that some of these have gained approval for clinical use in Europe (Glybera), gene therapies for the central nervous system (CNS) have proved more difficult. First, they often require the delivery of large genes or complex multigene cassettes that greatly exceed the capacity of LV and AAV vectors[1]. To accommodate larger payloads, larger viruses such as adenovirus (AdV) and HSV would be required. Although AdV vectors have limited capacity, "gutted" derivatives can incorporate up to 30 kb of foreign sequences[10]. However, gutted AdV vectors are typically contaminated with small percentages (but large particle numbers) of helper virus, and these contaminants engender antiviral responses that limit transgene expression, cause local inflammation and induce antiviral immunity impeding vector re-administration. Second, the ideal CNS vector should deliver to specific cell types after being injected into a highly heterogeneous tissue,

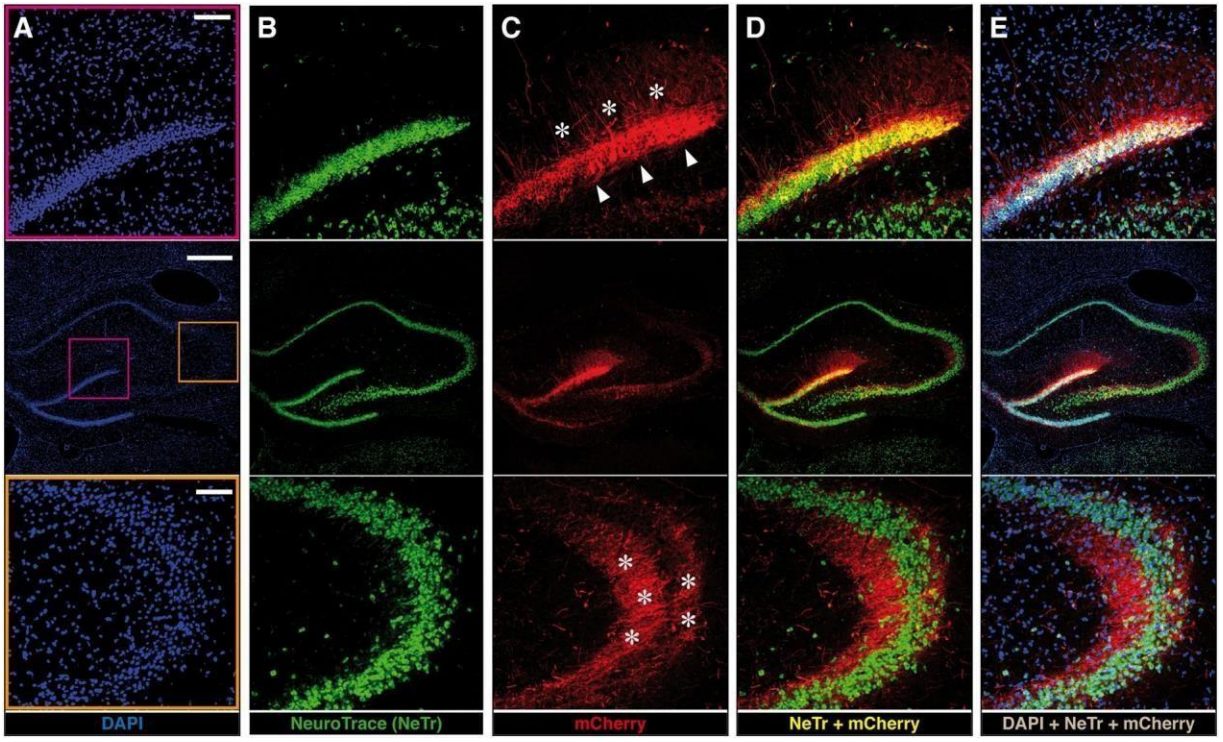

Figure 5. Localization of mCherry expression in the hippocampus. Representative images (5 sections/animal, 4 animals/group) taken from coronal sections prepared from animals killed 2 months after JΔNI6 injection into the right hippocampus. Middle panels show low magnification images of the whole hippocampus; upper panels show higher magnifications of the dentate gyrus including the granular layer (site of granule cell somas), framed in pink in the middle panel A; lower panels show higher magnifications of the CA3 areas (site of the axon terminals originating from the granule cells), framed in orange in the middle panel A. (**A**) Nuclei, stained in blue with DAPI. (**B**) Nuclei of neurons, stained in green with neurotrace. (**C**) Native mCherry florescence (red). Arrowheads, mCherry signals in granule cell bodies; asterisks, mCherry signals in dendrites (upper panel) and axon terminals (lower panel). (**D**) Neurotrace and mCherry double-fluorescence. Note overlapping signal (yellow) in granule cells (upper panel) but not in CA3 pyramidal cells (lower panel). (**E**) DAPI, neurotrace and mCherry triple-fluorescence. Note overlapping signal (white) in granule cells (upper panel) but not in CA3 pyramidal cells (lower panel). Also note that non-neuronal cells (blue nuclei) do not express mCherry. Horizontal bar in (**A**) (middle panel), 500 μm; horizontal bar in (**A**) (upper and lower panels), 100 μm.

Since failure to do so can lead to adverse or paradoxical effects[11]. Third, vectors whose genomes integrate into the host cell DNA can lead to transformation events that may result in harm to the patient.

Vectors derived from AAV, LV or AdV do not combine all features necessary for CNS applications. In principle, HSV is an attractive alternative, having a genome of 152 kb, ~25 kb of which can be deleted to accommodate up to 30 kb of foreign sequences. Moreover, the virus genes are expressed in a cascade fashion, such that deletion of the first expressed IE genes completely shuts down viral gene expression and replication. Finally, HSV does not integrate its DNA into the host cell genome like LV vectors, eliminating the risk of insertional mutagenesis. In spite of these advantages, HSV has thus far been relatively overlooked because of concerns over cytotoxicity, immunogenicity, and difficulty in achieving persistent expression in the CNS. The new generation of HSV vector designs described here and elsewhere[2] overcomes these problems while maintaining the ability to host large payloads of non-viral genes.

It has previously been shown that inactivation of all IE genes eliminates HSV cytotoxicity[12–14]. The present study expands these observations to the brain, documenting the absence of neurotoxicity and lymphocyte infiltration while confirming that ICP0 is a key inducer of both. Although amplicon vectors do not express any HSV gene, they are still toxic and pro-inflammatory, likely due to contamination with a low percentage but large number of helper viruses expressing ICP0 and other toxic IE proteins[15]. Elimination of ICP0 has proven problematic, however, since ICP0 counter-acts heterochromatinization of the viral genome[4] and is thereby essential for the maintenance of transgene expression in most cell types. We recently reported that genetic elements associated with the LAT gene can compensate to a degree for the absence of ICP0 in non-toxic vectors by protecting an embedded reporter gene from rapid silencing in non-neural cells[2], potentially by blocking heterochromatin encroachment. In the same study, we noticed that transgenes outside this protective environment, while silent in most cells, were active in sensory neurons for several days. The essential observation in the present study is that a reporter expression cassette in the ICP4 locus escaped global silencing of an IE gene-depleted HSV genome in CNS neurons for at least 6 months. A second reporter gene was silent throughout and we observed no overt

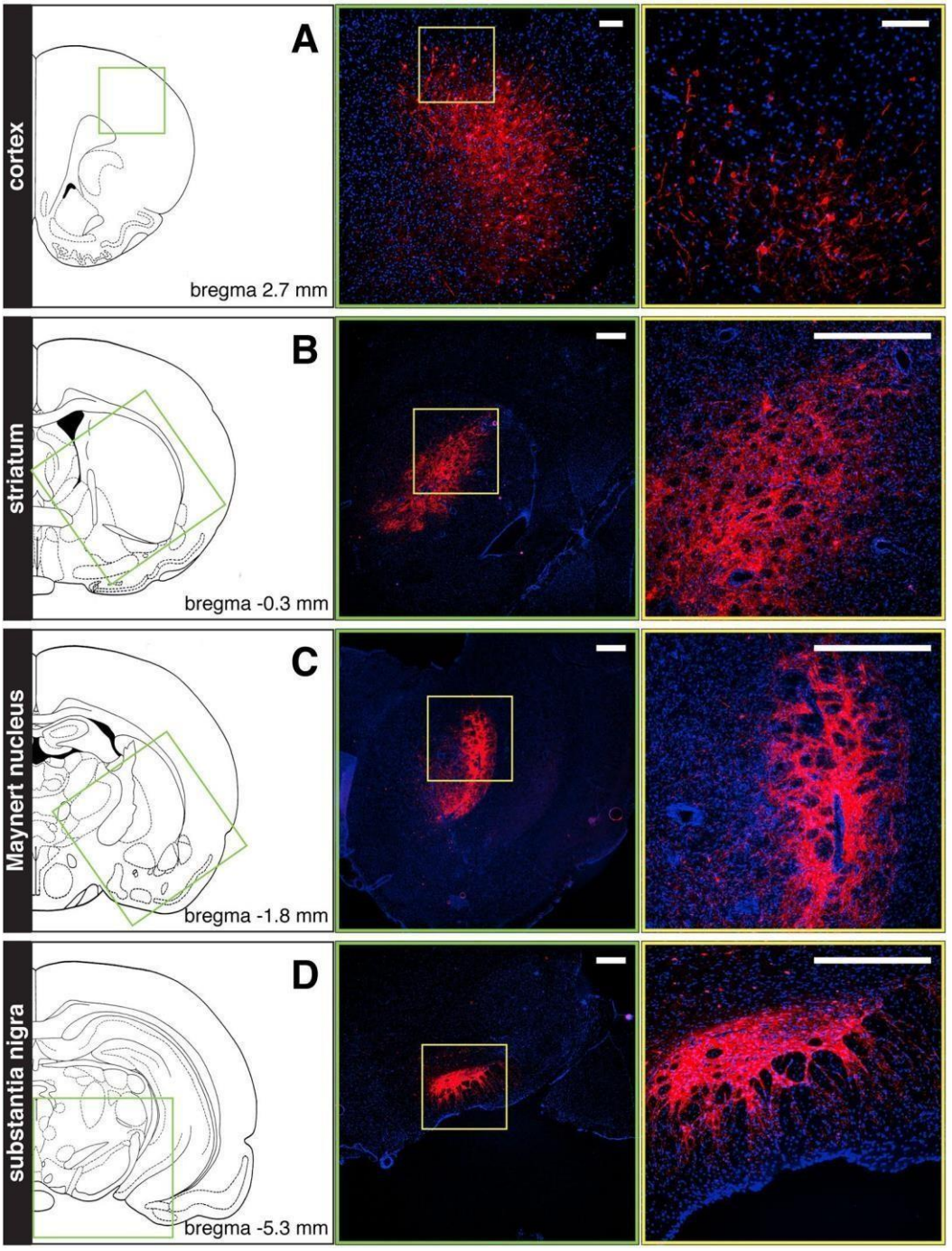

Figure 6. Transgene expression in different brain areas. Representative images (5 sections/animal, 4 animals/group) taken from coronal sections prepared from animals killed 2 weeks after JΔNI6 injection into the prefrontal cortex (**A**), striatum (**B**), Maynert nucleus (**C**) or substantia nigra (**D**). Native mCherry fluorescence in red; DAPI-stained nuclei in blue. Left panels are schematic drawings (adapted from Paxinos and Watson[22] with permission from Elsevier) of the brain structures at the level of vector injection; anteroposterior coordinates relative to bregma are indicated. Central panels are images of sections corresponding to the area framed in green in the corresponding left panel. Right panels are higher magnifications of the areas framed in yellow in the corresponding central panel. Horizontal bars in **A** = 100 µm; horizontal bars in **B**–**D** = 500 µm.

signs of toxicity or an immune response in vector-injected animals, arguing against genome-wide transcriptional derepression. These results raise the expectation that a safe and effective vector system for the delivery of large or multiple therapeutic transgenes for CNS disorders is within reach.

At this time we do not have a mechanistic explanation for the observation of sustained expression of mCherry, but not eGFP, in JΔNI6-infected CNS neurons. While potential differences in the stabilities of mCherry and eGFP mRNA and protein in these cells could be contributing factors, the more plausible hypothesis may be that

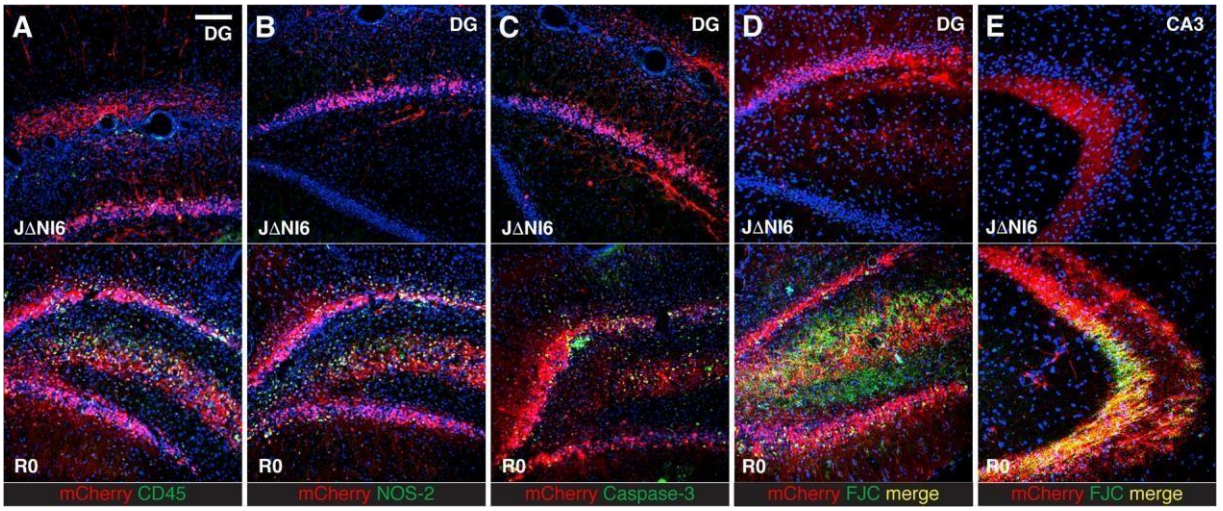

Figure 7. Safety of the JΔNI6 vector. Comparative effect of the JΔNI6 vector (upper panels) and the R0 vector (lower panels) on lymphocyte infiltration detected with anti-CD45 antibody (**A**), oxidative stress detected with anti-NOS-2 (**B**), apoptosis detected with anti-activated caspase 3 (**C**), and neuronal damage detected using fluoro-jade C (FJC, **D**–**E**). Animals (4 per group) were killed 1 week after vector injection into the hippocampus, and images were taken at the level of the dentate gyrus (DG), near the site of vector injection (**A**–**D**) and in the CA3 area, site of axon terminals from dentate gyrus granule cells (**E**). Native mCherry fluorescence in red; nuclei stained in blue with DAPI; CD45, NOS-2, caspase-3 and FJC staining in green in panels (A, B, C, and D, E), respectively. Horizontal bar in (**A**) (for all panels) = 100 μm.

the choice of transgene promoter and/or insertion site are critical for sustained expression. Further studies are ongoing to distinguish between these alternative possibilities.

Our data indicate that the mCherry gene was expressed in neurons, but not in astrocytes. Co-visualization of neurons (using NeuroTrace) and mCherry fluorescence showed hundreds of double-positive cells per field, but no mCherry-positive, NeuroTrace-negative cells. This result suggests that mCherry expression in astrocytes was at best orders of magnitude lower than in neurons. It will be of interest to determine whether this is a function of the transgene promoter (see below).

We found that JΔNI6 can induce transgene expression in multiple brain areas that are relevant to neurological diseases, including Parkinson's, Alzheimer's and several forms of epilepsy. The dramatic difference in both the level and duration of neuronal expression of the two transgenes of JΔNI6 raises several questions: (1) What is responsible for these differences, the promoter, the location of the expression cassette in the viral genome, or both? (2) If, as we suspect, location of the expression cassette is important, are there neuron-specific anti-silencing elements in the vicinity of the ICP4 locus? These may include regions enriched in CTCF-binding motifs flanking the ICP4 deletion in JΔNI6 on both sides[2,16] or yet unknown sequences. Of interest, it has been reported that transcriptional activity from an IE gene-depleted vector tends to be higher in neuronal cells in the repeat segments of the HSV genome than in the unique regions[17], but the mechanism is unknown. Examination of transgene expression from other loci in the viral repeats may reveal whether the sustained mCherry expression we see is a unique property of the ICP4 locus or more generally of locations with the repeats. (3) Can transgene expression from the ICP4 locus be switched to a different cell type using a cell-type-specific promoter or will this require additional manipulations to protect the site from heterochromatinization? Answers to these questions may provide the framework to expand the utility of our vectors to other cells of the CNS.

Our vector injection technique accomplished relatively broad transgene expression, spanning a distance of more than 3 mm across the injection point. It is likely that the vector spreads even more broadly because our distance estimate was based on detection of intrinsic mCherry fluorescence, i.e., of cells expressing the transgene at high levels; we have shown that additional infected cells can be detected by immunohistochemistry. While vector spread in the range we observed is perfectly suitable for studies in small rodents, translation to human diseases will require scale-up modeling in larger animals, such as mini-pigs or primates. Options are to design needles with multiple holes, to increase volumes and titers of vector injected, and/or to use convection-enhanced delivery systems for infusion[18,19]. Moreover, it may be possible to increase the efficiency of vector delivery to neurons by viral glycoprotein engineering to avoid virion attachment to other cells[20].

In conclusion, we report here a new generation of vectors that overcome the major limitations of HSV as a gene delivery vehicle for CNS disorders, namely short-term transgene expression and toxicity, while maintaining its advantages, in particular the ability to host large and/or multiple transgenes. These features represent a pivotal step forward in the development of vectors capable of selective expression of a single large therapeutic gene or entire regulatory networks in CNS neurons. Before first-in-man clinical experiments, however, remaining hurdles must be overcome. Aside from the need to increase virus spread in the injected brain, these include potential responses to re-dosing and inoculation of immunized individuals. Assuming these hurdles can be overcome in the future, our vectors may prove valuable for therapeutic intervention in the variety of diseases of the CNS that

require the expression of large and/or multiple therapeutic transgenes. In parallel, a better understanding of the mechanism(s) that allow persistent JΔNI6 reporter gene expression in neurons may lead to further improvements in vector design to benefit the treatment of CNS pathology.

Methods

Vector engineering. JΔNI6, previously referred to as JΔNI6GFP, was as described[2]. JΔNI5R0 was derived from JΔNI5, which is JΔNI6 without the eGFP expression cassette. A 7.5-kb *Dra*I-*Psi*I fragment spanning the ICP0 locus deletion in JΔNI5 was isolated from purified KOS-37 BAC DNA and cloned into pCRBlunt to generate plasmid pCRBluntICP0. The kanamycin-resistance gene flanked by an I-*Sce*I restriction site [I-*Sce*I-*aphAI* fragment[2]] was amplified from pEPkan-S2[21] [kindly provided by N. Osterrieder, Free University of Berlin, Berlin, Germany] by PCR with primers R0f and R0r specified below, providing terminal *Mfe*I restriction sites, and the *Mfe*I-digested product was cloned into the unique *Mfe*I site of pCRBluntICP0. The complete pCRBlunt insert was isolated and recombined with JΔNI5 DNA by Red-mediated recombination in *Escherichia coli*, essentially as described[2, 21], and the *aphAI* gene was removed by I-*Sce*I induction, also as described[2, 21]. Accurate repair of the ICP0 locus was confirmed by field inversion gel electrophoresis of restriction enzyme-digested BAC DNA, diagnostic PCR, and targeted DNA sequencing. Recombinant BAC DNA was converted to infectious virus by transfection of U2OS-ICP4/27 cells[2]. ICP0 expression was confirmed by Western blot analysis ofinfected U2OS cells.

Primer R0f:

5′-TATCAATTGCGCAACACCTGCCCGCTGTGCA ACGCCAAGCTGGTGTACCTGATAGTGGGAGG ATGACGACGATAAGTAGGGATA-3′

Primer R0r:

5′-AATCTGCAGCAATTGCTACAACCAATTAACCAATTCTGATTAG-3′

Virus production. HSV vectors were propagated on U2OS-ICP4/27 cells in T150 tissue culture flasks. Twenty-four h before infection, cells were seeded as a 50% confluent monolayer to reach a confluence of 90–100% the following day. Cells were infected in serum free medium at a multiplicity of 0.0001 plaque-forming units (pfu) per cell and incubated at 33 °C in 5% CO_2. After 5–7 days, the supernatant was collected and sequentially filtered through a 0.8 and a 0.45 μm nitrate cellulose membrane, and the virus was concentrated by high-speed centrifugation (45 min at 19,000 rpm in a JA-20 rotor). The viral pellet was re-suspended in phosphate-buffered saline (PBS) and stored at −80 °C in small aliquots. The JΔNI5R0 virus used in this study was deleted for the BAC region by passage through U2OS-ICP4/27-Cre cells, as described[2].

Virus titration by qPCR. Viral DNA was extracted with the DNeasy Blood and Tissue Kit (Qiagen, Hilden, Germany) according to the manufacturer's instructions. Quantitative (q) PCR was performed using the BioRad (Hercules, California, USA) CFX PCR System with customized primers and probe (BioRad) specific for the HSV glycoprotein D (gD) gene[2]. Viral genome copies were quantified by interpolation of a standard curve generated by tenfold serial dilution of a gD gene-containing plasmid of known concentration.

***In vivo* HSV injection.** Under ketamine (90 mg/kg i.p.) and xylazine (13 mg/kg i.p.) anesthesia, a total of ~2.5×10^8 viral genome copies were inoculated into the selected brain regions of Sprague Dawley male rats (300g; Harlan, San Pietro al Natisone, Italy). The stereotactic coordinates for inoculation, based on the Paxinos atlas[22], were as follows(0 bregma): dorsalhippocampus AP −3.5, ML+2.1, DV −3.5; prefrontalcortex AP +3, ML+2.5, DV −3; striatum AP +1.5, ML −2.7, DV −5.5; nucleus basalis of Maynert AP −1.3, ML +2.4, −7; substantia nigra AP −4.8, ML −2.4, DV −8.2. The viral vectors were injected by stereotactic implantation of a borosilicate glass needle, custom-made with a laser microdissector (CTR6000; Leica Microsystems, Wetzlar, Germany). The needle tips were chamfered through laser cutting (angle: 45 degrees; inner diameter at the tip: 60 μm; outer diameter at the tip: 80 μm) and an additional hole (diameter 10 μm) was opened 100 μm above the tip, to favor the spread of the injected solution. The needle was bottom-filled with the viral prepatration and linked to a microperfusion pump, in order to inject a total of 3 μl solution at a flow rate of 0.2 μl/min. These experiments were performed at the University of Ferrara in compliance with the guidelines for the ethical treatment of experimental animals (authorization from the Italian Ministry for Health D.M. 246/2012-B).

Tissue preparation. At the selected time points following vector injection, animals were deeply anesthetized with pentobarbital and perfused with 4% paraformaldehyde in 0.1 M PBS. Brains were isolated and postfixed in 4% paraformaldehyde for 1 h, then cryoprotected in 30% sucrose at 4 °C until tissue sank, and finally flash-frozen in isopentane chilled to −80 °C.

Native mCherry imaging and quantification. Frozen brains were cut into 20 μmthick coronal sections in a cryostat (Leica Microsystems). For direct imaging of native mCherry fluorescence, slices were immediately counterstained for nuclei with Pro-Long Gold antifade reagent with 4′,6-diamidino-2-phenylindole (DAPI; Thermo Fisher, Waltham, MA, USA) and mounted on microscope glass slides for observation. Image analy- ses were conducted using a DMRA2 microscope (Leica Microsystems), equipped with the Metamorph Image Analysis software (Universal Imaging Inc., Downingtown, PA, USA).

Immunofluorescence. Twenty μm coronal sections were cut at −20 °C in a cryostat, rinsed in 0.1 M PBS and blocked in 0.1 M PBS with 10% normal goat serum and 0.3% Triton X-100. Sections were then incubated overnight at 4 °C with primary antibodies dissolved in blocking solution: rabbit anti-mCherry (Thermo Fisher, 1:100); rabbit anti-cleaved caspase-3 (Cell Signaling, Danvers, MA, USA, 1:100); rabbit anti-nitric oxide synthase-2 (Santa Cruz, Dallas, TX, USA, 1:100); mouse anti-CD45 (Santa Cruz, 1:100); rabbit anti-Iba1 (Synaptic Systems, Gottingen, Germany, 1:200). The next day, sections were incubated with secondary antibodies for 2 h at room

temperature, as follows: Alexa Fluor 488 goat anti-rabbit (Molecular Probes, Eugene, OR, USA), 1:1,000; Alexa Fluor 488 goat anti-mouse (Molecular Probes), 1:1,000. In addition, 10 μM DAPI (Molecular Probes) was added to the secondary antibody solution in order to label cell nuclei.

NeuroTrace staining. After rehydration in 0.1 M PBS, sections were permeabilized with 0.1% Triton X-100 in PBS for 10 min, washed twice for 5 min in PBS and stained with NeuroTrace 640/660 Deep Red Fluorescent Nissl stain (ThermoFisher; dilution 1:200), for 20 min at room temperature. Sections were then washed in PBS and 0.1% Triton X-100, twice with PBS, and finally left for 2 h at room temperature in PBS before imaging.

FluoroJade-C staining. Cryostat brain sections were mounted on frosted microscope slides and pretreated for 5 min by immersion in 80% EtOH and 1% NaOH, followed by 2 min in EtOH 70% and 2 min washing in distilled water. These sections were then incubated for 10 min in 0.06% $KMnO_4$ and rinsed in distilled water for 3 min, before incubation for 10 min in a solution of 0.0001% FluoroJade-C (Immunological Sciences, Rome, Italy) and 0.1% acetic acid. After three washes in distilled water for 1 min, slides were dried, dehydrated with xylene, and coverslipped with DPX mountant for microscopy (Sigma, Saint Louis, MO, USA).

Quantification and statistical analysis. Images of the hippocampus were captured using a Hamamatsu C11440 camera (Hamamatsu, Japan) mounted on a Leica DMRA2 microscope, in 2^{16} gray levels. Using the Metamorph software, the area of the hippocampus was selected as the region of interest (ROI) and the minimum and average gray levels within the ROI were calculated. mCherry-positive pixels were identified by thresholding at the gray level corresponding to the mean plus the difference between average and minimum. Using this approach, only those pixels that were significantly above background (i.e., mCherry-positive) were selected. Data were then expressed as percent of mCherry-positive pixels over total hippocampal pixels. Five sections per animal were analyzed, one in every five 20 μm sections cut across the injection site, i.e., one every 100 μm with the 3rd at the site of injection. Numbers from these 5 sections were used as quintuplicates, i.e., the average was used for statistical analysis. Confocal images were captured using a HAL 100 camera (Zeiss, Oberkochen, Germany) mounted on a Zeiss LSM510 confocal microscope.

Statistical analysis of the comparison between native and immuno-fluorescence mCherry signal was performed using a non-parametric test (Mann-Whitney U test for unpaired data).

References

1. Simonato, M. *et al*. Progress in gene therapy for neurological disorders. *Nat Rev Neurol* **9**, 277–291, doi:10.1038/nrneurol.2013.56 (2013).
2. Miyagawa, Y. *et al*. Herpessimplex viral-vectordesign for efficient transduction of nonneuronalcells without cytotoxicity. *Proc Natl Acad Sci USA* **112**, E1632–1641, doi:10.1073/pnas.1423556112 (2015).
3. Ferenczy, M. W.& DeLuca, N. A. Reversal of heterochromatic silencing of quiescent herpes simplex virus type 1 by ICP0. *J Virol* **85**, 3424–3435, doi:10.1128/JVI.02263-10 (2011).
4. Boutell, C. & Everett, R. D. Regulation of alphaherpesvirus infections by the ICP0 family of proteins. *J Gen Virol* **94**, 465–481, doi:10.1099/vir.0.048900-0 (2013).
5. Uchida, H. *et al*. Adouble mutation in glycoprotein gB compensates for ineffective gD-dependent initiation of herpes simplex virus type 1 infection. *J Virol* **84**, 12200–12209, doi:10.1128/JVI.01633-10 (2010).
6. Woldbye, D. P.*et al*. Adeno-associated viral vector-induced overexpression of neuropeptide Y Y2 receptors in the hippocampus suppresses seizures. *Brain* **133**, 2778–2788, doi:10.1093/brain/awq219 (2010).
7. Samaniego, L. A., Wu, N. & DeLuca, N. A. The herpes simplex virus immediate-early protein ICP0 affects transcription from the viral genome and infected-cell survival in the absence of ICP4 and ICP27. *J Virol* **71**, 4614–4625 (1997).
8. Krisky, D. M. *et al*. Deletion of multiple immediate-early genes from herpes simplex virus reduces cytotoxicity and permits long-term gene expression in neurons. *Gene Ther* **5**, 1593–1603, doi:10.1038/sj.gt.3300766 (1998).
9. Paradiso, B. *et al*. Localized delivery of fibroblast growth factor-2 and brain-derived neurotrophic factor reduces spontaneous seizures in an epilepsy model. *Proc Natl Acad Sci USA* **106**, 7191–7196, doi:10.1073/pnas.0810710106 (2009).
10. Altaras, N. E. *et al*. Production and formulation of adenovirus vectors. *Adv Biochem Eng Biotechnol* **99**, 193–260, doi:10.1007/11542766 (2005).
11. Haberman, R. *et al*. Therapeutic liabilities of *in vivo* viral vector tropism: adeno-associated virus vectors, NMDAR1 antisense, and focal seizure sensitivity. *Mol Ther* **6**, 495–500, doi:10.1006/mthe.2002.0701 (2002).
12. Jackson, S. A. & DeLuca, N. A. Relationship of herpes simplex virus genome configuration to productive and persistent infections. *Proc Natl Acad Sci USA* **100**, 7871–7876, doi:10.1073/pnas.1230643100 (2003).
13. Samaniego, L. A., Neiderhiser, L. & DeLuca, N. A. Persistence and expression of the herpes simplex virus genome in the absence of immediate-early proteins. *J Virol* **72**, 3307–3320 (1998).
14. Terry-Allison, T., Smith, C. A. & DeLuca, N. A. Relaxed repression of herpes simplex virus type 1 genomes in Murine trigeminal neurons. *J Virol* **81**, 12394–12405, doi:10.1128/JVI.01068-07 (2007).
15. Suzuki, M., Chiocca, E. A. & Saeki, Y.Stable transgeneexpression from HSVamplicon vectorsinthebrain: potential involvement of immunoregulatory signals. *Mol Ther* **16**, 1727–1736, doi:10.1038/mt.2008.175 (2008).
16. Amelio, A. L., McAnany, P. K. & Bloom, D. C. A chromatin insulator-like element in the herpes simplex virus type 1 latency-associated transcript region binds CCCTC-binding factor and displays enhancer-blocking and silencing activities. *J Virol* **80**, 2358–2368, doi:10.1128/JVI.80.5.2358-2368.2006 (2006).
17. Harkness, J. M., Kader, M. & DeLuca, N. A. Transcription of the herpes simplex virus 1 genome during productive and quiescent infection of neuronal and nonneuronal cells. *J Virol* **88**, 6847–6861, doi:10.1128/JVI.00516-14 (2014).
18. Bankiewicz, K. S. *et al*. Convection-enhanceddelivery of AAVvector in parkinsonian monkeys; *invivo* detection of gene expression and restoration of dopaminergic function using pro-drug approach. *Exp Neurol* **164**, 2–14, doi:10.1006/exnr.2000.7408 (2000).
19. Kells, A. P.*et al*. Efficient genetherapy-based method for thedelivery of therapeutics toprimate cortex. *Proc Natl Acad Sci USA* **106**, 2407–2411, doi:10.1073/pnas.0810682106 (2009).
20. Laquerre, S. *et al*. Heparan sulfate proteoglycan binding by herpes simplex virus type 1 glycoproteins B and C, which differ in their contributions to virus attachment, penetration, and cell-to-cell spread. *J Virol* **72**, 6119–6130 (1998).
21. Tischer, B. K., von Einem, J., Kaufer, B. & Osterrieder, N. Two-step red-mediated recombination for versatile high-efficiency markerless DNAmanipulation in Escherichia coli. *Biotechniques* **40**, 191–197, doi:10.2144/000112096 (2006).
22. Paxinos, G. & Watson, C. *The Rat Brain In Stereotaxic Coordinates* (Academic Press, 1982).
23. Amaral, D. G. & Witter, M. P.In *The Rat Nervous System* (ed. Paxinos, G.) 443–493 (Academic Press, 1995).

Acknowledgements

This work was supported by grants to M.S. from the European Community (FP7-PEOPLE-2011-IAPP project 285827 [EPIXCHANGE]) and the Italian Ministry for Education, University and Research (PRIN project 2010N8PBAA [INBDNF]), and to J.C.G. from the NIH (NS064988, DK044935), the CHDI Foundation (A3777, A8790), and the Commonwealth of Pennsylvania (SAP #4100061184).

Author Contributions

G.V., Y.M., M.S. and J.C.G. conceived the experiments; Y.M. designed and produced recombinant plasmids, viral vectors and virus stocks; G.V. and S.I. performed animal injections, processing and imaging; G.V. and M.S. performed data quantifications; all authors conducted data analysis and interpretation; M.S., J.B.C. and J.C.G. wrote the manuscript.

Additional Information

Supplementary information accompanies this paper at doi:10.1038/s41598-017-01635-1

Competing Interests: G.V., M.S. and J.C.G. are founders of NuvoVec srl. Y.M., J.B.C. and J.C.G. are co-inventors of intellectual property licensed to SwitchBio, Inc. J.B.C. and J.C.G. are co-inventors of intellectual property licensed to Oncorus, Inc. J.C.G. is a founder and consultant of SwitchBio, Inc. and Oncorus, Inc.

Publisher's note: Springer Nature remains neutral with regard to jurisdictional claims in published maps and institutional affiliations.

Supplementary information

Engineered HSV vector achieves safe long-term transgene expression in the central nervous system

Gianluca Verlengia, Yoshitaka Miyagawa, Selene Ingusci, Justus B. Cohen, Michele Simonato, and Joseph C. Glorioso

Contents

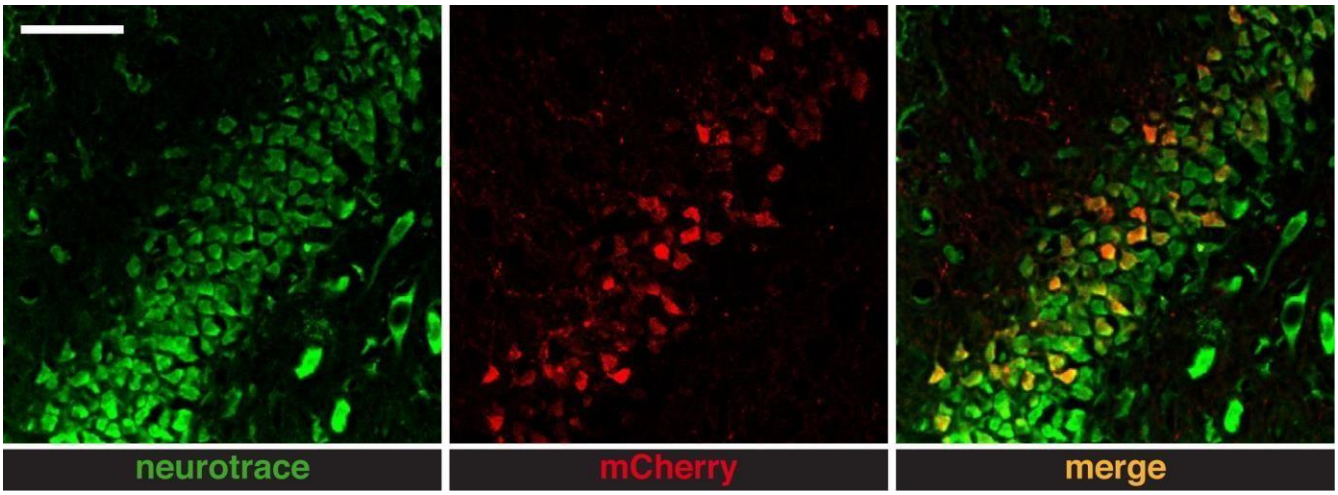

Supplementary Fig. S1. Neurons were the prevalent cell type expressing mCherry. Representative confocal images (4 animals/group) taken at the level of the dentate gyrus upper blade from coronal sections prepared from animals killed 2 months after JΔNI6 injection into the right hippocampus. Note overlapping signal (yellow) in granule cells bodies for all mCherry-expressing cells. Horizontal bar, 50 μm.

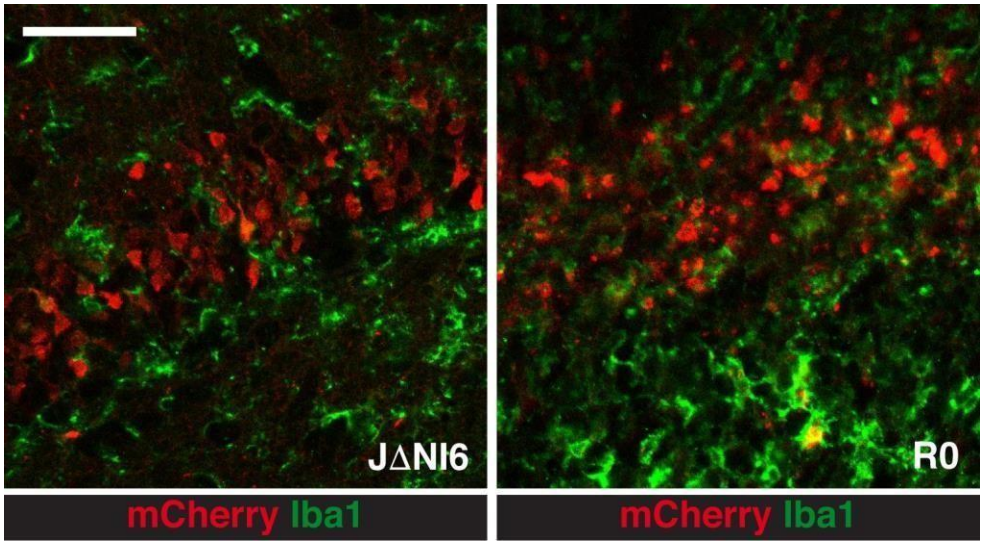

Supplementary Fig. S2. JΔNIR0 causes microglia activation. Representative confocal images (4 animals/group) taken at the level of the dentate gyrus upper blade from coronal sections prepared from animals killed 1 week after JΔNI6 (left) or JΔNI5R0 (right) injection into the right hippocampus. Note resting microglial cells after JΔNI6 injection, and activated microglial cells (i.e., cells with thicker ramifications) after JΔNI5R0 injection. Horizontal bar, 50 μm.

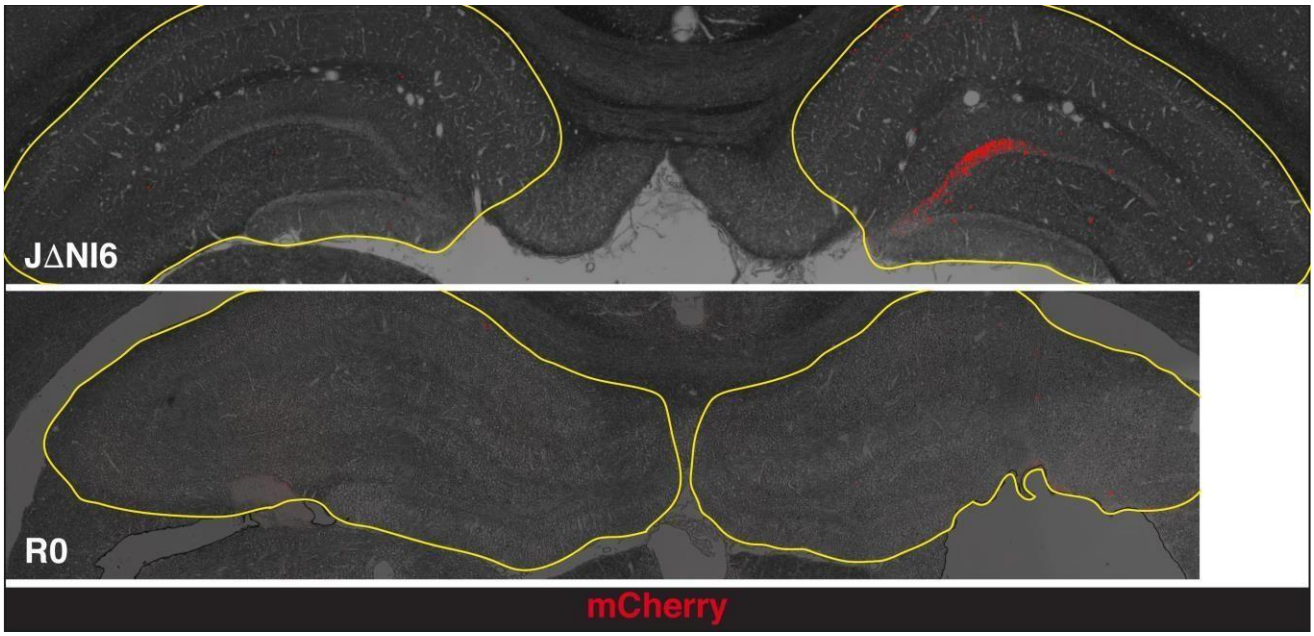

Supplementary Fig. S3. Neuropathological outcome of treatment with vector JΔNI6 (upper panel) or JΔNI5R0 (lower panel) 28 days after injection into the right hippocampus; hippocampi are circled in yellow. JΔNI5R0 causes an obvious reduction in hippocampal size, whereas JΔNI6 does not produce any detectable effect. Note that mCherry expression (red) is robust in the upper panel but is virtually absent in the lower panel, an indication that infected cells died because of vector toxicity. These images are representative of similar findings in 4 other animals per group.

3.2 Cellular Antisilencing Elements Support Transgene Expression from Herpes Simplex Virus Vectors in the Absence of Immediate Early Gene Expression

AMERICAN SOCIETY FOR MICROBIOLOGY | Journal of Virology®

GENE DELIVERY

Cellular Antisilencing Elements Support Transgene Expression from Herpes Simplex Virus Vectors in the Absence of Immediate Early Gene Expression

Fang Han,[a,b] Yoshitaka Miyagawa,[b]* Gianluca Verlengia,[c,d] Selene Ingusci,[c] Marie Soukupova,[c] Michele Simonato,[c,d] Joseph C. Glorioso,[b] Justus B. Cohen[b]

[a]School of Pharmaceutical Sciences, Tsinghua University, Beijing, China

[b]Department of Microbiology and Molecular Genetics, University of Pittsburgh School of Medicine, Pittsburgh, Pennsylvania, USA

[c]Section of Pharmacology, Department of Medical Sciences, University of Ferrara, Ferrara, Italy

[d]School of Medicine, University Vita-Salute San Raffaele, Milan, Italy

ABSTRACT Inactivation of all herpes simplex virus (HSV) immediate early (IE) genes to eliminate vector cytotoxicity results in rapid silencing of the viral genome, similar to the establishment of HSV latency. We recently reported that silencing of a nonvi- ral reporter cassette could be overcome in nonneuronal cells by positioning the cas- sette in the viral latency (LAT) locus between resident chromatin boundary elements. Here, we tested the abilities of the chicken hypersensitive site 4 insulator and the human ubiquitous chromatin opening element A2UCOE to promote transgene ex- pression from an IE-gene-inactivated HSV vector. We found that A2UCOE was partic- ularly active in nonneuronal cells and reduced reporter promoter occupancy by a re- pressive histone mark. We determined whether multiple transgenes could be expressed under the control of different promoters from different loci of the same virus. The results showed abundant coexpression of LAT-embedded and A2UCOE- flanked genes in nonneuronal cells. In addition, a third reporter gene without known protective elements was active in cultured rat sensory neurons. These findings indi- cate that cellular antisilencing sequences can contribute to the expression of multi- ple genes from separate promoters in fully IE gene-disabled HSV vectors, providing an opportunity for therapeutic applications requiring mutually independent expres- sion of different gene products from a single vector.

IMPORTANCE Gene therapy has now entered a phase of development in which a growing number of recessive single gene defects can be successfully treated by vector- mediated introduction of a wild-type copy of the gene into the appropriate tissue. However, many disease conditions, such as neurodegeneration, cancer, and inflammatory processes, are more complex, requiring either multiple gene correc- tions or provision of coordinated gene activities to achieve a therapeutic outcome. Although herpes simplex virus (HSV) vectors have the capacity to meet this need, the challenge has been to genetically engineer the HSV genome in a manner to pre- vent expression of any viral genes while retaining the ability to express multiple therapeutic transgenes under independent transcriptional control. Here, we show that non-HSV insulator elements can be applied to retain at least transient trans- gene activity from multiple viral loci, thereby opening the door for more complex gene therapy applications in the future.

KEYWORDS CTCF, HSV-1, ICP0, UCOE, cHS4, chromatin remodeling, gene therapy, insulator, transgene expression, viral vector

Received 29 March 2018 **Accepted** 13 June 2018

Accepted manuscript posted online 27 June 2018

Citation Han F, Miyagawa Y, Verlengia G, Ingusci S, Soukupova M, Simonato M, Glorioso JC, Cohen JB. 2018. Cellular antisilencing elements support transgene expression from herpes simplex virus vectors in the absence of immediate early gene expression. J Virol 92:e00536-18. https://doi.org/10.1128/JVI.00536-18.

Editor Rozanne M. Sandri-Goldin, University of California, Irvine

Address correspondence to Justus B. Cohen, jbc@pitt.edu.

* Present address: Yoshitaka Miyagawa, Department of Biochemistry and Molecular Biology, Nippon Medical School, Tokyo, Japan.

Studies over many years have extensively documented that progression of the herpes simplex virus (HSV) lytic life cycle relies on the coordinated expression of three classes of genes, the immediate early (IE), early (E), and late (L) genes (1). Key aspects of this regulation are, first, activation of unique enhancers associated with the promoters of the 5 IE genes by binding of the viral tegument protein VP16 and, second, absolute dependence of E and L viral gene expression on the products of the ICP4 and ICP27 IE genes. The remaining IE gene products have more specialized functions that include overcoming host innate immunity and preventing genome silencing (2). Stud- ies of the expression of members of the viral cascade have employed deletion mutants of the IE genes, and it has been shown that inactivation of all 5 IE genes completely silences the viral genome in nonneuronal cells (3, 4). Such highly defective recombinant HSV vectors are without cytotoxic activity but also fail to express transgenes from heterologous promoters (3, 4). In latently infected neurons, all IE genes are switched off, yet a unique HSV gene referred to as the latency-associated transcript (LAT) gene remains transcriptionally active. The molecular mechanism(s) underlying transition from latency to active infection has remained elusive, although breaking the silencing of the IE genes is undoubtedly an essential component (5, 6).

HSV is an attractive vehicle for transmitting genes to neurons due to its ability to persist in these cells in a nonintegrated state and deliver expansive foreign sequences. However, the challenge of eliminating all IE gene-associated cytotoxicity without losing transgene expression potential has long been a confounding obstacle. We recently showed that a foreign promoter introduced into the LAT locus was protected from genome-wide silencing in the absence of all IE gene products and that this protection was mediated in part by an upstream CTCF-binding repeat element referred to as CTRL1 (7, 8). Here, we have sought to extend these observations by evaluating the ability of cellular antisilencing elements to keep nonviral promoters active in an otherwise silent genome.

In our previous work, we described the replication-defective vector JΔNI5, which has all the IE genes functionally deleted, including the internal repeat (joint) region separating the two unique segments of the viral genome. JΔNI5 is transcriptionally silent in nonneuronal cells and devoid of cytotoxicity (7). We observed that a transgene expression cassette inserted into the JΔNI5 genome adjacent to a reported enhancer- type element (LATP2 or LAP2) (9, 10) in the LAT locus between CTRL1 and a second CTCF motif repeat element, CTRL2, remained robustly active for at least 4 weeks in contact- inhibited cells. While this vector can express multiple transgenes from a single promoter using "self-cleaving" 2A peptides (59; Y. Miyagawa, J. B. Cohen, and J. C. Glorioso, unpublished results), here, we explored the use of ectopic antisilencing elements to create additional active loci that would allow separately controlled expres- sion of multiple transgenes from a single vector. Unlike duplication of the LAT protec- tive elements to serve at more than one location, an ectopic element would not be expected to cause vector instability as a consequence of internal recombination events. In order to protect chromosomally integrated transgenes against heterochromatin formation, a number of genetic regulatory elements have been characterized and tested in gene transfer vectors. Some of these regulatory elements, including insulators and scaffold/matrix attachment regions (S/MARs), show border functions that shield the transgene promoter from the chromosomal environment to reduce position effects (11, 12). Other elements, including the locus control regions (LCRs) and ubiquitous chro- matin opening elements (UCOEs), exhibit a dominant chromatin-remodeling and transcription-activating function (13).

Chicken hypersensitive site 4 (cHS4) is among the most extensively characterized vertebrate insulators (11). It is located in the β-globin locus control region between an ~16-kb region of condensed chromatin and the β-globin gene cluster. It was found to have both enhancer-blocking and barrier activities. The activity of cHS4 was mapped to a 250-bp core element (14). While some studies have suggested that two copies of the core element on each side of a transgene cassette are sufficient to provide essentially full barrier activity (15, 16), others have used an extended (0.4-kb) core fragment (17,

18) or the 1.2-kb full-length insulator in retroviral (19) and lentiviral (20) vectors to achieve sustained, integration site-independent transgene expression.

UCOEs have also shown antisilencing effects. A prototypical UCOE, referred to as A2UCOE, is located in the human *HNRPA2B1-CBX3* locus. This locus contains a pair of divergently oriented promoters that are associated with active histone modification marks (21) within a methylation-free CpG island (22, 23). Based on these features, this region has been proposed to serve a dominant chromatin-remodeling function. Its core activity has been variously mapped, depending on the assay system, to 4.1-, 2.2-, 1.5-, and 1.2-kb subfragments roughly centered on the dual-promoter region (23–27). In a comparison among UCOE, MAR, stabilizing antirepressor (STAR), and cHS4 elements, the 1.5-kb A2UCOE was the most effective in creating cell pools that produced stable, high yields of a transgenic antibody (28). While other studies have shown that the *CBX3* component is essential or even sufficient for A2UCOE function (29), it has been reported that a 0.6-kb A2UCOE lacking *CBX3* sequences was able to stabilize transgene expression (30).

In this study, we explored the ability of cHS4 and the 4.1-kb A2UCOE encompassing the central CpG island and including unmethylated flanking *CBX3* and *HNRPA2B1* sequences (21) to increase and prolong transgene expression from a JΔNI5-derived vector in human dermal fibroblasts. We observed that the full-length versions of both elements were able to protect a cellular promoter positioned within a viral intergenic region from global silencing of the HSV-1 genome. The 4.1-kb A2UCOE was superior to cHS4 in terms of transgene expression level and duration and comparable in these regards to the full complement of LAT-protective elements. The antisilencing capacities of cHS4 and A2UCOE were also functional in virus-infected primary human muscle precursor cells and human epidermal keratinocytes. As observed in our previous study (7), the ubiquitin C (UbC) promoter driving mCherry expression in the ICP4 locus of JΔNI5 and derivatives was active in rat sensory neurons, but not in nonneuronal cells, suggesting that expression permissiveness at this site is neuronal cell dependent.

We took advantage of these observations to engineer a novel vector containing three different transgenes (enhanced green fluorescent protein [EGFP], firefly luciferase [fLuc], and mCherry genes) under the control of different promoters at different loci. All three transgenes were simultaneously expressed in individual rat dorsal root ganglion neurons in culture, and two of the three were coexpressed in rat hippocampus following intracranial vector delivery. This vector design has potential for gene therapy of peripheral and central nervous system (CNS) conditions that may benefit from independently regulated expression of more than a single external gene product.

RESULTS

cHS4 and A2UCOE improve transgene expression from a highly defective HSV vector. We created a series of HSV-1 recombinant viruses in which an EGFP expression cassette controlled by the cytomegalovirus (CMV) enhancer/þ-actin promoter fusion (CAG) was flanked in different configurations by all or components of the 1.2-kb cHS4 insulator or the 4.1-kb A2UCOE fragment. We assembled these extended cassettes in Gateway (GW) entry plasmids and recombined each with a GW destination cassette
located in the intergenic region between HSV-1 UL50 and UL51 genes in a previously described HSV-bacterial artificial chromosome (BAC) construct, JΔNI10GW, containing a highly defective HSV-1 genome (7) (Fig. 1). Viruses were produced by transfection of recombinant BAC DNAs into U2OS-ICP4/ICP27 or U2OS-ICP4/ICP27-Cre cells that complement the deleted ICP0, ICP4, and ICP27 genes; the latter cells also excise the BAC region located between *loxP* sites (7). Viruses were named according to their GW inserts, as indicated in Fig. 1. vCAG and vLAT are JΔNI10GFP and JΔNI10LAT-GFP, respectively, as described by Miyagawa et al. (7).

We examined EGFP and mCherry reporter gene expression from the different viruses in human dermal fibroblasts (HDFs) infected with equal numbers of virus particles based on genome copy (gc) titers listed in Table 1. At 7 days postinfection (dpi), none of the viruses showed detectable mCherry expression from the deleted ICP4 locus,

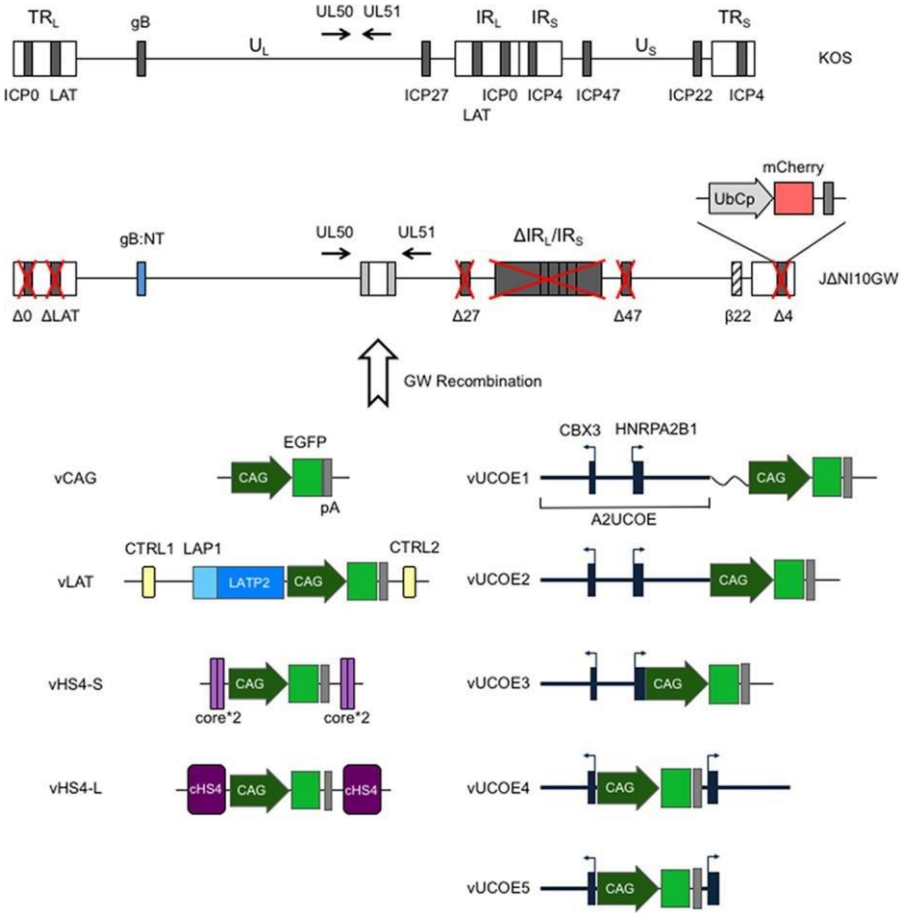

FIG 1 JΔNI10 genome engineering. (Top) Compared to the wild-type HSV-1 KOS genome represented at the top, JΔNI10GW (7) has the entire internal repeat (joint) region (IR_L and IR_S); the remaining ICP0 (Δ0), LAT (ΔLAT), and ICP4 (Δ4) loci; and the single-copy ICP27 (Δ27) gene deleted (red crosses). The promoter and translation initiation codon of the ICP47 (Δ47) gene are also deleted, and the ICP22 promoter acts as an early (þ22) promoter due to deletion of its regulatory sequences. The glycoprotein B gene contains a pair of entry-accelerating mutations (gB: NT) (58), and a GW destination cassette is located between the UL50 and UL51 genes, whose directions of transcription are indicated by arrows. A ubiquitin C promoter (UbCp)-mCherry gene cassette is located at the position of the deleted ICP4 gene (Δ4). U_L and U_S, unique long and short segments; TR_L and TR_S, terminal repeats flanking U_L and U_S, respectively; IR_L and IR_S, the cognate internal repeats of U_L and U_S, respectively. (Bottom) CAG promoter-EGFP cassettes flanked by antisilencing elements in different configurations were inserted into JΔNI10GW through GW recombination. vCAG contains a CAG promoter-controlled EGFP cassette and the rabbit þ-globin polyadenylation (pA) region. vLAT contains the EGFP expression cassette embedded in sequences from the LAT locus between the LATP2 enhancer-type element and CTRL2, with CTRL1 included upstream of the LAT promoter (LAP1). vHS4-S contains two tandem copies of the cHS4 core (core*2) at both sides of the expression cassette, while vHS4-L contains the cassette flanked on each side by a single copy of the full-length (1.2-kb) cHS4. vUCOE1 contains the complete 4.1-kb A2UCOE (black boxes; exons) and a 218-bp cloning sequence (wavy line) upstream of CAG. In vUCOE2, the linker sequence was deleted. vUCOE3 lacks both the linker and the first intron of *HNRPA2B1*. In vUCOE4 and vUCOE5, the EGFP expression cassette is located in the divergent promoter region separating the *CBX3* and *HNRPA2B1* transcription start sites, and in vUCOE5, the first intron of *HNRPA2B1* is deleted. Black boxes, UCOE exons; thick horizontal lines, UCOE introns and dual-promoter region; arrows, transcription start sites and directions.

while all the viruses produced detectable EGFP fluorescence, although at different levels (Fig. 2A). In agreement with our previous study (7), transplanted sequences from the LAT locus (vLAT) enabled prominent EGFP expression, whereas the CAG-EGFP cassette without additional elements (vCAG) produced a comparatively low level of EGFP fluorescence. Among the viruses, vUCOE2 generated the strongest EGFP fluores- cence, while vHS4-S and vUCOE5 produced low levels, similar to vCAG. These results were confirmed and extended by quantitative reverse transcription-PCR (qRT-PCR) measurement of EGFP mRNA levels at 7 and 14 dpi (Fig. 2B). While mRNA levels

TABLE 1 Virus titers

Virus name	No. of gc/ml	No. of PFU/ml	No. of gc/PFU
vCAG	1.86E12	1.03E9	1.80E3
vLAT	1.62E12	4.33E8	3.74E3
vHS4-S	1.75E12	4.33E8	4.05E3
vHS4-L	1.45E12	3.33E8	4.35E3
vUCOE1	1.97E12	1.13E9	1.74E3
vUCOE2	2.65E12	1.67E9	1.59E3
vUCOE3	2.85E12	1.77E9	1.61E3
vUCOE4	1.86E12	1.37E9	1.36E3
vUCOE5	1.84E12	9.33E8	1.97E3
vLuc	2.18E12	1.60E9	1.36E3
vU-Luc	1.52E12	1.33E9	1.14E3

decreased by an average of approximately 50% between the two time points, EGFP expression in vLAT-, vUCOE2-, and vUCOE1-infected cells was clearly enhanced compared to the vCAG baseline and other infected cells, whereas vHS4-L produced only a modest increase in EGFP RNA levels relative to vCAG (Fig. 2B). These data indicated that the 4.1-kb A2UCOE is capable of protecting a linked transgene expression cassette from the rapid global silencing of the HSV-1 genome that occurs in the absence of functional IE genes and that 2 copies of full-length cHS4 could provide some protection. Notably, omission of the *HNRPA2B1* intron abolished the antisilencing activity of A2UCOE (compare vUCOE2 and -3), but preservation of the intron in vUCOE4 did not rescue expression, indicating that disruption of the bidirectional promoter region of A2UCOE was detrimental. Although EGFP fluorescence waned over time, it remained detectable at 28 dpi in vUCOE1- and vUCOE2-infected HDFs (Fig. 2C). Together, these data showed that the uninterrupted 4.1-kb A2UCOE, and to a lesser extent the full-length cHS4, was capable of enhancing transgene expression from an extrachromosomal viral vector in the absence of viral *trans*-acting, antisilencing gene products. Table 2 summarizes the results of this analysis and our observations in additional cell types presented below. To extend these findings, we used a subset of the viruses to examine EGFP expression in other cell types. In human muscle-derived stem cells (hMDSCs) infected with vLAT or vUCOE2, EGFP fluorescence was elevated compared to vCAG-infected cells through at least 14 dpi, and elevated transcript levels persisted at 28 dpi. In contrast, EGFP expression in vHS4-L-infected cells was only slightly higher than in vCAG-infected cells (Fig. 3A). A similar pattern was observed in human epidermal keratinocytes (hEKs), although expression was more transient than in hMDSCs (Fig. 3B), likely a result of ongoing cell division reducing vector numbers per cell while hMDSCs underwent terminal differentiation. As in HDFs, mCherry fluorescence was not detected in any of the infected cultures (Fig. 3A and B). These results indicated that the antisilencing activity of A2UCOE in a highly defective HSV-1 vector is functional in different non-neuronal cell types.

Transcriptional activity of flanking genes. We asked whether cHS4 and A2UCOE affected the transcript levels of neighboring genes. The proximal UL50 and UL51 genes are transcribed in opposite directions toward the CAG-EGFP cassette (Fig. 1 and 4A). Surrounding CAG-EGFP with sequences from the LAT locus did not noticeably alter the expression of either UL50 or UL51 in infected HDFs at 7 and 14 dpi (Fig. 4B and C), indicating that the different elements of the LAT region (CTRLs and LATP2) neither activated neighboring promoters nor protected the promoters from putative stimulation by the CMV enhancer component of the CAG promoter. The cHS4 elements of vHS4-L caused a slight increase in UL50 expression but did not alter the expression of UL51 compared to vCAG, providing no evidence for either a boundary effect shielding these genes from silencing or a CAG enhancer-blocking activity. In contrast, A2UCOE had a stimulatory effect on the expression of both UL50 and UL51, albeit less pronounced than its stimulation of EGFP expression (see Fig. 2B). These results indicated that A2UCOE has an ability to enhance gene expression bidirectionally, although the

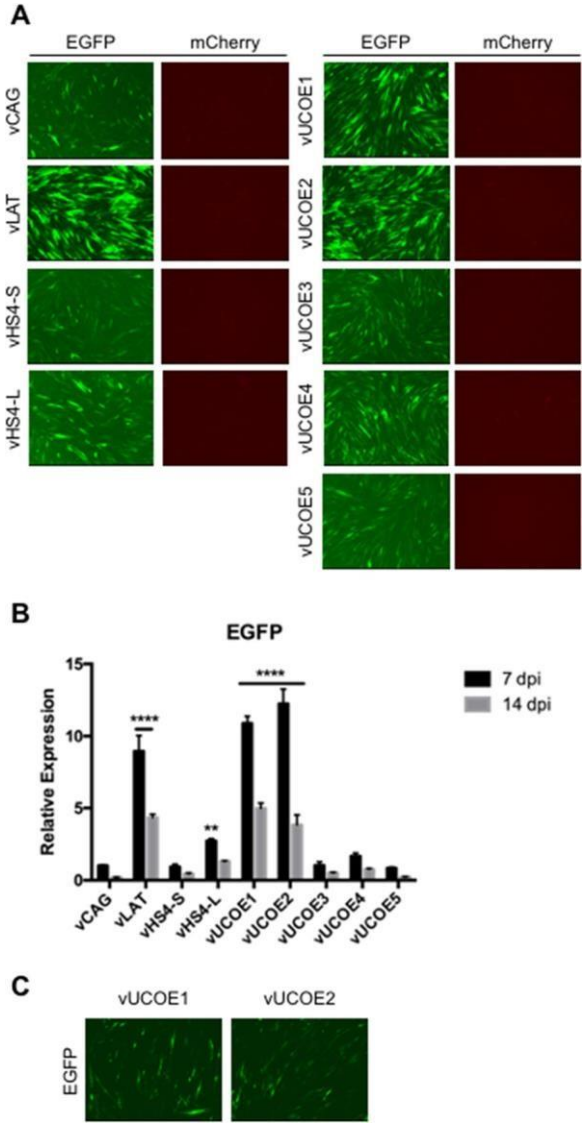

FIG 2 Transgene expression in infected HDFs at 7, 14, and 28 dpi. The cells were infected with the indicated viruses at 25,000 gc per cell. (A) EGFP and mCherry fluorescence in infected HDFs at 7 dpi. All the images of each marker were collected at a fixed exposure time and automatically adjusted for optimal contrast and brightness (autoscale setting; Meta Imaging Series 7.7 MetaMorph software; Molecular Devices). (B) Relative EGFP mRNA levels in infected HDFs as determined by qRT-PCR analysis. Expression levels were normalized to gc in the same samples and are presented as means and SD relative to the level in vCAG-infected cells at 7 dpi (see "Statistics" in Materials and Methods for details). ****, $P \leq 0.0001$; **, $P \leq 0.01$ compared to vCAG at the same time point (2-way ANOVA). (C) EGFP fluorescence in vUCOE1- and vUCOE2-infected HDFs at 28 dpi.

magnitude may vary with distance (Fig. 4A) and possibly the nature of the promoter (CAG versus non-IE HSV-1 promoters).

Histone modification contributes to the activity of A2UCOE in HDFs. To investigate the mechanism underlying the antisilencing effect of A2UCOE on genes in our highly defective HSV vector, we measured CAG promoter occupancy by total histone H3 and lysine 9-trimethylated histone H3 (H3K9Me3), a repressive histone mark, in vCAG- and vUCOE2-infected HDFs at 7 dpi. As shown in Fig. 5A, anti-H3 antibody precipitated similar fractions of CAG input DNA from vCAG- and vUCOE2-infected cells (~10%). However, CAG-associated H3K9Me3 was significantly less abundant in vUCOE2-infected cells (0.08%) than in vCAG-infected cells (0.12%) (Fig. 5B), indicating that A2UCOE provides protection against the accumulation of repressive histone marks on the CAG promoter in a quiescent HSV-1 genome.

TABLE 2 Summary of EGFP expression in UL50/UL51

Element	Virus	Feature	Position relative to CAG-EGFP	Fold change[a] HDF 7 dpi	HDF 14 dpi	hMDSC 14 dpi	hMDSC 28 dpi	hEK 3 dpi	hEK 7 dpi	rDRG 7 dpi	rDRG 14 dpi
cHS4	vHS4-S	Core*2 (2 × 250 bp)	5′+ 3′	0.92	0.44						
	vHS4-L	Full length (1.2 kb)	5′ + 3′	2.72	1.29	2.89	1.68	2.87	0.51	2.03	0.44
UCOE	vUCOE1	4.1-kb A2UCOE + 218-bp spacer	5′	10.88	4.98						
	vUCOE2	4.1-kb A2UCOE	5′	12.24	3.84	9.61	7.92	5.76	1.09	3.25	0.49
	vUCOE3	A2UCOE without HNRPA2B1 intron	5′	1.02	0.51						
	vUCOE4	Split 4.1-kb A2UCOE	CBX3 5′, HNRPA2B1 3′	1.66	0.75						
	vUCOE5	Split A2UCOE, no HNRPA2B1 intron	CBX3 5′, HNRPA2B1 3′	0.84	0.23						
LAT	vLAT	Split within 2-kb intron	CTRL1/LAP 5′, CTRL2 3′	8.90	4.30	12.20	8.40	8.74	0.70	1.72	0.67

[a]Fold change in mRNA relative to vCAG at the earlier time point per cell type.

Since A2UCOE encompasses methylation-free CpG islands, we also explored whether protection against DNA methylation played a role in the stimulatory effect of A2UCOE on transgene expression. Viral DNA extracted prior to infection and at 7 days post-HDF infection was treated with bisulfite to convert unmethylated cytosines to uracil, a portion of the þ-actin component of the CAG promoter was amplified by PCR, and a number of cloned fragments were sequenced. As illustrated in Fig. 5C and D, the CAG promoter was substantially free of methylation both in input viral DNA and in viral DNA from infected HDFs. Thus, methylation was not responsible for the repressed activity of the CAG promoter in vCAG-infected cells, and the A2UCOE insert in vUCOE2 did not act by preventing promoter methylation. Together, these results pointed to the involvement of histone modification, but not blockage of DNA methylation, in the mechanism of gene activation by A2UCOE in episomal HSV-1 DNA.

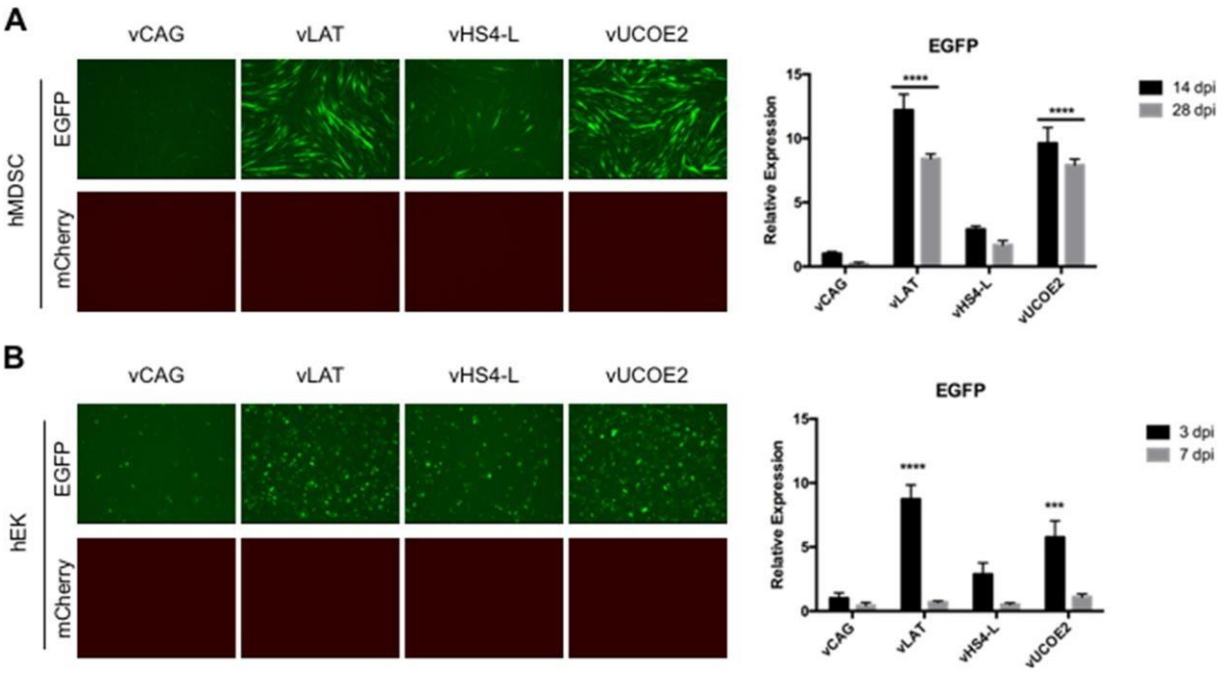

FIG 3 Transgene expression in infected hMDSC (50,000 gc/cell) (A) and hEK (25,000 gc/cell) (B) cell cultures. (A) EGFP and mCherry fluorescence at 14 dpi (left) and relative EGFP mRNA levels at 14 and 28 dpi (right). (B) Fluorescence at 3 dpi and relative EGFP mRNA levels at 3 and 7 dpi. Images were collected as for Fig. 2A. mRNA data were obtained by qRT-PCR with normalization to viral gc in the same samples and are presented as expression relative to that in vCAG-infected cells at 14 dpi (A) or 3 dpi (B). The data are means and SD; ***, $P \leq 0.001$, and ****, $P \leq 0.0001$ compared to vCAG at the same time point (2-way ANOVA).

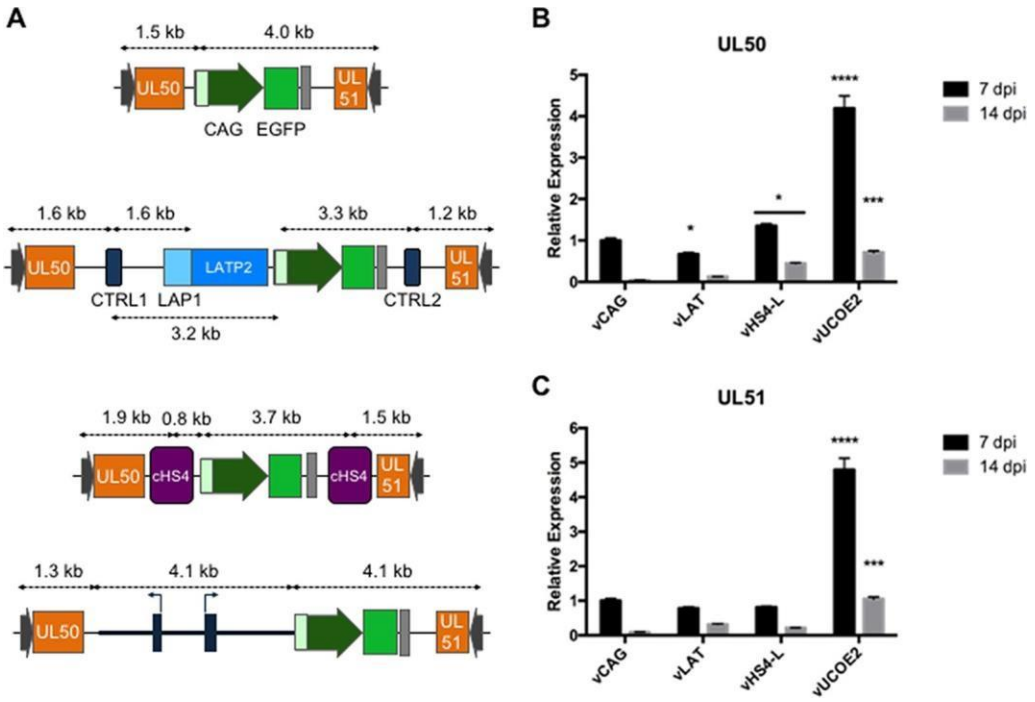

FIG 4 Structure of the UL50-UL51 locus in vCAG, vLAT, vHS4-L, and vUCOE2 (A) and relative UL50 (B) and UL51 (C) mRNA levels in infected HDFs. The data are means and SD; *, $P \leq 0.05$; ***, $P \leq 0.001$; ****, $P \leq 0.0001$ compared to vCAG at the same time point (2-way ANOVA).

A2UCOE activity in neuronal cells. In our previous study (7), we observed differences between primary human nonneuronal cells, including HDFs, hMDSCs, and hEKs, and rat dorsal root ganglion (rDRG) cultures in the expression of reporter genes from IE gene-inactive HSV-1 vectors. While the mCherry gene in the ICP4 locus was essentially silent in the human nonneuronal cells, it showed robust activity in rDRGs at 3 dpi. Moreover, while CAG-EGFP inserted between the viral UL3 and UL4 genes was inactive in the human cells, it too showed robust expression in rDRGs, matched in human cells only when the expression cassette was located in the LAT locus (7). Among different explanations, these results raised the unanticipated possibility that the IE gene-disabled genome backbone used in these studies was relatively derepressed in rDRGs compared to nonneuronal cells. Thus, it was of interest to determine whether CAG-EGFP located in the UL50-UL51 intergenic region was detectably expressed in rDRGs and whether its expression was enhanced by regulatory LAT, cHS4, or A2UCOE elements, as was seen in nonneuronal human cells. Infection with vCAG, vLAT, vHS4-L and vUCOE2 produced abundant expression of both EGFP and mCherry in rDRGs at 7 dpi (Fig. 6A) at a virus dose substantially lower than that used in the human cell infections shown in Fig. 2 and 3. Quantitative analysis by qRT-PCR showed small differences in mCherry transcript levels among the 4 viruses but increases in EGFP expression of ~1.5 to 3-fold per viral genome relative to vCAG (Fig. 6B). These results showed that the LAT, cHS4, and A2UCOE elements had a smaller impact in rDRGs than in the human cells examined earlier, consistent with the interpretation that the IE gene-deficient viral genome exists in DRGs in a less transcriptionally repressed state than in other cells. At 14 dpi, expression of EGFP and mCherry was reduced and was similar among the 4 viruses, indicating that the modest insulator effects observed at 7 dpi were transient in rDRG cultures.

Simultaneous expression of 3 distinct transgene cassettes from a single vector. Our observations suggested that A2UCOE would allow the expression in nonneuronal cells of 2 transgenes from different loci in the IE gene-inactive HSV-1 genome, raising the possibility of mutually independent regulation. Furthermore, they suggested that

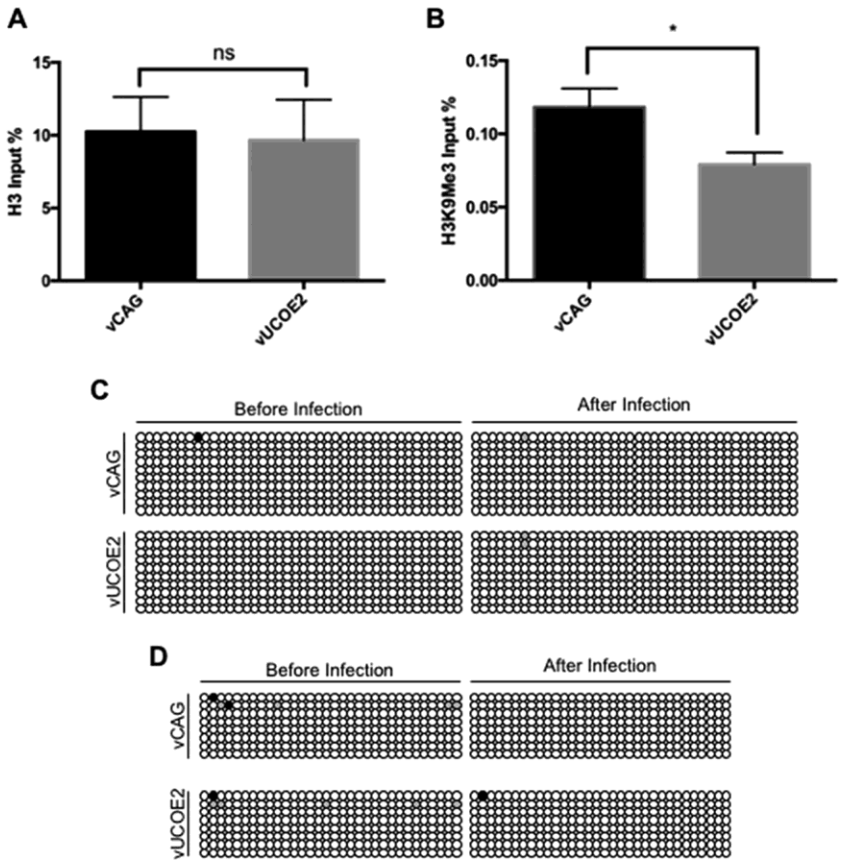

FIG 5 (A and B) Total H3 (A) and transcriptionally repressive H3K9Me3 (B) associated with the CAG promoters of vCAG and vUCOE2 7 days after infection of HDFs. qPCR was performed to determine the amount of CAG DNA precipitated by each antibody. The graphs show the percentages of CAG DNA precipitated with anti-histone H3 or K9Me3-specific anti-H3 as a percentage of total CAG DNA prior to precipitation. The error bars represent SD in the results of 4 experiments. ns, not significant; *, $P < 0.05$; Mann-Whitney test. (C and D) DNA methylation status of two different segments of the CAG promoter in vCAG and vUCOE2 before infection and at 7 days post-HDF infection. Each row of circles represents an individual cloned PCR product from the chicken β-actin component of the CAG promoter after bisulfite conversion. Each circle represents a CpG site. The white circles represent unmethylated CpG sites, and the black circles represent methylated CpG sites; the gray circles represent sites that could not be determined. (C) Primer set M2. (D) Primer set M4.

the same virus backbone would be able to express transgenes from 3 different loci in DRGs and perhaps other neuronal cells, at least short term. To test these suggestions, we introduced the fLuc gene under the control of the human EF1a promoter, with or without A2UCOE, into the UL50-UL51 intergenic region of a dual-reporter, IE gene-deficient vector, JΔNI7GFP (7), via a GW intermediate denoted JΔNI7GFP-GW (Fig. 7A); JΔNI7GFP-GW differs from JΔNI10GW (Fig. 1, top) in that it contains CAG-EGFP embedded within the native LAT locus. The resulting viruses, vLuc and vU-Luc (Fig. 7A), produced comparable levels of EGFP fluorescence (Fig. 7B) and mRNA (Fig. 7C, 7 and 14 dpi) in infected HDFs, and neither virus produced detectable mCherry fluorescence. In contrast, vU-Luc-infected cells contained substantially more luciferase enzymatic activity at 7 dpi than vLuc-infected cells, and this level remained relatively unchanged at 14 dpi (Fig. 7D). These results demonstrated directly that A2UCOE provides a means to express 2 transgenes in nonneuronal cells from different promoters in the vector genome. Furthermore, they indicated that A2UCOE, while capable of transiently stimulating the expression of nearby viral genes (Fig. 4), does not significantly affect the activity of distal genes (EGFP and mCherry).

We then sought to confirm that all three reporter genes of vLuc and vU-Luc could be expressed simultaneously in rDRGs. We used immunofluorescence to visualize fLuc

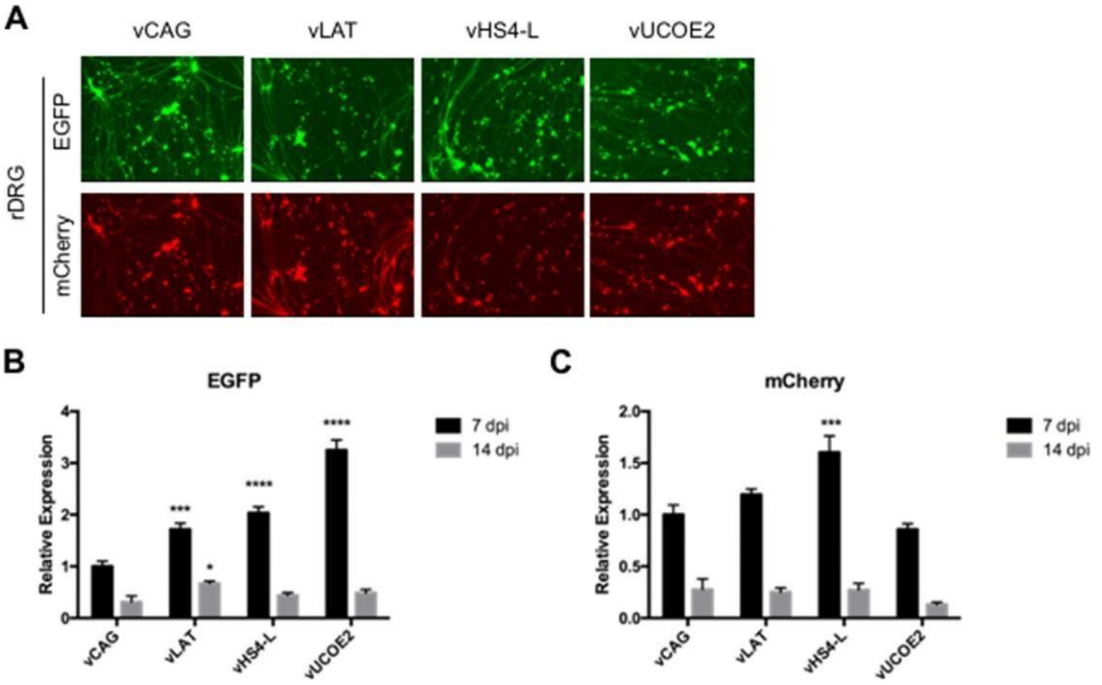

FIG 6 Fluorescence at 7 dpi (A) and relative EGFP (B) and mCherry (C) mRNA levels at 7 and 14 dpi in cultured rDRGs (3,000 gc/cell). The mRNA data were obtained by qRT-PCR with normalization to viral gc in the same samples and are presented as expression relative to that in vCAG-infected cells at 7 dpi. The data are means and SD; *, $P < 0.05$; ***, $P \leq 0.001$; ****, $P \leq 0.0001$ compared to vCAG at the same time point (2-way ANOVA).

protein in the same fields as EGFP and mCherry fluorescence and observed extensive overlap between the three types of signals from either virus (Fig. 8A). Although not statistically significant, luciferase activity appeared moderately higher in vU-Luc- than in vLuc-infected cells (Fig. 8B), consistent with the results shown in Fig. 6B. Likewise, EGFP transcript levels appeared somewhat elevated (Fig. 8C), but mCherry expression was essentially the same from the 2 viruses (Fig. 8D). It should be noted that in the episomal configuration adapted by these viruses, the EGFP and mCherry genes are located near one another while the fLuc locus is distal, arguing that any differential effect of A2UCOE on EGFP and mCherry expression is likely not a function of linear distance.

Lastly, we examined vLuc and vU-Luc transgene expression in mouse brain following stereotactic delivery of the vectors to the hippocampus. IVIS monitoring (see below) of luciferin-dependent bioluminescence (Fig. 9A) showed peak luciferase activity at 3 days post-vector inoculation, declining to undetectable at 28 days (Fig. 9B). Notably, at both 3 days and 7 days, the signal in vU-Luc-injected mice was stronger than in vLuc-injected mice (Fig. 9B). Hippocampal sections from animals sacrificed at 8, 15, and 29 days were tested by indirect immunofluorescence for EGFP and mCherry expression. Robust mCherry expression was observed at 8 days and persisted, albeit at reduced levels, at 29 days (Fig. 9C). In contrast, very little, if any, EGFP signal was detected at any time point. These results indicated that A2UCOE can enhance transient, independent expression of a second transgene in the central nervous system to complement the previously described durable expression of a first transgene positioned in the deleted ICP4 locus (31, 32). It remains to be determined what mechanisms can account for the rapid or immediate silencing of the LAT-based EGFP cassette of these vectors in mouse hippocampus.

DISCUSSION

Replication-defective HSV holds promise as a vector for gene therapy because of its large payload capacity and the establishment of its genome as an extrachromosomal episome without integration into cellular DNA. We recently developed an innocuous

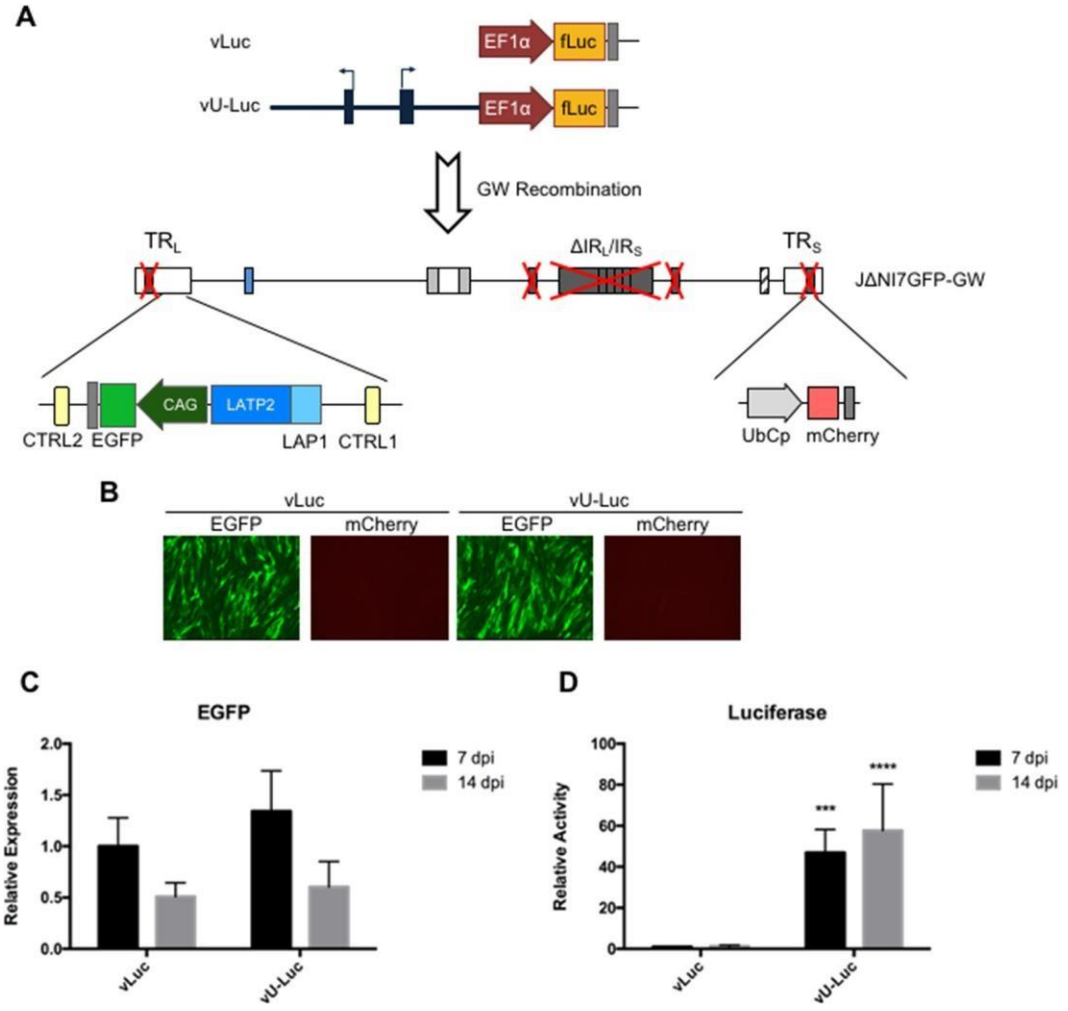

FIG 7 vLuc and vU-Luc genome structures and transgene expression in HDFs. (A) Schematic drawing of the vLuc and vU-Luc genomes. A CAG-EGFP cassette was located in the LAT loci of both vectors. A GW cassette positioned in the intergenic region between UL50 and UL51 was used to introduce an EF1a promoter-luciferase (fLuc) expression cassette with or without upstream A2UCOE. (B) EGFP and mCherry fluorescence in vLuc- and vU-Luc-infected HDFs at 7 dpi. (C) EGFP mRNA levels of vLuc- or vU-Luc-infected HDFs at 7 and 14 dpi expressed relative to vLuc at 7 dpi (qRT-PCR data were normalized to viral gc in the same samples). (D) Luciferase activity in vLuc- or vU-Luc-infected HDFs at 7 and 14 dpi relative to vLuc at 7 dpi. The data are means and SD; ***, $P \leq 0.001$, and ****, $P \leq 0.0001$ compared to vLuc at the same time point (2-way ANOVA).

HSV vector that is devoid of functional IE genes and is transcriptionally silent, with the exception of transgene expression cassettes inserted into the LAT locus, mimicking neuronal HSV latency in nonneuronal cells (7). We further showed that the privileged status of the LAT locus as a transcriptionally active site in an otherwise silent HSV episome is due in part to the presence of viral insulator-type elements in this region. To expand the utility of this vector platform, here, we explored the question of whether additional transcriptionally active sites can be created by insertion of cellular genetic elements that possess an ability to protect linked genes from epigenetic silencing. We found that the naturally hypomethylated cellular A2UCOE element enables adjacent reporter gene transcription from cellular promoters inserted into the defective HSV backbone, thereby providing a system for mutually independent expression of multiple transgenes from a single vector.

A2UCOE was first described in 2003 (22) and has since been tested in a variety of systems for its ability to support persistent transgene expression from the innate *HNRPA2B1* promoter or external promoters. Where comparisons have been performed, A2UCOE has been found to be more effective in blocking transgene silencing than cHS4

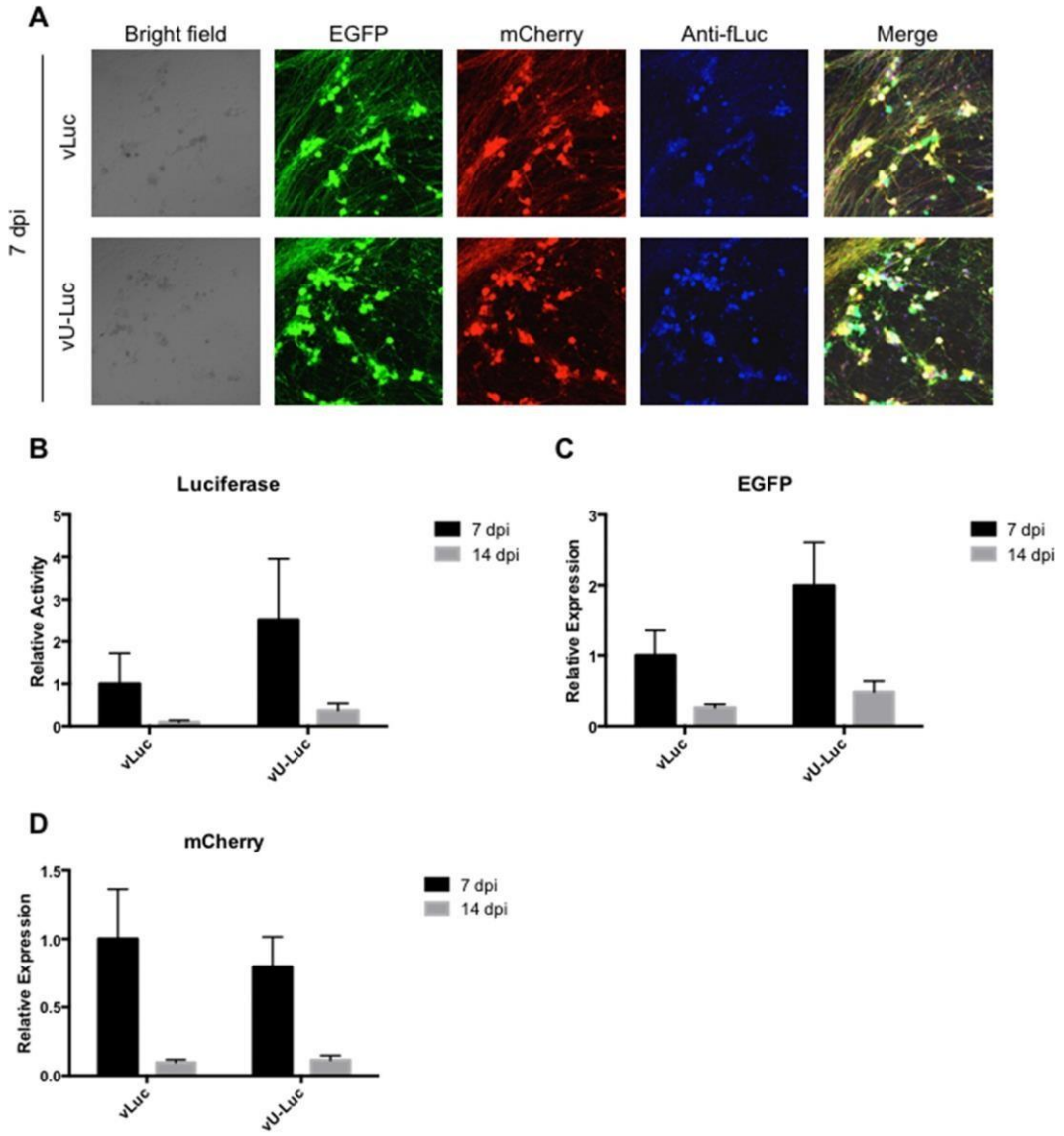

FIG 8 Expression of the three vLuc and vU-Luc transgenes in infected rDRG cultures (3,000 gc/cell). (A) EGFP and mCherry fluorescence and luciferase immunofluorescence (Anti-fLuc) at 7 dpi. Merge, overlay of the three fluorescence images. (B) Luciferase activities at 7 and 14 dpi relative to vLuc at 7 dpi. (C and D) EGFP (C) and mCherry (D) mRNA levels at 7 and 14 dpi relative to vLuc-infected cells at 7 dpi. The mRNA data were obtained by qRT-PCR with normalization to viral gc in the same samples. The data are means and SD; $P > 0.05$ (not significant) for all vU-Luc compared to vLuc at the same time point (2-way ANOVA).

(28, 33), consistent with our results. The majority of UCOE studies concern the protection of transgene transcription from position effects at chromosomal integration sites, showing that UCOEs provide uniformity in expression that directly correlates with the transgene copy number and is stable through numerous cell divisions. Nonreplicating, large episomal vectors like the defective HSV vectors used in this study (~138 to 150 kb) represent a different situation. Most importantly, the transgene position and genetic context are predetermined and unique, excluding variable position effects. The advantage of this situation is that it facilitates the study of regulatory elements in a defined chromatin environment that in some instances can be manipulated. For example, the HSV IE protein ICP0 blocks global heterochromatinization of the viral genome (34), and its deletion, as in our study, allows an assessment of the heterochromatin-blocking activity of *cis*-acting sequences by comparison of transgene expression in populations of infected cells. HSV DNA, including that of replication-

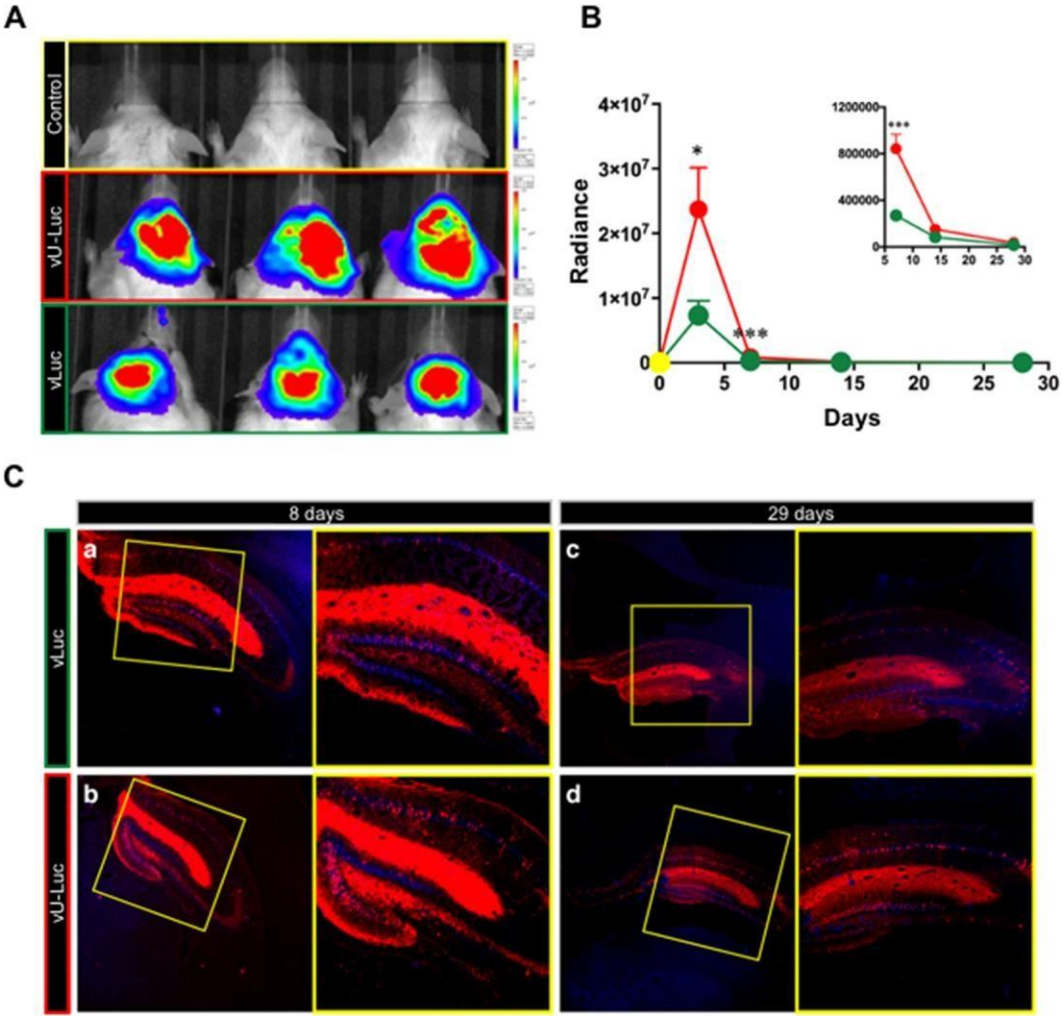

FIG 9 Transgene expression in the brains of mice injected with vLuc, vU-Luc, or vehicle (PBS). (A) Luciferase activity in 3 representative mice per group at 3 dpi. The colors indicate activity levels. (B) Quantification of bioluminescence signals (photons per second per square centimeter). Green, vLuc ($n = 12$ at 3 days and 7 days; $n = 8$ at 14 days; $n = 4$ at 28 days); red, vU-Luc ($n=12$ at 3 days and 7 days; $n=8$ at 14 days; $n=4$ at 28 days); yellow, PBS ($n=3$ at 3 days and 7 days; $n=2$ at 14 days; $n = 1$ at 28 days). The inset shows differences at the 7-, 14-, and 28-day time points in a lower bioluminescence range. The data are means and standard errors of the mean (SEM) per group. *, $P < 0.05$; ***, $P < 0.001$; Mann-Whitney U test.
(C) Representative images of coronal sections from animals injected with vLuc (top) or vU-Luc (bottom) sacrificed on the indicated days post-vector delivery. Blue, nuclei of neurons stained with Neurotrace; red, mCherry-positive cells. Higher magnifications of the boxed areas are shown on the right.

defective virions produced in complementing cells, is largely free of CpG methylation during replication (35). On infection of noncomplementing cells, transgenes are initially expressed from replication-defective vectors lacking ICP0, a cytotoxic protein, but are then rapidly silenced, similar to virus entry into latency in neurons. However, in latency, the viral genome remains unmethylated, and it has been shown that HSV gene expression is regulated by posttranscriptional histone modification (36). In dividing cells, such as preconfluent HDFs, partitioning of replication-defective viral genomes into daughter cells, in addition, reduces viral gene expression per cell by a nonepigenetic mechanism. In nondividing cells (e.g., DRG neurons), the viral genome copy number per cell remains essentially constant.

Previous studies have shown that a 4.0-kb A2UCOE fragment similar to the 4.1-kb region used in our work provided robust, stable transgene expression from the CMV promoter in transfected cells through numerous passages; a 1.5-kb A2UCOE fragment extending from *CBX3* intron 1 to *HNRPA2B1* intron 1 mediated moderately lower but equally stable expression (23). Likewise, Zhang and colleagues (27) showed that the

1.5-kb fragment and a 1.2-kb subfragment extending to the end of *HNRPA2B1* exon 1 enabled stable lentivirus transgene expression from the spleen focus-forming virus (SFFV) long terminal repeat (LTR), whereas the transgene was rapidly silenced in the absence of the UCOE. These authors, in addition, showed that the antisilencing activities of both fragments correlated with orientation-dependent blockage of SSFV promoter methylation. In our study, the CAG promoter was largely unmethylated even in the absence of A2UCOE sequences, and thus, UCOE-mediated promoter protection from methylation was not responsible for the increased transgene expression we observed from vUCOE1 and vUCOE2 compared to vCAG. By the same argument, it is unlikely that the loss of transgene expression we observed on deletion of the *HNRPA2B1* intron was due to promoter methylation. Instead, our H3K9Me3 analysis is consistent with the suggestion that A2UCOE prevents the deposition of repressive histone marks on proximal promoters, as previously proposed (37).

We have not excluded the formation of *HNRPA2B1*-transgene fusion transcripts resulting from transcription read-through from the *HNRPA2B1* promoter, as previously observed from the *CBX3* promoter (25, 38), and subsequent *HNRPA2B1* exon 1 splicing to splice acceptors at the ends of our CAG and EF1a constructs just upstream of the transgene. The intron 1 deletion (vUCOE3) would prevent these splicing events, as it includes the *HNRPA2B1* splice donor. Moreover, when we exchanged the positions of the *HNRPA2B1* promoter/transcribed region and the CAGp-EGFP cassette by inserting CAGp-EGFP into the A2UCOE dual-divergent promoter region (vUCOE4), transgene expression in HDFs was barely higher than in the absence of A2UCOE (Fig. 2B). Thus, in both cases, reduced green fluorescent protein (GFP) expression was correlated with the predicted absence of a productive read-through/splicing product. In vU-Luc-infected cells, the putative *HNRPA2B1*-Luc transcription/splicing event would create a short open reading frame (ORF) upstream of the luciferase ORF that might not interfere with luciferase translation. In vUCOE2-infected cells, however, translation from the *HNRPA2B1* start codon in exon 1 would read out of frame into the EGFP ORF and prevent the formation of a fluorescent product, arguing against a contribution of read-through transcription to the EGFP signal. As the effect of A2UCOE on expression of the linked reporter gene was larger in vU-Luc-infected than in vUCOE2-infected HDFs, it remains possible that transcripts initiating at the *HNRPA2B1* promoter contrib- uted to the vU-Luc luciferase signal in these cells but not to the vUCOE2 EGFP signal and not in neurons, where the difference was minimal.

We found that the 4.1-kb A2UCOE had a greater enhancing effect on transgene expression in HDFs and hMDSCs than in rDRGs. It is possible that this is related to differences between rDRG neurons and other host cells in the activity of the *CBX3* promoter, since it has been proposed that the cell-type-dependent strength of the promoter pointing away from the transgene is a key determinant of the chromatin-remodeling and antisilencing activities of A2UCOE (13, 27). However, the additional expression of mCherry in rDRGs is consistent with the alternative suggestion that our highly defective HSV vectors exist in a less transcriptionally repressed state in DRG neurons than in other cultured cells. While our images of vLuc/vU-Luc-infected rDRGs (Fig. 8A) suggest that most of the cells express all three transgenes, mCherry in particular is notably absent in some. This is reminiscent of observations in trigeminal ganglion (TG) cultures infected with the IE gene-disabled *d*109 vector (39) and likely reflects differences between different neuronal subtypes present in both DRG and TG cultures.

The suggestion that rDRGs in culture are relatively supportive of gene expression from highly defective HSV backbones agrees with our previous observation that an IE gene-inactive vector containing CAG-EGFP in the UL3-UL4 intergenic region produced substantially more EGFP-positive cells per input gc in rDRGs at 3 dpi than in nonneu-ronal cells (7). In contrast, we did not detect EGFP expression in rat hippocampus from the UL3-UL4 locus in previous work (31). Likewise, while CAG-EGFP in the LAT locus was active in cultured DRG neurons (reference 7 and this study), hippocampal expression was not observed (but see below). These results are suggestive of significant differences

between DRG and CNS neurons, although both are predominantly capable of transgene expression from the terminal ICP4 locus, unlike the different nonneuronal cell types we tested here and elsewhere (7).

The absence of detectable EGFP expression from the vLuc and vU-Luc vectors in mouse brain is unexplained. Lilley and coworkers introduced a strong promoter (CMV)-reporter gene cassette downstream of the LAP1-LATP2 components of the LAT gene in an arrangement very similar to our CAG promoter-EGFP insertion in a vector backbone that had the essential ICP4 and ICP27 genes and the IE gene-transactivating activity of VP16 deleted. At 7 days post-vector injection into rat striatum, strong reporter expression was observed in both the striatum and the substantia nigra, increasing from a moderate level at 3 days, and expression remained readily detectable at 1 month (40). While the authors acknowledged the possibility of an apparently nontoxic, undetected residual level of ICP0 expression from their VP16 mutant vector, we note that their vector also differed from ours in other respects, including the strain background (17*syn*$^+$ versus KOS), a complete deletion of the ICP34.5 neurovirulence gene, and the retention of CTCF-binding sites deleted in our vectors. Guided by these observations, we anticipate that further engineering may provide our vector with the ability to express LAT-based transgene cassettes in the CNS.

The HSV genome contains multiple CTCF-binding regions, in addition to CTRL1 and -2 (8). All of these regions are located within or near the long inverted repeats of the viral genome, and each of the 5 IE genes, in addition to the LAT gene, is flanked by at least one of these sites (8, 36). CTCF has insulator activity, defining chromatin boundaries that allow differential regulation of adjacent transcription domains (41–43). Moreover, in concert with cohesin, CTCF mediates DNA looping to distal CTCF-binding sites (44, 45), suggesting the potential for various types of regulatory interactions among the CTCF-binding regions of HSV (46, 47). Several laboratories have begun to unravel the role of CTCF and its partners in the regulation of HSV latency and reactivation, painting a complex picture of short- and potential long-range effects that may be influenced by the products of some of the regulated genes, LAT and ICP0 in particular (47–53). The extensive deletions in our vectors, which include all but 4 of the CTCF-binding sites in most of the vectors shown in Fig. 1, the ICP0 promoter and coding region, and large portions of the LAT gene, including key splicing signals for the formation of the stable LAT introns (Fig. 7A) or the promoter, enhancer, intron, including CTRL2, and upstream region, including CTRL1 (Fig. 1), can be predicted to profoundly alter the normal CTCF-mediated regulation of viral gene expression in latency compared to the latent- like state assumed by our vectors. We hypothesize that the unexpected long-term reporter gene expression from the terminal ICP4 locus of our defective vectors in central nervous system neurons *in vivo* (Fig. 9C) (31, 32) and the simultaneous lack of reporter expression from the LAT locus reported here are consequences of the disrup- tion of CTCF interactions and the loss of LAT and ICP0 functions. However, it is uncertain whether A2UCOE activity is influenced by the same mechanisms. While we suspect that the effects of A2UCOE can be duplicated in other locations distant from known CTCF-binding sites, this remains to be shown. Likewise, while we may expect that our vectors will act in human neurons much like they do in rodent neurons, this comparison has yet to be performed.

In conclusion, our study shows that the 4.1-kb A2UCOE can be a valuable component of highly defective HSV gene therapy vectors, particularly in nonneuronal cells. The stimulatory effect of A2UCOE on transgene expression in neuronal cells is short term but may be useful to increase the transient level of a regulator that induces an expression cascade. This work holds promise for the development of increasingly complex vectors for tightly controlled treatment of a variety of pathological conditions.

MATERIALS AND METHODS

Cells. HDFs, hMDSCs, hEKs, and rDRGs were cultured as described previously (7). For hMDSCs, the medium was changed at 1 dpi to 2% (vol/vol) fetal bovine serum (FBS) with 100 U/ml penicillin and 100 μg/ml streptomycin to induce myogenic differentiation. U2OS-ICP4/ICP27 and U2OS-ICP4/ICP27-Cre cells were as described previously (7).

TABLE 3 Primer sequences

Primer name	Orientation[a]	Sequence
P1	F	ACTAGTGCGCGCGGCGCGCCACCCAGCTTTCTTGTACAAAGTTGG
	R	CCAACTTTGTACAAAAAAGCAGGCTATTTAAATGGCCGGCCCATATG GTTAACAGATCTTCTAGAGCTAGCGGGCCC
P2	F	TTGGGAGCATGCGAATGGAG
	R	CGCCGGTTCGAAATTCTGGGCACTTATGAATG
P3	F	GGCCGCTTCGAAGCGTTACATAACTTACGG
	R	CGCCGCTCTGATTGGCTGCCGCCGCACCTC
P4	F	CGAATTAGGGACCCTTCGAAGCAAGCTTTATTCCAAGAGGTAGTAACT
	R	AGCACCTCCGCACGGGACCC
O1	F	ACCGGTGTATACTGGCCATGGCCGGCCTTAATATC
	R	GATATTAAGGCCGGCCATGGCCAGTATACACCGGT
Q1	F	ATCATGGCCGACAAGCAGAAGAAC
	R	GTACAGCTCGTCCATGCCGAGAGT
Q2	F	CCTGTCCCCTCAGTTCATGT
	R	GCTTCAAGTAGTCGGGGATG
Q3	F	GTGACTACGGCCCTACCG
	R	GAAACCGGCATCCTCCTCG
Q4	F	AGCACATCCGCGGACTTGTC
	R	ACCACCCCGGGTTCGAGG
Q5	F	CTGACTGACCGCGTTACTCC
	R	CGTCATTAAACCAAGCGCTAA
M1	F	GTGAAAGTTTTGAGGGGTTT
	R	AAAAATACAAAAAAAATTACAACCC
M2	F	GTTTGTTTTTTTTTTGTGGTTG
	R	AAAAATACAAAAAAAATTACAACCC
M3	F	GTAGGGATTTTTTTTGTTTTAAATT
	R	CATAATTAACAAAAACTCTAAAACC
M4	F	GTAGTTATTGTTTTTTATGGTAAT
	R	CATAATTAACAAAAACTCTAAAACC

[a]F, forward; R, reverse.

Plasmids. (i) pHS4-S. Plasmid pENTR-CAG-EGFP contains a CAG promoter (CMV enhancer/chicken þ- actin promoter/chimeric intron)-driven EGFP expression cassette between *attL* sites (7). To introduce multiple-cloning sites (MCS) both between *attL1* and the promoter and between the poly(A) region and *attL2*, we performed a PCR with primer pair P1 (all the primers mentioned are listed in Table 3) to amplify the plasmid backbone with terminal *attL* sites and digested the product at unique, *attL*-external XbaI and StuI sites specified by the respective primers. A SpeI-StuI fragment containing the EGFP expression cassette of pENTR-CAG-EGFP was isolated and ligated to the digested backbone PCR product to generate pCAG-EGFP-MCS1. A SwaI-AscI fragment containing two tandem copies of the 250-bp cHS4 core (54) on both sides of a tdTomato expression cassette was isolated from pBT268 (Addgene plasmid 36880; Liqun Luo laboratory) and cloned between the two MCS loci flanking the CAG-EGFP cassette in pCAG-EGFP- MCS1. The tdTomato cassette of the resulting plasmid, pENTR-cHS4-S, was then replaced with the EGFP expression cassette from pCAG-EGFP-MCS1 to generate pHS4-S containing *attL1*-(2xcHS4)- [CAG-EGFP- poly(A)]-(2xcHS4)-*attL2*.

(ii) pHS4-L. A SacI fragment containing the full-length 1.2-kb cHS4 insulator region was isolated from pJC13-1 (54) (kindly provided by G. Felsenfeld, NIH/NIDDK) and cloned into the SacI site of pBluescript to create pBS-cHS4. The SacI fragment was excised, its 3=overhangs were removed with T4 DNA polymerase, and it was cloned into the filled-in SpeI site upstream of the CAG promoter in pENTR-CAG-EGFP (pENTR-CAG-EGFP-HS4-L-up). The same blunt-ended SacI fragment was then cloned in the same orientation into the StuI site downstream of the poly(A) region in pENTR-CAG-EGFP-HS4-L-up.

(iii) pUCOE1. A synthetic MCS generated by annealing oligonucleotides O1 was introduced between the SwaI and FseI sites in the upstream MCS of pCAG-EGFP-MCS1 to create pCAG-EGFP-MCS2. A2UCOE

(22) was isolated from UCOE Hu-P (Millipore) as an AgeI-MscI fragment and inserted between the same sites in the new MCS of pCAG-EGFP-MCS2.

(iv) pUCOE2. A 3′ segment of A2UCOE and a 5′ segment of the CAG promoter were separately amplified from pUCOE1 using primer sets P2 and P3, respectively. The two PCR products joined at a BstBI site were cloned into pUCOE1 between an SphI site in the amplified portion of the HNRPA2B1 intron and a SnaBI site in the amplified CAG portion.

(v) pUCOE3. pUCOE2 was digested with Tth111I and BstBI, cutting at both ends of the HNRPA2B1 intron, and the large fragment was gel purified, its 5′ overhangs were filled in with T4 DNA polymerase, and it was self-ligated.

(vi) pUCOE4. pUCOE2 was digested with BstBI and HindIII, the 5′ overhangs were filled in with T4 DNA polymerase, and the large fragment was self-ligated to generate pUCOE2 with CAG-EGFP deleted. Adjacent BstBI and HindIII sites were inserted into this plasmid in the CBX3-HNRPA2B1 dual-divergent promoter region by replacing a SanD1 fragment, extending from the center of the region into the HNRPA2B1 exon, with a corresponding PCR fragment generated on pUCOE2 as the template with SanDI-overlapping primers P4-F, specifying the inserted sites, and P4-R. The resulting plasmid was then modified by BstBI-HindIII digestion and ligation to the CAG-EGFP BstBI-HindIII fragment from pUCOE2.

(vii) pUCOE5. pUCOE2 was digested with Tth111I and HindIII, the 5′ overhangs were filled in with T4 DNA polymerase, and the large fragment was self-ligated to delete CAG-EGFP, along with the HNRPA2B1 intron. Introduction of cloning sites into the CBX3-HNRPA2B1 promoter region, followed by CAG-EGFP insertion, was as described for pUCOE4 above.

(viii) pLuc. The mir-941 precursor in pEP-mir (Cell Biolabs) was removed by digestion with BamHI and NheI, and the vector piece was blunt ended and self-ligated to generate an EF1α promoter-intron-mCherry/Puro plasmid termed pEP-mCherry. The mCherry/Puro cDNA was replaced by EGFP from pCAG-GFP (7) to create pEP-EGFP. EGFP was subsequently replaced with a blunted BamHI-SacI fragment containing the firefly luciferase gene from pMIR-report (Ambion), producing pEP-luc. The complete EF1α-luc cassette was then isolated from pEP-luc by partial digestion with ClaI and SpeI and used to replace the CAG-EGFP cassette in pENTR-CAG-EGFP.

(ix) pU-Luc. The EF1α-luc cassette from pEP-luc was isolated as a 5′ ClaI-EcoRI fragment and a 3′ EcoRI-BglII fragment. The two fragments were subcloned into BstBI-BglII-digested pUCOE2, replacing the CAG-EGFP cassette. The PacI-NheI fragment separating A2UCOE from the EF1α-luc cassette was replaced with the PacI-NheI fragment of pLuc to remove differences between pLuc and pU-Luc outside the A2UCOE region.

Viral genome engineering. Viral genome constructs containing CAG-EGFP in the UL50-UL51 intergenic region were generated by LR clonase (Invitrogen)-mediated recombination between appropriate pENTR-based plasmids and the GW region of JΔNI10GW BAC DNA, essentially as described previously (7). vLuc and vU-Luc were generated by GW recombination between pLuc or pU-Luc, and JΔNI11GW. JΔNI11GW was engineered by Red/ET (Gene Bridges, Heidelberg, Germany)-mediated recombination of a PCR-amplified GW-Zeo cassette (7) into the intergenic region between UL50 and UL51 of JΔNI7GFP BAC (7) in *Escherichia coli*. All the BAC recombinants were confirmed by PCR analysis, field inversion gel electrophoresis (FIGE) analysis of restriction enzyme digests, and targeted DNA sequencing.

Virus production. Recombinant viruses were produced by transfection of U2OS-ICP4/ICP27 cells with purified BAC DNA, as described previously (7). Following cytopathic effect (CPE), supernatants were harvested for standard virus amplification in the same cell line. The titers of virus stocks were determined on U2OS-ICP4/ICP27 cells as PFU/ml. Genome copy titers (gc per milliliter) were determined by real-time quantitative PCR (qPCR) for the viral gD gene (7). Deletion of the BAC region, including the associated chloramphenicol resistance and *lacZ* genes, was essentially as described previously (7). Briefly, viruses were passaged twice through U2OS-ICP4/ICP27-Cre cells, and isolated plaques generated by limiting dilution were screened by PCR across the expected deletion and by staining for β-galactosidase activity. Isolates with the BAC deleted were propagated on U2OS-ICP4/ICP27 cells.

Luciferase assay. Luciferase assays were performed with a luciferase assay system (Promega) according to the manufacturer's instructions. Cells were lysed with cell culture lysis reagent (CCLR; Promega), and the lysate was used for both luciferase activity measurement in a BioTek Synergy2 microplate reader and PCR determination of viral genome copy numbers for normalization.

Quantitative reverse transcription-PCR. qRT-PCR was performed as previously described (7) using a Cells-to-cDNA II kit (Ambion) for mRNA extraction and cDNA synthesis. The qPCR primers for GFP (Q1), mCherry (Q2), UL50 (Q3), and UL51 (Q4) are listed in Table 3. The results were normalized to the viral genome copy numbers measured in lysates prior to the DNase step for RNA isolation.

Immunofluorescence. Transduced rDRGs were fixed in Buffered Formalde-Fresh (Fisher Scientific) at room temperature for 10 min and blocked with 5% normal goat serum–0.2% Triton X-100 in phosphate-buffered saline (PBS) for 1 h at room temperature. After blocking, the cells were incubated with anti-luciferase antibody (Abcam; ab21176; 1:500) at 4°C overnight, and biotin (Sigma; B7389; 1:1,000)- avidin (Invitrogen; A11236; 1:1,000) was added the next day for a 1-h incubation at room temperature. Fluorescence images were collected with an Olympus FV1000 confocal microscope.

ChIP. Two million HDFs were plated in 10-cm dishes for infection the following day (5,000 gc/cell). At 7 dpi, chromatin immunoprecipitation (ChIP) was carried out as described by Nelson and colleagues (55). Briefly, infected HDFs were cross-linked with 37% formaldehyde for 15 min, and the reaction was quenched with 1 M glycine. Cells were collected by centrifugation, washed in cold PBS, and lysed in immunoprecipitation (IP) buffer (150 mM NaCl, 50 mM Tris-HCl, pH 7.5, 5 mM EDTA, 0.5% [vol/vol] NP-40, and 1.0% [vol/vol] Triton X-100). The lysates were sonicated using an S-3000 Misonix sonicator. Immunoprecipitations were carried out overnight at 4°C with normal rabbit IgG (Santa Cruz; sc-2027), rabbit

anti-histone H3 antibody (Millipore; 06-755), or rabbit anti-H3K9Me3 (Millipore; 07-442). Dynabeads M-280 sheep anti-rabbit IgG (Life Technologies) was used to precipitate the antibody-bound DNA. A fraction of the sonicated cells was used as the input control. qRT-PCR was carried out using primer set Q5 within the CAG promoter.

Bisulfite conversion and sequencing. Viral DNA was extracted with a DNeasy blood and tissue kit (Qiagen) prior to (input) and at 7 days after infection of HDFs. Bisulfite conversion was carried out using an Epitech kit (Qiagen) according to the manufacturer's instructions. The converted input DNA was amplified with primer pair M1, and the converted DNA from infected HDFs was amplified with primer pair M2, followed by a nested PCR with primer pair M1 using GoTaq DNA polymerase M300 (Promega) to examine the viral DNA methylation status of a 5′ portion of the β-actin component of the CAG promoter. Likewise, primer pairs M3 and M4 were used for pre- and postinfection viral DNA PCR to determine the methylation status of a 3′ portion of the β-actin segment of the CAG promoter. The PCR products were gel purified and cloned into pCR2.1-TOPO using a TOPO TA Cloning kit (no. 450641; Invitrogen). Inserts of individual clones were sequenced using the M13 reverse primer.

Animals. Male CD1 mice were purchased from Charles River Italy (Calco, Lecco, Italy). Experiments were performed at the University of Ferrara in compliance with the guidelines for the ethical treatment of experimental animals (authorization from the Italian Ministry for Health D.M. 18/2017-PR).

HSV-1 infusion *in vivo*. General anesthesia was induced in 25- to 30-g mice by coadministration of ketamine (45 mg/kg of body weight intraperitoneally [i.p.]) and xylazine (7 mg/kg i.p.) and was maintained with 1.4% isoflurane in air (flow, 1.2 ml/min). The animals were placed in a stereotactic frame on a temperature-controlled heating pad, and a total of 2×10^9 viral genome copies was injected into the right dorsal hippocampus. Viral vectors (vLuc and vU-Luc; $n = 12$ mice/vector) or PBS ($n = 3$) was injected by stereotactic placement of a custom-made borosilicate glass needle (56). The needle tips were chamfered by laser microdissector cutting (LMD6500 Laser Microdissection System; Leica Microsystems, Wetzlar, Germany) (angle, 140°; inner and outer diameters at the tip, 80 and 100 μm, respectively). An additional hole (diameter, 10 μm) was opened 100 μm above the tip to favor spreading of the injected virus (56). The needle was bottom filled with the viral solution and linked to a microperfusion pump set to inject a total of 2 μl at a flow rate of 0.3 μl/min. The stereotactic coordinates (57) were 1.6 mm lateral,
1.9 mm posterior to bregma, and 1.9 mm deep from dura. Carprofen (5 mg/kg i.p.) was administered after surgery to prevent pain.

***In vivo* bioluminescence imaging.** At selected time points (3, 7, 14, and 28 days postsurgery), mice were anesthetized with 2% isoflurane and oxygen, and D-luciferin substrate (Roche) was injected i.p. at a dose of 200 mg/kg. *In vivo* bioluminescence was detected 8 min after the injection in a total-body luminometer (IVIS Lumina; Caliper-PerkinElmer, Hopkinton, MA, USA). Photon emissions in the region of interest were quantified with Living Image software (Caliper).

Tissue preparation. Animals were deeply anesthetized with pentobarbital and transcardially perfused with PBS, followed by 4% paraformaldehyde in 0.1 M PBS. Brains were isolated and postfixed in 4% paraformaldehyde for 1 h, cryoprotected in 30% sucrose at 4°C until the tissue sank, and flash-frozen in isopentane prechilled at −80°C.

Tissue immunofluorescence. Twenty-micrometer coronal sections were cut at −20°C in a cryostat (Leica), rinsed in 0.1 M PBS, permeabilized for 10 min in 0.3% Triton X-100 –PBS, and blocked for 30 min in 0.1 M PBS with 10% normal goat serum. The sections were then incubated overnight at 4°C with primary antibodies diluted in 0.1 M PBS: rabbit anti-mCherry (Abcam), 1:500; chicken anti-GFP (Abcam), 1:200. The sections were washed twice in PBS and stained for 2 h at room temperature with 1:500-diluted Alexa Fluor 594 goat anti-rabbit or Alexa Fluor 488 goat anti-chicken antibody (Molecular Probes, Eugene, OR, USA).

NeuroTrace staining. After rehydration in 0.1 M PBS, sections were permeabilized with 0.1% Triton X-100 in PBS for 10 min, washed twice for 5 min each time in PBS, and stained with NeuroTrace 435/455 Blue Fluorescent Nissl stain (ThermoFisher; dilution, 1:200) for 20 min at room temperature. The sections were then washed twice in PBS and finally left for 2 h at room temperature in PBS before imaging.

Statistics. For quantitative analyses in cell culture, two plaque-purified isolates per vector construct were tested in parallel in duplicate wells in 48- or 96-well plates. Each experiment was then repeated once on a separate day with one of the two isolates per construct. Data were recorded for each well, and the mean of the duplicate wells was calculated. Viral genome qPCR and mRNA qRT-PCR measurements were performed in duplicate or triplicate per well, and the mean qRT-PCR value was normalized to the mean viral genome qPCR value for each well. The data were analyzed separately for each isolate and repeat experiments by 2-way analysis of variance (ANOVA), with the exception of Fig. 5 (Mann-Whitney test). The representative data shown (means and standard deviations [SD] of duplicate wells) are from one isolate per vector construct, with the exception of Fig. 7 (combined data from duplicate wells for 2 isolates). *In vivo* bioluminescence results were analyzed by Mann-Whitney U test.

Data availability. The materials described in this publication are available on request to members of the scientific community for noncommercial purposes.

ACKNOWLEDGMENTS

We are grateful to G. Felsenfeld for the pJC13-1 plasmid, Johnny Huard and Xueqin Gao for hMDSCs, Mingdi Zhang for rat DRG culturing and immunostaining, William Goins for technical advice, and Bonnie Hall for helpful discussions.

This work was supported by grants to J. C. Glorioso from the NIH (NS064988 and DK044935) and the CHDI Foundation (A3777 and A8790) and to M. Simonato from the

European Community (FP7-PEOPLE-2011-IAPP project 285827 [EPIXCHANGE]), the Italian Ministry for Education, University and Research (PRIN project 2010N8PBAA [INBDNF]), and the Regione Lombardia (POR FESR 2014-2020 project ID 239047 [NeOn]).

F. Han was supported by funding from the China Scholarship Council.

Experiments were designed by F. Han, Y. Miyagawa, G. Verlengia, M. Simonato, J. C. Glorioso, and J. B. Cohen; vector engineering, virus production, and *in vitro* analyses were performed by F. Han and Y. Miyagawa; animal experiments were carried out by G. Verlengia, S. Ingusci, and M. Soukupova; all the authors conducted data analysis and interpretation; F. Han, Y. Miyagawa, J. C. Glorioso, and J. B. Cohen wrote the manuscript.

G. Verlengia, M. Simonato, and J. C. Glorioso are founders of NuvoVec srl. Y. Miyagawa, J. C. Glorioso and J. B. Cohen are coinventors of intellectual property licensed to Coda Biotherapeutics, Inc., J. C. Glorioso and J. B. Cohen are coinventors of intellectual property licensed to Oncorus, Inc., and J. C. Glorioso is a founder and consultant of Coda Biotherapeutics, Inc., and Oncorus, Inc.

REFERENCES

1. Roizman B, Zhou G. 2015. The 3 facets of regulation of herpes simplex virus gene expression: a critical inquiry. Virology 479-480:562–567. https://doi.org/10.1016/j.virol.2015.02.036.
2. Knipe DM. 2015. Nuclear sensing of viral DNA, epigenetic regulation of herpes simplex virus infection, and innate immunity. Virology 479-480: 153–159. https://doi.org/10.1016/j.virol.2015.02.009.
3. Samaniego LA, Neiderhiser L, DeLuca NA. 1998. Persistence and expres- sion of the herpes simplex virus genome in the absence of immediate- early proteins. J Virol 72:3307–3320.
4. Harkness JM, Kader M, DeLuca NA. 2014. Transcription of the herpes simplex virus 1 genome during productive and quiescent infection of neuronal and nonneuronal cells. J Virol 88:6847– 6861. https://doi.org/10.1128/JVI.00516-14.
5. Du T, Zhou G, Roizman B. 2011. HSV-1 gene expression from reactivated ganglia is disordered and concurrent with suppression of latency-associated transcript and miRNAs. Proc Natl Acad Sci U S A 108: 18820 –18824. https://doi.org/10.1073/pnas.1117203108.
6. Raja P, Lee JS, Pan D, Pesola JM, Coen DM, Knipe DM. 2016. A herpesviral lytic protein regulates the structure of latent viral chromatin. mBio 7:e00633-16. https://doi.org/10.1128/mBio.00633-16.
7. Miyagawa Y, Marino P, Verlengia G, Uchida H, Goins WF, Yokota S, Geller DA, Yoshida O, Mester J, Cohen JB, Glorioso JC. 2015. Herpes simplex viral-vector design for efficient transduction of nonneuronal cells with- out cytotoxicity. Proc Natl Acad Sci U S A 112:E1632–E1641. https://doi.org/10.1073/pnas.1423556112.
8. Amelio AL, McAnany PK, Bloom DC. 2006. A chromatin insulator-like element in the herpes simplex virus type 1 latency-associated transcript region binds CCCTC-binding factor and displays enhancer-blocking and silencing activities. J Virol 80:2358 –2368. https://doi.org/10.1128/JVI.80.5.2358-2368.2006.
9. Palmer JA, Branston RH, Lilley CE, Robinson MJ, Groutsi F, Smith J, Latchman DS, Coffin RS. 2000. Development and optimization of herpes simplex virus vectors for multiple long-term gene delivery to the pe- ripheral nervous system. J Virol 74:5604 –5618. https://doi.org/10.1128/ JVI.74.12.5604-5618.2000.
10. Goins WF, Sternberg LR, Croen KD, Krause PR, Hendricks RL, Fink DJ, Straus SE, Levine M, Glorioso JC. 1994. A novel latency-active promoter is contained within the herpes simplex virus type 1 UL flanking repeats. J Virol 68:2239 –2252.
11. Emery DW. 2011. The use of chromatin insulators to improve the expression and safety of integrating gene transfer vectors. Hum Gene Ther 22:761–774. https://doi.org/10.1089/hum.2010.233.
12. Argyros O, Wong SP, Harbottle RP. 2011. Non-viral episomal modifica- tion of cells using S/MAR elements. Expert Opin Biol Ther 11:1177–1191. https://doi.org/10.1517/14712598.2011.582035.
13. Antoniou MN, Skipper KA, Anakok O. 2013. Optimizing retroviral gene expression for effective therapies. Hum Gene Ther 24:363–374. https://doi.org/10.1089/hum.2013.062.
14. Chung JH, Bell AC, Felsenfeld G. 1997. Characterization of the chicken beta-globin insulator. Proc Natl Acad Sci U S A 94:575–580. https://doi.org/10.1073/pnas.94.2.575.
15. Recillas-Targa F, Pikaart MJ, Burgess-Beusse B, Bell AC, Litt MD, West AG, Gaszner M, Felsenfeld G. 2002. Position-effect protection and enhancer blocking by the chicken beta-globin insulator are separable activities. Proc Natl Acad Sci U S A 99:6883– 6888. https://doi.org/10.1073/pnas.102179399.
16. Yao S. 2003. Retrovirus silencer blocking by the cHS4 insulator is CTCF independent. Nucleic Acids Res 31:5317–5323. https://doi.org/10.1093/nar/gkg742.
17. Aker M, Tubb J, Groth AC, Bukovsky AA, Bell AC, Felsenfeld G, Kiem HP, Stamatoyannopoulos G, Emery DW. 2007. Extended core sequences from the cHS4 insulator are necessary for protecting retroviral vectors from silencing position effects. Hum Gene Ther 18:333–343. https://doi.org/10.1089/hum.2007.021.
18. Suttiprapa S, Rinaldi G, Brindley PJ. 2012. Prototypic chromatin insulator cHS4 protects retroviral transgene from silencing in Schistosoma man- soni. Transgenic Res 21:555–566. https://doi.org/10.1007/s11248-011-9556-0.
19. Emery DW, Yannaki E, Tubb J, Nishino T, Li Q, Stamatoyannopoulos G. 2002. Development of virus vectors for gene therapy of beta chain hemoglobinopathies: flanking with a chromatin insulator reduces gamma-globin gene silencing in vivo. Blood 100:2012–2019. https://doi.org/10.1182/blood-2002-01-0219.
20. Arumugam PI, Scholes J, Perelman N, Xia P, Yee JK, Malik P. 2007. Improved human beta-globin expression from self-inactivating lentiviral vectors carrying the chicken hypersensitive site-4 (cHS4) insulator ele- ment. Mol Ther 15:1863–1871. https://doi.org/10.1038/sj.mt.6300259.
21. Lindahl Allen M, Antoniou M. 2007. Correlation of DNA methylation with histone modifications across the HNRPA2B1-CBX3 ubiquitously-acting chromatin open element (UCOE). Epigenetics 2:227–236. https://doi.org/10.4161/epi.2.4.5231.
22. Antoniou M, Harland L, Mustoe T, Williams S, Holdstock J, Yague E, Mulcahy T, Griffiths M, Edwards S, Ioannou PA, Mountain A, Crombie R. 2003. Transgenes encompassing dual-promoter CpG islands from the human TBP and HNRPA2B1 loci are resistant to heterochromatin- mediated silencing. Genomics 82:269 –279. https://doi.org/10.1016/ S0888-7543(03)00107-1.
23. Williams S, Mustoe T, Mulcahy T, Griffiths M, Simpson D, Antoniou M, Irvine A, Mountain A, Crombie R. 2005. CpG-island fragments from the HNRPA2B1/CBX3 genomic locus reduce silencing and enhance trans- gene expression from the hCMV promoter/enhancer in mammalian cells. BMC Biotechnol 5:17. https://doi.org/10.1186/1472-6750-5-17.
24. Boscolo S, Mion F, Licciulli M, Macor P, De Maso L, Brce M, Antoniou MN, Marzari R, Santoro C, Sblattero D. 2012. Simple scale-up of recombinant antibody production using an UCOE containing vector. N Biotechnol 29:477– 484. https://doi.org/10.1016/j.nbt.2011.12.005.
25. Brendel C, Muller-Kuller U, Schultze-Strasser S, Stein S, Chen-Wichmann L, Krattenmacher A, Kunkel H, Dillmann A, Antoniou MN, Grez M. 2012. Physiological regulation of transgene expression by a lentiviral vector containing the A2UCOE linked to a myeloid promoter. Gene Ther 19: 1018 –1029. https://doi.org/10.1038/gt.2011.167.
26. Zhang F, Thornhill SI, Howe SJ, Ulaganathan M, Schambach A, Sinclair J,

Kinnon C, Gaspar HB, Antoniou M, Thrasher AJ. 2007. Lentiviral vectors containing an enhancer-less ubiquitously acting chromatin opening element (UCOE) provide highly reproducible and stable transgene expression in hematopoietic cells. Blood 110:1448 –1457. https://doi.org/10.1182/blood-2006-12-060814.
27. Zhang F, Frost AR, Blundell MP, Bales O, Antoniou MN, Thrasher AJ. 2010. A ubiquitous chromatin opening element (UCOE) confers resistance to DNA methylation-mediated silencing of lentiviral vectors. Mol Ther 18: 1640 – 1649. https://doi.org/10.1038/mt.2010.132.
28. Saunders F, Sweeney B, Antoniou MN, Stephens P, Cain K. 2015. Chromatin function modifying elements in an industrial antibody production platform— comparison of UCOE, MAR, STAR and cHS4 elements. PLoS One 10:e0120096. https://doi.org/10.1371/journal.pone.0120096.
29. Muller-Kuller U, Ackermann M, Kolodziej S, Brendel C, Fritsch J, Lach- mann N, Kunkel H, Lausen J, Schambach A, Moritz T, Grez M. 2015. A minimal ubiquitous chromatin opening element (UCOE) effectively pre- vents silencing of juxtaposed heterologous promoters by epigenetic remodeling in multipotent and pluripotent stem cells. Nucleic Acids Res 43:1577–1592. https://doi.org/10.1093/nar/gkv019.
30. Uchiyama T, Adriani M, Jagadeesh GJ, Paine A, Candotti F. 2012. Foamy virus vector-mediated gene correction of a mouse model of Wiskott- Aldrich syndrome. Mol Ther 20:1270 –1279. https://doi.org/10.1038/mt.2011.282.
31. Verlengia G, Miyagawa Y, Ingusci S, Cohen JB, Simonato M, Glorioso JC. 2017. Engineered HSV vector achieves safe long-term transgene expression in the central nervous system. Sci Rep 7:1507. https://doi.org/10.1038/s41598-017-01635-1.
32. Miyagawa Y, Verlengia G, Reinhart B, Han F, Uchida H, Zucchini S, Goins WF, Simonato M, Cohen JB, Glorioso JC. 2017. Deletion of the virion host shutoff gene enhances neuronal-selective transgene expression from an HSV vector lacking functional IE genes. Mol Ther Methods Clin Dev 6:79 –90. https://doi.org/10.1016/j.omtm.2017.06.001.
33. Hagedorn C, Antoniou MN, Lipps HJ. 2013. Genomic cis-acting se- quences improve expression and establishment of a nonviral vector. Mol Ther Nucleic Acids 2:e118. https://doi.org/10.1038/mtna.2013.47.
34. Ferenczy MW, DeLuca NA. 2011. Reversal of heterochromatic silencing of quiescent herpes simplex virus type 1 by ICP0. J Virol 85:3424 –3435. https://doi.org/10.1128/JVI.02263-10.
35. Hoelzer K, Shackelton LA, Parrish CR. 2008. Presence and role of cytosine methylation in DNA viruses of animals. Nucleic Acids Res 36:2825–2837. https://doi.org/10.1093/nar/gkn121.
36. Bloom DC, Giordani NV, Kwiatkowski DL. 2010. Epigenetic regulation of latent HSV-1 gene expression. Biochim Biophys Acta 1799:246 –256. https://doi.org/10.1016/j.bbagrm.2009.12.001.
37. Majocchi S, Aritonovska E, Mermod N. 2014. Epigenetic regulatory elements associate with specific histone modifications to prevent silencing of telomeric genes. Nucleic Acids Res 42:193–204. https://doi.org/10.1093/nar/gkt880.
38. Talbot GE, Waddington SN, Bales O, Tchen RC, Antoniou MN. 2010. Desmin-regulated lentiviral vectors for skeletal muscle gene transfer. Mol Ther 18:601– 608. https://doi.org/10.1038/mt.2009.267.
39. Terry-Allison T, Smith CA, DeLuca NA. 2007. Relaxed repression of herpes simplex virus type 1 genomes in murine trigeminal neurons. J Virol 81:12394 –12405. https://doi.org/10.1128/JVI.01068-07.
40. Lilley CE, Groutsi F, Han Z, Palmer JA, Anderson PN, Latchman DS, Coffin RS. 2001. Multiple immediate-early gene-deficient herpes simplex virus vectors allowing efficient gene delivery to neurons in culture and wide- spread gene delivery to the central nervous system in vivo. J Virol 75:4343– 4356. https://doi.org/10.1128/JVI.75.9.4343-4356.2001.
41. Ong CT, Corces VG. 2014. CTCF: an architectural protein bridging ge- nome topology and function. Nat Rev Genet 15:234 –246. https://doi.org/10.1038/nrg3663.
42. Kim S, Yu NK, Kaang BK. 2015. CTCF as a multifunctional protein in genome regulation and gene expression. Exp Mol Med 47:e166. https://doi.org/10.1038/emm.2015.33.
43. Ghirlando R, Felsenfeld G. 2016. CTCF: making the right connections. Genes Dev 30:881– 891. https://doi.org/10.1101/gad.277863.116.
44. Merkenschlager M, Nora EP. 2016. CTCF and cohesin in genome folding and transcriptional gene regulation. Annu Rev Genomics Hum Genet 17:17– 43. https://doi.org/10.1146/annurev-genom-083115-022339.
45. Barrington C, Finn R, Hadjur S. 2017. Cohesin biology meets the loop extrusion model. Chromosome Res 25:51– 60. https://doi.org/10.1007/s10577-017-9550-3.
46. Busslinger GA, Stocsits RR, van der Lelij P, Axelsson E, Tedeschi A, Galjart N, Peters JM. 2017. Cohesin is positioned in mammalian genomes by transcription, CTCF and Wapl. Nature 544:503–507. https://doi.org/10.1038/nature22063.
47. Lee JS, Raja P, Pan D, Pesola JM, Coen DM, Knipe DM. 2018. CCCTC- binding factor acts as a heterochromatin barrier on herpes simplex viral latent chromatin and contributes to poised latent infection. mBio 9. e02372-17. https://doi.org/10.1128/mBio.02372-17.
48. Wang QY, Zhou C, Johnson KE, Colgrove RC, Coen DM, Knipe DM. 2005. Herpesviral latency-associated transcript gene promotes as- sembly of heterochromatin on viral lytic-gene promoters in latent infection. Proc Natl Acad Sci U S A 102:16055–16059. https://doi.org/10.1073/pnas.0505850102.
49. Cliffe AR, Knipe DM. 2008. Herpes simplex virus ICP0 promotes both histone removal and acetylation on viral DNA during lytic infection. J Virol 82:12030 –12038. https://doi.org/10.1128/JVI.01575-08.
50. Ferenczy MW, DeLuca NA. 2009. Epigenetic modulation of gene expression from quiescent herpes simplex virus genomes. J Virol 83: 8514 – 8524. https://doi.org/10.1128/JVI.00785-09.
51. Ertel MK, Cammarata AL, Hron RJ, Neumann DM. 2012. CTCF occupation of the herpes simplex virus 1 genome is disrupted at early times postreactivation in a transcription-dependent manner. J Virol 86: 12741–12759. https://doi.org/10.1128/JVI.01655-12.
52. Lang F, Li X, Vladimirova O, Hu B, Chen G, Xiao Y, Singh V, Lu D, Li L, Han H, Wickramasinghe JM, Smith ST, Zheng C, Li Q, Lieberman PM, Fraser NW, Zhou J. 2017. CTCF interacts with the lytic HSV-1 genome to promote viral transcription. Sci Rep 7:39861. https://doi.org/10.1038/ srep39861.
53. Washington SD, Musarrat F, Ertel MK, Backes GL, Neumann DM. 2018. CTCF binding sites in the herpes simplex virus 1 genome display site- specific CTCF occupation, protein recruitment, and insulator function. J Virol 92. e00156-18. https://doi.org/10.1128/JVI.00156-18.
54. Chung JH, Whiteley M, Felsenfeld G. 1993. A 5element of the chicken beta-globin domain serves as an insulator in human erythroid cells and protects against position effect in Drosophila. Cell 74:505–514. https://doi.org/10.1016/0092-8674(93)80052-G.
55. Nelson JD, Denisenko O, Bomsztyk K. 2006. Protocol for the fast chromatin immunoprecipitation (ChIP) method. Nat Protoc 1:179 –185. https://doi.org/10.1038/nprot.2006.27.
56. Paolone G, Falcicchia C, Verlengia G, Barbieri M, Binaschi A, Paliotto F, Paradiso B, Soukupova M, Zucchini S, Simonato M. 2018. Personalized needles for microinjections in the rodent brain. J Vis Exp https://doi.org/10.1128/JVI.00156-18.
57. Paxinos GT, Franklin KBJ. 2001. The mouse brain in stereotaxic coordinates, 2nd ed. Academic Press, San Diego, CA.
58. Uchida H, Chan J, Goins WF, Grandi P, Kumagai I, Cohen JB, Glorioso JC. 2010. A double mutation in glycoprotein gB compensates for ineffective gD-dependent initiation of herpes simplex virus type 1 infection. J Virol 84:12200 –12209. https://doi.org/10.1128/JVI.01633-10.
59. Szymczak AL, Vignali DA. 2005. Development of 2A peptide-based strategies in the design of multicistronic vectors. Expert Opin Biol Ther 5:627–638. https://doi.org/10.1517/14712598.5.5.627.

3.3 Noninvasive Bioluminescence and Ex Vivo Histological Evaluation of Long and Short Term Expression of Herpes Simplex Virus Type-1 Based Amplicon vectors in the Mouse Brain

Noninvasive Bioluminescence and Ex Vivo Histological Evaluation of Long and Short Term Expression of Herpes Simplex Virus Type-1 Based Amplicon vectors in the Mouse Brain

Marie Soukupová[1], Selene Ingusci[1], Francesca Lovisari[1], Chiara Falcicchia[1], Silvia Zucchini[1], Mario Barbieri[1], Pascal Trempat[2], Coline Perrier-Biollay[2], Simonetta Falzoni[3], Francesco Di Virgilio[3], Hervé Berthommé[2], Michele Simonato[1]

[1]Department of Medical Sciences, Section of Pharmacology, Neuroscience Center, University of Ferrara and National Institute of Neuroscience, Via Fossato di Mortara 17-19, Ferrara, Italy, [2]Bioviron, Université Claude Bernard Lyon 1, Villeurbanne, France, [3]Department of Morphology, Surgery and Experimental Medicine, University of Ferrara, Ferrara, Italy

Corresponding author:
Marie Soukupová (marie.soukupova@unife.it)
Tel: (0039)-0532455859

KEYWORDS:
amplicon vectors, hippocampus, luciferase imaging, green fluorescent protein, gene therapy, mice

ABSTRACT:
Gene therapy, where DNA or RNA packed into a vector is used as a pharmacologically active agent, represents a promising approach for the treatment of many neurological diseases. Different types of viral and non-viral vectors can be used to vehicle therapeutic genes into specific cells or brain areas. All viral vectors currently used for central nervous system gene therapy are able to insert genetic material into host cells and to target the pathological cell function; however, only Herpes Simplex Virus (HSV) based vectors are capable to carry a large amount of genetic material. Among the various viral vectors derived from HSV, the amplicon vectors, i.e. viral particles containing a genome of about 150 kb constituted of concatameric repetitions of an expression cassette, enable the expression of the gene of interest in multiple-copies and for a defined time period. HSV-1 based amplicon vectors are non-pathogenic and have been successfully employed in the past for gene delivery into the brain of living animals. In this study, different amplicon vectors were designed using a set of specific promoters, to allow a short or long lasting expression of the transgene in a given cell population. In particular, four amplicon vectors were tested (each containing the luciferase and GFP reporter genes) at different time points for 6 months after injection into the dorsal hippocampus of mice. All tested amplicons were found to be able to infect principal cells and not to induce immune cell infiltration or neuronal damage. These findings, together with the high efficiency of infection, make the amplicon vectors a promising system for the delivery of therapeutic genes in the central nervous system and, thereby, the treatment of diseases like epilepsy, Parkinson's disease or Alzheimer's disease.

MAIN FINDINGS:

We tested in vivo the following portfolio of amplicons (Figure 1):
1) vAm-ESYN-LiG2
2) vAm-ECBA-LiG2
3) vAm-IE4/5-LiG2
4) vSAm-ESYN-LiG2
The first three amplicon vectors differ for the promoter which drives the expression of the 2 reporter genes: GFP and luciferase. One of the amplicon vectors, vSAm-ESYN-LiG2, was developed using a new technology of construction, called SAm technology, that was expected to ensure stable transgene expression over time.
With all amplicon vectors, we carried out longitudinal in vivo studies to evaluate the transgenes expression. Specifically, we examined: first, the bioluminescence level induced by luciferase expression, acquired using the IVIS Lumina in vivo imaging system (Perkin-Elmer); second, the number of GFP positive cells detectable around the site of injection. Amplicon vectors were produced at low titer (1x108 TU/ml), only two also at high titer (1x1010 TU/ml (Figure 1).

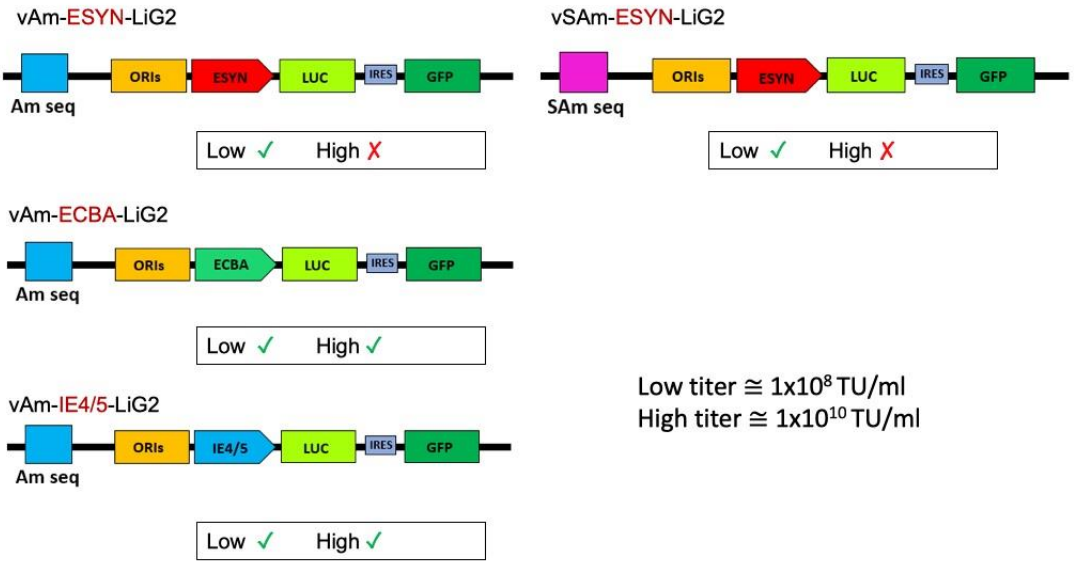

Figure 1. The amplicon portfolio.

All the amplicon vectors were injected into the right dorsal hippocampus of CD1 mice and the expression of luciferase and GFP reporting genes was evaluated at different time points, from 5 days to 6 months after injection (Figure 2).

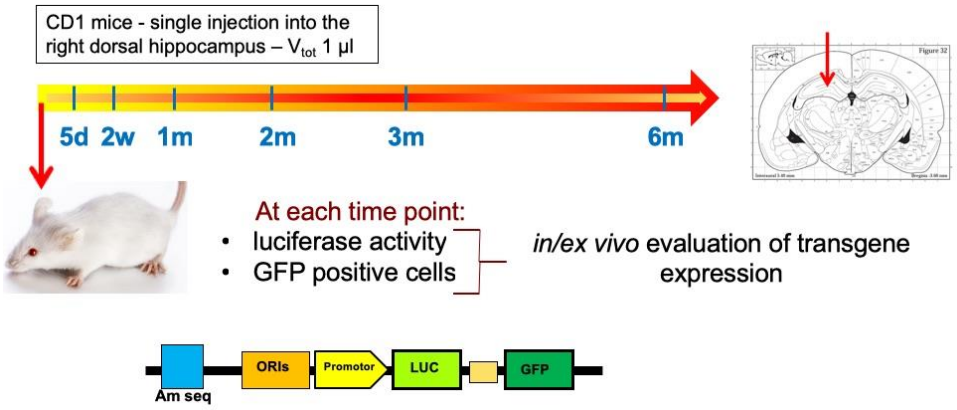

Figure 2. The experimental design.

When injected at the same (low) titer, amplicons containing the ESYN or ECBA promotor expressed the luciferase transgene for 6 months with similar kinetics: the bioluminescence signal (BLI) peaked at the 5 days and decreased dramatically over 4 weeks, subsequently maintaining low but stable levels until 6 months (Figure 3).

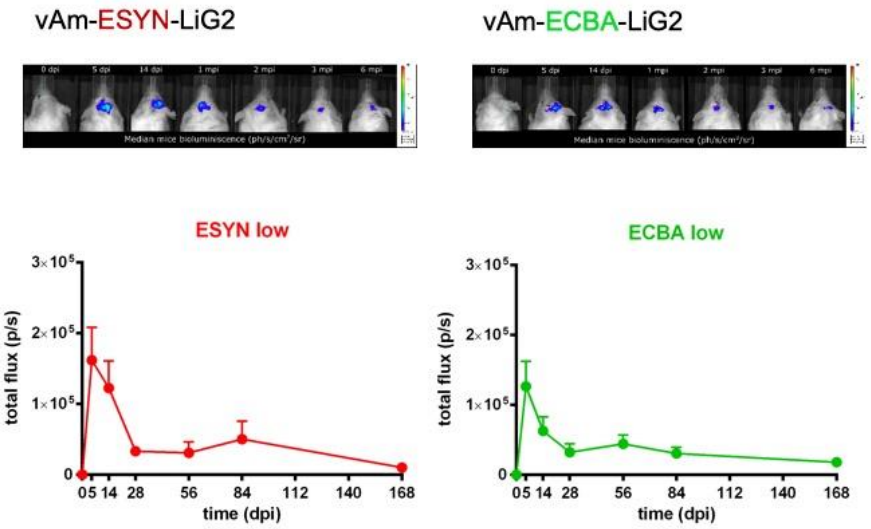

Figure 3. Time-course of luciferase driven by the ESYN and ECBA promoters.

On the other hand, the BLI signal in mice injected with IE4/5 amplicon reached high levels at 1 dpi to rapidly diminish in few days and totally disappear at 7 days (Figure 4).

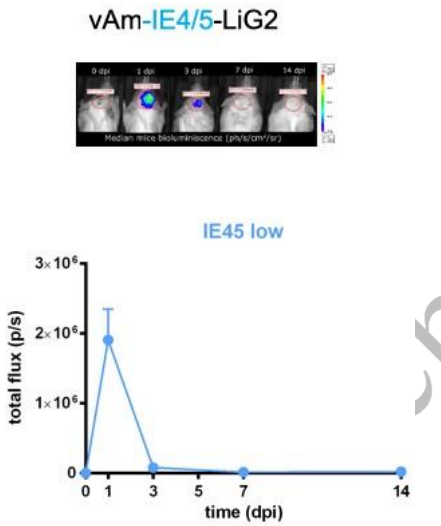

Figure 4. Time-course of luciferase driven by the IE4/5 promoter.

Comparing the vectors vAm-ECBA-LiG2 and vAm-IE4/5-LiG2 used at low or high titer, the BLI kinetic profile was the same but the signal intensity was much greater, 1 or 2 log higher when using the high with respect to the low titer (see Figure 5 for vAm-ECBA).

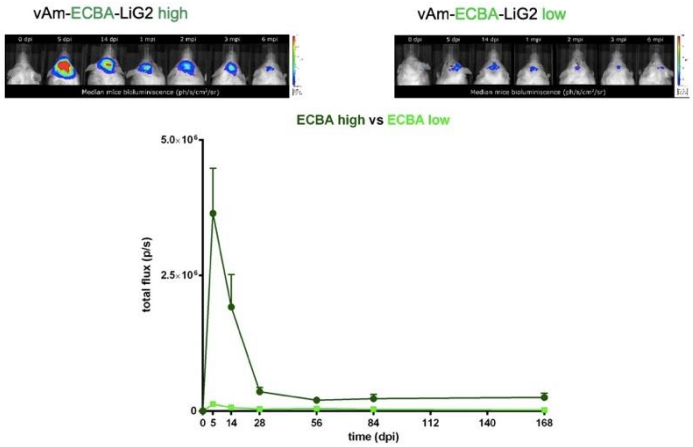

Figure 5. Comparison of low and high titer vAm-ECBA.

Finally, mice injected with vSAm-ESYN-LIG2 displayed a steady and high BLI signal lasting from 5 days up to 6 months post injection, demonstrating that the SAM technology can ensure a stable and long-lasting transgene expression (Figure 6).

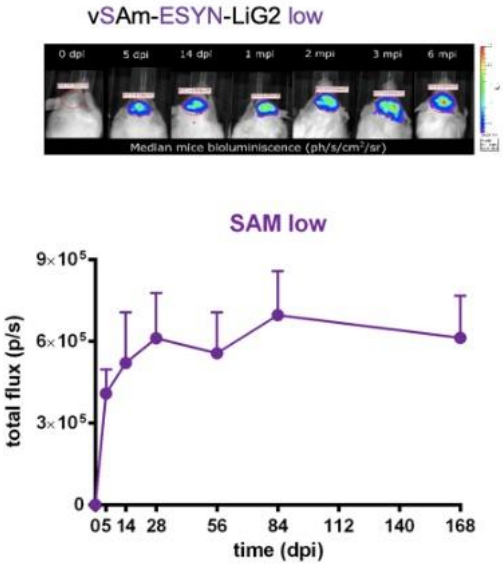

Figure 6. Time-course of luciferase expression with vSAm-ESYN-LIG2.

Using immunohistochemistry, we were able to detect GFP expression and identify the cell type infected by the amplicon vectors. After injection of all tested amplicons, many GFP positive cells were found at the level of principal cells in the injected hippocampus (Figure 7) and no infected cell was observed in the contralateral hippocampus, indication that the vectors lost its ability to be retrogradely transported. Double immunofluorescence demonstrated that amplicon infected cells were prevalently neuronal cells. Only when using vAm-IE4/5-LiG2, some infected cells were also GFAP positive, indicating the ability of this amplicon also to infect astrocytes.

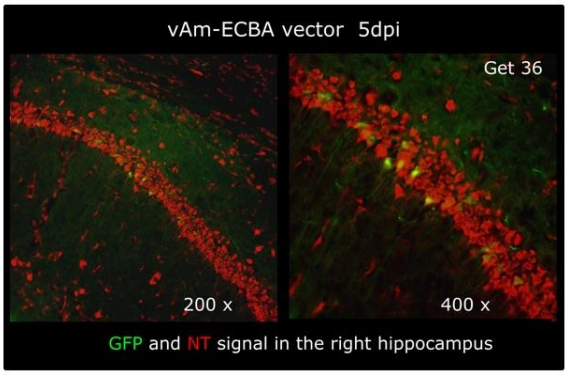

Figure 7.

In sum:

- the level of transgene expression depends on the promotor and (mainly) on the number of infectious viral particles in the preparation,
- the SAm technology confers stable and long-lasting expression of the transgenes;
- neurons are the main cellular target of all tested amplicon vectors.

We also performed an assessment of the safety of these amplicons. We performed hematoxylin-eosin and Fluoro Jade C staining, at early time points (3-5 dpi) and observed the lack of immune cell infiltration and no ongoing neurodegeneration.

In conclusion, any amplicon vector from our portfolio may be useful for gene therapy and the choice

of promotor and technology would affect such use; IE4/5 driven amplicons may be used for short-term gene therapy, whereas ESYN driven SAm amplicon vectors would be best for long-term treatments.

4. Summary and discussion

Epilepsy and neurodegenerative diseases (NDs), such as Alzheimer's, Parkinson's or Huntington's disease, are debilitating pathologies characterized by the slow and progressive loss of one or more functions of the nervous system. In general, these diseases are treated with poor results through the administration of purely symptomatic drugs, that reduce the symptoms without however interrupting or modifying the course of the disease. Today, neurodegenerative disorders account for a significant and increasing proportion of morbidity and mortality and have a high economic burden [70; 71; 72]. Not to be overlooked are the comorbidities associated with these pathologies. Several studies have reported executive function deficits, in particular deficits in cognitive functions like planning, monitoring, cognitive flexibility and inhibition of automated responses; but also psychiatric disorders, such as anxiety or depression, and motor disorders like coordination and stereotypic movement [73; 74; 75; 76]. Finding effective treatments is a goal of increasing urgency. It is therefore necessary to identify novel strategies to meet this relevant clinical demand, that is, preventing the development of the disease or improving the clinical scenario for millions of people worldwide affected by these invalidating disorders.

Gene therapy arises as an emerging new field of medical research that ambitiously promises to cure a wide range of untreatable diseases. Novel approaches of gene therapy are constantly emerging, prompted by encouraging results from a variety of preclinical and clinical studies. Several strategies have been explored to achieve the highest efficiency for gene transfer while minimizing side effects, but the challenge to set up final tools for an efficient and safe gene delivery is still open. The complex CNS poses several challenges to gene therapy. First of all, the CNS represents a highly heterogeneous environment with many different cell types, which often require to be targeted specifically. Moreover, in some cases, a cell-specific targeting into the non-dividing cells, that many viral vectors cannot infect, may be necessary. Second, neurological diseases often display a complex pathophysiology that would require co-transfection of several genes. Third, the difficult access to the CNS imposes a built-in regulation of transgene expression. To date, probably the most employed approach for gene delivery is to take advantage of genetically engineered non-toxic viral vectors with features essential for CNS infection. The optimal vector should allow delivery to specific cell types, should have a high efficacy of transgene expression and should have a large capacity to host single and/or multiple inserts. It should be safe for the receiver, exert a long-lasting transgene expression, and should contain an adjustable mechanism to regulate expression. These are the features that we have considered for the characterization of vectors derived from Herpes virus type 1 (HSV-1) proposed in this PhD thesis. The goal of my PhD project was to develop new gene transfer tools based on herpetic vectors, characterizing the different vectors in vitro and testing their properties in vivo in order to prepare and, later, produce in greater amounts a new generation of therapeutic vectors for CNS applications.

HSV-1 is the vector that best approaches the needs of a good gene delivery tool for the CNS: it is an enveloped, double stranded DNA virus with a big genome of 152 kb, of which at least 30 kb can be deleted to accommodate foreign sequences. It shows a natural neurotropism and does not integrate its DNA in the host cell genome. However, the development of HSV vectors that include all the desired properties together is not easy. We modified step-by-step the viral vector in order to achieve low cytotoxicity and immunogenicity as well as persistent expression in the CNS.

Our first point, the absence of replication in vivo, was relatively simple to achieve as the viral genes are expressed in a cascade fashion: to obtain replication defective vectors derived, it is sufficient the deletion of first expressed (immediate early, IE) genes. However, such intervention is not without its pitfalls, because these replication defective HSV-1 vectors, unlike the wild type viruses which are able to establish latency in neurons without host cell destruction, usually show a high in vitro cytotoxicity, which limits their usefulness as gene transfer tools [77]. Due to the many functions of IE proteins on host cell metabolism, the lack of their expression does not ensure normal cell function and viability. Interestingly, according to the studies from the last two decades, the severity of the host cell impairment seems to be dependent on the number of IE genes deleted. It was observed a severe rapid cell death, chromosomal damage and nuclear structure alteration in single mutant vectors, while

replication defective vectors mutant for two or three IE genes result in progressive reduction of cytotoxicity [77; 78; 79]. Similarly, Wu and colleagues has shown that Vero cells infected with viruses deleted for combination of IE genes ICP4, ICP22 and ICP27, survive longer than the same cells infected with sole ICP4$^-$ or ICP27$^-$ IE gene mutant viruses [78]. The host cells infected with vectors that display the combined deletion of IE genes retain a relatively normal morphology and express genes from the viral and cellular genomes for at least 3-day post infection (dpi) [78]. Additional studies have concluded that to completely eliminate the toxicity it is mandatory to abrogate all IE genes (ICP0, ICP4, ICP27, ICP22 and ICP47) [65; 80] and Samaniego and colleagues further extended such observations by reporting that the simultaneous deletion of ICP0, ICP4, ICP27 and ICP22 may completely eliminates vector toxicity. However, a low-level transgene expression was observed with these backbones. In particular, it was seen that the deletion of the ICP0 IE gene reduces the vector cytotoxicity, but at the same time dramatically reduces transgene expression [79]. Such observation is in line with known functions of ICP0. Indeed, ICP0 is a potent transactivator involved in inhibiting the host cell system, it promotes viral replication and reactivation of latency and prevents the transcriptional repression of viral genes by protecting them from cellular epigenetic silencing mechanisms. The lack of ICP0 functions in HSV-1 replication-defective vectors clearly compromises the vector efficacy. To overcome this problem, different HSV vectors have been engineered to dramatically reduce but not eliminate ICP0 expression by knocking it down partially or by substituting it with similar IE genes from other herpesviruses, presuming that low levels of the ICP0 protein or protein with similar function would maintain transgene activity without loss of cell proliferation or viability. Unfortunately, neither of the two strategies resolve completely the problem [81; 82; 83; 84]. Thus, other genome modifications must be employed to promote transgene expression in ICP0 deleted HSV vectors.

We developed a new generation of HSV-1 replication defective vectors, known as the JDNI family. These vectors employ a boundary elements strategy for transgene expression and show extremely low levels of viral lytic genes that can be detected only by RT-PCR. They were obtained by functional deletion of ICP0, ICP4, ICP27 ICP47 and the JOINT region (thus providing a total of ~25kb of space for transgene insertion). Additionally, ICP22 was converted to later expression kinetics. First in vitro investigations in a variety of primary non-neuronal cells indicated that the use of boundary elements of the viral latency locus, positioned in different loci of the viral backbone, allows to protect the foreign DNA from cellular mechanisms of transcriptional repression, thus obtaining the expression of a transgene driven by a foreign promoter for up to 1-month. These observations are in contrast with the previously mentioned works, in which the complete deletion of sets of IE genes compromised gene expression [85]. Once established the viral vector efficacy in vitro, the challenge has been to confirm its functionality in vivo. The first vector tested in vivo belonging to this family was JDNI6. The JDNI6 backbone was designed to contain two expression cassettes for reporter genes driven by two different promoters: (i) the reporter gene enhanced green fluorescent protein (eGFP) is located in the intergenic region UL3, UL4 under the control of the CAG promoter and (ii) the mCherry gene, driven by the ubiquitin C promoter, is inserted into the deleted ICP4 locus. After injection of JDNI6 in the rat hippocampus, we observed a high level and robust mCherry transgene expression. In a subset of experiments, the vector provided a durable transgene expression in multiple brain areas that are relevant to neurological diseases, including Parkinson, Alzheimer and several forms of epilepsy. Since JDNI6 does not contain ICP0 which may act in both, the apoptotic and necrosis pathways, we investigated the presence of viral vector induced toxicity using markers for lymphocyte infiltration (CD45), oxidative stress (iNOS), apoptosis (Cas3) and neurodegeneration (FJ-C). Absence of neurotoxicity and lymphocyte infiltration was observed in brain tissue injected with JDNI6 at the dose effective in infecting a good percentage of hippocampal neurons. No activation of apoptotic pathways and microglia was observed. In the studies of vector infection localization, we confirmed that the mCherry expression is specific for neurons, and absent in astrocytes and oligodendrocytes [86]. The essential information we obtained from the in vivo studies is that a reporter gene inserted in the ICP4 locus was able to escape the global silencing of an IE-gene-depleted HSV genome in the CNS, thus allowing a long-term expression. In fact, the eGFP reporter gene expression declined very fast, within one week. Thus, we further investigated the question testing the two different

hypotheses: (i) the expression differences observed between the two transgenes are dependent on the promoter kinetics (employing the switch between the promoters) and/or (ii) the differences depend on the transgene location sites (by inverting the expression cassettes). What was concluded from the additional studies is that the location of the expression cassettes is much more important than the promoter used (unpublished data), probably for the presence of neuron-specific anti-silencing elements, including regions enriched in CTCF-binding elements, which are naturally present in the herpes genome and in the JDNI6 backbone. Seven conserved CTCF-binding domains has been described in the HSV-1 genome [52]. These binding sites individually flank the latency-associated transcript (LAT) and the immediate early gene regions. Recently, Washington and colleagues showed that three of these CTCF-binding sites may be occupied by CTCF during latency, including the CTC repeat long 2 (CTRL2) site downstream from the LAT enhancer, CTa'm upstream from ICP0 and CTRS3 upstream from ICP4 and that the protein recruitment and insulator function are independent on the specific site. Furthermore, the same authors reported that the insulators CTRL1 and CTRS3 exert different enhanced blocking mechanism, depending on the cell type [61]. These findings support our hypothesis, in which the differences observed in the expression of the two transgenes placed into two distant cassettes depend on the locus and the particular regulation elements that surround it. Furthermore, Washington´s work supports our previous findings, i.e. CTRL1 and LATP2 are essential for preventing the rapid silencing of an ectopic promoter in the LAT locus in non-neuronal cells in the absence of all viral IE gene products, and these elements provide protection against the silencing of an embedded promoter when moved away from its native position in the viral genome [85].

Given the importance of the CTRL1 and LATP2 regulatory elements on gene expression, we have further extended the previous observations with evaluations of different chromatin insulators for their ability to keep a non-viral promoter active in an otherwise silent genome. Chromatin insulators are long-range cis-acting DNA elements that have the ability to regulate transcriptional domains and gene expression through protein recruitment and through the formation of three-dimensional chromatin loops [87; 88]. We tested the ability of ectopic anti-silencing elements on protection from epigenetic silencing mechanisms to create additional active loci that would allow separately controlled expression of multiple transgene from a single vector. In vitro evaluations allowed us to test the different combinations of the analyzed elements: a. ubiquitous chromatin opening element (A2UCOE), b. chicken hypersensitive site 4 (cHS4) insulator and c. the previously described latency elements CTRL1, CTRL2 and LAP1. A2UCOE was then chosen for in vivo testing because it increased transgene more than the others. This element was for the first time described in 2013 and several studies reported its ability to increase transgene expression in different types of viral vectors by different mechanisms [89]. For example, it has been demonstrated that the A2UCOE element is able to interfere with epigenetic modifications, in particular by reducing the methylation of the CpG islands and by intervening on the deacetylation of the N-terminal extremities of the histone tails, allowing the maintenance of chromatin in the euchromatin form, accessible to transcription [88; 90]. In our study, we obtained similar results, confirming the involvement of A2UCOE in histone modification, but we did not observe the block of DNA methylation. In the light of new promising results with the use of the A2UCOE element in the vector backbone, a novel vector containing A2UCOE has been engineered to express three different reporter transgenes (eGFP, fLuc and mCherry) under the control of different promoters localized at different loci. In particular, eGFP was inserted between the UL3 an UL4 genes under the control of the CAG promoter and protected by CTRL1, CTRL2 and the enhanced-like latency active promoter 2 (LAP2); the mCherry gene was driven by the ubiquitin C promoter and inserted into the deleted ICP4 locus while the A2UCOE element was positioned between the intergenic regions UL50 and UL51 and specifically upstream of the third reporter, fLuc (fly luciferase), whose expression was under the control of elongation factor 1 promoter. All three transgenes were simultaneously expressed in individual rat DRG neurons in vitro and two of them (mCherry and fLuc) were co-expressed in the mouse hippocampus following intracranial vector delivery for at least 1-month, the last time point considered in this study [91]. It remains unexplained why eGFP expression was not detectable in the mouse brain, but these diverging results may be explained by significant differences between DRG and CNS neurons [85]. In contrast to what we have observed, a similarly engineered HSV vector has been reported to express GFP under the CMG promoter at 1 month after injection into the rat striatum. However, our vector differs significantly from this last one, as we used different viral strain background,

promoter, IE gene deletion strategy [83]. Further experiments are needed to better understand the role of different elements controlling transgene expression in the JDNI constructs. Nevertheless, we demonstrated that the insertion of ectopic regulatory elements in the viral backbone of defective herpetic vectors can enhance the strength of transgene transcription from multiple viral loci.

In conclusion, we developed a new generation of brain tissue safe, high capacity recombinant HSV vectors with ability to target specific cell populations in a heterogeneous environment and with the capacity to transfer multiple-transgene cassettes by insertion of non-HSV insulator elements. These features make our HSV defective vectors suitable for many CNS application and promising for the development of increasingly complex vectors for strictly controlled treatment of a variety of pathological conditions.

The same procedures described above for HSV-1 replication defective vectors were followed during the testing of suitable HSV-1 based amplicon vectors with respect to efficacy of transgene expression in the CNS, specificity and safety. Amplicon vectors are defective, helper-dependent vectors that carry no viral genes and ensure the largest payload capacity [63]. However, amplicon vectors still carry several undesired features that compromises their utility for gene therapy: their major disadvantage is a transient expression of transgenes and, despite the absence of any viral gene, an activation of the immune adaptive response associated to mild cytotoxicity due to helper virus contamination. To date, different strategies have been employed to overcome the problem of residual cytotoxicity. New production technologies reduce the percentage of helper virus present in the stock to 0.01% by using helper viruses deleted of the packaging sequence or lacking essential genes that ensure the inability of encapsulation or the inability to replicate in the host organism [92; 93; 94]. The transient expression of the transgene may be caused by the same epigenetic silencing mechanisms that strike HSV-defective vectors. The suppression of transgene expression observed in amplicon vectors may depend on the absence of the ICP0 IE gene but also on the activation of an immune response induced by type I interferons, due to the presence of bacterial sequences in the amplicon genome [95; 96].

We have recently tested a new series of amplicon vectors for safe delivery and long-term transgene expression in the CNS. Four amplicon vectors that differ for the promoter used to control the duration of transgene expression and for the production technology were tested in vivo after being injected into the mice brain. In particular, vAm-IE4/5-LiG2, driven by the ubiquitous immediate-early 4/5 (IE4/5) promoter, vAm-ESYN-LiG2 and vSAm-ESYN-LiG2 amplicon vectors, driven by the neuron-specific human synapsin 1 promoter and vAm-ECBA-LiG2 driven by the ubiquitous chicken β actin promoter. All tested amplicon vectors contained two reporter genes: (i) fLuc (Li) and (ii) eGFP.

We observed a long-term (6-months) transgene expression of both reporter genes after vAm-ESYN-LiG2 and vAm-ECBA-LiG2 delivery in mice hippocampi, with similar kinetics (peaking at the beginning, 5dpi). The kinetic expression profile with these two promoters are similar to those reported in other works [97; 98; 99]. The ESYN promoter allowed higher fLuc expression during the first two weeks compared to ECBA promoter. In contrast, short-term transgene expression was observed for both transgenes when using the vAm-IE4/5-LiG2 vector. The fLuc signal peaked at 1 dpi and reached a tenfold higher difference compared to vAm-ESYN-LiG2 and vAm-ECBA-LiG2, but then decreased dramatically at 5 dpi to completely vanish at 7 dpi. This last result is clearly dependent on the effect of the promoter, because IE4/5 genes are activated in the first few hours and days after host infection. Many similar studies employing viral promoters, such as IE4/5 or HCMV IE enhancer, are in line with our observation of a strong but also short-term expression [100; 101; 102; 103]. The use of neurospecific promoters, such as those for preproenkephalin, tyrosine hydroxylase and synapsin results in a significant increase in the duration of transgene expression compared to viral promoters [104; 105; 106; 107].

We then tested amplicon vectors as regards to the engineering technology. After in vivo delivery of vAm-ESYN-LiG2 and vSAm-ESYN-LiG2 we observed long-term transgene expression in both reporter genes until 6

months. However, in mice infected with vAm-ESYN-LiG2 the transgene expression achieved its maximum at about 5 dpi and then declined, whereas in vSAm-ESYN-LiG2 injected animals the expression peaked at about 1 mpi and then maintained its plateau levels for at least 6 mpi. Such different kinetics obviously depend on the different production technology. Unfortunately, the vSAm-ESYN-LiG2 technology is currently under a patent application and cannot be described in detail in this thesis.

vAm-ESYN-LiG2, vSAm-ESYN-LiG2 and vAm-ECBA-LiG2 all showed a high specificity for neurons without any signs of inflammatory response activation. Consistent with previous reports [108; 109], the synapsin I promoter shows preferential expression in excitatory neurons (94.4%), with weaker expression in inhibitory neurons (5.6%), in the rat motor cortex. In addition, the specificity of the ECBA ubiquitous promoter was confirmed, with a 99.5% specific expression in neurons [110].

Our finding of absence of toxicity is in contrast with previously published results in which a robust transgene expression was associated with dose-dependent inflammation and infiltration of immune cells around injection sites [111]. However, we detected some degenerating cells in the animals injected with IE4/5-LiG2 vector during the first two-days post-infection. In addition, this amplicon vector expressed the transgene not only in neurons, but also in astrocytes. This is an unexpected result, as there are no data in the literature that confirm the ability of amplicon vectors to infect and express transgenes in astrocytic cells. Future experiments are needed to better understand and validate our data.

Remaining hurdles like host innate and acquired immunity against HSV-1 or a tight, on demand control of transgene expression must be overcome before the first-in-man clinical experiment can be performed. As mentioned, the efficacy of HSV-1 defective vectors might potentially be compromised by the pre-existing immunity to viral antigens in the host cell. Indeed, HSV-1 infection is so widespread, that its seropositivity covers more than 70% of the world population [112]. However, when considering a HSV-1 based gene therapy that targets exclusively a CNS, the problem of potential intrinsic immunity would be relevant only in the very few cases of patients in whom HSV-1 entered the central nervous system (e.g. as a consequence of HSV-1 induced encephalitis) [113]. Caution is always commendable. AdV vectors used in gene therapy clinical trials provoked a lethal immunotoxicity including extravasation of blood cells from the pulmonary circulation, congestion of the tracheobronchial lymph nodes, decreased respiratory rates and pulmonary hypotension [114], and this case greatly limits their further clinical use [115]. Similarly, vectors like AAV, known for their low immunogenicity, were described to confer a residual toxicity which was sufficient to eliminate the transduced cells in many clinical trials, hindering the therapeutic effect [116]. These and similar observation are alarming. The potential effect of pre-existing immunity on HSV-1 based vectors should be further studied, as it remains rather controversial, with some studies showing strong immune response and other studies reporting that preexisting immunity does not interfere with the HSV-1 induced transgene expression [117; 118]. Altogether, a deeper knowledge of the immune response against viral antigens and the possibility to modulate or bypass it will be crucial for a concrete clinical development of gene therapy, especially in disorders requiring repeated administration of the vector or long-lasting expression of the transgene. Therefore, the vectors developed in the course of this project should be tested on previously immunized animals.

At the moment, we have in our hands HSV-1 based vectors with which we have obtained a broad, dose-dependent distribution of the transgene in the rodent tissue. In the future, it will be necessary to scale-up vector distribution by performing experiments in larger animals, such as mini-pigs or primates, and to further increase the vector's spread using higher titers, larger volumes or multiple-injection.

In addition, mechanism should be implemented into the new HSV-1 based vectors to obtain strictly controlled regulation of transgene expression. The use of inducible promoters may allow to halt the treatment at the occurrence of adverse reactions or activate it only when needed [119].

[1] A.J. Davison, R. Eberle, B. Ehlers, G.S. Hayward, D.J. McGeoch, A.C. Minson, P.E. Pellett, B. Roizman, M.J. Studdert, and E. Thiry, The order Herpesvirales. Arch Virol 154 (2009) 171-7.
[2] A.R. Frampton, Jr., W.F. Goins, K. Nakano, E.A. Burton, and J.C. Glorioso, HSV trafficking and development of gene therapy vectors with applications in the nervous system. Gene Ther 12 (2005) 891-901.
[3] I. Steiner, and P.G. Kennedy, Molecular biology of herpes simplex virus type 1 latency in the nervous system. Mol Neurobiol 7 (1993) 137-59.
[4] T.J. Liesegang, Biology and molecular aspects of herpes simplex and varicella-zoster virus infections. Ophthalmology 99 (1992) 781-99.
[5] S.J. Macdonald, H.H. Mostafa, L.A. Morrison, and D.J. Davido, Genome sequence of herpes simplex virus 1 strain KOS. J Virol 86 (2012) 6371-2.
[6] R. Manservigi, R. Argnani, and P. Marconi, HSV Recombinant Vectors for Gene Therapy. Open Virol J 4 (2010) 123-56.
[7] R.J. Watson, M. Sullivan, and G.F. Vande Woude, Structures of two spliced herpes simplex virus type 1 immediate-early mRNA's which map at the junctions of the unique and reiterated regions of the virus DNA S component. J Virol 37 (1981) 431-44.
[8] P. O'Hare, and G.S. Hayward, Three trans-acting regulatory proteins of herpes simplex virus modulate immediate-early gene expression in a pathway involving positive and negative feedback regulation. J Virol 56 (1985) 723-33.
[9] B.L. Trus, F.P. Booy, W.W. Newcomb, J.C. Brown, F.L. Homa, D.R. Thomsen, and A.C. Steven, The herpes simplex virus procapsid: structure, conformational changes upon maturation, and roles of the triplex proteins VP19c and VP23 in assembly. J Mol Biol 263 (1996) 447-62.
[10] G. Cardone, D.C. Winkler, B.L. Trus, N. Cheng, J.E. Heuser, W.W. Newcomb, J.C. Brown, and A.C. Steven, Visualization of the herpes simplex virus portal in situ by cryo-electron tomography. Virology 361 (2007) 426-34.
[11] B.J. Kelly, C. Fraefel, A.L. Cunningham, and R.J. Diefenbach, Functional roles of the tegument proteins of herpes simplex virus type 1. Virus Res 145 (2009) 173-86.
[12] T.C. Mettenleiter, Budding events in herpesvirus morphogenesis. Virus Res 106 (2004) 167-80.
[13] M.E. Campbell, J.W. Palfreyman, and C.M. Preston, Identification of herpes simplex virus DNA sequences which encode a trans-acting polypeptide responsible for stimulation of immediate early transcription. J Mol Biol 180 (1984) 1-19.
[14] A.D. Kwong, and N. Frenkel, The herpes simplex virus virion host shutoff function. J Virol 63 (1989) 4834-9.
[15] S.L. McKnight, R.C. Kingsbury, A. Spence, and M. Smith, The distal transcription signals of the herpesvirus tk gene share a common hexanucleotide control sequence. Cell 37 (1984) 253-62.
[16] C. Duffy, E.F. Mbong, and J.D. Baines, VP22 of herpes simplex virus 1 promotes protein synthesis at late times in infection and accumulation of a subset of viral mRNAs at early times in infection. J Virol 83 (2009) 1009-17.
[17] W.H. Cai, B. Gu, and S. Person, Role of glycoprotein B of herpes simplex virus type 1 in viral entry and cell fusion. J Virol 62 (1988) 2596-604.
[18] D. WuDunn, and P.G. Spear, Initial interaction of herpes simplex virus with cells is binding to heparan sulfate. J Virol 63 (1989) 52-8.
[19] B.C. Herold, R.J. Visalli, N. Susmarski, C.R. Brandt, and P.G. Spear, Glycoprotein C-independent binding of herpes simplex virus to cells requires cell surface heparan sulphate and glycoprotein B. J Gen Virol 75 (Pt 6) (1994) 1211-22.
[20] R.I. Montgomery, M.S. Warner, B.J. Lum, and P.G. Spear, Herpes simplex virus-1 entry into cells mediated by a novel member of the TNF/NGF receptor family. Cell 87 (1996) 427-36.
[21] A. Turner, B. Bruun, T. Minson, and H. Browne, Glycoproteins gB, gD, and gHgL of herpes simplex virus type 1 are necessary and sufficient to mediate membrane fusion in a Cos cell transfection system. J Virol 72 (1998) 873-5.
[22] V. Jovasevic, L. Liang, and B. Roizman, Proteolytic cleavage of VP1-2 is required for release of herpes

simplex virus 1 DNA into the nucleus. J Virol 82 (2008) 3311-9.
[23] P.M. Ojala, B. Sodeik, M.W. Ebersold, U. Kutay, and A. Helenius, Herpes simplex virus type 1 entry into host cells: reconstitution of capsid binding and uncoating at the nuclear pore complex in vitro. Mol Cell Biol 20 (2000) 4922-31.
[24] B. Sodeik, M.W. Ebersold, and A. Helenius, Microtubule-mediated transport of incoming herpes simplex virus 1 capsids to the nucleus. J Cell Biol 136 (1997) 1007-21.
[25] J. Matis, and M. Kudelova, Early shutoff of host protein synthesis in cells infected with herpes simplex viruses. Acta Virol 45 (2001) 269-77.
[26] J. Rajcani, and V. Durmanova, Early expression of herpes simplex virus (HSV) proteins and reactivation of latent infection. Folia Microbiol (Praha) 45 (2000) 7-28.
[27] J. Wysocka, and W. Herr, The herpes simplex virus VP16-induced complex: the makings of a regulatory switch. Trends Biochem Sci 28 (2003) 294-304.
[28] R. Hagglund, and B. Roizman, Role of ICP0 in the strategy of conquest of the host cell by herpes simplex virus 1. J Virol 78 (2004) 2169-78.
[29] I.H. Gelman, and S. Silverstein, Co-ordinate regulation of herpes simplex virus gene expression is mediated by the functional interaction of two immediate early gene products. J Mol Biol 191 (1986) 395-409.
[30] D.A. Leib, T.E. Harrison, K.M. Laslo, M.A. Machalek, N.J. Moorman, and H.W. Virgin, Interferons regulate the phenotype of wild-type and mutant herpes simplex viruses in vivo. J Exp Med 189 (1999) 663-72.
[31] G.G. Maul, A.M. Ishov, and R.D. Everett, Nuclear domain 10 as preexisting potential replication start sites of herpes simplex virus type-1. Virology 217 (1996) 67-75.
[32] H. Gu, and B. Roizman, The two functions of herpes simplex virus 1 ICP0, inhibition of silencing by the CoREST/REST/HDAC complex and degradation of PML, are executed in tandem. J Virol 83 (2009) 181-7.
[33] M.J. Carrozza, and N.A. DeLuca, Interaction of the viral activator protein ICP4 with TFIID through TAF250. Mol Cell Biol 16 (1996) 3085-93.
[34] M. Shapira, F.L. Homa, J.C. Glorioso, and M. Levine, Regulation of the herpes simplex virus type 1 late (gamma2) glycoprotein C gene: sequences between base pairs -34 to +29 control transient expression and responsiveness to transactivation by the products of the immediate early (alpha) 4 and 0 genes. Nucleic Acids Res 15 (1987) 3097- 111.
[35] J.S. Orlando, T.L. Astor, S.A. Rundle, and P.A. Schaffer, The products of the herpes simplex virus type 1 immediate-early US1/US1.5 genes downregulate levels of S-phase-specific cyclins and facilitate virus replication in S-phase Vero cells. J Virol 80 (2006) 4005-16.
[36] S.A. Rice, and D.J. Davido, HSV-1 ICP22: hijacking host nuclear functions to enhance viral infection. Future Microbiol 8 (2013) 311-21.
[37] H.E. Bryant, S.E. Wadd, A.I. Lamond, S.J. Silverstein, and J.B. Clements, Herpes simplex virus IE63 (ICP27) protein interacts with spliceosome-associated protein 145 and inhibits splicing prior to the first catalytic step. J Virol 75 (2001) 4376-85.
[38] A.J. Easterfield, B.M. Austen, and O.M. Westwood, Inhibition of antigen transport by expression of infected cell peptide 47 (ICP47) prevents cell surface expression of HLA in choriocarcinoma cell lines. J Reprod Immunol 50 (2001) 19-40.
[39] S.M. Brown, J. Harland, A.R. MacLean, J. Podlech, and J.B. Clements, Cell type and cell state determine differential in vitro growth of non-neurovirulent ICP34.5-negative herpes simplex virus types 1 and
2. J Gen Virol 75 (Pt 9) (1994) 2367-77.
[40] R.K. Mattila, K. Harila, S.M. Kangas, H. Paavilainen, A.M. Heape, I.J. Mohr, and V. Hukkanen, An investigation of herpes simplex virus type 1 latency in a novel mouse dorsal root ganglion model suggests a role for ICP34.5 in reactivation. J Gen Virol 96 (2015) 2304-13.
[41] S.L. Deshmane, and N.W. Fraser, During latency, herpes simplex virus type 1 DNA is associated with nucleosomes in a chromatin structure. J Virol 63 (1989) 943-7.
[42] D.L. Rock, and N.W. Fraser, Latent herpes simplex virus type 1 DNA contains two copies of the virion DNA joint region. J Virol 55 (1985) 849-52.
[43] M.J. Farrell, A.T. Dobson, and L.T. Feldman, Herpes simplex virus latency-associated transcript is a

stable intron. Proc Natl Acad Sci U S A 88 (1991) 790-4.

[44] M.P. Nicoll, J.T. Proenca, and S. Efstathiou, The molecular basis of herpes simplex virus latency. FEMS Microbiol Rev 36 (2012) 684-705.
[45] S. Tang, A. Patel, and P.R. Krause, Novel less-abundant viral microRNAs encoded by herpes simplex virus 2 latency-associated transcript and their roles in regulating ICP34.5 and ICP0 mRNAs. J Virol 83 (2009) 1433-42.
[46] J.L. Umbach, M.F. Kramer, I. Jurak, H.W. Karnowski, D.M. Coen, and B.R. Cullen, MicroRNAs expressed by herpes simplex virus 1 during latent infection regulate viral mRNAs. Nature 454 (2008) 780-3.
[47] H. Zhao, C. Zhang, G. Hou, and J. Song, MicroRNA-H4-5p encoded by HSV-1 latency-associated transcript promotes cell proliferation, invasion and cell cycle progression via p16-mediated PI3K-Akt signaling pathway in SHSY5Y cells. Int J Clin Exp Med 8 (2015) 7526-34.
[48] G.C. Perng, C. Jones, J. Ciacci-Zanella, M. Stone, G. Henderson, A. Yukht, S.M. Slanina, F.M. Hofman, H. Ghiasi,
A.B. Nesburn, and S.L. Wechsler, Virus-induced neuronal apoptosis blocked by the herpes simplex virus latency- associated transcript. Science 287 (2000) 1500-3.
[49] N.J. Kubat, R.K. Tran, P. McAnany, and D.C. Bloom, Specific histone tail modification and not DNA methylation is a determinant of herpes simplex virus type 1 latent gene expression. J Virol 78 (2004) 1139-49.
[50] R.J. Klose, and Y. Zhang, Regulation of histone methylation by demethylimination and demethylation. Nat Rev Mol Cell Biol 8 (2007) 307-18.
[51] Q. Chen, L. Lin, S. Smith, J. Huang, S.L. Berger, and J. Zhou, CTCF-dependent chromatin boundary element between the latency-associated transcript and ICP0 promoters in the herpes simplex virus type 1 genome. J Virol 81 (2007) 5192-201.
[52] A.L. Amelio, P.K. McAnany, and D.C. Bloom, A chromatin insulator-like element in the herpes simplex virus type 1 latency-associated transcript region binds CCCTC-binding factor and displays enhancer-blocking and silencing activities. J Virol 80 (2006) 2358-68.
[53] D.C. Bloom, N.V. Giordani, and D.L. Kwiatkowski, Epigenetic regulation of latent HSV-1 gene expression. Biochim Biophys Acta 1799 (2010) 246-56.
[54] A.G. West, M. Gaszner, and G. Felsenfeld, Insulators: many functions, many mechanisms. Genes Dev 16 (2002) 271-88.
[55] H. Zhao, and A. Dean, An insulator blocks spreading of histone acetylation and interferes with RNA polymerase II transfer between an enhancer and gene. Nucleic Acids Res 32 (2004) 4903-19.
[56] G. Felsenfeld, B. Burgess-Beusse, C. Farrell, M. Gaszner, R. Ghirlando, S. Huang, C. Jin, M. Litt, F. Magdinier, V. Mutskov, Y. Nakatani, H. Tagami, A. West, and T. Yusufzai, Chromatin boundaries and chromatin domains. Cold Spring Harb Symp Quant Biol 69 (2004) 245-50.
[57] H.N. Cai, and M. Levine, The gypsy insulator can function as a promoter-specific silencer in the Drosophila embryo. EMBO J 16 (1997) 1732-41.
[58] M. Du, L.G. Beatty, W. Zhou, J. Lew, C. Schoenherr, R. Weksberg, and P.D. Sadowski, Insulator and silencer sequences in the imprinted region of human chromosome 11p15.5. Hum Mol Genet 12 (2003) 1927-39.
[59] R. Ohlsson, R. Renkawitz, and V. Lobanenkov, CTCF is a uniquely versatile transcription regulator linked to epigenetics and disease. Trends Genet 17 (2001) 520-527.
[60] J.E. Phillips, and V.G. Corces, CTCF: master weaver of the genome. Cell 137 (2009) 1194-211.
[61] S.D. Washington, F. Musarrat, M.K. Ertel, G.L. Backes, and D.M. Neumann, CTCF Binding Sites in the Herpes Simplex Virus 1 Genome Display Site-Specific CTCF Occupation, Protein Recruitment, and Insulator Function. Journal of Virology 92 (2018).
[62] J.C. Glorioso, Herpes simplex viral vectors: late bloomers with big potential. Human gene therapy 25 (2014) 83- 91.
[63] A.L. Epstein, HSV-1-derived amplicon vectors: recent technological improvements and remaining difficulties--a review. Mem Inst Oswaldo Cruz 104 (2009) 399-410.
[64] A.I. Geller, K. Keyomarsi, J. Bryan, and A.B. Pardee, An efficient deletion mutant packaging system for

defective herpes simplex virus vectors: potential applications to human gene therapy and neuronal physiology. Proc Natl Acad Sci U S A 87 (1990) 8950-4.

[65] P.A. Johnson, A. Miyanohara, F. Levine, T. Cahill, and T. Friedmann, Cytotoxicity of a replication-defective mutant of herpes simplex virus type 1. J Virol 66 (1992) 2952-65.
[66] B.K. Jin, M. Belloni, B. Conti, H.J. Federoff, R. Starr, J.H. Son, H. Baker, and T.H. Joh, Prolonged in vivo gene expression driven by a tyrosine hydroxylase promoter in a defective herpes simplex virus amplicon vector. Hum Gene Ther 7 (1996) 2015-24.
[67] A.I. Brooks, D.A. Cory-Slechta, W.J. Bowers, S.L. Murg, and H.J. Federoff, Enhanced learning in mice parallels vector-mediated nerve growth factor expression in hippocampus. Hum Gene Ther 11 (2000) 2341-52.
[68] P. Marconi, D. Krisky, T. Oligino, P.L. Poliani, R. Ramakrishnan, W.F. Goins, D.J. Fink, and J.C. Glorioso, Replication-defective herpes simplex virus vectors for gene transfer in vivo. Proc Natl Acad Sci U S A 93 (1996) 11319-20.
[69] R. Argnani, M. Lufino, M. Manservigi, and R. Manservigi, Replication-competent herpes simplex vectors: design and applications. Gene Ther 12 Suppl 1 (2005) S170-7.
[70] N.A. Fineberg, P.M. Haddad, L. Carpenter, B. Gannon, R. Sharpe, A.H. Young, E. Joyce, J. Rowe, D. Wellsted, D.J. Nutt, and B.J. Sahakian, The size, burden and cost of disorders of the brain in the UK. Journal of psychopharmacology 27 (2013) 761-70.
[71] D. Weintraub, C.L. Comella, and S. Horn, Parkinson's disease--Part 1: Pathophysiology, symptoms, burden, diagnosis, and assessment. Am J Manag Care 14 (2008) S40-8.
[72] S.H. Mehta, and C.H. Adler, Advances in Biomarker Research in Parkinson's Disease. Curr Neurol Neurosci Rep 16 (2016) 7.
[73] W. Ding, L.J. Ding, F.F. Li, Y. Han, and L. Mu, Neurodegeneration and cognition in Parkinson's disease: a review. Eur Rev Med Pharmacol Sci 19 (2015) 2275-81.
[74] J.A. Santiago, V. Bottero, and J.A. Potashkin, Biological and Clinical Implications of Comorbidities in Parkinson's Disease. Frontiers in aging neuroscience 9 (2017) 394.
[75] M. Montero-Odasso, F. Pieruccini-Faria, R. Bartha, S.E. Black, E. Finger, M. Freedman, B. Greenberg, D.A. Grimes, R.A. Hegele, C. Hudson, P.W. Kleinstiver, A.E. Lang, M. Masellis, P.M. McLaughlin, D.P. Munoz, S. Strother, R.H. Swartz, S. Symons, M.C. Tartaglia, L. Zinman, M.J. Strong, O. Investigators, and W. McIlroy, Motor Phenotype in Neurodegenerative Disorders: Gait and Balance Platform Study Design Protocol for the Ontario Neurodegenerative Research Initiative (ONDRI). Journal of Alzheimer's disease : JAD 59 (2017) 707-721.
[76] D.C. Hesdorffer, Comorbidity between neurological illness and psychiatric disorders. CNS spectrums 21 (2016) 230-8.
[77] D.M. Krisky, D. Wolfe, W.F. Goins, P.C. Marconi, R. Ramakrishnan, M. Mata, R.J. Rouse, D.J. Fink, and J.C. Glorioso, Deletion of multiple immediate-early genes from herpes simplex virus reduces cytotoxicity and permits long-term gene expression in neurons. Gene Ther 5 (1998) 1593-603.
[78] N. Wu, S.C. Watkins, P.A. Schaffer, and N.A. DeLuca, Prolonged gene expression and cell survival after infection by a herpes simplex virus mutant defective in the immediate-early genes encoding ICP4, ICP27, and ICP22. J Virol 70 (1996) 6358-69.
[79] L.A. Samaniego, L. Neiderhiser, and N.A. DeLuca, Persistence and expression of the herpes simplex virus genome in the absence of immediate-early proteins. J Virol 72 (1998) 3307-20.
[80] P.A. Johnson, M.J. Wang, and T. Friedmann, Improved cell survival by the reduction of immediate-early gene expression in replication-defective mutants of herpes simplex virus type 1 but not by mutation of the virion host shutoff function. J Virol 68 (1994) 6347-62.
[81] C.M. Preston, R. Mabbs, and M.J. Nicholl, Construction and characterization of herpes simplex virus type1 mutants with conditional defects in immediate early gene expression. Virology 229 (1997) 228-39.
[82] C.M. Preston, and M.J. Nicholl, Human cytomegalovirus tegument protein pp71 directs long-term gene expression from quiescent herpes simplex virus genomes. J Virol 79 (2005) 525-35.
[83] C.E. Lilley, F. Groutsi, Z. Han, J.A. Palmer, P.N. Anderson, D.S. Latchman, and R.S. Coffin, Multiple immediate- early gene-deficient herpes simplex virus vectors allowing efficient gene delivery to neurons in culture and widespread gene delivery to the central nervous system in vivo. J Virol 75 (2001) 4343-56.

[84] E.G. Homer, A. Rinaldi, M.J. Nicholl, and C.M. Preston, Activation of herpesvirus gene expression by the human cytomegalovirus protein pp71. J Virol 73 (1999) 8512-8.

[85] Y. Miyagawa, P. Marino, G. Verlengia, H. Uchida, W.F. Goins, S. Yokota, D.A. Geller, O. Yoshida, J. Mester, J.B. Cohen, and J.C. Glorioso, Herpes simplex viral-vector design for efficient transduction of nonneuronal cells without cytotoxicity. Proceedings of the National Academy of Sciences of the United States of America 112 (2015) E1632- 41.
[86] G. Verlengia, Y. Miyagawa, S. Ingusci, J.B. Cohen, M. Simonato, and J.C. Glorioso, Engineered HSV vector achieves safe long-term transgene expression in the central nervous system. Sci Rep 7 (2017) 1507.
[87] R. Ghirlando, and G. Felsenfeld, CTCF: making the right connections. Genes Dev 30 (2016) 881-91.
[88] D.W. Emery, The Use of Chromatin Insulators to Improve the Expression and Safety of Integrating Gene Transfer Vectors. Hum Gene Ther 22 (2011) 761-774.
[89] M.N. Antoniou, K.A. Skipper, and O. Anakok, Optimizing retroviral gene expression for effective therapies. Hum Gene Ther 24 (2013) 363-74.
[90] F. Zhang, A.R. Frost, M.P. Blundell, O. Bales, M.N. Antoniou, and A.J. Thrasher, A ubiquitous chromatin opening element (UCOE) confers resistance to DNA methylation-mediated silencing of lentiviral vectors. Molecular therapy: the journal of the American Society of Gene Therapy 18 (2010) 1640-9.
[91] F. Han, Y. Miyagawa, G. Verlengia, S. Ingusci, M. Soukupova, M. Simonato, J.C. Glorioso, and J.B. Cohen, Cellular Antisilencing Elements Support Transgene Expression from Herpes Simplex Virus Vectors in the Absence of Immediate Early Gene Expression. Journal of virology 92 (2018).
[92] P.A. Pechan, M. Fotaki, R.L. Thompson, R. Dunn, M. Chase, E.A. Chiocca, and X.O. Breakefield, A novel 'piggyback' packaging system for herpes simplex virus amplicon vectors. Human gene therapy 7 (1996) 2003-13.
[93] C. Logvinoff, and A.L. Epstein, Genetic engineering of herpes simplex virus and vector genomes carrying loxP sites in cells expressing Cre recombinase. Virology 267 (2000) 102-10.
[94] C. Zaupa, V. Revol-Guyot, and A.L. Epstein, Improved packaging system for generation of high-level noncytotoxic HSV-1 amplicon vectors using Cre-loxP site-specific recombination to delete the packaging signals of defective helper genomes. Human gene therapy 14 (2003) 1049-63.
[95] M. Suzuki, K. Kasai, and Y. Saeki, Plasmid DNA sequences present in conventional herpes simplex virus amplicon vectors cause rapid transgene silencing by forming inactive chromatin. Journal of virology 80 (2006) 3293-300.
[96] M. Suzuki, E.A. Chiocca, and Y. Saeki, Early STAT1 activation after systemic delivery of HSV amplicon vectors suppresses transcription of the vector-encoded transgene. Mol Ther 15 (2007) 2017-26.
[97] R.L. Klein, M.E. Hamby, Y. Gong, A.C. Hirko, S. Wang, J.A. Hughes, M.A. King, and E.M. Meyer, Dose and promoter effects of adeno-associated viral vector for green fluorescent protein expression in the rat brain. Experimental neurology 176 (2002) 66-74.
[98] K.L. Jackson, R.D. Dayton, B.E. Deverman, and R.L. Klein, Better Targeting, Better Efficiency for Wide-Scale Neuronal Transduction with the Synapsin Promoter and AAV-PHP.B. Frontiers in molecular neuroscience 9 (2016) 116.
[99] K.L. Jackson, R.D. Dayton, J.M. Fisher-Perkins, P.J. Didier, K.C. Baker, M. Weimer, A. Gutierrez, C.D. Cain, J.M. Mathis, M.A. Gitcho, B.A. Bunnell, and R.L. Klein, Initial gene vector dosing for studying symptomatology of amyotrophic lateral sclerosis in non-human primates. Journal of medical primatology 44 (2015) 66-75.
[100] C. Fraefel, S. Song, F. Lim, P. Lang, L. Yu, Y. Wang, P. Wild, and A.I. Geller, Helper virus-free transfer of herpes simplex virus type 1 plasmid vectors into neural cells. J Virol 70 (1996) 7190-7.
[101] Y. Saeki, T. Ichikawa, A. Saeki, E.A. Chiocca, K. Tobler, M. Ackermann, X.O. Breakefield, and C. Fraefel, Herpes simplex virus type 1 DNA amplified as bacterial artificial chromosome in Escherichia coli: rescue of replication-competent virus progeny and packaging of amplicon vectors. Hum Gene Ther 9 (1998) 2787-94.
[102] T.A. Stavropoulos, and C.A. Strathdee, An enhanced packaging system for helper-dependent herpes simplex virus vectors. J Virol 72 (1998) 7137-43.
[103] A. Gimenez-Cassina, R. Wade-Martins, S. Gomez-Sebastian, J.C. Corona, F. Lim, and J. Diaz-Nido, Infectious delivery and long-term persistence of transgene expression in the brain by a 135-kb iBAC-FXN genomic DNA expression vector. Gene Ther 18 (2011) 1015-9.

[104] M.G. Kaplitt, A.D. Kwong, S.P. Kleopoulos, C.V. Mobbs, S.D. Rabkin, and D.W. Pfaff, Preproenkephalin promoter yields region-specific and long-term expression in adult brain after direct in vivo gene transfer via a defective herpes simplex viral vector. Proc Natl Acad Sci U S A 91 (1994) 8979-83.

6. References

[105] D.Y. Ho, J.R. McLaughlin, and R.M. Sapolsky, Inducible gene expression from defective herpes simplex virus vectors using the tetracycline-responsive promoter system. Brain Res Mol Brain Res 41 (1996) 200-9.
[106] S. Song, Y. Wang, S.Y. Bak, P. Lang, D. Ullrey, R.L. Neve, K.L. O'Malley, and A.I. Geller, An HSV-1 vector containing the rat tyrosine hydroxylase promoter enhances both long-term and cell type-specific expression in the midbrain. J Neurochem 68 (1997) 1792-803.
[107] S. Kugler, E. Kilic, and M. Bahr, Human synapsin 1 gene promoter confers highly neuron-specific long-term transgene expression from an adenoviral vector in the adult rat brain depending on the transduced area. Gene therapy 10 (2003) 337-47.
[108] J.L. Nathanson, Y. Yanagawa, K. Obata, and E.M. Callaway, Preferential Labeling of Inhibitory and Excitatory Cortical Neurons by Endogenous Tropism of Adeno-Associated Virus and Lentivirus Vectors. Neuroscience 161 (2009) 441-450.
[109] T. Dittgen, A. Nimmerjahn, S. Komai, P. Licznerski, J. Waters, T.W. Margrie, F. Helmchen, W. Denk, M. Brecht, and P. Osten, Lentivirus-based genetic manipulations of cortical neurons and their optical and electrophysiological monitoring in vivo. P Natl Acad Sci USA 101 (2004) 18206-18211.
[110] M. Yaguchi, Y. Ohashi, T. Tsubota, A. Sato, K.W. Koyano, N. Wang, and Y. Miyashita, Characterization of the properties of seven promoters in the motor cortex of rats and monkeys after lentiviral vector-mediated gene transfer. Hum Gene Ther Methods 24 (2013) 333-44.
[111] M. Suzuki, E.A. Chiocca, and Y. Saeki, Stable transgene expression from HSV amplicon vectors in the brain: potential involvement of immunoregulatory signals. Mol Ther 16 (2008) 1727-36.
[112] J. Zhang, H. Liu, and B. Wei, Immune response of T cells during herpes simplex virus type 1 (HSV-1) infection. J Zhejiang Univ Sci B 18 (2017) 277-288.
[113] P.A. Sheridan, and M.A. Beck, The immune response to herpes simplex virus encephalitis in mice is modulated by dietary vitamin E. J Nutr 138 (2008) 130-7.
[114] A.W. Harmon, and A.P. Byrnes, Adenovirus Vector Toxicity. in: N. Brunetti-Pierri, (Ed.), Safety and Efficacy of Gene-Based Therapeutics for Inherited Disorders, 2017, pp. 37-60.
[115] S. Lehrman, Virus treatment questioned after gene therapy death. Nature 401 (1999) 517-8.
[116] F. Mingozzi, and K.A. High, Immune responses to AAV vectors: overcoming barriers to successful gene therapy. Blood 122 (2013) 23-36.
[117] P.K. Hocknell, R.D. Wiley, X. Wang, T.G. Evans, W.J. Bowers, T. Hanke, H.J. Federoff, and S. Dewhurst, Expression of human immunodeficiency virus type 1 gp120 from herpes simplex virus type 1-derived amplicons results in potent, specific, and durable cellular and humoral immune responses. J Virol 76 (2002) 5565-80.
[118] M.A. Brockman, and D.M. Knipe, Herpes simplex virus vectors elicit durable immune responses in the presence of preexisting host immunity. J Virol 76 (2002) 3678-87.
[119] Y.B. Lee, C.P. Glover, A.S. Cosgrave, A. Bienemann, and J.B. Uney, Optimizing regulatable gene expression using adenoviral vectors. Exp Physiol 90 (2005) 33-7.

A new selective JNK2 inhibitor is neuroprotective in epilepsy

Silvia Zucchini[1], Marco Feligioni[2], Selene Ingusci[1] & Michele Simonato[1]

[1]Department of Medical Sciences, Section of Pharmacology, Neuroscience Center, University of Ferrara and National Institute of Neuroscience, Via Fossato di Mortara 17-19, Ferrara, Italy, [2]Laboratory of Pharmacology of Synaptic Plasticity, EBRI "Rita Levi-Montalcini" Foundation, Rome, 00143, Italy.

Epilepsy is generated by alterations of the balance between inhibitory (γ-aminobutyric acid, GABA) and excitatory (glutamate) neurotransmission. In particular, N-Methyl-D-aspartate receptors (NMDARs) have been shown to play a key role in the pathophysiology of epilepsy and NMDAR antagonists proved effective antiepileptic agents in both preclinical and clinical studies. Neuronal cell death is a severe outcome of epileptic seizures, and several studies demonstrate that NMDA antagonist are highly effective to protect brain tissue during seizures. Unfortunately, because of serious side effects, these compounds are not used in clinical practice. Remarkably, activation of c-Jun N-terminal kinase (JNK) seems to play a fundamental role in regulating cell death in epilepsy. It has been shown that JNK inhibitors can exert antiepileptic effects and reduce NMDAR-mediated neuronal death. We found that presynaptic JNK2 isoforms regulate NMDAR-evoked glutamate release and that JNK2 knockout mice display a reduced activity of cortical presynaptic NMDARs. We found that presynaptic NMDA activity is regulated by interaction with JNK2/Syntaxin 1a (STX1a), and that the inhibition of JNK2/STX1a interaction by a cell permeable peptide, JGRi1, reduces NMDA-evoked release of glutamate. Intracerebroventricular injection of JGRi1 in a mouse model of epilepsy (i.p kainate) is able to reduce neural cell death both in the cortex and in the hippocampus by about 70%, but susceptibility to kainate-induced seizures and seizure severity remain unchanged. These results indicate a neuroprotective role of JGRi1.

Target autophagy as a new therapeutic approach to recover myelination in multiple sclerosis

Simone Patergnani[1], S. Ingusci[2], E. Bertelè[1], M. Bonora[1], M. Castellazzi[3], C. Giorgi[1], S. Marchi[1], E. Granieri[3], M. Simonato[2],
P. Pinton[1]

[1]Department of Morphology, Surgery and Experimental Medicine Section of General Pathology Paolo Pinton's Lab c/o CUBO and LTTA center, University of Ferrara; [2]Department of Medical Sciences and National Institute of Neurosciences, Section of Pharmacology, University of Ferrara; [3]Department of Biomedical and Specialist Surgical Sciences, Section of Neurological, Psychiatric and Psychological Sciences, University of Ferrara

It has been recently demonstrated how autophagy plays a key role in neurodegenerative processes. Given its major role in cell survival during unfavourable conditions, it is not surprising that autophagy protects from neuronal death. However, autophagy has been also described as a mechanism of cytotoxicity. Indeed, autophagy seems to play a dual role in neurodegenerative disease. Multiple sclerosis (MS), a chronic inflammatory demyelinating disorder, is an auto-immune disease of the central nervous system. Several studies have shown that autophagy directly participates in the progress of MS, suggesting that enhanced autophagic levels may be a very harmful condition for oligodendrocyte precursor cells (OPCs) differentiation and MS progression. Different compounds may be used as autophagy inhibitors, including anti- psychotic drugs like clozapine and haloperidol. To address the role of autophagy in OPCs differentiation and MS, we employed an *in vitro* multicellular system that maintains physiological cell-to-cell interactions (organotypic cerebellar slice, OCS, cultures) and an *in vivo* mouse model based on treatment with a copper chelator (cuprizone). Clozapine and haloperidol treatment of OCSs after lysolecithin-induced demyelination enhanced remyelination, as evaluated using alignment to axons and immunoreactivity for myelin markers. When administered to cuprizone-treated mice, clozapine and haloperidol significantly improved motor coordination, gait ability and balance. This data supports an off-label use of clozapine and haloperidol as remyelinating drugs.

Video Article

Microdialysis of Excitatory Amino Acids During EEG Recordings in Freely Moving Rats

Marie Soukupová[1], Chiara Falcicchia[1], Francesca Lovisari[1], Selene Ingusci[1], Mario Barbieri[1], Silvia Zucchini[1], Michele Simonato[1]

[1]Department of Medical Sciences, Section of Pharmacology, Neuroscience Center, University of Ferrara and National Institute of Neuroscience

Correspondence to: Marie Soukupová at marie.soukupova@unife.it

URL: https://www.jove.com/video/58455
DOI: doi:10.3791/58455

Keywords: microdialysis, glutamate, aspartate, epilepsy, pilocarpine model, stereotaxic surgery, potassium stimulation, electroencephalography, liquid chromatography

Date Published: 11/6/2018

Citation: Soukupová, M., Falcicchia, C., Lovisari, F., Ingusci, S., Barbieri, M., Zucchini, S., Simonato, M. Microdialysis of Excitatory Amino Acids During EEG Recordings in Freely Moving Rats. *J. Vis. Exp.* (), e58455, doi:10.3791/58455 (2018).

Abstract

Microdialysis is a well-established neuroscience technique that correlates the changes of neurologically active substances diffusing into the brain interstitial space with the behavior and/or with the specific outcome of a pathology (*e.g.,* seizures for epilepsy). When studying epilepsy, the microdialysis technique is often combined with short-term or even long-term video-electroencephalography (EEG) monitoring to assess spontaneous seizure frequency, severity, progression and clustering. The combined microdialysis-EEG is based on the use of several methods and instruments. Here, we performed *in vivo* microdialysis and continuous video-EEG recording to monitor glutamate and aspartate outflow over time, in different phases of the natural history of epilepsy in a rat model. This combined approach allows the pairing of changes in the neurotransmitter release with specific stages of the disease development and progression. The amino acid concentration in the dialysate was determined by liquid chromatography. Here, we describe the methods and outline the principal precautionary measures one should take during *in vivo* microdialysis-EEG, with particular attention to the stereotaxic surgery, basal and high potassium stimulation during microdialysis, depth electrode EEG recording and high-performance liquid chromatography analysis of aspartate and glutamate in the dialysate. This approach may be adapted to test a variety of drug or disease induced changes of the physiological concentrations of aspartate and glutamate in the brain. Depending on the availability of an appropriate analytical assay, it may be further used to test different soluble molecules when employing EEG recording at the same time.

Video Link

The video component of this article can be found at https://www.jove.com/video/58455/

Introduction

To provide insight into the functional impairment of glutamate-mediated excitatory and GABAergic inhibitory neurotransmission resulting in spontaneous seizures in temporal lobe epilepsy (TLE), we systematically monitored extracellular concentrations of GABA[1] and later the levels of glutamate and aspartate[2] by microdialysis in the ventral hippocampus of rats at various time-points of the disease natural course, *i.e.*, during development and progression of epilepsy. We took advantage of the TLE pilocarpine model in rats, which mimics the disease very accurately in terms of behavioral, electrophysiological and histopathological changes[3,4] and we correlated the dialysate concentration of amino acids to its different phases: the acute phase after the epileptogenic insult, the latency phase, the time of the first spontaneous seizure and the chronic phass[5,6,7]. Framing the disease phases was enabled by long-term video-EEG monitoring and the precise EEG and clinical characterization of spontaneous seizures. Application of the microdialysis technique associated with long-term video-EEG monitoring allowed us to propose mechanistic hypotheses for TLE neuropathology. In summary, the technique described in this manuscript allows the pairing of neurochemical alterations within a defined brain area with the development and progression of epilepsy in an animal model.

Paired devices, made up of a depth electrode juxtaposed to a microdialysis cannula, are often employed in epilepsy research studies where changes in neurotransmitters, their metabolites, or energy substrates should be correlated to neuronal activity.In the vast majority of cases, it is used in freely behaving animals, but it can be also conducted in a similar way in human beings, *e.g.*, in pharmaco-resistant epileptic patients undergoing depth electrode investigation prior to surgery[8]. Both EEG recording, and dialysate collection may be performed separately (*e.g.*, implanting the electrode in one hemisphere and the microdialysis probe in the other hemisphere or even performing the microdialysis in one group of animals while performing the sole EEG in another group of animals). However, coupling the electrodes to probes may have multiple advantages: it simplifies stereotaxic surgery, limits tissue damage to only one hemisphere (while leaving the other, intact, as a control for histological studies), and homogenizes the results as these are obtained from the same brain region and the same animal.

On the other hand, the preparation of the coupled microdialysis probe-electrode device requires skills and time if it is home-made. One could spend relatively high amounts of money if purchased from the market. Moreover, when microdialysis probes (probe tips are typically 200-400 µm in diameter and 7-12 mm long)[9], and EEG electrodes (electrode tips are usually of 300-500 µm in diameter, and long enough to reach the brain structure of interest[10]) are coupled, the mounted device represents a bulky and relatively heavy object on one side of the head, which is troublesome for animals and prone to be lost especially when it is connected to the dialysis pump and the hard-wire EEG recording system.

This aspect is more relevant in epileptic animals that are difficult to handle and less adaptive to the microdialysis sessions. Proper surgical techniques and appropriate post-operative care can result in long-lasting implants that cause minimal animal discomfort and should be pursued for combinatory microdialysis-EEG experiments[10,11,12].

The advantages and limitations of the microdialysis technique have been reviewed in detail by many neuroscientists. Its primary advantage over other *in vivo* perfusion techniques (*e.g.*, fast flow push-pull or cortical cup perfusion) is a small diameter of the probe which covers a relatively precise area of interest[13,14,15]. Second, the microdialysis membrane creates a physical barrier between the tissue and the perfusate; therefore, high-molecular weight substances do not cross and do not interfere with the analysis[16,17]. Moreover, the tissue is protected from the turbulent flow of the perfusate[18]. Another important advantage is the possibility to modify the perfusate flow for maximizing the analyte concentration in the perfusate (*i.e.*, the process of microdialysis can be well defined mathematically and can be modified to yield high concentrations of the analyte in the sample)[19]. Finally, the technique may be used to infuse the drugs or pharmacologically active substances into the tissue of interest and to determine their effect at the site of intervention[20]. On the other hand, microdialysis has a limited resolution time (typically more than 1 min due to the time needed for collecting samples) in comparison to electrochemical or biological sensors; it is an invasive technique that causes tissue damage; it compromises the neurochemical balance within the space around the membrane due to the continuous concentration gradient of all soluble substances which enters the perfusate together with the analyte of interest. Finally, the microdialysis technique is highly influenced by the limits of the analytical techniques employed for the quantification of substances in the perfusate[9,21,22,23]. The high-performance liquid chromatography (HPLC) after derivatization with orthophthaldialdehyde for glutamate and aspartate analysis in biological samples has been well validated[24,25,26,27] and its extensive discussion is out of the scope of this manuscript, but the data produced by using this method will be described in detail.

When performed properly and without modifications of the perfusate composition, microdialysis can provide reliable information about the basal levels of neurotransmitter release. The largest portion of the basal levels is likely the result of the transmitter spillover from the synapses[9]. Because in many instances the simple sampling of the neurotransmitter in the extra synaptic space is not sufficient to pursue the goals of an investigation, the microdialysis technique can be also employed to stimulate neurons or to deprive them of important physiological ions such as K^+ or Ca^{2+}, in order to evoke or prevent the release of the neurotransmitter.

High K^+ stimulation is often used in neurobiology to stimulate neuronal activity not only in awake animals but also in primary and organotypic cultures. The exposure of a healthy central nervous system to solutions with high concentrations of K^+ (40-100 mM) evokes the efflux of neurotransmitters[28]. This ability of neurons to provide an additional release in response to high K^+ may be compromised in epileptic animals [1] and in other neurodegenerative diseases[29,30]. Similarly, the Ca^{2+} deprivation (obtained by perfusing Ca^{2+} free solutions) is used to establish calcium-dependent release of most neurotransmitters measured by microdialysis. It is generally believed that Ca^{2+} dependent release is of neuronal origin, whereas Ca^{2+} independent release originates from glia, but many studies raised controversy over the meaning of Ca^{2+}-sensitive measurements of e.g. glutamate or GABA[9]: thus, if possible, it is advisable to support microdialysis studies with microsensor studies, as these latter have higher spatial resolution and the electrodes allows to get closer to synapses[31].

Regarding microdialysis studies in epileptic animals, it is important to stress that the data obtained from most of them rely upon video or video-EEG monitoring of seizures, *i.e.*, of the transient occurrence of signs and/or symptoms due to abnormal excessive or synchronous neuronal activity in the brain[32]. There are some specifics of electrographic seizures in pilocarpine treated animals which should be considered when preparing the experiment. Spontaneous seizures are followed by depressed activity with frequent EEG interictal spikes[3] and occur in clusters[33,34]. Sham operated non-epileptic animals may exhibit seizure-like activity[35] and therefore the parameters for EEG recordings evaluation should be standardized[36] and, if possible, the timing of microdialysis sessions should be well defined. Finally, we highly recommend following the principles and methodological standards for video-EEG monitoring in control adult rodents outlined by experts of International League Against Epilepsy and American Epilepsy Society in their very recent reports[37,38].

Here, we describe microdialysis of glutamate and aspartate in parallel with the long-term video-EEG recordings in epileptic animals and their analysis in the dialysate by HPLC. We will emphasize the critical steps of the protocol that one should take care of for best result.

Protocol

All experimental procedures have been approved by the University of Ferrara Institutional Animal Care and Use Committee and by the Italian Ministry of Health (authorization: D.M. 246/2012-B) in accordance with guidelines outlined in the European Communities Council Directive of 24 November 1986 (86/609/EEC). This protocol is specifically adjusted for glutamate and aspartate determination in rat brain dialysates obtained under EEG control of microdialysis sessions in epileptic and non-epileptic rats. Many of the materials described here may be easily replaced with those that one uses in his laboratory for EEG recordings or microdialysis.

1. Assembly of the Microdialysis Probe-electrode Device

1. Use a 3-channel two-twisted electrode (with at least a 20 mm cut length of the registering electrode and a 10 cm long grounding electrode) and couple it to a guide cannula to prepare the device. See examples of 3-channel electrode and guide cannula for dialysis in **Figure 1A-1B.**
2. Remove (**Figure 1C**) and insert (**Figure 1D**) the metal guide cannula into the dummy plastic cannula a few times prior to the usage in order to ease its removal at the moment of its switch for microdialysis probe in animal.
3. Bend the twisted wires of registering electrode two times (**Figure 1E-1F**) in order to align the wires with the dummy cannula of the guide and cut the electrode tip (**Figure 1G**) to be 0.5 mm longer than the tip of the guide cannula (**Figure 1H**) using the digital caliper.
4. Have ready the 1 mm long silicon circlet (O.D. 2 mm, thickness 0.3 mm; **Figure 1I**) and insert the tip of the guide cannula and the tip of the twisted electrodes into the silicon circlet using the tweezers (**Figure 1J**). Fix it onto the foot of the guide cannula pedestal with polymer glue of rapid action or resin (**Figure 1K**). See the example of the completed devices in **Figure 1L and Figure 2A**.
5. Sterilize the device under germicidal UV light for 4 h. Turn over the device four times so as each of its sides is exposed to the light for 1 h. Note: Many home-made electrodes and microdialysis probes may be assembled in a similar way. The head of above described implant for rats has the following dimensions: 7 mm width x 5 mm depth x 10 mm length from the top to pedestal toe; the implant tip is about 11 mm

long, 600 µm in diameter and all the device weights about 330-360 mg. The device may be reused two or three times if (i) a sufficient length of the ground electrode is left on the skull during the surgery for the next use and (ii) when the animal is killed, and the device recovered together with the dental cement it is left in acetone overnight, such that the cement may be mechanically disaggregated, and the device washed and sterilized again.

2. Stereotaxic Surgery

1. Use a stereotaxic apparatus and probe clip holder (**Figure 2B**) for the device implantation following the contemporary standards for aseptic and pain-free surgeries[39,40,41].
    1. Anesthetize the adult Sprague-Dawley rats with ketamine/xylazine mixture (43 mg/kg and 7 mg/kg, i.p.) and fix it onto the stereotaxic frame. Add isoflurane anesthesia (1.4% in air; 1.2 mL/min) to initial ketamine/xylazine injection as it allows to control the depth of anesthesia in time. Shave the fur on animal's head.

2. Swab the head skin surface by iodine-based solution followed by 70% ethanol to prepare it for aseptic surgery[39].
    1. Implant the guide cannula-electrode device prepared in precedence (1.1 – 1.5) into the right ventral hippocampus using the following coordinates: nose bar + 5.0 mm, A – 3.4 mm, L + 4.5 mm, P + 6.5 mm to bregma[1,2]. Follow standard techniques for stereotaxic surgeries[10,11,12].
    2. Ensure that it does not cover the anchoring screws. When mounting it onto the stereotaxic apparatus, grasp the device for the guide cannula head as this may be easily aligned to the probe holder.

3. Anchor the device to the skull with at least four stainless screws screwing them into the skull bone (1 screw into the left and 1 screw into the right frontal bone plates, 1 screw into the left parietal and 1 screw into the interparietal bone plates). Add a drop of tissue glue to further fix each screw to the skull bone.
    1. Cover half of screw threads with methacrylic cement. Promote the binding of the cement by making shallow grooves in the bone to increase the adherence.

4. Once the tip of the device is positioned into the brain tissue, twist the wire of the ground electrode around 3 anchoring screws. Cover all mounted screws and the device with the dental cement[12,42,43].
5. Monitor the animals during the surgery and for about 1 h thereafter until upright and moving around the cage. Keep them on a warming pad to avoid hypothermia. Allow the rats to recover for at least 7 days after the device implantation.
6. Monitor the animals at least once daily for 3 days after the surgery for signs of pain or distress. Give the animals with the antibiotic cream (gentamycin 0.1%) close to the incised site to prevent the infection and an analgesic (tramadol 5 mg/kg, i.p.) for 3 days to prevent the post-surgical pain.

3. Temporal Lobe Epilepsy Induction by Pilocarpine and Assignment of Animals to Experimental Groups

1. After a week of post-surgical recovery, assign the animals randomly to groups: (i) control animals receiving vehicle and (ii) epileptic animals that will receive pilocarpine. Use a proportionally higher number of animals for epileptic group since not all of the pilocarpine administered rats will develop the disease.
2. Inject a dose of methylscopolamine (1 mg/kg, s.c.) and 30 min after, a single injection of pilocarpine (350 mg/kg, i.p.) to induce the status epilepticus (SE). Inject methylscopolamine and the vehicle (saline) to the control rats. Use 1 mL syringe with 25G needle for all i.p. administrations.
    1. Check visually the animals to start to have behavioral seizures (moving vibrissa within 5 min, nodding head, cloning the limbs) and within 25 min to clone continuously all the body (SE).

3. Arrest the SE 2 h after the onset to have a mortality about 25% and a mean latent period of approximately 10 days by administration of diazepam (20 mg/kg, i.p.). Observe and record any seizure behavior beginning immediately after the pilocarpine injection and continue for at least 6 h thereafter.
4. Give the animals saline (1 mL, i.p.) using 1 mL syringe with 25G needle and sucrose solution (1 mL, p.o.) using 1 mL syringe and flexible feeding 17G needle for 2-3 days after SE to promote the recovery of body weight loss.
    1. Exclude the animals that do not achieve the initial body weight within the first week after pilocarpine SE from the study (except for the acute group killed 24 h after SE, where the body weight follow up is not possible).

5. Assign post-SE animals randomly to different experimental groups (**Figure 3**): acute phase (where the microdialysis takes place 24 h after SE), latency (7-9 days after SE), first spontaneous seizure (approximately 11 days after SE), and chronic period (starts about 22-24 days after SE, i.e. about 10 days after the first seizure). Monitor the animals for the occurrence of spontaneous seizures.
Note: Use the following inclusion/exclusion criteria for further experiments in epileptic rats: development of convulsive SE within 1 h after pilocarpine administration; weight gain in the first week after SE and the correct positioning of the microdialysis probe and electrode.

4. Epileptic Behavior Monitoring and Analysis

1. Long-term monitoring of epileptic behavior
    1. Approximately 6 h after pilocarpine administration (*i.e.*, at the end of direct observation by the researchers), place the animals into the clean home cages and start the 24 h video monitoring.
    2. Continue the 24 h video monitoring until day 5, using a digital video surveillance system.
    3. Beginning at day 5, connect the rats in their home rectangular cages to tethered EEG recording system and continue the 24 h video monitoring.

4. Set the parameters on the amplifier positioned outside of the Faraday cage (set amplification factor on each channel according to the specificity of the EEG signal of each single animal) and start the EEG acquisition observing the EEG signal produced by unconnected cables. Use sampling rate 200 Hz and low pass filter set to 0.5 Hz.
5. Connect the animal to cables holding an animal's head between two stretched fingers of one hand and screwing down the connectors to the electrode pedestal using the other free hand. Start the acquisition.
   Caution: Ensure that the signal is free of artifacts. Common artifacts are the spikes greatly exceeding the scale.
6. A day before the microdialysis experiment, transfer the animals into the tethered EEG system equipped with plexiglass cylinders for microdialysis. Disconnect the animals from the EEG tethering system in home cage screwing up the connectors from the electrode without restrain the animal. Place the animal into the high plexiglass cylinders.

2. Monitoring of epileptic behavior a day before and during the microdialysis session
   1. Switch on the amplifier positioned outside of the Faraday cage. Open the EEG software. Start the EEG acquisition observing the EEG signal produced by unconnected cables.
   2. Connect the animal to the tethered EEG recording system holding an animal's head between two stretched fingers of one hand and screwing down the connectors to the electrode pedestal using the other free hand. Set an amplification factor (gain) on each channel of amplifier according to electrode signal of single animal so the EEG signal is in scale. Let the animal explore the new cage (cylinder) for at least 1 h under the direct observation of the researcher.
   3. **Note:** 24 h before the microdialysis experiment, the rats are briefly anesthetized with isoflurane for the switch of guide cannulas to microdialysis probe. Take advantage of the moment when they are anesthetized to connect them to the EEG recording system.
   4. Shorten or prolong pendulous cable according to animal's commodity. Make sure that the cables do not interfere with animal's movements and lying posture.
   5. Check for the correct image framing of the video cameras. Start the video-EEG recording.

3. Identification of seizures and EEG activity
   1. Use a software player to watch the videos. Scroll the movie 8 times faster than the real time playing and individuate the generalized seizures (see animal to rear with forelimb clonus or animal rearing and falling with forelimb clonus). Slow down the video and note the precise time of the beginning and of the end of the behavioral seizure.
   2. Process the data by counting the number of generalized seizures observed in 24 h of video records and express them in terms of seizure frequency and duration as mean values of all seizures observed in 24 h.
   3. Define the EEG seizures as the periods of paroxysmal activity of high frequency (>5 Hz) characterized by a >3-fold amplitude increment over baseline with progression of the spike frequency that lasts for a minimum of 3 s[2,44] or similar[28]. Use EEG software to process the raw EEG recordings. Split the EEG traces into 1 h fractions. Copy the EEG tracing fractions to file for software automatic spike analysis.
   4. Analyze the EEG activity data using EEG software and predefined parameters (4.3.3.). Conduct all video analyses in two independent investigators who are blind for the group of analyzed animals. In case of divergence, make them re-examine the data together to reach a consensus[45].

5. Microdialysis

1. *In vitro* probe recovery
   1. Prepare the probe for its first use according to the manufacturer's instructions, handling it in its protective sleeve.
   2. Run the experiment in triplicate: prepare three 1.5 mL test tubes loading them with 1 mL of Ringer's solution containing the mixture of standards (2.5 µM of glutamate and 2.5 µM of aspartate). Put three loaded 1.5 mL test tubes into the block heater set to 37 °C and position it on the stirrer.
      Note: Use the same standard solutions for chromatography calibrations.
   3. Seal the 1.5 mL test tubes with paraffin film and puncture it by sharp tweezers to make a hole of about 1 mm in diameter.
   4. Take the probe and insert it into the hole made in paraffin film. Immerse the membrane at least 2 mm under the solution level. Fix further the probe to 1.5 mL test tube by paraffin film.
      Caution: Ensure that the tip does not touch the walls of the 1.5 mL test tube.
   5. Connect the probe inlet to the syringe mounted on the infusion pump using FEP-tubing and tubing adapters. Optionally, use fine bore polythene tubing of 0.28 mm ID and 0.61 mm OD and colored tubing adapters (red and blue tubing adapters) for connections.
   6. Start the pump at 2 µL/min and let the fluid appear at the outlet tip. Connect the probe outlet to the 0.2 mL collecting test tube using FEP-tubing and tubing adapters.
      Note: Use FEP-tubing for all connections. Cut the desired length of tubing by using a razor blade. Use tubing adapters of different color for inlet and outlet of the probe. Let the pump run for 60 min. Check for leaks and air bubbles. These should not be present.
   7. Set the pump to the flow rate 2 µL/min and start to collect the samples on the outlet side of the tubing.
   8. Collect three 30 min perfusate samples and three equal volume samples of the solution in the 1.5 mL test tube. Take the equal volume samples from the 1.5 mL test tube every 30 min using the microsyringe immersed into the standard solution in the 1.5 mL test tube.
   9. Repeat the experiment (5.1.1-5.1.8) setting up the pump to the flow rate 3 µL/min (5.1.7) to have a probe recovery comparison when using two different perfusion flow rates.
   10. When finished, stop the pump and rinse the tubing with distilled water, 70% ethanol and push the air into it. Store the probe in a vial filled with clean distilled water. Rinse the probe thoroughly by perfusing it at 2 µL/min by distilled water prior the storage.
   11. Analyze the concentration of the glutamate and aspartate in the samples by chromatography (see the details below; 6.3).
   12. Calculate the recovery using the following equation:
       Recovery (%) = ($C_{perfusate}$ /$C_{dialysed\ solution}$) x 100.

2. Microdialysis sessions in freely moving rats
   1. Preparative procedures: probe insertion and testing, infusion pump setting and start

1. Prepare the microdialysis probes for the first use according to the manufacturer user's guide and fill them with Ringer's solution. Cut about 10 cm long pieces of FEP-tubing and connect them to inlet and outlet cannulas of the probe using the tubing adapters of different colors.
2. Make sure that the tubing touches the adapters with no dead space in all connections.
3. 5.2.1.3. 24 h before the microdialysis experiment, anesthetize briefly the animal with isoflurane (5% in air) in an induction chamber until recumbent. Remove the dummy cannula from its guide using the tweezers and holding the animal's head firmly. Insert the microdialysis probe, endowed with a dialyzing membrane, into the guide cannula and firm further the microdialysis cannulas inserted in their guide by modeling clay.
   Caution: Do not let the probe touch the walls of the protective probe sleeve when extracting.
4. Put the animal into the plexiglass cylinder and let it explore the new ambience. Connect the animal to the tethered EEG recording system as described above (follow the points 4.2.2 and 4.2.3).
5. Follow the awake and freely moving rat movements and connect the inlet of the probe to the 2.5 mL syringe with blunted 22G needle containing Ringer's solution using the tubing adapters. Push Ringer's solution inside the probe ejecting 1 mL of Ringer's solution in 10 s pushing continuously the piston of 2.5 mL syringe. Check for the drop of the liquid appearing on the outlet. The probe is now ready for use.
6. Fill up the 2.5 mL syringes connected to FEP-tubing by tubing adapters with Ringer's solution and mount them onto the infusion pump. Start the pump at 2 µL/min. Let it run overnight.
   Note: Use the desired length of all FEP-tubing but calculate the tubing dead volume to know when the high K^+ stimulation should be started and to correlate the quantification data with neurochemical changes in animal brain. Use the air bubble created in the tubing under the working flow to calculate this time.

2. Collection of samples during EEG recording and potassium stimulation
   1. Verify the absence of seizures in the 3 h preceding the onset of sample collection (video-EEG recordings) and continue to monitor seizure activity during microdialysis.
   2. Stop the pump carrying the FEP-tubing cannulated syringes filled up with Ringer's solution. Mount onto the pump another set of 2.5 mL syringes connected to FEP-tubing with tubing adapters filled up with a modified Ringer's solution containing 100 mM K^+ solution.
   3. Start the pump at 2 µL/min and let it run. For more rapid filling of the tubing, set the pump at 5 µL/min for the time of filling. Check for the absence of air bubbles in the system. Ensure that the tubing touches the adapters with no dead space in all connections.
   4. Test the probe if ready for use in animal as described above (5.2.1.5).
      Note: If for some reason the probe does not work, change it. For these cases, keep a few prepared microdialysis probes ready to use near the microdialysis-EEG workstation. Disconnect the animal from EEG cables and anesthetize it briefly with isoflurane if necessary to realize the change.
   5. Connect the FEP-tubing of syringes filled up with Ringer's solution to the inlet cannula of the probe in each animal and wait for the appearance of the liquid drop on the tip of the outlet.
   6. Connect the outlet of the probe to the FEP-tubing, which leads to collection in the test tube. Insert the FEP-tubing into the closed 0.2 mL test tube with a perforated cap. Ensure that the tube stays in the place by fixing with a piece of modeling clay.
   7. Continue to run the pump at 2 µL/min for 60 min without collecting samples to equilibrate the system (zero sample).
   8. Collect 5 consecutive 30 min dialysate samples (60 µL respective volume) under baseline conditions (perfusion with normal Ringer's solution). Store samples on ice.
   9. Calculate the time it takes liquid to pass from the pump into the animal's head (it depends on dead volume of tubing, *i.e.*, air bubble time) and switch the FEP-tubing that goes from the syringes containing normal Ringer's solution to syringes containing modified (100 mM K^+) Ringer's solution at this time without stopping the pump. Check for the absence of the air bubbles in the system. Let the pump run for 10 min.
      Caution: In 10 min of high K^+ stimulation, the animals tend to move themselves frenetically and usually present a great number of wet dog shakes (control and out of seizure cluster animals) or behavioral seizures (epileptic animals), so be ready to intervene to protect the tubing and cables from twisting.
   10. After 10 min, switch the tubing from the syringes containing 100 mM K^+ Ringer's solution to normal Ringer's solution and let the pump run. Do not turn off the pump during the solution changes so that that there will be a drop of the liquid at the end of the tubing to be connected in line.
   11. From the moment at which the dialysate contains high potassium, *i.e.*, after collection of the fifth post-equilibration dialysate, collect the dialysate fractions every 10 min (20 µL) for 1 h. Collect 3 additional 30 min dialysate samples and stop the pump. Store the samples on ice.
   12. Store the samples at -80 °C after the experiment until HPLC analysis.
   13. Repeat the microdialysis experiment for 3 consecutive days, except for the acute (24 h) and first seizure group, in which only one microdialysis session takes place 24 h after SE or within 24 h after the first spontaneous seizure (**Figure 3**).
   14. On completion of each experiment, euthanize the animal with an anesthetic overdose and remove the brain for verification of probe and electrode placement.

3. Post-microdialysis procedures
   1. Rinse the used microdialysis probes with distilled water and store them in a vial filled with clean distilled water until next use.
      Note: The reused membranes may have increased permeability; check for the probe recovery before its repeated use.
   2. Rinse the entire microdialysis set up (tubing, connectors and syringes) with distilled water followed by 70% ethanol. Replace ethanol with air and store the set up in a sterile environment.
   3. Split the basal dialysate samples into 20 µL fractions and use only one 20 µL fraction for amino acid basal concentration analysis. Store the remaining sample volume for further or confirmatory analysis at -80 °C.
   4. Fix the brains in 10% formalin and preserve them by paraffin-embedding[1]. Coronally section the brains into slices and stain them with hematoxylin and eosin. Examine the brains for correct probe and electrode placement[1,2].

Note: Fix the brains in cooled 2-methylbutane and store them at -80 °C. Use any other proven staining on the nervous tissue sections which permits to visualize the probe and electrode tract.

6. Chromatographic Analysis of Glutamate and Aspartate

1. Preparation of derivatizing agent
    1. Mix the respective volumes 20:1 (v/v) of orthophthaldialdehyde reagent (OPA) and 2-mercaptoethanol (5-ME) in the vial. Close the vial using the cap and air tight septum.
    Caution: Work under the chemical hood.
    2. Vortex the prepared solution and put it into the autosampler into the position for derivatizing agent.

2. Preparation of dialysate samples
    1. Put the glass insert with bottom spring into the 2 mL brown autosampler vial. Prepare the vials for all samples measured in one batch.
    2. Take the 20 µL dialysis samples from -80 °C freezer and let them melt. Remove 1 µL of the solution and add 1 µL of internal standard (IS) L-Homoserine (50 µM) to 19 µL of the sample, thus the sample contains 2.5 µM of IS. Pipette 20 µL of the dialysis sample into the glass insert in vial and seal it with an air tight septum.
    3. Place the vials containing the samples into the autosampler using the chromatographic software to label the samples in their positions.

3. Chromatographic analysis of samples to determine glutamate and aspartate concentration
    1. Run the analyses on the liquid chromatograph system with spectrofluorometric detection. Detect the amino acids after 2 min pre-column derivatization with 20 µL of orthophthaldialdehyde/5-mercaptoethanol 20:1 (v/v) added to 20 µL of sample.
    2. Prepare the system for amino acids analysis. Switch on the autosampler, the pump, the degasser, the detector and controlling unit together with computer.
    3. Immerse the siphons into the bottles containing the mobile phase and purge the channels of the chromatographic pump to be used for the analysis.
    4. Start to increase the flow of the mobile phase checking the pressure on the column (*e.g.*, start at 0.2 mL/min and increase the flow for additional 0.2 mL/min every 5 min until achieving the working flow). Let the system run at working flow 0.8 mL/min for at least 1 h to equilibrate the column.
    Caution: Unstable pressure indicates the presence of the air in the system. The pressure should not exceed 25 MPa.
    5. Set the gain, high sensitivity and the excitation and emission wavelengths on the detector to 345/455 nm respectively. Reset the detector signal (AUTOZERO).
    6. Using the chromatographic software, send the method to the instrument. Now, the chromatograph should be ready to measure.
    7. Separate the dialysate samples, standard spiked dialysate samples as well as standards (0.25 µM – 2.5 µM aspartate and glutamate in Ringer's solution) on the appropriate chromatographic column. Calibrate the chromatographic method and establish the detection and quantification limits before any dialysis samples analysis.
    8. Activate the single analysis or create the sequence of the samples to be analyzed using the chromatography software and run the sequence.
    Caution: Run more than one blank sample and different standard samples within the sequence of dialysate samples in order to control the method accuracy.
    9. Once the chromatograms are acquired, analyze them with chromatography software. Check the integration of the peaks of the interest into the calibration plot. Use peak height or peak area for quantification.
    10. Once the sample recording is finished fill the column and the system with an organic solvent (*e.g.*, 50% acetonitrile in ultrapure water) to prevent its aging and mold growth in it.
    11. Shut down the system.

Representative Results

Probe recovery

The mean recovery (*i.e.,* the mean amino acid content in the perfusate as a percentage of the content in an equal volume of the vial solution) was 15.49 ± 0.42% at a flow rate of 2 µL/min and 6.32 ± 0.64 at 3 µL/min for glutamate and 14.89 ± 0.36% at a flow rate of 2 µL/min and 10.13 ± 0.51 at 3 µL/min for aspartate when using the cuprophane membrane probe. If using the polyacrylonitrile membrane probe, the mean recovery was 13.67 ± 0.42% at a flow rate of 2 µL/min and 6.55 ± 1.07 at 3 µL/min for glutamate and 14.29 ± 0.62% at a flow rate of 2 µL/min and 8.49 ± 0.15 at 3 µL/min for aspartate (**Figure 4A-4B**). As it can be clearly seen in **Figure 4A**, the slower flow rate (2 µL/min) enhances the dialyzing performance of both probes. For the following experiments the cuprophane membrane endowed probe perfused at a flow rate 2 µL/min was chosen, because its mean recovery was higher (even if not significantly) at this flow rate for both analytes and because of experimental continuity (these probes were used for analyzing GABA in precedence[1]).

Seizures development and progression of the disease after status epilepticus

The behavioral and EEG monitoring of seizures, their evaluation, was done in all the animals employed in this study to confirm the development and progression of TLE disease in these.

The robust convulsive SE, that was interrupted after 3 h using diazepam, occurred 25±5 min after the pilocarpine injection. Then, all the animals entered a latency state in which they were apparently well and they were continuously video-EEG monitored in order to verify that no spontaneous seizures occurred in the first 9 days or to identify the first spontaneous seizure, respectively for the latency and the first seizure group. The first spontaneous seizure occurred 11.3 ± 0.6 days after SE (mean ± SEM, n=21). Thereafter, seizures occurred in clusters, and aggravated in time. In late chronic phase (days 55-62 after SE) the epileptic rats experienced 3.3±1.2 (mean ± SEM, n=12) generalized seizures

daily. There was a clear progression of the disease. Many, but not all EEG seizures, corresponded with behavioral seizure activity. **Figure 5B** shows the recorded paroxysmal epileptiform activity that was observed about 500 ms before and during behavioral seizures. **Figure 5A** shows control traces in non- epileptic rats.

Representative basal values of amino acids found in microdialysis perfusate and potassium stimulated release of glutamate

Basal glutamate concentration found in chronic epileptic rats (0.87 ± 0.06 µM) was significantly higher than in control animals (0.59 ± 0.03 µM; $p < 0.05$ vs. controls; one-way ANOVA and post hoc Dunnett's test). There was no statistically significant difference between chronic epileptic (0.31 ± 0.04 µM) and non-epileptic animals (0.30 ± 0.05 µM) in basal or high K^+ evoked aspartate concentrations. See the original article for details[2]. The reported basal levels of glutamate in control rats are in line with those found by others in similar studies (*i.e.*, about 0.75 µM when using a 2 µL/min flow and membranes of 2 mm effective length)[46,47,48,49,50,51,52,53]. However, many different factors can influence the results of microdialysis, for example the effective length of the probe and the membrane cut off.

High K^+-evoked an additional release of glutamate for about 30 min in control rats and for about 60 min in chronic epileptic rats (**Figure 6**). See the original article for details[2]. As can be seen from the depicted time course, the 10 min time resolution of microdialysis was sufficient to capture the variances in glutamate release found in both groups of animals.

HPLC calibration and limits

The data were calculated based on calibration curves obtained with standard solutions of glutamate and aspartate and the internal standard L-homoserine. The concentration of the neurotransmitters glutamate and aspartate in the perfusates was expressed in absolute values (µmol/L). Each calibration plot was constructed by analysis of solutions of glutamate and aspartate at four concentration levels (five replicates at each level).Regression coefficients were calculated for calibration plots: $y = \mathbf{k}x + \mathbf{q}$, where x was the concentration ratio of aspartate or glutamate to L-homoserine (IS) and y was the corresponding peak-area ratio of aspartate or glutamate to L- homoserine (IS). The coefficient of determination (r^2) was calculated. The applicability of HPLC method was within the limits; the lower limit of quantification was determined as the lowest concentration in the standard calibration curve and the upper limit of quantification as the highest used concentration of amino acid analytes for calibration, respectively. Limit of detection (LOD) was also calculated. Some of these values are delineated in **Table 1**. A model chromatogram of blank sample, standards sample and collected dialysis sample obtained with above described method are shown in **Figure 7**.

Probe localization

Microdialysis probe and recording electrode were implanted into the right ventral hippocampus and their correct placement was verified. Only those animals where the implantation was maximally in 500 µm distant from stabilized coordinates (see **Figure 8**) were included in analysis.

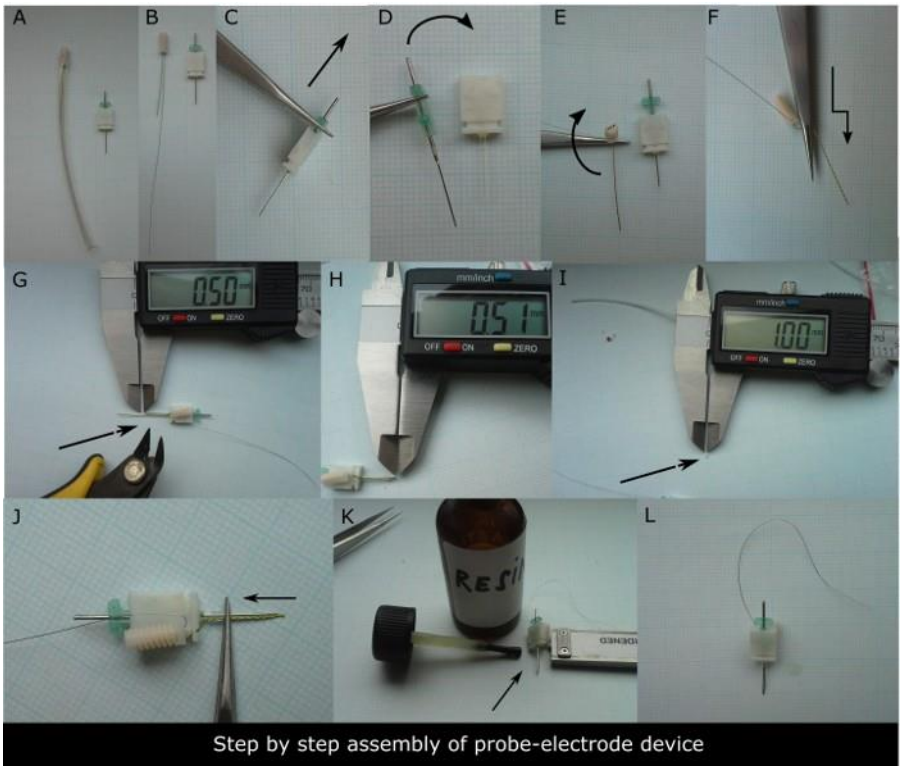

Figure 1. Step-by-step preparation of the device to be implanted. (A) 3-channel electrode with 10 cm long grounding electrode in its protective sleeve on the left and guide cannula for microdialysis on the right needed to assemble the device. (B). The bare electrode and guide cannula in detail. The first step is to remove (C) and insert (D) the metal guide cannula from and into its plastic dummy few times to ease its release once implanted into the animal's head. The second step is to bend two times the twisted registering electrode to be aligned to dialysis guide cannula (E, F). (G) The electrode tip should be cut to be 0.5 mm longer than the tip of the metal guide cannula. (H) Check for the precision of the cut using the digital caliper. Subsequently, about 1 mm long silicon circlet should be used to fix the alignment of electrode to guide cannula foot (I). (J) The photograph showing how to ring the electrode and guide cannula shaft. The final step is to put a drop of resin or glue onto the guide cannula pedestal fixing the silicon circlet to it (K). (L) Assembled device ready to be sterilized. Please click here to view a larger version of this figure.

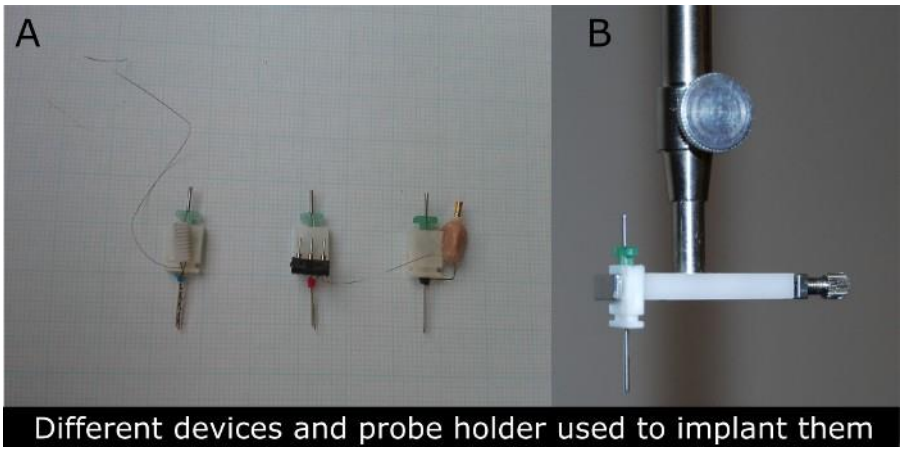

Figure 2. Photographs of different types of devices for microdialysis-EEG in rats used (A) and the photograph of the probe clip holder (B) used to implant these devices. (A) The guide cannula (in green) is replaced by a microdialysis cannula typically 24 h before the experiment. The electrical connector of the device (first left was used for the recordings described in this manuscript) permits the attachment of wires that conduct electrical signal to amplifier and data collection equipment. The device is surgically attached to the skull of anesthetized rats and recordings may be obtained later without causing pain or discomfort in freely behaving rats. Please click here to view a larger version of this figure.

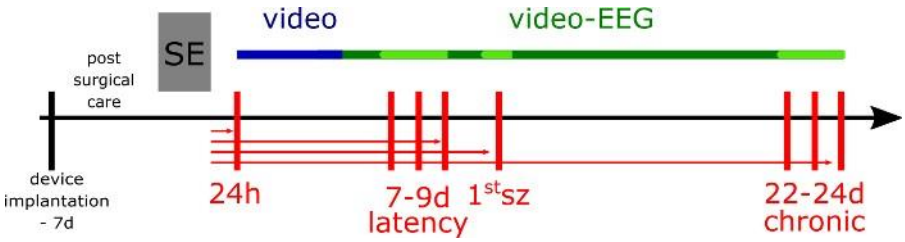

Figure 3. Experimental design. The week before status epilepticus (SE) induction, the rats are implanted with the device. SE is induced by pilocarpine and animals (if not dialyzed and killed at 24 h after SE; the rats from acute group) are video monitored for 5 days (blue line), then video-EEG monitored to assess the seizure frequency and duration in their home cages (green line). For the microdialysis experiment, the epileptic and respective non-epileptic control rats are transferred to another EEG set up equipped with cylinder cages in 24 h before the microdialysis session and still video-EEG monitored (light green line). The vertical red lines represent the dialysis sessions at different time-points of epileptic disease development. The horizontal red lines represent the different groups of epileptic animals (and respective non-epileptic animals), where the arrow indicates the last day of the microdialysis and the day of animal's death. Please click here to view a larger version of this figure.

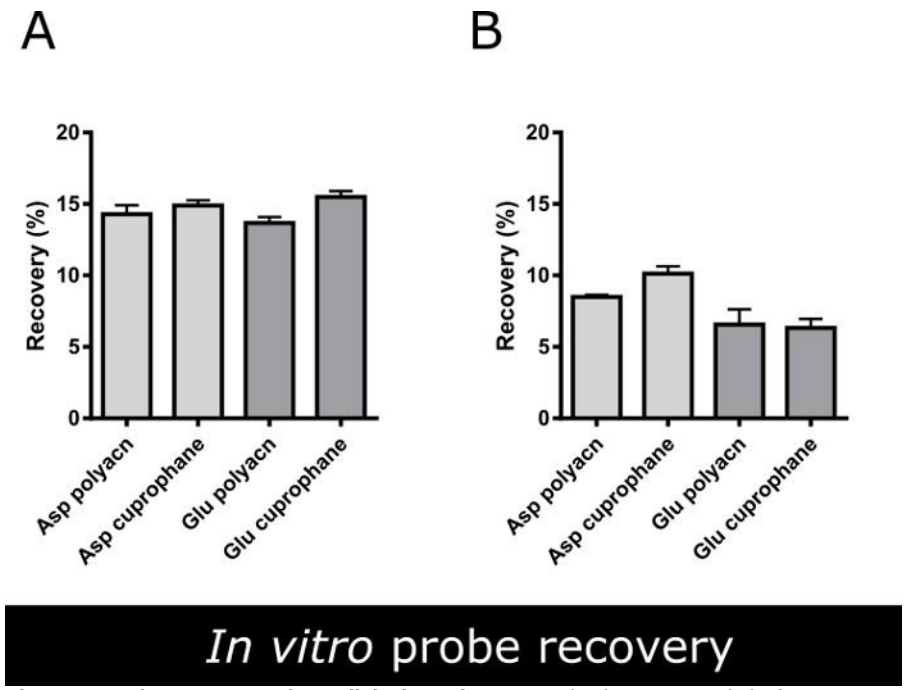

Figure 4. *In vitro* recovery of two dialysis probes. Mean *in vitro* recovery (%) of aspartate and glutamate using two different commercially available microdialysis probes (both endowed with 1 mm long dialyzing membrane) at (A) 2 µL/min and (B) 3 µL/min flow rate. Data are the mean ± SEM of 3 independent experiments run in triplicates. There are not statistically significant differences between the efficiency of various probes (Student's unpaired t-test, $p<0.05$). Using a flow rate 2 µL/min the glutamate recovery increased about 5% compared to 3 µL/min flow rate, thus the slower flow rate was used for microdialysis experiments. Please click here to view a larger version of this figure.

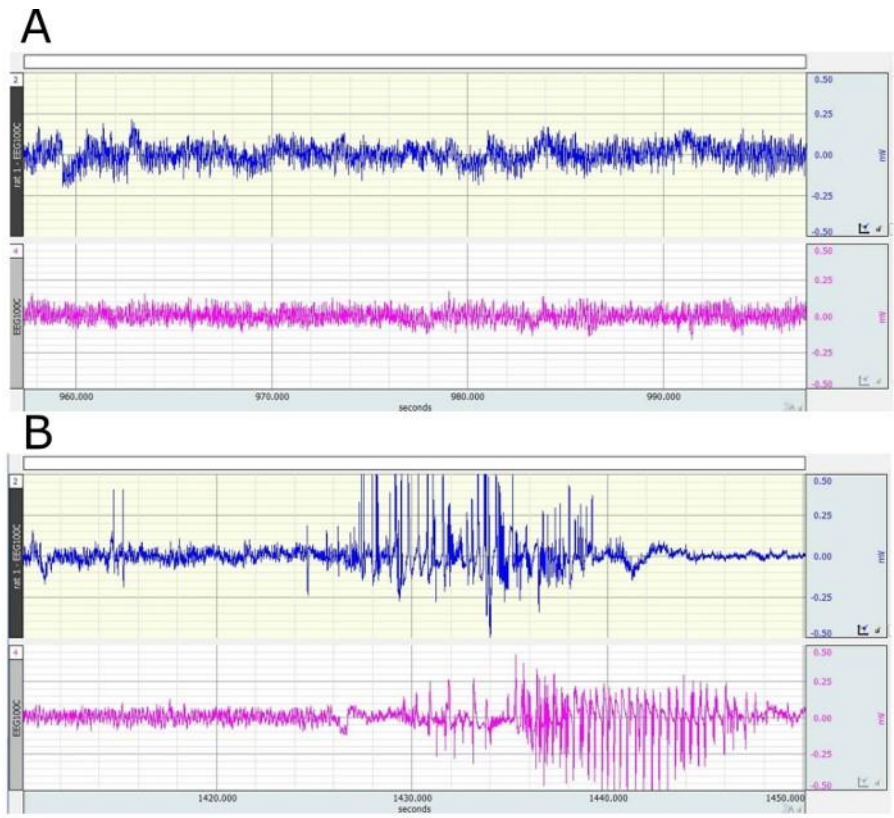

Figure 5. Illustrative EEG recordings from ventral hippocampus of paraoxystic activities as can be seen at chronic phase in control and epileptic rats. (A) Two representative traces recorded in two saline treated non-epileptic rats. (B) Traces recorded in two epileptic rats. Epileptiform discharges correspond with class 3 behavioral seizures in these rats. Please click here to view a larger version of this figure.

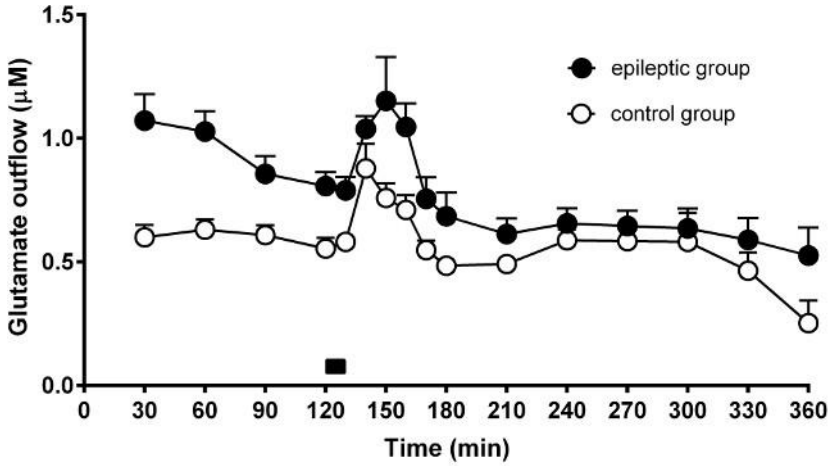

Figure 6. Time-course of the effect of potassium stimulation on glutamate release from the rat hippocampus. Representative result of the microdialysis experiment performed in 6 control (open circles) and 6 chronic epileptic rats (black circles). The graph shows the temporal changes of dialysate glutamate concentration in the course of microdialysis experiments and during high 100 mM K^+ stimulation. The time of high K^+ stimulus (10 min) is indicated by the black bar on bottom of the graph. The data are the means ± SEM of 6 animals per group. Please click here to view a larger version of this figure.

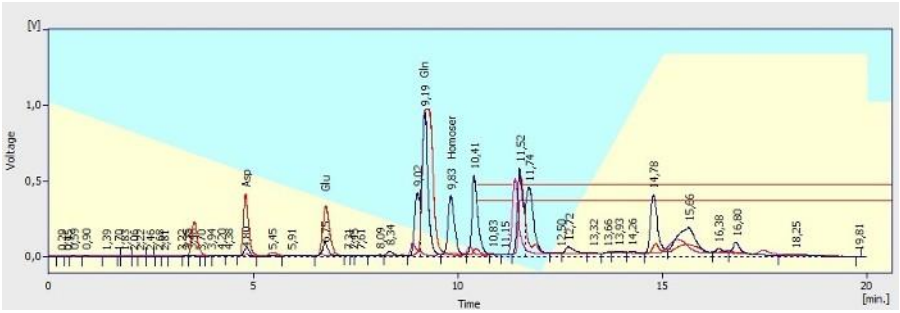

Figure 7. Illustration of chromatograms. Known peaks are labeled. Pink trace: chromatogram of Ringer's solution without intentionally added amines after OPA/5-ME derivatization (blank sample). Blue trace: chromatogram of dialysate sample after derivatization showing the peaks of amino acids: aspartate (t_R 4.80 min), glutamate (t_R 6.75 min) and glutamine (t_R 9.19 min) and the peak of IS L-homoserine (2.5 µM, retention time, t_R 9.83 min). Red trace: Chromatogram of standard of aspartate (2.5 µM) and glutamate (2.5 µM) in Ringer's solution. Azure and yellow background of the picture stands for mobile phase A (azure) and mobile phase B (yellow) portion used for analytes elution. A red rectangle indicated area (t_R 10.41 min and further) shows the peaks of unknown substances and OPA degradation products. All injection volumes were 20 µL. The derivatives were separated at a flow rate of 0.8 mL/min. Please click here to view a larger version of this figure.

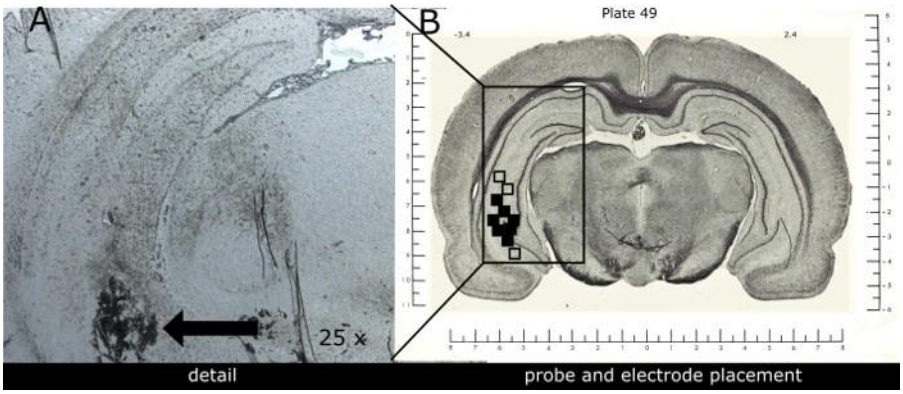

Figure 8. Representative image of combined electrode-probe placement within the ventral hippocampus. (A) Photograph shows the scare left by the device tip in detail (black arrow). (B) Schematic illustration of the electrode-probe tip positions within the implanted ventral hippocampus of 12 rats. The solid squares (some overlapping) indicate correctly localized probe-electrode tips. Open squares indicate incorrectly localized probe-electrode tips in animals excluded from the study (n=3). Coronal brain slices containing probes and recording sites were processed after experiments for histological analysis. The numbers above the illustration show the distance from Bregma (according to Pellegrino *et al.* 1979 atlas of rat brain; nose bar + 5.0 mm, co-ordinates used: A -3.4 mm, L+5.4 mm; P + 7.5 mm from dura). Please click here to view a larger version of this figure.

Analyte	**c (µmol/l)**	***k***	***q***	***r²***	**LOD (pmol/l)**
Glutamate	0.25-2.5	5.215	1043.79	0.999	19.4
Aspartate	0.25-2.5	2.258	1994.72	0.998	31.7

Table 1. Quantification characteristics of HPLC method used for amino acids determination. Concentration range of standards (c), slope (k), intercept (q), coefficient of determination (r^2) and limit of detection (LOD) describing the calibration plots obtained with standard solutions of glutamate and aspartate (0.25, 0.5, 1.0 and 2.5 µM) and internal standard L-homoserine (2.5 µM) using the described HPLC method with spectrofluorometric detection.

Discussion

In this work, we show how a continuous video-EEG recording coupled with microdialysis can be performed in an experimental model of TLE. Video-EEG recording techniques are used to correctly diagnose the different phases of the disease progression in animals and the microdialysis technique is used to describe the changes in glutamate release that occur in time (no changes have been found for aspartate in a previously published study[2]). We strongly recommend the use of a single device/implant to perform them both in each animal for the reasons discussed in the Introduction.

Whenever available, radiotelemetry should be preferred to tethered systems for chronic EEG recording as it minimizes interferences with behavior and reduces harm risk and distress for the animals[54]. However, the tethered EEG recording is much less expensive than telemetry.

In our laboratory, we use the connectors to the EEG recording system and microdialysis tubing in parallel, such that wires and tubings are attached to two different swivels. This is the most critical issue for these experiments: the wires and tubing tend to cross frequently due to the animal's movements. Therefore, we use connectors and tubing long enough to let the animal chase its own tail (a behavior that is typically observed with potassium stimulation) or fall down and roll during generalized epileptic seizures. It is advisable to firm further the microdialysis cannulas inserted in their guide by modeling clay, in order to strengthen their contact with the guide (sometimes, microdialysis cannulas are

bumped against the walls of the cage during generalized seizures and may slip off). On the other hand, it is advisable to keep the tubing as short as possible, to minimize the delay between neurochemical time and collection time. This is particularly important when collection periods are short. In general, the microdialysis tubing should be of adequate length and capacity to ensure that the sampling time does not exceed the time between dialysis outlet and collection. It was observed that the solutes tend to diffuse more between some plugs if the tubing dead time is superior to the sampling rate[55]. Therefore, the experimental dead time/volume of microdialysis tubing should be reduced as much as possible and determined very precisely in order to correlate the neurochemistry data with the animal's behavior. Finally, it is important to note that both swivels and electrodes coupled with cannula for combined EEG and microdialysis studies are commercially available. Therefore, whenever possible, set up the EEG system with the option to perform the microdialysis experiments.

The minor recommendations are: (i) before beginning any experiment, check that the EEG recording system and/or microdialysis set up are functioning properly and troubleshoot any problem; we suggest that having one reserve set up ready (another pump with syringes mounted on and completed of tubing filled up with working solutions) when performing the experiment, as well as a sufficient number of ready to use microdialysis probes for changing broken ones; (ii) when transferring animal into the working EEG-microdialysis cage it is helpful to have a second person assisting and starting the acquisitions; (iii) make sure that the column and autosampler reached the appropriate temperatures before chromatography; in addition, use standards and construct the calibration plots before any dialysate samples are injected on the chromatographic column; (v) whenever needed, try to develop the chromatographic or other analytical method to measure multiple analytes at the same time.

Alterations in neurotransmission have implications in many CNS disorders (including epilepsy) and there has been a great interest over the decades to quantify these changes during the progression from a healthy to a diseased phenotype. Today, only a few techniques allow the measurement of changes in neurotransmitter levels over days or months. Microdialysis is one of these techniques. In a large number of cases, like that described here, it is performed in freely moving animals and coupled to conventional offline analytical assays like high performance liquid chromatography (HPLC) or capillary electrophoresis (CE), with which it reaches 5-30 min temporal resolution[31,56]. Clearly, these sampling intervals do not reflect the rapid neurotransmitter dynamics in the vicinity of synapses, but may be convenient for some long term microdialysis applications (*e.g.*, disease development or drug effect studies) which require coupling neurochemical, EEG and behavioral data. However, other studies are primarily concerned with measuring real-time or close to real-time changes in neurotransmitter release. For these, the microdialysis technique must be refined to increase the speed of sampling (therefore decreasing sample volumes). Indeed, the classic microdialysis technique is often criticized for its poor temporal (minutes) and spatial resolution (the conventional probe is much larger than the synaptic cleft)[9,21,56,57]. However, it is the mass sensitivity of the analytical method coupled to microdialysis what determines the microdialysis time resolution (*i.e.*, its resolution is equal to the time required to have enough sample to be detected by an analytical technique[56]). Thus, when the microdialysis produces tiny amounts of samples, the sensitivity of quantification techniques must be increased. To date, such improvements in temporal resolution of the microdialysis technique followed 3 different lines. One of these is represented by miniaturization of the columns and/or detection cells of classic HPLC methods; these are called UHPLC (ultra-performant HPLC) techniques and allow to achieve 1-10 min time resolution[58,59,60]. Another approach is to couple a classic HPLC to mass spectrometry (MS) or tandem (MS/MS) for multiplex analysis of neurotransmitters in brain dialysates. Combined HPLC-MS assays have an excellent sensitivity and reach about 1-5 min time resolution[56,61,62,63]. A third line of improvement exists in modifications of capillary electrophoresis (CE). If CE uses laser induced fluorescence detection (CE-LIFD), it enables the determination of submicromolar concentrations of various neurotransmitters in nanoliter fractions obtained every 5 min[55,64,65] or even at 10 s intervals[56]. A clear advantage that emerges from UHPLCs or advanced CEs analytical approaches is that the sampling may be done in freely moving animals, not compromising experiments in which spontaneous behavior must be observed and analyzed. On the other hand, there are methods that permits the brain dialysate sampling at even hundred milliseconds temporal resolution (*e.g.,* enzyme reactor based on-line assays or droplet collection of dialysate coupled to MS techniques), but these are typically used in restrained animals[66] or under general anesthesia[67,68,69], not allowing to couple microdialysis with behavioral studies.

When considering the second most important weakness of microdialysis, *i.e.,* relatively low spatial resolution due to the membrane dimensions (often about 0.5 mm in diameter and 1-4 mm long), an alternative may be the microprobes developed with low-flow push-pull sampling. These probes consist of two silica capillaries (of 20 µm ID and 200 µm OD) fused side-by-side and sheathed with a polymeric tubing. During the experiment, these capillaries are perfused at very low flow rates, such that fluid is pulled out of one capillary and a sample is retrieved from the other at the same flow rate. Because the sampling occurs only at the probe tip, the spatial resolution is greater than with the probe for microdialysis[70]. Another possibility is to switch from miniaturized probes to microelectrode arrays (biosensors) for real-time neurotransmitter evaluation. Different electrochemical techniques (based principally on voltammetry or amperometry) permit analyte sampling very close to the synapse (micron scale) and in less than 1 s[31,70,71]. These devices can measure the concentration of multiple analytes from multiple brain regions. However, they also require some refinements, for example to avoid artifacts and a relatively rapid deterioration.

Considering the latest advances in *in vivo* neurochemical monitoring, it seems likely that the different transmitter sampling methods will be combined in one sensor in the near future. The work on microfabricated sampling probes has already started, and we believe that further progress in microfabrication technologies together with analytical advances will further facilitate *in vivo* neurochemical monitoring investigation. At this time, however, the conventional microdialysis correlated to EEG remains a valid method for many neuroscience applications.

Disclosures

The authors have nothing to disclose.

Acknowledgements

The authors wish to thank Anna Binaschi, Paolo Roncon and Eleonora Palma for their contribution to manuscripts published in precedence.

References

1. Soukupova, M., *et al.* Impairment of GABA release in the hippocampus at the time of the first spontaneous seizure in the pilocarpine model of temporal lobe epilepsy. *Experimental Neurology.* **257** 39-49 (2014).
2. Soukupova, M., *et al.* Increased extracellular levels of glutamate in the hippocampus of chronically epileptic rats. *Neuroscience.* **301** 246-253 (2015).
3. Curia, G., Longo, D., Biagini, G., Jones, R. S., & Avoli, M. The pilocarpine model of temporal lobe epilepsy. *Journal of Neuroscience Methods.* **172** (2), 143-157 (2008).
4. Scorza, F.A., *et al.* The pilocarpine model of epilepsy: what have we learned? *Anais da Academia Brasileira de Ciencias.* **81** (3), 345-365 (2009).
5. Pitkanen, A., & Sutula, T. P. Is epilepsy a progressive disorder? Prospects for new therapeutic approaches in temporal-lobe epilepsy. *The Lancet Neurology.* **1** (3), 173-181 (2002).
6. Pitkanen, A., & Lukasiuk, K. Mechanisms of epileptogenesis and potential treatment targets. *The Lancet Neurology.* **10** (2), 173-186 (2011).
7. Reddy, D. S. Role of hormones and neurosteroids in epileptogenesis. *Frontiers in Cellular Neuroscience.* **7** (115) (2013).
8. Engel, J., Jr. Research on the human brain in an epilepsy surgery setting. *Epilepsy Research.* **32** (1-2), 1-11 (1998).
9. Watson, C. J., Venton, B. J., & Kennedy, R. T. In vivo measurements of neurotransmitters by microdialysis sampling. *Analytical Chemistry.* **78** (5), 1391-1399 (2006).
10. Jeffrey, M., *et al.* A reliable method for intracranial electrode implantation and chronic electrical stimulation in the mouse brain. *BMC Neuroscience.* **14** 82 (2013).
11. Oliveira, L. M. O., & Dimitrov, D. Surgical techniques for chronic implantation of microwire arrays in rodents and primates. *Frontiers in Neuroscience.Methods for Neural Ensemble Recordings. 2nd edition. Boca Raton (FL): CRC Press/Taylor & Francis; 2008. Chapter 2.* (2008).
12. Fornari, R.V., *et al.* Rodent stereotaxic surgery and animal welfare outcome improvements for behavioral neuroscience. *Journal of Visualized Experiments: JoVE.* (59), e3528 (2012).
13. Horn, T. F., & Engelmann, M. In vivo microdialysis for nonapeptides in rat brain--a practical guide. *Methods.* **23** (1), 41-53 (2001).
14. Kennedy, R. T., Thompson, J. E., & Vickroy, T. W. In vivo monitoring of amino acids by direct sampling of brain extracellular fluid at ultralow flow rates and capillary electrophoresis. *Journal of Neuroscience Methods.* **114** (1), 39-49 (2002).
15. Renno, W. M., Mullet, M. A., Williams, F. G., & Beitz, A. J. Construction of 1 mm microdialysis probe for amino acids dialysis in rats. *Journal of Neuroscience Methods.* **79** (2), 217-228 (1998).
16. Nirogi, R., *et al.* Approach to reduce the non-specific binding in microdialysis. *Journal of Neuroscience Methods.* **209** (2), 379-387 (2012).
17. Zhou, Y., Wong, J. M., Mabrouk, O. S., & Kennedy, R. T. Reducing adsorption to improve recovery and in vivo detection of neuropeptides by microdialysis with LC-MS. *Analytical Chemistry.* **87** (19), 9802-9809 (2015).
18. Wisniewski, N., & Torto, N. Optimisation of microdialysis sampling recovery by varying inner cannula geometry. *Analyst.* **127** (8), 1129-1134 (2002).
19. Morrison, P. F., *et al.* Quantitative microdialysis: analysis of transients and application to pharmacokinetics in brain. *Journal of Neurochemistry.* **57** (1), 103-119 (1991).
20. Westerink, B. H., & De Vries, J. B. A method to evaluate the diffusion rate of drugs from a microdialysis probe through brain tissue. *Journal of Neuroscience Methods.* **109** (1), 53-58 (2001).
21. Chefer, V. I., Thompson, A. C., Zapata, A., & Shippenberg, T. S. Overview of brain microdialysis. *Current Protocols in Neurosciences.* **Chapter 7** Unit 7.1 (2009).
22. Westerink, B. H. Brain microdialysis and its application for the study of animal behaviour. *Behavioural Brain Research.* **70** (2), 103-124 (1995).
23. Zhang, M. Y., & Beyer, C. E. Measurement of neurotransmitters from extracellular fluid in brain by in vivo microdialysis and chromatography-mass spectrometry. *Journal of Pharmaceutical and Biomedical Analysis.* **40** (3), 492-499 (2006).
24. Allison, L. A., Mayer, G. S., & Shoup, R. E. o-Phthalaldehyde derivatives of amines for high-speed liquid chromatography/electrochemistry. *Analytical Chemistry.* **56** (7), 1089-1096 (1984).
25. Boyd, B. W., Witowski, S. R., & Kennedy, R. T. Trace-level amino acid analysis by capillary liquid chromatography and application to in vivo microdialysis sampling with 10-s temporal resolution. *Analytical Chemistry.* **72** (4), 865-871 (2000).
26. Hanczko, R., Jambor, A., Perl, A., & Molnar-Perl, I. Advances in the o-phthalaldehyde derivatizations. Comeback to the o-phthalaldehyde-ethanethiol reagent. *Journal of Chromatography A.* **1163** (1-2), 25-42 (2007).
27. Molnar-Perl, I. Quantitation of amino acids and amines in the same matrix by high-performance liquid chromatography, either simultaneously or separately. *Journal of Chromatography A.* **987** (1-2), 291-309 (2003).
28. Solis, J.M., *et al.* Variation of potassium ion concentrations in the rat hippocampus specifically affects extracellular taurine levels. *Neuroscience Letters.* **66** (3), 263-268 (1986).
29. Boatell, M. L., Bendahan, G., & Mahy, N. Time-related cortical amino acid changes after basal forebrain lesion: a microdialysis study. *Journal of Neurochemistry.* **64** (1), 285-291 (1995).
30. Sutton, A.C., *et al.* Elevated potassium provides an ionic mechanism for deep brain stimulation in the hemiparkinsonian rat. *The European Journal of Neuroscience.* **37** (2), 231-241 (2013).
31. Hascup, K. N., & Hascup, E. R. Electrochemical techniques for subsecond neurotransmitter detection in live rodents. *Comparative Medicine.* **64** (4), 249-255 (2014).
32. Fisher, R.S., *et al.* Epileptic seizures and epilepsy: definitions proposed by the International League Against Epilepsy (ILAE) and the International Bureau for Epilepsy (IBE). *Epilepsia.* **46** (4), 470-472 (2005).
33. Goffin, K., Nissinen, J., Van Laere, K., & Pitkanen, A. Cyclicity of spontaneous recurrent seizures in pilocarpine model of temporal lobe epilepsy in rat. *Experimental Neurology.* **205** (2), 501-505 (2007).
34. Pitsch, J., *et al.* Circadian clustering of spontaneous epileptic seizures emerges after pilocarpine-induced status epilepticus. *Epilepsia.* **58** (7), 1159-1171 (2017).

35. Pearce, P.S., *et al.* Spike-wave discharges in adult Sprague-Dawley rats and their implications for animal models of temporal lobe epilepsy. *Epilepsy and Behavior.* **32** 121-131 (2014).
36. Twele, F., Tollner, K., Bankstahl, M., & Loscher, W. The effects of carbamazepine in the intrahippocampal kainate model of temporal lobe epilepsy depend on seizure definition and mouse strain. *Epilepsia Open.* **1** (1-2), 45-60 (2016).
37. Kadam, S.D., *et al.* Methodological standards and interpretation of video-electroencephalography in adult control rodents. A TASK1-WG1 report of the AES/ILAE Translational Task Force of the ILAE. *Epilepsia.* **58 Suppl 4** 10-27 (2017).
38. Hernan, A.E., *et al.* Methodological standards and functional correlates of depth in vivo electrophysiological recordings in control rodents. A TASK1-WG3 report of the AES/ILAE Translational Task Force of the ILAE. *Epilepsia.* **58 Suppl 4** 28-39 (2017).
39. Bernal, J., *et al.* Guidelines for rodent survival surgery. *Journal of Investigative Surgery: the official journal of the Academy of Surgical Research.* **22** (6), 445-451 (2009).
40. Flecknell, P. Rodent analgesia: Assessment and therapeutics. *Veterinary Journal (London, England: 1997).* **232** 70-77 (2018).
41. Miller, A. L., & Richardson, C. A. Rodent analgesia. *The Veterinary Clinics of North America. Exotic Animal Practice.* **14** (1), 81-92 (2011).
42. Geiger, B. M., Frank, L. E., Caldera-Siu, A. D., & Pothos, E. N. Survivable stereotaxic surgery in rodents. *Journal of Visualized Experiments: JoVE.* (20) (2008).
43. Gardiner, T. W., & Toth, L. A. Stereotactic Surgery and Long-Term Maintenance of Cranial Implants in Research Animals. *Contemporary Topics in Laboratory Animal Science.* **38** (1), 56-63 (1999).
44. Williams, P.A., *et al.* Development of spontaneous recurrent seizures after kainate-induced status epilepticus. *The Journal of Neuroscience: The official journal of the Society for Neuroscience.* **29** (7), 2103-2112 (2009).
45. Paradiso, B., *et al.* Localized overexpression of FGF-2 and BDNF in hippocampus reduces mossy fiber sprouting and spontaneous seizures up to 4 weeks after pilocarpine-induced status epilepticus. *Epilepsia.* **52** (3), 572-578 (2011).
46. Kanamori, K. Faster flux of neurotransmitter glutamate during seizure - Evidence from 13C-enrichment of extracellular glutamate in kainate rat model. *PLoS One.* **12** (4), e0174845 (2017).
47. Kanamori, K., & Ross, B. D. Chronic electrographic seizure reduces glutamine and elevates glutamate in the extracellular fluid of rat brain. *Brain Research.* **1371** 180-191 (2011).
48. Kanamori, K., & Ross, B. D. Electrographic seizures are significantly reduced by in vivo inhibition of neuronal uptake of extracellular glutamine in rat hippocampus. *Epilepsy Research.* **107** (1-2), 20-36 (2013).
49. Luna-Munguia, H., Meneses, A., Pena-Ortega, F., Gaona, A., & Rocha, L. Effects of hippocampal high-frequency electrical stimulation in memory formation and their association with amino acid tissue content and release in normal rats. *Hippocampus.* **22** (1), 98-105 (2012).
50. Mazzuferi, M., Binaschi, A., Rodi, D., Mantovani, S., & Simonato, M. Induction of B1 bradykinin receptors in the kindled hippocampus increases extracellular glutamate levels: a microdialysis study. *Neuroscience.* **135** (3), 979-986 (2005).
51. Meurs, A., Clinckers, R., Ebinger, G., Michotte, Y., & Smolders, I. Seizure activity and changes in hippocampal extracellular glutamate, GABA, dopamine and serotonin. *Epilepsy Research.* **78** (1), 50-59 (2008).
52. Ueda, Y., *et al.* Collapse of extracellular glutamate regulation during epileptogenesis: down-regulation and functional failure of glutamate transporter function in rats with chronic seizures induced by kainic acid. *Journal of Neurochemistry.* **76** (3), 892-900 (2001).
53. Wilson, C.L., *et al.* Comparison of seizure related amino acid release in human epileptic hippocampus versus a chronic, kainate rat model of hippocampal epilepsy. *Epilepsy Research.* **26** (1), 245-254 (1996).
54. Lidster, K., *et al.* Opportunities for improving animal welfare in rodent models of epilepsy and seizures. *Journal of Neuroscience Methods.* **260** 2-25 (2016).
55. Parrot, S., *et al.* High temporal resolution for in vivo monitoring of neurotransmitters in awake epileptic rats using brain microdialysis and capillary electrophoresis with laser-induced fluorescence detection. *Journal of Neuroscience Methods.* **140** (1-2), 29-38 (2004).
56. Kennedy, R. T., Watson, C. J., Haskins, W. E., Powell, D. H., & Strecker, R. E. In vivo neurochemical monitoring by microdialysis and capillary separations. *Current Opinion in Chemical Biology.* **6** (5), 659-665 (2002).
57. Kennedy, R. T. Emerging trends in in vivo neurochemical monitoring by microdialysis. *Current Opinion in Chemical Biology.* **17** (5), 860-867 (2013).
58. Ferry, B., Gifu, E. P., Sandu, I., Denoroy, L., & Parrot, S. Analysis of microdialysate monoamines, including noradrenaline, dopamine and serotonin, using capillary ultra-high performance liquid chromatography and electrochemical detection. *Journal of Chromatography B, Analytical Technologies in the Biomedical and Life Sciences.* **951-952** 52-57 (2014).
59. Jung, M. C., Shi, G., Borland, L., Michael, A. C., & Weber, S. G. Simultaneous determination of biogenic monoamines in rat brain dialysates using capillary high-performance liquid chromatography with photoluminescence following electron transfer. *Analytical Chemistry.* **78** (6), 1755-1760 (2006).
60. Parrot, S., Lambas-Senas, L., Sentenac, S., Denoroy, L., & Renaud, B. Highly sensitive assay for the measurement of serotonin in microdialysates using capillary high-performance liquid chromatography with electrochemical detection. *Journal of Chromatography B, Analytical Technologies in the Biomedical and Life Sciences.* **850** (1-2), 303-309 (2007).
61. Hershey, N. D., & Kennedy, R. T. In vivo calibration of microdialysis using infusion of stable-isotope labeled neurotransmitters. *ACS Chemical Neuroscience.* **4** (5), 729-736 (2013).
62. Vander Weele, C.M., *et al.* Rapid dopamine transmission within the nucleus accumbens: dramatic difference between morphine and oxycodone delivery. *The European Journal of Neuroscience.* **40** (7), 3041-3054 (2014).
63. Zestos, A. G., & Kennedy, R. T. Microdialysis Coupled with LC-MS/MS for In Vivo Neurochemical Monitoring. *The AAPS journal.* **19** (5), 1284-1293 (2017).
64. Benturquia, N., Parrot, S., Sauvinet, V., Renaud, B., & Denoroy, L. Simultaneous determination of vigabatrin and amino acid neurotransmitters in brain microdialysates by capillary electrophoresis with laser-induced fluorescence detection. *Journal of Chromatography B, Analytical Technologies in the Biomedical and Life Sciences.* **806** (2), 237-244 (2004).
65. Chefer, V., *et al.* Repeated exposure to moderate doses of ethanol augments hippocampal glutamate neurotransmission by increasing release. *Addiction Biology.* **16** (2), 229-237 (2011).
66. Morales-Villagran, A., Pardo-Pena, K., Medina-Ceja, L., & Lopez-Perez, S. A microdialysis and enzymatic reactor sensing procedure for the simultaneous registration of online glutamate measurements at high temporal resolution during epileptiform activity. *Journal of Neurochemistry.* **139** (5), 886-896 (2016).
67. Petit-Pierre, G., *et al.* In vivo neurochemical measurements in cerebral tissues using a droplet-based monitoring system. *Nature Communication.* **8** (1), 1239 (2017).

68. Renaud, P., Su, C. K., Hsia, S. C., & Sun, Y. C. A high-throughput microdialysis-parallel solid phase extraction-inductively coupled plasma mass spectrometry hyphenated system for continuous monitoring of extracellular metal ions in living rat brain. *Nature Communication.* **1326** 73-79 (2014).
69. Zilkha, E., Obrenovitch, T. P., Koshy, A., Kusakabe, H., & Bennetto, H. P. Extracellular glutamate: on-line monitoring using microdialysis coupled to enzyme-amperometric analysis. *Journal of Neuroscience Methods.* **60** (1-2), 1-9 (1995).
70. Ngernsutivorakul, T., White, T. S., & Kennedy, R. T. Microfabricated Probes for Studying Brain Chemistry: A Review. *Chemphyschem: a Eurepean journal of chemical physics and physical chemistry.* **19** (10), 1128-1142 (2018).
71. Mirzaei, M., & Sawan, M. Microelectronics-based biosensors dedicated to the detection of neurotransmitters: a review. *Sensors (Basel, Switzerland).* **14** (10), 17981-18008 (2014).

My last words in this thesis are dedicated to the people who guided me during my PhD. None of my personal improvement and scientific achievements could have happened without the talented scientists I worked with during these three years.

First of all, I'm very grateful to my tutor Prof. Michele Simonato, for giving me a chance to study and learn in a welcoming, collegial, and intellectually stimulating environment. His mentorship, guidance, and friendship have made the past three years truly rewarding.

I would also like to thank Dr.ssa. Silvia Zucchini, for taking always time to meet with me and providing a guidance. The encouragement and the unconditional faith she had in me stimulated me to grow day by day. Ms. Michela Nanni, the most incredible laboratory manager I ever meet. Thank you so much for your help with all – and I say all – the paperwork and for supporting words.

Lots of thanks also even to Dr. Mario Barbieri, Dr.ssa Marie Soukupova and Dr.ssa Chiara Falcicchia, who shared with me their huge knowledge. I never had the pleasure of working closely with people who brought so much collaboration and genial ideas. Thanks for complicity… Also, thanks Mario for giving me my first lab name "Number 31". I like the special person you are!

Francesca "Donna Francisca" Lovisari, I'm very grateful to have faced this path with you, thank you for support, strength and everything we shared.

Last but not least, an immense thanks to my brothers – Mattia e Simone – for always being on my side. For unconditional love and support I need thank my grandparents. And thanks to my loving mom, to which I want to dedicate this thesis. Thanks, you for – everything. Without you nothing would have been possible. Thank you for endless support and love and for always providing me a warm and cosy home. You are always with me deep, deep down in my heart. I love you!

Another thesis would not sufficent to thank you all: Dr.ssa Simonetta Falzoni, Dr.ssa Michelina Lauriola, Dr.ssa Annunziata Guarino, Ram, my little girls – Chiara Marchetti, Nicole Mistroni, Maria Orsola Francesca –, Pinton Lab, Monchi and collegues to make this experience even more enjoyable (Sara, Gabriele et al. 2018).

Sara, Gabriele, Alberto, Federico, Anna, Silvia, Elena, Bara, Vir, Isa, Antonis and Daniela (2018). "Il mio grazie speciale." Journal Of a Life **1**: 2015-2018.